UCGE Reports
Number 20195

Department of Geomatics Engineering

Numerical Solutions to Altimetry-Gravimetry Boundary Value Problems in Coastal Regions

(URL: http://www.geomatics.ucalgary.ca/links/GradTheses.html)

by

Rossen Grebenitcharsky

May 2004

UNIVERSITY OF CALGARY

NUMERICAL SOLUTIONS TO ALTIMETRY-GRAVIMETRY BOUNDARY VALUE PROBLEMS IN COASTAL REGIONS

by

Rossen Grebenitcharsky

A THESIS

SUBMITTED TO THE FACULTY OF GRADUATE STUDIES

IN PARTIAL FULFILMENT OF THE REQUIREMENTS FOR THE

DEGREE OF DOCTOR OF PHILOSOPHY

DEPARTMENT OF GEOMATICS ENGINEERING

CALGARY, ALBERTA

May, 2004

Abstract

This thesis presents novel solutions of altimetry-gravimetry boundary value problems (AGBVPs) with compatibility (smoothness) conditions along the coastline for geoid determination. After an analysis of the state of the art for AGBVPs it was found that a lot of work has already been done in terms of theoretical problem formulation and solution investigation of AGBVPs. The conditions under which the solutions of different AGBVPs exist and are unique have been provided. It has been shown that without additional compatibility conditions along the coastline a solution with higher level of regularity does not exist. This was the starting point of this work and, after three preliminary experiments, it was found that the effect of smoothness along the coast line is significant for cm-geoid determination. Further theoretical investigations by the author resulted in the following achievements and contributions to local and regional determination of the geoid. The theory of spherical pseudo-differential operators (PDOs), spherical wavelets and spherical harmonics was combined for local and regional geoid determination in coastal areas. Using the theory of PDOs, it has been proven that the fixed AGBVP II has a unique solution and different methods applied to solve this problem yield the same solution. It has been shown that the compatibility conditions given by Svensson (1988) are equivalent to the condition that the data and their first and second order gradients coincide with each other along the coastline. It has been proven that PDOs are uniformly Lipschitz α; in this case, they can be combined with wavelets that are locally Lipschitz α to increase the regularity (smoothness) of the solution along the coastline. A modified algorithm for reconstruction of a signal using wavelet modulus maxima points is suggested to detect and to smooth existing discrepancies and irregularities along the coastline. Any kind of functionals of disturbing potential is presented in a discrete form, which allows spherical PDOs and wavelets to be applied numerically; even the compatibility conditions are expressed in an *explicit form* in discrete form as a sum of two functionals described above. Final numerical solution with spherical H-Shannon wavelets was proposed and conclusions are drawn about its advantages from an application point of view. Finally, as a result of the proposed procedure a smooth transition of the geoid from land to sea can be achieved, which will result in an improved geoid model in coastal areas.

Acknowledgements

I would like to express my gratitude to my supervisor, Dr. Michael Sideris, for his guidance and support throughout my graduate studies, as well as for his constructive criticisms of my research. This thesis would not have been possible without his constant cooperation and support. I am grateful to Dr. J.A.R. Blais for very helpful discussions about the theoretical part of the thesis and his help with reference materials and also for very useful suggestions related to the final version of this thesis. I would like to acknowledge very helpful discussions with Dr. B. Heck and Dr. W. Keller, which have helped me to clarify the main objectives of the thesis. Thank you Dr. Sneeuw and Dr. Kotsakis for the constructive suggestions in the gravity group meetings.

I would like to thank Dr. Georgia Fotopoulos for her help and advices, especially in the final step of the thesis preparation. Thanks to George Vergos, for being my friend and officemate for two years, and for our very useful discussions and collaborations.

Special thanks to my friend, colleague and officemate Elena Rangelova for her constant support and for many professional discussions. Thank you Elena and Dimitar for your help in the last stage of the thesis preparation.

Thanks to all my friends in the gravity group and in the Geomatics Department for their constant support.

Special thanks to my family for supporting me from the very beginning and to my son and wife for their great patience and sacrifice.

Financial support for this work was provided from research grants awarded to Dr. Sideris by the Geomatics for Informed Decisions (GEOIDE) Network of Centres of Excellence (NCE) and by NSERC.

Contents

List of Tables

List of Figures

LIST OF SYMBOLS

General theory of BVPs, PDOs and wavelets

$\mathbf{R}^1$, $\mathbf{R}^2$ and $\mathbf{R}^3$	1D, 2D and 3D spaces of real numbers
Au	partial differential operator A applied on a function u
$Au = f$	partial differential equation, needs to be solved
u	the dependent variable, giving the solution of a PDE and BVP
u_i and u_{jj}	the first and second order partial derivatives
Δ, ∇^2	Laplace's operator (Laplacian)
$u(x',x_3)$	solution of PDE and BVP
G and Γ	space $G \subset \mathrm{R}^3$ outside a boundary surface $\Gamma \subset \mathrm{R}^2$
$x' = (x_1 , x_2) \in \Gamma$;	point on the 2D boundary surface
$B_1(x')$	the boundary condition (measurement, observation or data);
$\partial u / \partial n$	the normal derivative (the derivative in the direction of the normal vector to the boundary surface)
$\overline{G} = G \cup \Gamma$	the closure of G
Γ_1 and Γ_2	are the two parts of the boundary surface and $\Gamma = \Gamma_1 \cup \Gamma_2$
$\gamma_c = \Gamma_1 \cap \Gamma_2$	γ_c the coastline
$\mathbf{W}_\alpha, \overline{\mathbf{W}}_\alpha$	Sobolev spaces of generalized derivatives and their closures of order α, where α is a real number
$\mathbf{C}^\infty(\mathbf{R}^3)$	space of functions with continuous partial derivatives of all orders
$\mathbf{C}_0^\infty(\mathbf{R}^3)$	space of functions in 3D which have continuous partial derivatives of any order on a compact support
$v(x)$	base (test) functions
$\mathbf{S} = \mathbf{S}(\mathbf{R}^3)$	space of (fundamental) base functions
$D^k(\bullet)$	partial derivative of order $k = (k_1, k_2, k_3)$
$v_1 * v_2$	convolution of a pair of functions $v_1(x), v_2(x) \in \mathbf{S}$
$\overline{(\bullet)}, \bullet^*$	complex conjugate of a variable or function
f	functional
$\mathbf{S}' = \mathbf{S}'(\mathbf{R}^3)$	space of generalized functions
$(D^k f, \varphi)$	derivative of k^{th}-order of a functional
$\mathbf{U}$	domain in $\mathbf{R}^3$

$\mathbf{C}_0^\infty(\mathbf{U})$	the space of all inifinitely differentiable functions with compact support in **U**
$\mathbf{S}'(\mathbf{U})$	space of generalized functions on finite domain
$p : pF = f$	restriction operator
$lf : F = lf$	extension operator
$\mathrm{supp}F$	support of the functional F
k	integer index giving the order of derivative of a generalized function
$\xi = (\xi_1, \xi_2, \xi_3)$	frequency represented in $\mathbf{R}^3$
$\xi' = (\xi_1, \xi_2)$	representation of the frequency in 2D
$\hat{\bullet}, F\{\bullet\}$	Fourier transform
$\mathbb{F}^{-1}\{\bullet\}$	Inverse Fourier transform
Au	pseudo-differential operator A
$A(\xi)$	symbol of PDO A
$A_0(t\xi) = t^{\alpha+i\beta}A_0(\xi), \quad \forall t > 0$	homogeneous operator
$O^\infty_{\alpha+i\beta}$	class of homogeneous functions of degree $\alpha + i\beta$
$A(\xi', \xi_3) = A_-(\xi', \xi_3)A_+(\xi', \xi_3)$	homogeneous factorization with respect to the variable ξ_3
$\mathbf{k} = \mathbf{k}_1 + i.\mathbf{k}_2$	factorization index of an elliptic symbol
$\mathfrak{R}_0 \in \mathbf{S}'(\mathbf{R}^3)$	generalized function induced by homogeneous function $A_0(\xi)$
$p.v.$	Cauchy principal value
$L(D)$	linear operator containing partial derivatives up to second order
a_{jk}	constants
$\mathbf{R}^3_+$	the halfspace defined by $x_3 \geq 0$
$\mathbf{R}^2 \equiv \Gamma$	the 2-dimensional boundary plane
$\mathbf{R}^2_+ \equiv \Gamma_1 \subset \mathbf{R}^2$	the 2-dimensional halfspace $x_2 > 0, x_3 = 0$
$\mathbf{R}^2_- \equiv \Gamma_2 \subset \mathbf{R}^2$	the halfspace $x_2 < 0, x_3 = 0$
$x_2 = 0$	presenting the coastline in AGBVPs
$B_1(D), B_2(D)$	boundary conditions (observations)
$a_k^{(1)}, a_k^{(2)}$	coefficients in the symbol representation $\hat{B}_1(\xi), \hat{B}_2(\xi)$ of both operators representing the boundary conditions
$d = \sqrt{x_3^2 + x_2^2}$	distance of the point to the coastline
$d^{k_0}, d^{k_0} \ln d$	smoothness of the solution

A	differential operator of n[th]-order
f	continuous function with continuous n^{th} order derivatives in the domain G
$\mathbf{D}_A$	the space of classical pointwise solutions
$(u,v)_A$	scalar product in space $\mathbf{D}_A$
$\mathbf{L}^2(a,b)$	space of square integrable functions on interval a,b
$\mathbf{S}_A$	functional space defined by the scalar product $(u,v)_A$
$\mathbf{H}_A$	space of weak solutions for a BVP
$\mathbf{W}_k$	Sobolev spaces of all functions with genealized derivatives up to k^{th} order
$\mathbf{H}$	is a Hilbert space
P,Q	frame limits
$\widetilde{U}^{-1}$	left pseudo-inverse operator
$\widetilde{v}_n = \left(U^* U\right)^{-1} v_n$	dual frame family corresponding to the reconstruction step
$\mathrm{W}g(x,s), \left(g, \psi_{x,s}\right)$	continuous wavelet transform
s	scale of continuous wavelet
$s_j = a^j$	sampling of the scale based on dilation step a
$\psi_{j,n}, \widetilde{\psi}_{j,n}$	discrete wavelet and corresponding dual wavelet
$s_j = 2^j$	dyadic scale
$\hat{\psi}_{j,n}, \hat{\widetilde{\psi}}_{j,n}$	Fourier transforms of wavelet and dual wavelet
A_j, D_j	Approximation and detail coefficients for j-level of wavelet decomposition
l_{j+1}, h_{j+1}	orthogonal projections
$A_j = A_{j+1} \oplus D_{j+1}$	wavelet decomposition of approximated coefficients at j-level
$\otimes$	space addition operator
l,h	low and high-pass filters corresponding to the scaling and wavelet functions of a dyadic MRA
$\hat{l}, \hat{h}$	Fourier transform of low and high-pass filters
$\widetilde{l}, \widetilde{h}, \hat{\widetilde{l}}, \hat{\widetilde{h}},$	dual low and high-pass filters and their Fourier transforms
$a_0[n]$	samples of discrete input signal

$a_j[n], d_j[n]$	approximated and detail dyadic coefficients at *j*-level of decomposition
$\uparrow, \downarrow$	up-sampling and down-sampling
$p_x(t), e_x(t)$	Taylor polynomial series of order *m* and their errors
$\tau(t)$	function which n^{th}-derivative is equal to the wavelet with *n* vanishing moments
(x_0, s_0)	pair representing local maximum
$W\tilde{g}(x,2^j)$	wavelet coefficients for reconstructed signal at the modulus maxima points

Gravity potential, gravity and geoid determination

W	the gravity potential outside the physical Earth's surface
ω_E	the Earth's angular velocity
G	the 3D space outside the physical Earth's surface
$\Gamma(x')$	the physical Earth surface
grad$W$	the gradient of gravity potential – the vector of the gravity force (gravity) $g(x')$
$B_1(x')$ and $B_2(x')$	functionals of the gravity potential
U	normal potential
$L_i(U)$	functionals of normal potential
T	disturbing potential
$\gamma = \|\boldsymbol{\gamma}\|$	the magnitude of the normal gravity vector
N	the geoidal height above the ellipsoid
h	the ellipsoidal height above the ellipsoid
Σ	telluroid as boundary surface
ζ	height anomaly
$\boldsymbol{\gamma}, \boldsymbol{\Delta g}, \mathbf{M}$	normal gravity vector, vectorial gravity anomaly and Hesse matrix of normal potential
ΔW	potential anomaly
$r = \|\mathbf{r}\|$	the length of the radius vector $\mathbf{r}$
$\Delta g'$	the gravity anomaly along the isozenithal direction
$\sigma(\varphi, \lambda)$	a point on the boundary surface with spherical coordinates - latitude and longitude - horizontal coordinates
$\bullet_L, \bullet_S$	indices for land and sea part of the boundary surface

$\Omega, \delta\Omega_L, \delta\Omega_S$	the space outside the sphere $\delta\Omega$, land and sea part of the sphere
a, b	constants representing systematic differences
$C = W_0 - W$	geopotential number
W_0	gravity potential on the geoid
$\mathbf{W_i}(\delta\Omega_k), \bar{\mathbf{W}}_i(\delta\Omega_k)$	Sobolev spaces of order i and their closures defined on land and at sea part of the sphere ($k = L, S$)
E, F, L, M	PDOs presenting mappings between different Sobolev spaces from land or sea part of the sphere to the entire sphere, which are extensions in terms of generalized functions
Δg_L	gravity anomalies on land
δg_S	gravity disturbances at sea
$a(\delta g_S, \Delta g_L)$	constant representing the systematic differences between gravity anomalies on land and gravity anomalies at sea along the coastline
Δ_σ	Laplace's (Beltrami) operator on the sphere with radius R
A, C, AC	PDOs on sphere
$S = A^{-1}$	Stokes' operator as a PDO
T_1	the first term in the representation of disturbing potential
$P = L + M$	operator for merging data on land and at sea
I	identity operator
$((T, v))_B$	variational equation for representing disturbing potential
$B(T, v)$	bilinear form representing variational equation for disturbing potential
$g(T, v)$	inner product of boundary conditions as functionals of disturbing potential
$F(T)$	functional needs to be minimized
$\sigma = \eta(\eta_1, \eta_2, \eta_3)$	point outside the sphere $\delta\Omega$ with radius R
$\eta(\eta_1, \eta_2, \eta_3) = \sigma(\varphi, \lambda, h)$	for spherical coordinates
$\mathbf{W}_1$	space of functions that are square integrable on $\delta\Omega$ under the weight $\lvert\eta\rvert^{-2}$ and have first derivatives in a generalized sense
$c_j^{(n)}$	coefficients of Galerkin system
$e = (e_1, e_2, e_3)$	orthonormal basis
$Y_n(x/r)$	spherical harmonics of order n
$H_n(x) = r^n Y_n(x/r)$	solid harmonics outside the sphere $\delta\Omega$

L_p	Legendre operator of variable $p = \cos(90^\circ - \varphi)$
P_n	Legendre polynomial of order n
P_{nm}	Legendre functions of order n and degree m
$Harm_n$	space of spherical harmonics of order n
Y_{nm}	spherical harmonics of order n and degree m
$\omega = (\omega_1, \omega_2, \omega_3), \eta = (\eta_1, \eta_2, \eta_3),$ $\varsigma = (\varsigma_1, \varsigma_2, \varsigma_3)$	points on unit sphere
δ_{nm}	2D Dirac δ function
$d\sigma(\eta)$	surface element at point η on the sphere $\delta\Omega$
θ	spherical distance between two points on the sphere
$(\omega, \eta) = \cos\theta$	scalar product of two vectors presenting points on the unit sphere
$\hat{\bullet}$	spherical Fourier transform, spherical symbol, Legendre transform
$l^2(\mathbf{N})$	space of all sequences of spherical symbols $\mathbf{N} = \{(n, j) \mid n = 0,1,2,..., j = -n,...-1,0,1...n\}$
$\{\Phi_s\}$	kernel of singular interval
$I_s = \Phi_s * g$	spherical singular integral
$\rho = e^{-s}$	the radius of Abel-Poisson kernel
A_ρ	operator for downward continuation from the unit sphere to the internal space
$Q_r(\omega.\eta)$	Abel-Poisson kernel
$\mathbf{E}$	linear space of all sequences $\{E_{n,j}\}$ of real numbers
$\{E_n\} \in \mathbf{E}$	sequence $E_{n,j} = E_n$, for $j = -n,...,-1,0,1,...,n$
$\mathbf{E}^\infty(\{E_n\})$	set of all infinitely differentiable functions g on $\delta\Omega$
$\mathbf{W}_\alpha^{\delta\Omega} = \mathbf{W}_\alpha(\delta\Omega)$	Sobolev spaces of degree α on sphere $\delta\Omega$, completion of space E^∞ in the norm (5.25)
$Bg = (-\Delta_\sigma + 1/4)^{\alpha/2} g$	operator used to define generalized derivatives and PDOs on unit sphere
$\Lambda(g), \hat{\Lambda}(n)$	PDO on sphere and its spherical symbol
N	degree of truncation of spherical harmonic expansion
$\mathbf{R}_\eta, \mathbf{D}_s$	rotation and dilation operator on sphere

$WT_{\psi} g(s;\eta)$	continuous wavelet transform
$\varphi_R, \hat{\varphi}(n)$	continuous scale function and ist spherical symbol
$\psi_j^P, \hat{\psi}_j^P(n)$	discrete spherical wavelet packet (P-wavelets) and their spherical symbol
$\psi_j^M, \hat{\psi}_j^M(n)$	discrete spherical wavelet modified (M-wavelets) and their spherical symbol
$\psi_j^D, \hat{\psi}_j^D(n)$	discrete Daubechies spherical (D-wavelets) and their spherical symbol
$\widetilde{\psi}_j^A, \hat{\widetilde{\psi}}_j^A(n)$	dual discrete wavelets and their spherical symbols for $A = P, M, D$
$\varphi_J^D, \hat{\varphi}_J^D(n)$	D-scaling function corresponding to the *J*-level of spherical MRA given by (5.63)
$\Phi, \widetilde{\Psi}$	scale function and the dual wavelet
$\hat{\Phi}, \hat{\Psi}$	the spherical symbols for scale function and wavelet function
J	the level of wavelet decomposition
b_n^0, b_n^j, a_s^k	coefficients
M, M_0, M_j	number of discrete points on the sphere j- level of decomposition
ξ, η	points on the sphere
K_{Λ}	kernel of corresponding PDO
$\Lambda T(\xi)$	PDO presenting a functional of disturbing potential at point ξ on the sphere
$r = R + h$	r is the distance to the center of the sphere, R is the radius of the sphere, h is the height above the sphere
$\hat{A}, \hat{C}, AC^{\wedge}$	spherical symbols of PDOs
χ, ϑ	"land" and "ocean" functions
$\hat{L}(\Delta g), \hat{M}(\delta g)$	Fourier transforms of extension operators L and M applied to
$\hat{L}(n), \hat{M}(n)$	spherical symbols for both extension operators in case of spherical cap
$\Lambda_L(T), \Lambda_S(T)$	PDOs on land and at sea part of the boundary surface used to give the compatibility conditions in an explicit form

LIST OF ABBREVIATIONS

BVP	boundary value problem
FFT	fast Fourier transform
GPS	global positioning system
FA	free-air anomalies
RMS	root mean square (error)
EGM96	Earth geopotential model 96
AGBVP	altimetry-gravimetry boundary value problem
GBVP	geodetic boundary value problem
PDO	pseudo-differential operator
MRA	multi-resolution analysis
PDE	partial differential equation
SST	sea surface topography
1D	one dimensional
2D	two dimensional
3D	three dimensional
KMS	Kort&Matrikelstyrelesen – Ministry of the Environment of Denmark
GEOSAT GM	altimetry satellite geodetic mission
MIMOST	multiple input multiple output system theory
PSD	power spectral density
GSD	Geodetic Survey Division
NOAA	National Oceanographic and Atmospheric Administration
CGG2000	most recent geoid of Canada
QSST	quasi-stationary sea surface topography

Chapter 1

Introduction

1.1 Background

Altimetry-gravimetry boundary value problems (AGBVPs) provide a framework in which the combination of different types of data is possible for gravity field and geoid determination. A general definition is given in Svenson (1983a): *"The altimetry-gravimetry problem consists in combining the altimetry observations over the oceans with the gravimetric observations over the continents in order to estimate geoid heights all over the Earth"*. More specifically, an AGBVP can be defined as a mixed type of boundary value problem (BVP), the goal of which is to find the disturbing potential as the solution of Laplace's equation; an AGBVP uses two different types of data (boundary conditions) on land and at sea, in what essentially is a devided type of boundary surface. In Figure 1.1 one type of AGBVP is presented when geoid heights from altimetry at sea and gravity anomalies on land are available to determine the geoid both on land and sea.

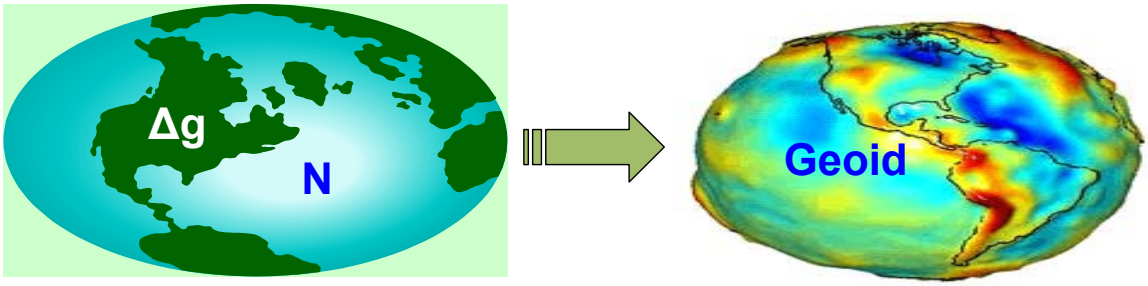

Figure 1.1: Altimetry-gravimetry boundary value problem – data distribution

Three types of AGBVPs exist:

- AGBVP I – geoid heights at sea and gravity anomalies on land (the boundary surface on land is unknown)
- AGBVP II – gravity disturbances at sea and gravity anomalies on land (the boundary surface on land unknown)

- AGBVP III - gravity disturbances at sea and gravity anomalies on land (the boundary surface on land known)

Although the solution can be smooth enough separately on the land and the sea parts, it must account for discrepancies, singularities and irregularities that occur along the coastline due to the different nature of available measurements, their accuracies and their resolutions. Additional compatibility conditions along the coastline are necessary to overcome these problems. They can be defined as constraints on the solution in coastal areas to:

- guarantee the existence and uniqueness of the solution;
- solve the datum problem between land and sea by introducing additional constants in the model, which can be considered as the major part of compatibility conditions;
- increase the regularity (smoothness) of the solution along the coastline by forcing higher order gradients of the solution to coincide along the coastline.

The entire thesis is focused only on the compatibility conditions as a tool to smooth and minimize the discrepancies along the coastline assuming that the systematic differences (datum problems, different biases, etc.) between land and sea segments are eliminated.

The formulation of the problem from a mathematical point of view is continuous but all applications are discrete. It is known that the discretization of data themselves can help the problem to become well-posed. But, irregularities in data along the coastline will still exist and as a result the solution (geoid) will have a sharp transition across the coastline. Increasing the smoothness of the solution means that it will become closer to the physical reality – the geoid. The application of so-called pseudo-differential operators (PDOs) as an averaging in the neighbourhood of the computational points can be useful in two aspects:

- to insure enough smoothness off the coastline;
- to provide the tools for imposing compatibility conditions which applied through wavelet filtering will increase the smoothness of the solution along the coastline.

The main problem consists of two parts: (i) how to apply, numerically, the compatibility (smoothness) conditions along the coastline for solutions of AGBVPs; and (ii) how compatibility conditions, in terms of pseudo-differentialoperators and wavelets, will increase the regularity of the solution across the coastline. The problem is explored in terms of identifying the difficulties and complexity of each situation, and proposing and testing a solution to achieve maximum efficiency.

1.1.1. Literature review

Historically, the first formulation of an AGBVP appeared when gravity data became available at sea (Holota, 1980). Another type of AGBVP appeared in Sansò (1981) and Arnold (1983), known later as AGBVP I. Holota treated both problems in a linearized form (Holota, 1983a and 1983b). Later, with the availability of GPS/levelling data, a new AGBVP appeared, known as AGBPV III (Lehmann, 1999b). All AGBVPs consist of two different types of geodetic boundary value problems (GBVPs): one on land and one at sea. They are distinguished by the type of boundary surface and boundary conditions used. In Sansò (1993), different types of AGBVPs are described both on land and at sea. The most recent definitions of both problems can be found in Sansò (1995) and Lehmann (1999b). Different types of solutions for AGBVP I and AGBVP II have been suggested for global and local applications. Table 1.1 summarizes the characteristics of most AGBVP solutions, their properties and areas of applicability in view of the global or local case. AGBVP I is suitable for global applications and AGBVP II for local and regional applications. There is a small number of references in which the additional compatibility conditions along the coastline are treated.

The role of compatibility conditions for altimetry-gravimetry boundary-value problems is quite complicated from several perspectives: guaranteeing the existence of the solution, smoothing the data (boundary conditions) at the boundary, and providing higher levels of regularization and smoothness in the solution. They are usually used to ensure the well-posedness of the problem (Sacerdote and Sansò, 1987; Svensson, 1988). The uniqueness and existence of the solution of AGBVPs depend upon the smoothness assumptions

applied along the coastline (Svensson, 1988). In Lehmann (1999a) it has been concluded that "*Incompatibility of the data does not produce significant distortions along the coastline"*. In Keller (1996) the addition of compatibility conditions is mentioned in terms of increasing the regularity of the solution. According to Svensson (1988), unless the compatibility conditions are satisfied, the mixed problems cannot be solved with a higher degree of smoothness. Additional constraints on the data for the regularization of the solution along the coastline were derived in Sacerdote and Sansò (1987).

One of the most often used methods for the solution of AGBVPs – the variational method for solving differential equations (Rektorys, 1977; Holota, 1997) – requires both the boundary surface and the boundary conditions (observations) to have a specified degree of smoothness, i.e., to have continuous derivatives up to a certain order. The *classical solution* of an AGBVP is defined as one which satisfies both the partial differential equation and boundary conditions *pointwise* everywhere. If boundary surface and boundary conditions are smooth enough the weak (generalized) solution will be close enough to the classical solution for the given problem. The complete theory behind this statement is based on the Sobolev spaces of generalized derivatives and can be found in (Rektorys, 1977; pp. 546-548). Sobolev embedding theorems have been used to show that, if the given data (boundary conditions) are smooth enough, the weak solution is also smooth enough and as a result it is regarded as the classical solution. In reality, however, irregularities exist on the coastline because different types of data with different observation procedures, accuracies and resolutions are used. To overcome these problems, compatibility conditions along the coastline can be used. Compatibility (smoothness) conditions in an implicit form based on the theory of pseudo-differential operators (PDOs) have been discussed by Svensson (1988). In this case, PDOs are applied as tools for imposing compatibility conditions assuming that they will increase the smoothness of the solution of AGBVPs.

Generalized derivatives from Sobolev spaces can be considered as a complement of generalized functions (see Chapter 3) having a real number for the degree of generalized

derivatives. PDOs have a bounded and continuous inverse Fourier transform and are invertible even when singularities exist along the coastline exist. All PDOs are generalized functions (Gelfand and Shilov, 1968; Eskin, 1980) which are globally defined (on the entire region of support) but compatibility conditions along the coastline have to be locally applied. The addition of compatibility conditions along the coastline may force the problem to become well-posed, but it is questionable whether such conditions upon the data are realistic for practical use. To answer this question, three preliminary numerical experiments have been conducted; see Grebenitcharsky and Sideris (2001a and 2002b), and Grebenitcharsky et al. (2001b), discussed in detail in Chapter 6 of this dissertation. In all three experiments, the applied smoothing procedure using wavelet filtering had an effect which can be considered significant from the perspective of cm-geoid determination; the changes in data and final solutions occurred only in the coastal area but not in other regions located away from the coastline.

These preliminary numerical results were the starting point of a further theoretical investigation for finding solutions of AGBVPs based on the combination of spherical harmonics, spherical pseudo-differential operators, spherical wavelets together with variational methods for solving differential equations; for a full treatment, see Grebenitcharsky and Sideris (2002a) and detailed discussion in Chapter 6. The compatibility conditions in Svensson (1988) are given in an implicit form. They need to be provided in an explicit form but, for current purposes, the so-called symbols of an ocean-land function (Simons et al., 1997) are necessary. Another way of using Svensson's compatibility conditions is to clarify their meaning and find a way to apply them numerically.

Spherical harmonic expansion and spherical wavelets for global applications are studied in Blais and Provins (2002). Applying spherical harmonic expansions to determine the definition of pseudo-differential operators (PDOs) will give us the so-called spherical PDOs in the finite spherical domain. They have been derived from the theory of singular integrals. For AGBVPs, PDOs can be applied not only for reformulation of AGBVPs in a

simple way but also for imposing compatibility conditions at the coastline. The theory of spherical PDOs has been described in Freeden and Windheuser (1997) and in Freeden et al. (1998). The definition of spherical PDOs in the finite spherical domain is slightly different from that of PDOs in an infinite domain (Eskin, 1980), due to the use of spherical harmonic expansions. Planar projections of PDOs on a manifold have been discussed in Keller (2003) in terms of their geodetic applications, to address the question of how PDOs can be used in local and regional applications on a plane instead of on a part of a sphere. The effect of the selected projection on the solution of Laplace's equation has been discussed in Svensson (2003). It has been shown that the Laplacian solution in a projection plane will differ from the solution of the sphere by a constant for local conformal map projections.

A study related to the application of spherical wavelets in the global case of investigating global potential models for geophysical applications has been conducted in Provins (2004). The numerical application of wavelet theory is related to the application of multiresolution analysis (MRA) described in, e.g., Mallat (1998) and Keller (2000). The use of MRA for solving problems in geodesy using gridded data is discussed in detail in Kotsakis (2000). The transition from variational methods to frame theory (Christensen, 2000; Mallat, 1998; Kotsakis, 2000) provides the theoretical motivation to restrict the wavelet coefficients in a dyadic MRA for the application of compatibility conditions as smoothness conditions to the irregularities and discrepancies along the coastline. The uniform regularity (Mallat, 1998) of PDOs can be combined with the local regularity (Mallat, 1998; Jaffard and Meyer, 1996) of wavelets to localize the PDOs, which are described as smooth generalized functions (Eskin, 1980).

The application of multiresolution analysis (MRA) and wavelets with well known planar types of wavelet transforms is not suitable for the solution of AGBVPs because known wavelets for an infinite (planar) domain are not harmonic functions on the sphere. To solve this problem, new wavelet methods for approximating harmonic functions have been suggested in Freeden and Schreiner (1995). Spherical wavelets are useful for the

solution of AGBVPs, since they are harmonic and have good spatial and spectral localization properties, which are necessary for the application of compatibility (smoothness) conditions. Spherical wavelets are a result of applying "rotation" and "dilation" operators. In the case of classical wavelets, the operators are "translation" and "dilation" of a mother wavelet. Another characteristic of spherical wavelets is the way of obtaining the mother wavelet. The kernels of spherical singular integrals are used as spherical scaling functions. As a spherical scaling function for solution of AGBVPs, the most suitable kernel is the Abel-Poisson kernel because it is harmonic (Freeden and Windheuser, 1996). When the harmonic Legendre polynomials are used as base functions, the corresponding spherical scaling function is harmonic as well. Some problems from the computational point of view related to the application of spherical wavelets on the sphere can be encountered (Blais and Provins, 2002). It is known that the Abel-Poisson kernel will produce non-orthogonal spherical wavelets. As a result, numerical difficulties can be expected. The application of a spherical MRA will require an orthogonalization procedure and the so-called "belt" Slepian problem can be applied to transform the coefficients of the spherical wavelets into coefficients of orthogonal Slepian functions (Albertella et al., 1999). Also, numerical difficulties are expected on the sphere because of the fact that a grid of spherical coordinates is non-equidistant. To overcome this problem, a hierarchical equidistributed grid described in (Freeden and Windheuser, 1997; pp. 28) can be applied. Such a grid will allow us to apply the orthogonalization procedure with "belt" Slepian functions in two directions along the two families of curvilinear coordinates. Another way to overcome this problem is to use *H*-Shannon spherical wavelets with the Abel-Poisson kernel as a scale function (Freeden and Michel, 2002). They are orthogonal and have a narrow local support, which makes them very useful for the local application of compatibility conditions along the coastline in the numerical solution of AGBVPs.

Table 1.1: Solutions of AGBVPs

AGBVP	Reference	Properties and characteristics	Area of application
AGBVP I, Least squares method	Arnold (1983)	1. Numerical 2. Uses least-squares condition 3. Orthonormalized surface spherical harmonics up to Nmax 4. With irregular data	global case
AGBVP I, orthonornalized approach	Mainville (1986)	1. Solution on sphere with spherical harmonics as base functions 2. Minimizing a functional – corresponds to variational methods on sphere	global case plus global coverage of the ocean with ship gravity data
AGBVP I, generalized spectral analysis	Xu (1992)	Substitution of the orthonormalization by an iterative technique. There is no proof if it is a workable method in practice	global case
AGBVP II	Sansò and Stock (1985)	1. Numerical solution of integral equation – Hotine's integral 2. Extension of Hotine integral to a Fredholm integral over land 3. Use of Galerkin method with base functions 4. The method is very close to the method of finite element technique 5. Finite element technique - constant function over an element	1. local case 12 °x 12° area with 6'x6' blocks 2. GPM is extracted from the data 3. around coastline
AGBVP II - fixed BVP	Mayer (1997)	1. Semi-linearized form only for gravity 2. On land this is a fixed problem using ellipsoidal heights 3. Variant 1 - Numerical, using Boundary Element Method 4. Variant 2 - Analytical with integral equation	local case, closed seas and around the coastline
AGBVP I	Svensson (1988)	1. Numerical solution 2. Proof that AGBVP I does not have stable least-squares solution 3. Disturbing potential across coastlines is not square integrable *4. Additional compatibility conditions in terms of pseudo-differential operators for AGBVP 1 and AGBVP II are introduced to increase the regularity of the solution*	global case and spherical cap for AGBVP I - 74.5 degree and for AGBVP II -

AGBVP	Reference	Properties and characteristics	Area of application
		5. Least-squares norm does not have finite value	52..2 degree
AGBVP I	Martinec (1995)	1. Numerically stable solution up harmonic degree 500 2. Shows that ill-posed problems some times become well posed after discretization	global case
AGBVP I, II and III, "Axisymetric experiment"	Lehmann (1999a)	1. Not only GPM has influence but whole global reference. 2. After exclusion of long wavelengths the prediction errors may be correlated in space over land part - in the case of AGBVP I,II for ellipsoidal heights, and in the case of AGBVP III for the potential 3. Different spectral contents of the boundary data for AGBVP I and AGBVP III 4. Nmax is optimal when the information is fully exploited. At sea Nmax is lower than land data. 5. *Incompatibility of the data does not produce significant distorsions along coastlines*	global case, local case and regions around coastlines
AGBVP I, construction of global models	Sansò (1993)	1. Analytical solution 2. Transformation from potential disturbances to gravity anomalies by the inverse Stokes' equation 3. Uniform BVP over the whole Earth with gravity anomalies all over the world 4. Estimation of coefficients of spherical harmonic expansion	global case
AGBVP II "Local approximation"	Sansò (1993)	1. Analytical solution 2. Integral solution for a wider area than the area where we need solution 3. Use of Hotine's integral extended to the land area 4. The difference between gravity anomalies and disturbances is around 1 mGal and this solution is possible only if the accuracy of marine gravity data is 0.1 mGal	local cases, closed seas with subtracted GPM information
AGBVP II, using "Global reference field"	Lehmann and Klees (1999)	1. Numerical solution 2. Adaptation of finite element methods (FEM) and boundary element methods (BEM) to use information from GPM 3. Use of wavelet transform or multiscale basis	local case
MIXED BVP	Jinghai and	1. Analytical	global

AGBVP	Reference	Properties and characteristics	Area of application
solution	Xiaoping (1997)	2. With reference ellipsoid as boundary	
AGBVP III - Fixed scalar BVP	Keller (1996)	1. Proof of existence and uniqueness of the solution 2. Has a unique solution for an arbitrary data distribution on land and sea 3. *To obtain a higher degree of regularity of the solution some compatibility conditions have to be fulfilled*	global and local case
New Pseudo Boundary Value problems (ψ -BVP)	Sansò (1995)	1. The usual remove-restore technique and the Residual Terrain Corrections (RTC) introduce new kind of BVP-Pseudo BVPs 2. What kind of boundary surface is used? 3. Contains boundary conditions where the boundary operators act on gravity disturbance at two boundaries	mostly in local case
Global Potential Model determination, using AGBVP	Sansò (1995)	1. GPM become itself a new kind of data with very high accuracy 2. Use of AGBVP II for wavelength between 440 km and 800km 3. Solution of an inverse Stokes' problem at sea to obtain gravity anomalies and then solution of Stokes problem all over the world for wavelength between 110km and 440 km.	global case
Free datum and multi datum BVP	Rummel and Teunissen (1988)	1. Change of Bruns formula 2. Change of fundamental equation 3. Introduction of new unknowns in the model	global solution and local solution
AGBVPI,II and III	Lehmann (1999b)	1. Proof of wellposedness of simple AGBVP II, III with free vertical datum 2. AGBVP I can be ill-posed for some distributions at sea and on land	global, local cases

Table 1.1 provides the characteristics of existing AGBVP solutions, their properties and areas of applicability. Finally, different types of numerical solutions of AGBVPs are possible based on the combined use of variational methods, spherical harmonic expansions, spherical PDOs and spherical wavelets. Most of them are appropriate for the solution of AGBVP II because, for local and regional applications, this AGBVP type or AGBVP III are the more suitable.

1.1.2. Open problems related to the application of compatibility conditions for the solution of AGBVPs

By way of summarizing the foregoing literature review, the following open problems exist with respect to the application of compatibility (smoothness) conditions in solutions of AGBVPs:

- Are the compatibility (smoothing) conditions at coastline necessary for the solution of AGBVPs - either from a theoretical point of view or from a practical point of view?

- How to account for the compatibility (smoothing) conditions at the coastline - including both the pointwise (classical) form of compatibility conditions and the generalized form of compatibility conditions - in terms of pseudo-differential operators and wavelets?

- How can wavelet transforms be used as multilevel differential operators for detection of discrepancies along the coastline and their application as smoothing conditions?

- What are the main properties of variational methods for the solution of boundary value problems, and of pseudo-differential operators, spherical harmonics and spherical wavelets from the perspective of the application of compatibility conditions?

- How to combine the advantages of variational methods for the solution of boundary value problems, pseudo-differential operators, spherical harmonics and spherical wavelets to obtain numerical solutions of AGBVPs with compatibility conditions along the coastline?

- How to find numerical solutions of different AGBVPs, while taking into account compatibility (smoothing) conditions?

- From the theoretical point of view, what is the quality of the numerical solutions obtained? Aspects of the problem, and the criteria of this evaluation, include: increasing the regularity of the solution across the coastline; smoothing irregularities and discrepancies by suppressing wavelet coefficients; obtain a generalized solution close to the classical solution; and the harmonic solution for disturbing potential by combining harmonic Abel-Poisson wavelets, PDOs and spherical harmonic expansions.

- From the application point of view, what is the quality of the numerical solutions obtained? Aspects of the problem, and the criteria of this evaluation, include: tests of numerical solutions of AGBVPs with actual data from coastal areas of Newfoundland and the Pacific coast of Canada and the US; data used - land and shipborne gravity data, multi-satellite altimetry missions data, GPS/leveling data; the effect of compatibility (smoothing) conditions along the coastline in found numerical solutions of AGBVPs; comparison of the test results with existing geoid solutions and other methods of geoid determination in the area under study.

- What conclusions can be drawn about the applicability of the proposed numerical solutions of AGBVPs using compatibility conditions along the coastline?

- Open questions for future work on the application of compatibility conditions include:
  - orthogonalization of spherical wavelets by application of Slepian functions;
  - providing an equidistant grid on the sphere for local and regional application;
  - computing spherical symbols for an ocean-land function for a general distribution of land and sea by applying spherical harmonic expansions;
  - application of compatibility conditions in explicit form based on a combination of spherical harmonics, PDOs and wavelets together with the spherical symbol for the ocean-land function.

1.2 Objectives

The following three scientific hypotheses comprise the basis of this dissertation: 1) Because of the different types of data, different accuracies and different levels of resolutions used for geoid determination both on land and ocean (sea) areas, conceptual discrepancies exist between the various forms of data; 2) A generalized solution, which is a result of the application of different variational methods and pseudo-differential operators, is closer to the classical solution of a boundary value problem if the boundary surface and boundary conditions (measurements) are sufficiently smooth; 3) The classical solution of AGBVPs in an integral form such as Stokes's formula does not exist. It is important to have a generalized solution of AGBVPs as close as possible to the classical solution and, to satisfy this condition, the discrepancies between data along the coastline must be smoothed using compatibility (smoothing) conditions. According to these hypotheses, the main purpose of this dissertation is twofold: *(i) to analyze altimetry-gravimetry boundary value problems (AGBVPs) with compatibility (smoothing) conditions along coastlines for geoid determination; and (ii) to find numerical solutions using a combination of variational methods, pseudo-differential operators, spherical harmonics and spherical wavelets*.

The objectives of the research related to the above-mentioned purpose include the following:

(i) The first objective of this research is to study the role of compatibility conditions in AGBVPs both from theoretical and practical points of view; having been formulated in an implicit form by Svensson (1988), it is necessary to discuss their meaning and their contribution to the final solutions of AGBVPs. From a practical point of view, the magnitude of their effect on the solutions must be investigated primarily to motivate a further theoretical investigation for the use of compatibility conditions in numerical solutions of AGBVP.

(ii) The second objective is to represent the compatibility conditions in an explicit form in terms of spherical harmonics, spherical PDOs and spherical wavelets. Having them in an explicit form is necessary for developing a procedure to incorporate them compatibility conditions in the numerical solutions of different types of AGBVPs.

(iii) The third and final objective is to conduct numerical experiments to test the quality of the solutions and the impact of the compatibility conditions on the final geoid determination in a regional case. Comparisons with existing geoid models and well-known methods of geoid determination will show possible advantages and disadvantages of the proposed numerical solutions for two different areas: the flat area of Newfoundland, along the eastern Canadian coastline, and the mountainous and very complicated coastline along the west coast of Canada and the U.S.

1.3 Thesis outline

A short description of each chapter is provided to show how the main objectives of the thesis will be achieved.

Chapter 1 contains the necessary background in terms of a definition of the problem which needs to be solved; a literature review related to this problem; open questions which exist and which must be solved in this dissertation or in future work; and the main objectives of the dissertation.

Chapter 2 presents in detail what comprises an AGBVP, starting from very basic definitions of a partial differential equation, boundary value problems, mixed boundary value problems, main geodetic boundary value problems and the role of compatibility conditions in the solution of AGBVPs. In addition, the general concept of the combined use of pseudo-differential operators and wavelets for imposing compatibility conditions is described. Finally, the main tasks of the thesis are defined.

Chapter 3 provides the theory of generalized functions and pseudo-differential operators, answering the question of why they are necessary for the application of compatibility conditions along the coastline. A proof is provided to show that compatibility conditions are actually conditions for coincidence of data and their gradients of first and second order along the coastline. The role of compatibility conditions in increasing the regularity of the solution is discussed and the impact of the so-called factorization index is considered. It is proven that the AGBVP II has a unique solution depending on the value of the factorization index; if the factorization index is increased by additional compatibility conditions, a higher level of regularity is achievable along the coastline.

Chapter 4 is related to the transition from variational methods with base functions to the frame theory of wavelet application. A short description of variational methods and frame theory is presented to explain how wavelet coefficients can be used to apply compatibility (smoothness) conditions. It is shown that PDOs are uniformly Lipschitz α and they can be combined with local regular wavelets to increase the smoothness of the solution along the coastline. A procedure for detecting and smoothing singularities and edges along the coastline is discussed, which is based on the local maxima of wavelets. Dyadic multiresolution analysis is discussed as well, explaining the numerical application of scale functions and wavelets as low-pass and high-pass filters.

Chapter 5 provides the background for spherical harmonics, spherical PDOs and spherical wavelets together with their use in combination to produce solutions of AGBVPs. Compatibility conditions are derived in an explicit form as the summation of two functionals of the disturbing potential. It is shown that they can be expressed in terms of spherical harmonics, spherical PDOs and wavelets; in addition, their spherical symbols are derived. Two possible solutions for AGBVP II are considered from a theoretical point of view: one is based on the Neumann boundary-value problem, while the second is based on the explicit form of the compatibility conditions.

Chapter 6 discusses three preliminary numerical experiments to investigate the effect of smoothness on the final geoid determination for flat and mountainous areas. The third one is in the form of a solution of the Neumann problem with the suppression of wavelet coefficients along the coastline. The effect of smoothing on a boundary surface and on boundary conditions is investigated. The three preliminary experiments show that the effect of smoothing along the coastline can be considered to be significant from the cm-geoid point of view. A numerical experiment is conducted to test a numerical solution of AGBVP II by combining spherical PDOs and wavelets so as to impose compatibility conditions along the coastline. Conclusions about the applicability and advantages of this solution from a practical point of view are drawn.

Chapter 7 summarizes the main contributions made in this dissertation, the main conclusions related to the application of compatibility conditions for increasing the regularity (smoothness) of the geoid in coastal regions, and recommendations for future work in this area of investigation.

Chapter 2

Altimetry-gravimetry boundary value problems and compatibility conditions along the coastline

2.1 Boundary value problems – general aspects

Solving partial differential equations (PDEs) with boundary conditions (data, measurements or observations) on a boundary surface leads to different types of boundary value problems (BVPs). An important role in gravity field and geoid determination plays the solution of Laplace's differential equation using different kind of boundary data on different boundary surfaces. For a better understanding of altimetry-gravimetry boundary value problems (AGBVPs) as mixed type BVPs a general view of the theory of BVPs will be presented in this chapter.

2.1.1 Boundary value problems in terms of partial differential equations

In general, different physical phenomena (gravity and gravitational potential of the Earth), can be described by equations containing space and time partial derivatives of unknown variables which have to be found. The variable which is differentiated is called dependent variable and very often it corresponds to the solution needed to be found. The variables with respect to which the differentiation takes place are called independent variables and in physical geodesy they usually correspond to the coordinates where the boundary conditions are known. The partial derivatives with respect to time variables are called initial conditions and the partial space derivatives on a boundary surface or a combination of them can be considered as boundary conditions. If a time independent physical phenomenon is modelled the initial conditions are not presented in the mathematical model. Only space derivatives are used, which leads to the so-called *boundary value problems*. From now on, considering the Earth potential field as a non time varying physical phenomenon, boundary value problems with known boundary

conditions (data, measurement or observations) on a certain boundary surface will be considered. There are two main issues in the description of a physical problem.

1) How to formulate a BVP which corresponds to this physical problem. The objective is to construct the mathematical model defining the corresponding PDE together with the available boundary conditions. The main part of a BVP is the PDE which has to be solved. Its type will determine the class of the BVP and there are the following characteristics of PDEs: *Order of the PDE* – the highest partial derivative in the equation; *Number of variables* – the number of independent variables, usually related to the dimensions of the functional space in which the PDEs is described; *Linearity* – the partial differential equations are linear or nonlinear, where a linear model means that the dependent variable (the solution of the problem) and all its derivatives appear in a linear manner. For example, the following equation

$$au_{x_1x_1} + bu_{x_1x_2} + cu_{x_2x_2} + du_{x_1} + eu_{x_2} + fu = g \tag{2.1}$$

where u is the dependent variable, u_i and u_{jj} are the first and second order partial derivatives with respect to the Cartesian coordinates $i, j = x_1, x_2$, is considered as a *second–order linear equation in two variables*; *Homogeneity* - if $g(x_1, x_2)$ is equal to zero for all x_1 and x_2 variables the PDE is called homogeneous, if not the PDE is non-homogeneous; *Type of coefficients* – the coefficients are either constants or functions. If they are constants, then the PDE is with *constant coefficients*; *Types of linear equations* – parabolic $\left((b)^2 - 4ac = 0\right)$, hyperbolic $\left((b)^2 - 4ac < 0\right)$ and elliptic $\left((b)^2 - 4ac > 0\right)$. In physical geodesy, most BVPs are based on Laplace's PDE, which represents the Earth's gravitational potential field in the 3D geometrical space outside the Earth surface

$$\Delta u = \nabla^2 u = u_{x_1x_1} + u_{x_2x_2} + u_{x_3x_3} = 0\,. \tag{2.2}$$

The Laplacian operator $\Delta \equiv \nabla^2$ is most important not only in physical geodesy but in mathematical physics in general. The reason is the fact that functions satisfying the Laplacian are harmonic (analytic). The physical meaning of the Laplacian after Farlow (1993) is:

1. If $\Delta u<0$ at a point then u is smaller than the average of all u at its neighbouring points;
2. If $\Delta u=0$ at a point then u is *equal* to the average of all u at its neighbouring points;
3. If $\Delta u>0$ at a point then u is greater than the average of all u at its neighbouring points.

In other words, in potential theory all harmonic (analytical) functions satisfying the Laplace equation ($\Delta u=0$) are infinitely smooth functions. According to the classification above the Laplace PDE is a *second-order homogeneous elliptic linear equation in three variables with constant coefficients, but only if Laplace PDE is given in Cartesian coordinates*.

The second important part for a BVP is the boundary conditions. They determine the types of BVPs with respect to the observations, measurements or data available on the boundary surface (Earth surface, equipotential surface, geoid etc.). In physical geodesy, an unknown boundary surface is used and the corresponding BVPs, taking into account the type of the boundary surface are called *geodetic boundary value problems* (GBVPs). Also, the boundary surface can be broken into several parts on which different types of boundary conditions exist. In such case, a BVP is formulated as a *mixed* BVP. Typical examples of mixed GBVPs are the altimetry-gravimetry boundary value problems (AGBVPs). The boundary surface consists of two parts, covering the land and the ocean parts of the Earth surface, respectively. In geodesy, considering the boundary conditions and the boundary surface, several types of GBVPs exist and they will be discussed in more detail in the next section.

2) How to solve the PDE using the boundary conditions is the second issue in describing a physical phenomenon by BVP. The classification mentioned above will generally provide the methods and theory applied certain class of PDEs. According to Farlow (1993), there exist ten techniques to solve a BVP: separation of variables, integral transforms, change of coordinates, transformation of the dependent variable, numerical methods, perturbation methods, impulse-response technique, integral equations, variational methods and eigenfunction expansions. In case the solution of a certain BVP exists and is unique, all techniques mentioned above have to provide the same results in the frame of the assumed computational precision and the accuracy of used data and measurements. All the solutions of BVPs can be classified in two main groups – analytical and numerical solutions. By the definition given in Farlow (1993), the *analytical solutions* for continuous case are those where the unknown variable is given as a mathematical expression in terms of the independent variables and the parameters of the system which are expressed as infinite series or integrals. The *numerical solutions* to discrete model refer to finding the solution of PDEs by replacing the differential equation with an approximation equation and solving the easier one. A numerical solution can be considered as the discretization of the continuous one. The following advantages can be considered for both types of solutions:

- Analytical solutions – a formula provides more information than a table of numbers. The solution is available at any single point (not only at certain points or a grid of points) with any degree of accuracy. It gives an idea how the physical parameters and boundary conditions affect the solution.
- Numerical solutions – the major advantage is that a lot of problems do not have analytical solutions and the only solutions which are possible are numerical solutions. For example, all mixed type BVPs do not have analytical solutions.

A solution (either analytical or numerical) of a BVP exists if the problem is *normally solvable*. According to Eskin (1980) a problem is normally solvable if the homogeneous

equation has a finite number of linearly independent solutions, and the non-homogeneous one is solvable under the fulfilment of a finite number of conditions.

2.1.2 Geodetic boundary value problems

In general, the boundary surface is assumed to be known, but in physical geodesy the boundary surface needs to be determined. According to Moritz (1980), a GBVP is formulated as the *determination of the physical Earth surface using gravity and gravity potential data on this surface*. The type of boundary conditions and the type of the boundary surface determine different types of BVPs.

2.1.2.1 Boundary value problems in mathematical physics

In general, a boundary condition can be represented in the form $B(x') = a\partial u / \partial n + bu$, where the coefficients a, b can be constant or functions. The main three BVPs used in mathematical physics and applied in physical geodesy are:

1) The Dirichlet BVP (a=0, b=1, the boundary surface is known)

$$\begin{vmatrix} \Delta u = 0 & \text{in } G \\ B_1(x') = u\big|_{\Gamma} = g_1(x') & \text{on } \Gamma \end{vmatrix} \tag{2.3}$$

where $x' = (x_1, x_2)$ represent 2D coordinates on the boundary surface. *The problem is to find a harmonic function* $u(x', x_3)$ *in the domain* $G \subset \mathrm{R}^3$ *outside a known boundary surface* Γ*, considering that the function u(x') itself is known and equal to* $g_1(x')$ *on the boundary.* A similar problem can arise when the geoid height (or disturbing gravity potential) from satellite altimetry (after removing the effect of sea surface topography) has been used as boundary condition. *The solution of this BVP defined on a sphere is the well known Poisson integral providing the downward (upward) continuation of the potential. According to Blais and Provins (2002) it can be presented as a spherical*

convolution and applying the Green function approach, the Poisson integral can be transformed into a spherical harmonic series. It is interesting to mention that the application of spherical PDOs and wavelets for upward continuation discussed in Chapter 5 (see Grebenitcharsky and Sideris, 2002a) lead to the same discrete form of the Poisson's integral.

2) The Neumann BVP (a=1, b=0, the boundary surface is known)

$$\begin{vmatrix} \Delta u = 0 & \text{in G} \\ B_2(x') = \left.\dfrac{\partial u}{\partial n}\right|_{\Gamma} = g_2(x') & \text{on } \Gamma \end{vmatrix} \tag{2.4}$$

The problem is to find a harmonic function $u(x', x_3)$ *in the domain* $G \subset \mathrm{R}^3$ *outside a known boundary surface* Γ*, considering that the normal derivative of the function u(x') is known and equal to* $g_2(x')$ *on the boundary.* It is known that an additional condition must always be satisfied for the Neumann problem, i.e.

$$\int_{\Gamma} \frac{\partial u}{\partial n} d\sigma = 0 \,. \tag{2.5}$$

It means that – the mean- there is no change in the described physical phenomenon (the potential in physical geodesy) across the boundary. Another specific characteristic of the Neumann problem is that the solution is not unique – there exists an infinite number of solutions, but if one solution is available the others will be possible by adding a constant. The last property of the solution can be explained by the fact that an integral is known up to a constant. An example of a Neumann BVP is when gravity disturbances are known on the boundary surface (geoid) and the solution for the gravity potential outside the boundary has to be found.

3) The Robin BVP (General 3D case: a≠0, b≠0, the boundary surface is known)

$$\begin{vmatrix} \Delta u = 0 & \text{in } G \\ B_3(x') = a\dfrac{\partial u}{\partial n} + bu\Big|_{\Gamma} = g_3(x') & \text{on } \Gamma \end{vmatrix} \tag{2.6}$$

The problem is to find a harmonic function $u(x', x_3)$ *in the domain* $G \subset \mathrm{R}^3$ *outside a boundary surface (known)* Γ *, satisfying the boundary conditions* $g_3(x')$ *on the boundary, where* $x' = (x_1, x_2) \in \Gamma$ *;* a, b can be constants or functions as well; $B_3(x')$ is the functional corresponding to the boundary condition (measurement, observation or data); $\partial u / \partial n$ is the normal derivative (the derivative in the direction of the vector normal to the boundary surface). A typical example for such boundary conditions in physical geodesy are gravity anomalies measured on the boundary surface, gravity anomalies are given on the geoid.

All three BVPs described above are known in potential theory as the first BVP – Dirichlet's problem; the second BVP – Neumann's problem and the third BVP – Robin's BVP.

In potential theory there exist a fourth type BVP, called oblique-derivative (Poincari). It appears when the boundary surface is known, which corresponds to so-called "fixed" GBVP.

2.1.2.2 Geodetic boundary value problems – unknown boundary surface

The GBVP is defined in a very general form in Moritz (1980) as follows:
"The geodetic boundary-value problem is the determination of the Earth's physical surface from the values of the gravity vector and the gravity potential given on it."

This very general definition can be presented in a stronger mathematical way by using the following assumptions (Sansó, 1981) and (Heck, 1997): *The Earth is assumed to behave like a rigid, non-deformable body, uniformly rotating with a constant angular velocity about a space and body fixed axis in Newtonian absolute space, which is by definition three dimensional Euclidian space. All attracting masses are located in the interior of the closed boundary surface* Γ*, which represents the Earth's physical surface. On the other hand, all time-varying gravitational or non-gravitational effects are extracted from the measurements by means of reductions previously applied to the original measurements. Furthermore, atmospheric masses need to be extracted as well.*

Mathematically, a GBVP is expressed in the form

$$\begin{vmatrix} \Delta W = 2\omega_E^2 & \text{in } G \\ B_1(x') = \left\| \text{grad} W(x') \right\| \Big|_\Gamma = \left\| \mathbf{g}(x') \right\| & \text{on } \Gamma \\ B_2(x') = W(x')\big|_\Gamma & \text{on } \Gamma \\ W \text{ regular at infinity} \end{vmatrix} . \tag{2.7}$$

In principle, potential differences $\delta W = W(x')\big|_\Gamma - W_0$ have to be introduced in the boundary condition because the absolute potentials are not measurable. *The problem is to determine the physical Earth's surface Γ(x') from the known gravity potential W(x') and gravity g(x') on it.* The following notations have been used: W is the gravity potential outside the physical Earth's surface; ω_E is the Earth's angular velocity; G is the 3D space outside the physical Earth's surface; $\Gamma(x')$ is the physical Earth's surface, which has to be determined; *gradW* is the gradient of gravity potential – the vector of the gravity acceleration (gravity) $\mathbf{g}(x')$; $B_1(x')$ and $B_2(x')$ are functionals of the gravity potential. In this general form the GBVP is a non-linear, non-homogeneous second order BVP with constant coefficients and unknown boundary surface. To solve the problem, the boundary conditions have to be linearized and must be transformed from Poisson's equation to the Laplace equation. In other words, a non-homogeneous PDE needs to be transformed to a homogeneous one. The linearization procedure consists of decomposing the gravity field

(W, $B_i(W)$) into a normal part (U – normal potential, $B_i(U)$ – functionals of normal potential) and a disturbing part (T, - disturbing potential, $B_i(T)$ – functionals of disturbing potential) where the normal part is due to a mathematical model (sphere, ellipsoid). Then the following relationships hold under the assumption that W and U contain identical centrifugal parts, or T is harmonic:

$$\begin{aligned} W &= U + T \\ B_i(W) &= B_i(U) + B_i(T), \qquad \mathrm{i} = 1,2 \end{aligned} \tag{2.8}$$

The last is valid only if B_i is a linear operator. The linearization procedure has been described in the literature (Moritz, 1980) and it will not be discussed in detail. After the linearization, the GBVP is transformed in a way that the disturbing potential T has to be determined and satisfy the boundary conditions, known on the boundary surface and expressed in terms of the disturbing potential. The last step in finding the solution of a GBVP is to formulate the GBVP on an ellipsoid, or on a sphere with a radius R, or on a plane ($R \to \infty$). Next two GBVPs will be finally given in spherical approximation because AGBVPs and the compatibility conditions need to be presented on a sphere in terms of spherical pseudo-differential operators.

Depending on the choice of boundary surface two main GBVPs are known. The first one – the classical Stokes' problem - uses the geoid as an approximation of the physical Earth surface and the second one – the Molodensky's problem - uses the real Earth's surface as a boundary surface. In both cases the boundary surface is unknown. The major difference is in the fact the geoid is an equipotential surface (all points on it have the same gravity potential and the normal to the boundary surface coincides with the direction of the gravity vector) but the Earth's surface is not equipotential and the normal to the boundary surface does not coincide with the gravity vector. In the first case, the problem is called *normal derivative* BVP and the second problem is an *oblique derivative* BVP. The Stokes problem is simple from a theoretical point a view but difficult to apply in practice because the measurements done on the Earth's surface have to be reduced to the geoid

and this procedure requires the knowledge of the density of the masses above the geoid. The Molodensky problem seems to be complicated from a theoretical point of view because of the non-equipotential boundary surface used. An additional information (e.g. astronomical deflections of the vertical) is necessary do describe the oblique derivatives. But from a practical point of view the knowledge of the density is not necessary, because the measurements have been used as they are on the Earth's surface – the downward continuation procedure is not applied. Both BVPs will be presented in the general linearized form and in their spherical approximation. Originally, two boundary conditions for two unknowns (disturbing potential and height of the Earth's surface) exist. The elimination of the height provides the reduced boundary condition for T, presented in the following.

4a) Stokes' problem in a general 3D linearized form corresponds to

$a = -1,\ b = \frac{1}{\gamma}\frac{\partial \gamma}{\partial n} = \frac{1}{\gamma}\frac{\partial \gamma}{\partial h}, g_1(x') = \Delta g$, $u \equiv T$, *and the boundary surface (the geoid* Γ*) is unknown.*

This GBVP has boundary conditions similar to the Robin BVP - gravity anomalies Δg - but on the geoid which is the unknown boundary surface. It is assumed that the derivative along the normal to the boundary surface coincides with the derivative in the direction of the ellipsoidal height *h*.

$$\begin{vmatrix} \Delta T = 0 & \text{in G (outside the geoid } \Gamma) \\ -\frac{\partial T}{\partial h} + \frac{1}{\gamma}\frac{\partial \gamma}{\partial h} T \Big|_{\Gamma} = \Delta g & \text{on } \Gamma \text{ (geoid)} \\ T \sim O(r^{-1}),\ r \to \infty \end{vmatrix}, \qquad (2.9)$$

where γ is the magnitude of the normal gravity vector, and $\frac{T}{\gamma} = N$ is the geoid height above the ellipsoid.

4b) Stokes' problem in spherical approximation on the sphere with radius R corresponds to $a=-1,\ b=\frac{1}{\gamma}\frac{\partial\gamma}{\partial h}=\frac{1}{\gamma}\frac{\partial\gamma}{\partial r}=-\frac{2}{R},\ g_1(x')=\Delta g$, $u \equiv T$, *and the boundary surface (the geoid* Γ*) is unknown.*

In spherical approximation the derivative along the height *h* above the sphere coincides with the radial derivative in the direction of the vector $\mathbf{r}=(x_1,x_2,x_3)$ to the data point on the geoid.

$$\begin{vmatrix} \Delta T = 0 & \text{in G (outside the geoid } \Gamma) \\ -\frac{\partial T}{\partial r}-\frac{2}{R}T\Big|_{\Gamma} = \Delta g & \text{on } \Gamma \text{ (geoid)} \\ T \sim O(r^{-1}),\ r\to\infty & \end{vmatrix}, \qquad (2.10)$$

where $\frac{\partial T}{\partial h}=\frac{\partial T}{\partial r}$, and $\frac{\partial\gamma}{\partial h}=\frac{\partial\gamma}{\partial r}=-\frac{2}{R}$. The solution of Eq. (2.10) is given by well known Stokes' integral which according to Blais and Provins (2002) is a spherical convolution and can be expressed in spherical harmonic series using Green's function approach. On the other hand, this solution can be represented by pseudo-differential operators and both spherical series representations are identical.

5a) Molodensky's problem in a general 3D linearized form (fundamental boundary condition) corresponds to $a=\boldsymbol{\gamma}^T\boldsymbol{M}^{-1},\ b=-1, g_1(x')=\boldsymbol{\gamma}^T\boldsymbol{M}^{-1}\boldsymbol{\Delta g}-\Delta W$, $u \equiv T$, *and the boundary surface (Earth's surface* Γ_E*) is unknown.*

The measurements are used on the Earth's surface as they are measured (besides tidal and atmospheric reductions). The Earth's surface itself is very rough and another surface is necessary as its approximation.

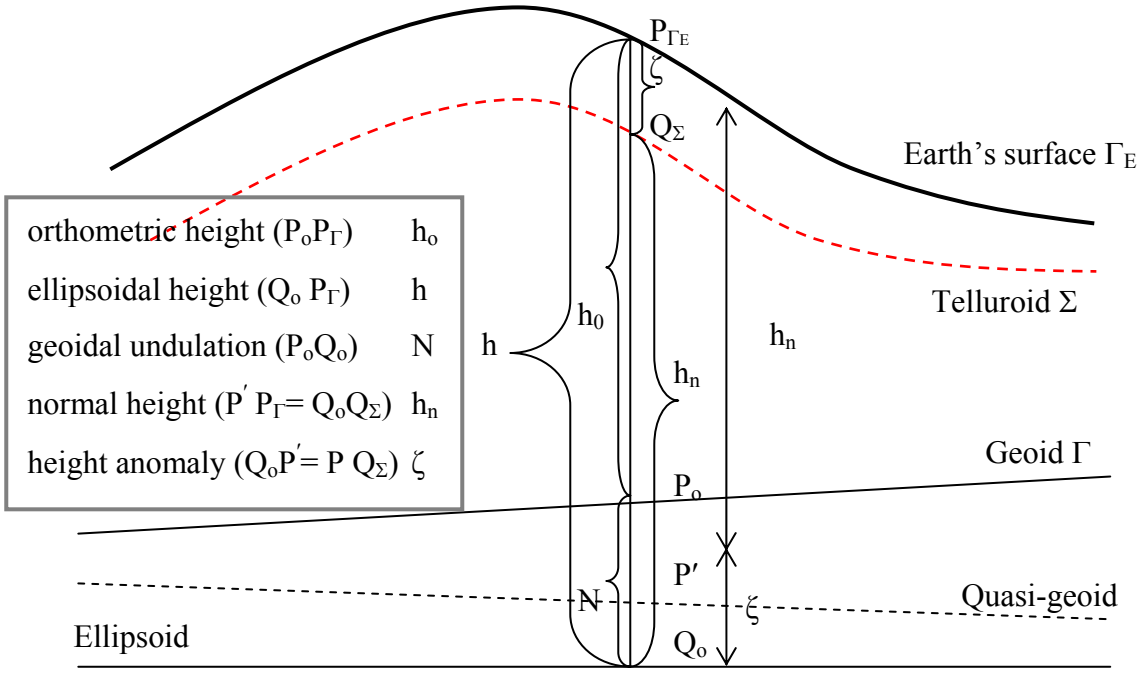

Figure 2.1: Geoid and quasigeoid

The normal gravity field is related to this surface called *telluroid,* see Fig. 2.1. By definition the telluroid is the surface close to the Earth's where the actual gravity potential W at point P_Γ on the real Earth's surface is equal to the normal potential U at the point Q_Σ on this surface Σ. For more precise representation it is valid $W(P_{\Gamma_E}) - W_0 = U(Q_\Sigma) - U_0$, where in general $W_0 - U_0$ is unknown. The height difference between points P_{Γ_E} and Q_Σ along the normal to the ellipsoid is called height anomaly ς and it is considered as the height of quasi-geoid above the reference ellipsoid. Because the telluroid is not equipotential the normal vector to this surface is different from the gravity vector. This is the reason the coefficient a and the boundary condition $g_1(x')$ to be represented as a matrix product. Let us assume following notations: $\boldsymbol{M}$ is the Hesse matrix of the normal potential, $\boldsymbol{\gamma}$ is the normal gravity vector, $\boldsymbol{\gamma}^T$ is its transpose vector, $\boldsymbol{\Delta g}$ is the vectorial gravity anomaly and ΔW (not the Laplace operator) is the potential anomaly between points Q_Σ and P_{Γ_E}. These have the following relationships

$$\Delta W = W_P - U_Q = T_P + U_P - U_Q$$
$$\boldsymbol{g}_P - \boldsymbol{\gamma}_Q = \boldsymbol{\Delta g} \quad . \tag{2.11}$$
$$\boldsymbol{M} = \left[\boldsymbol{M}_{ij}\right] = \left[\frac{\partial^2 U}{\partial x_i \partial x_j}\right] = \left[\frac{\partial \gamma_i}{\partial x_j}\right]$$

More natural representation for ΔW could be: $\Delta W = (W(P_{\Gamma_E}) - W_0) - (U(Q_\Sigma) - U_0)$. Now, the Molodensky problem in its fundamental form is

$$\begin{cases} \Delta T = 0 & \text{in G (outside the telluroid } \Sigma) \\ \boldsymbol{\gamma}^T \mathbf{M}^{-1} \text{grad } T - T\big|_{\Gamma_E} = \boldsymbol{\gamma}^T \mathbf{M}^{-1} \boldsymbol{\Delta g} \text{ -}\Delta\text{W} & \text{on } \Sigma \text{ (telluroid } \Sigma) \\ T \sim O(r^{-1}), \quad r \to \infty \end{cases}$$

5b) Molodensky's problem in spherical approximation (simple problem) corresponds to $a = -1, \quad b = -\frac{2}{r}, \; g_1(x') = \Delta g' - \frac{2}{r}\Delta W$ *, u ≡ T, and the boundary surface (Earth's surface* Γ_E*) is unknown.*

$$\begin{cases} \Delta T = 0 & \text{in G (outside the telluroid } \Sigma) \\ -\frac{\partial T}{\partial r} - \frac{2}{r} T\Big|_{\Gamma_E} = \Delta g' - \frac{2}{r}\Delta W & \text{on } \Sigma \text{ (telluroid)} \\ T \sim O(r^{-1}), \quad r \to \infty \end{cases} \tag{2.12}$$

where *r* is the length of the radius vector ***r*** from the coordinate origin to the measurement point; $\Delta g'$ is the gravity anomaly along the isozenithal direction (the line which links the points with the same normal direction). For a non-rotating sphere the isozenithal coincides with the radius vector. It can be assumed that $\Delta g \approx \Delta g'$ and $\Delta W = 0$ on the telluroid. The Molodensky's problem in spherical approximation with boundary conditions on the telluroid Σ is

$$\begin{cases} \Delta T = 0 & \text{in G (outside the telluroid } \Sigma) \\ \left(-\frac{\partial T}{\partial r} - \frac{2}{r} T \right)\Big|_{\Sigma} = \Delta g - \frac{2}{r} \Delta W_0 & \text{on } \Sigma \text{ (telluroid)} \end{cases} . \qquad (2.13)$$

The linear Molodensky problem corresponds to the oblique-derivative BVP defined previously. This form of the Molodensky problem can be compared to the classical Stokes problem. The difference is that gravity anomalies are on the telluroid instead of on the geoid and instead of the radius *R* of the sphere the length *r* of the radius vector is used. After downward continuation of the gravity anomalies from the telluroid to the geoid, the Molodensky problem is formally transformed to the classical Stokes BVP.

2.1.2.3 Geodetic boundary value problems - partially or completely known boundary surface

The GBVPs with unknown boundary surface are called free BVPs. New GBVPs arose after the Global Positioning System (GPS) and other techniques (satellite altimetry, airborne gravimetry, satellite gradiometry, new gravity missions) became available. The boundary surface can be completely or partially known. If GPS/leveling data are available the geoid can be considered as known (in the frame of the measurement accuracy and the resolution of the GPS/leveling points). The corresponding free GBVPs become fixed GBVPs.

Different GBVPs are discussed in Heck (1997) and Sansò (1995) with respect to the type of the boundary surface. Common BVPs are summarized in Table 2.1. The main criterion for this classification is whether the horizontal and vertical coordinates of the points on the boundary surface are known or unknown. The classical Molodensky GBVP is with completely unknown boundary surface and the scalar free Molodensky GBVP is with known geodetic latitude and longitude for every point. The first type of BVP, called vectorial free classical Molodensky BVP, has an important role from a theoretical point of view because it has a more general character. From the application point of view,

astronomical observations are necessary to solve this GBVP. This fact causes complications in the application of the classical Molodensky BVP.

Table 2.1: Classification of BVPs with respect to the type of boundary surface

BVPs	Boundary surface	Horizontal components	Vertical component
Dirichlet BVP	known (regular surface)	known	known
Neumann BVP	known (regular surface)	known	known
Robin BVP	known (regular surface)	known	known
Stokes GBVP	unknown (equipotential surface, geoid)	unknown	unknown
Molodensky BVP	unknown (Earth's surface)	unknown	unknown
Vector-free GBVP	unknown (Earth's surface)	unknown	unknown
Scalar-free GBVP	unknown (Earth's surface)	known	unknown
Fixed GBVP	known (geoid, Earth's surface)	known	known

AGBVPs are mixed type boundary value problems, where different BVPs are defined on the land and at sea parts of the boundary surface. Different combinations of the above discussed BVPs can be used in the definition of an AGBVP.

2.1.3 Mixed boundary value problems

Altimetry-gravimetry boundary value problems represent the class of mixed BVPs, where the boundary surface is broken in two parts – on land and at sea. The theory of mixed boundary value problems for elliptic differential equations in *n*-dimensional functional space of all rational functions has been developed in Eskin (1980). This theory, applied in $\mathbf{R}^3$ for the solution of the Laplace equation will be used to explain AGBVPs in a better way and to clarify the role of compatibility conditions along the coastline. This theory is

based on pseudo-differential operators (PDOs) in bounded domains (Eskin, 1980). More details are presented in the next chapter dedicated to the application of PDOs in the solutions of AGBVPs. To illustrate an AGBVP in a general way the following mixed BVP in a 3D domain $G \subset \mathrm{R}^3$ outside the Earth, with boundary surface Γ will be considered:

$$\begin{cases} \Delta u = 0 \\ u\big|_{\Gamma_1} = g_1(x') & \Gamma_1 \text{ ocean} \\ a\partial u/\partial n + bu\big|_{\Gamma_2} = g_2(x') & \Gamma_2 \text{ land} \\ u \sim O(r^{-1}), \ \ r \to \infty \end{cases} \tag{2.14}$$

In this formulation the smooth boundary surface Γ ($\overline{G} = G \cup \Gamma$, is the closure of G) is divided into two parts Γ_1 and Γ_2 and $\Gamma = \Gamma_1 \cup \Gamma_2$, $\gamma_c = \Gamma_1 \cap \Gamma_2$; γ_c is 1-dimensional line on the boundary surface. In case of an AGBVP, Γ_1 and Γ_2 are the ocean and land part of the Earth's surface and γ_c represents the coastline. The pair $x' = (x_1, x_2)$ represents the 2D coordinates on the boundary surface and x_3 is the third coordinate above or below the boundary surface. It is valid for $(x', x_3) \in G$. The notation $\partial u/\partial n\big|_{\Gamma_2}$ denotes the partial derivative along the normal to the boundary surface (normal derivative). The coefficients a and b in the second boundary condition are constants. In this example, the boundary conditions $g_1(x')$ and $g_2(x')$ are the measurements on the boundary surface. For an AGBVP they can represent the geoid heights from satellite altimetry at sea and gravity anomalies on land. To illustrate the AGBVPs as a mixed type BVP the Fig. 3.1 can be used, although it only presents the problem in a general way.

There are two main questions that must be asked concerning the solution of a mixed BVP - the first is the normal solvability of the BVP and the second one is the behavior of the solution in the neighborhood of γ_c, taking into account that the solution of a mixed problem is not smooth at the boundary γ_c. Both questions are closely inter-related. An example for arising the second question can be considered so called elliptic singular

integral equation (s.i.e.) (see Chapter 3) in $G \subset \mathbf{R}^3$. According to Eskin (1980), *whereas the ellipticity condition is the only necessary and sufficient condition for the normal solvability in the space of square integrable functions* $\mathbf{L}^2$*, on a manifold without boundary, additional normal solvability characteristics exist in the case of a s.i.e. on a bounded domain in* $\mathbf{R}^3$. Because the boundary surface for a mixed BVP consists of two different parts (two bounded domains Γ_1, $\Gamma_2 \subset \mathbf{R}^3$ related to the land and sea) and singularities expected across γ_c the question for existence of additional normal solvability characteristics need to be discussed (see Chapter 3). Depending on the value of that characteristic (every elliptic PDO in a bounded domain has such characteristic) different levels of regularity (smoothness) on the boundary surface and especially on the boundary γ_c can be expected. For mixed BVPs for an elliptic equation of order two (such as the Laplacian applied to the gravity potential) it is possible according to Eskin (1980) to select function spaces with weight factors vanishing on γ_c and to ensure the smoothness of the solution everywhere off γ_c. In this case the problem can become normally solvable. This fact can be considered as a starting point to investigate the application of wavelet filtering because of their very good space-scale (frequency) localizing properties. Restricting the wavelet coefficients on the coastline to zero (or certain limit) can insure a satisfactory level of regularity (smoothness) of the solution.

Introducing *compatibility conditions* (Svensson, 1988) to a mixed AGBVP can cause the problem to become normal solvable and at the same time it will increase the regularity of the solution (smoothness). Eskin (1980) has applied the theory of pseudo-differential operators (PDOs) to answer both questions for normal solvability of mixed BVPs and asymptotic behavior of the solution at γ_c. This theory will be presented in more details in the next chapter, focusing on their application for solutions of AGBVPs. Special attention will be paid to the representation of compatibility conditions in terms of PDOs and their abilities to provide a certain level of smoothness off the coastline.

2.2 Altimetry-gravimetry boundary value problems – mixed type BVPs

In general, AGBVPs appeared after satellite altimetry data became available. The definition of AGBVPs changed over time depending on the development of this new technology for height determination of the sea surface. In the very beginning only one type of AGBVP was known and it was synonymous to what is known as AGBVP I. The first discusion of AGBVP as a mixed BVP can be found in Arnold (1983, 1984), and Svensson (1983). In Svensson (1983a) we can find the following general definition of AGBVP.

Definition 2.1: *"The altimetry-gravimetry problem consists in combining the altimetry observations over the oceans with the gravimetric observations over the continents in order to estimate geoid height all over the Earth"*

2.2.1 Definitions of AGBVP I and AGBVP II

The following definition of the altimetry-gravimetry problem is given by Sansò (1981) and later was called AGBVP I. In a general way it can be presented below as:

$$
\begin{array}{ll}
\Delta W = 2\omega_E{}^2 & \text{in } G \text{ (outside the Earth's surface } \Gamma) \\
\left.\begin{array}{l} B_{1L}(x') = W_L \\ B_{2L}(x') = g_L \end{array}\right\} & \text{on } \Gamma_L \text{ (unknown land part of } \Gamma) \\
B_{1S}(x') = \bar{W} = const. & \text{at } \Gamma_S \text{ (known sea part of } \Gamma) \\
B_{2S}(x') = N_S = S_S(x') - SST(x') & \\
V = W - \frac{1}{2}\left|x \times \omega_E\right|^2 = O\left(\left|\mathbf{r}\right|^{-1}\right), & \text{at } \left|\mathbf{r}\right| \to \infty \\
\text{where} \quad V = W - \omega_E{}^2/2 & \text{is the gravitational potential;} \\
N_S(x'), SST(x') & \text{are the known geoid heights and} \\
 & \text{sea surface topography} \\
\bar{W}, S_S(x') & \text{are the gravity potential corresponding} \\
 & \text{to the geoid and the sea surface height}
\end{array}
\qquad (2.15)
$$

This definition supposes that the sea surface topography (SST) can be subtracted and thus geoid heights at sea are known. As the geoid is assumed to be an equipotential surface (after substracting the SST from the known sea surface) the gravity potential is equal to a constant. On land gravity and the gravity potential (using gravity data and leveling) are known. The AGBVP I at sea is a typical Dirichlet problem. In fact the AGBVP I consists of two parts: on land where the boundary surface is not known - and on sea - Dirichlet problem with known boundary surface.

The second form (later called AGBVP II) of altimetry-gravimetry problem has been presented first by Holota (1980). In a general way it has the form

$$
\begin{aligned}
&\Delta W = 2\omega_E{}^2 && \text{in } G \text{ (outside the Earth's surface } \Gamma) \\
&\left.\begin{aligned} B_{1L}(x') &= W_L \\ B_{2L}(x') &= g_L \end{aligned}\right\} && \text{on } \Gamma_L \text{ (unknown land part of } \Gamma) \\
&B_{1S}(x') = g_S. && \text{at } \Gamma_S \text{ (known sea part of } \Gamma) \\
&B_{2S} = N_S(x') = S_S(x') - SST(x') && \\
&V = W - \frac{1}{2}\left|x \times \omega_E\right|^2 = O\left(|\mathbf{r}|^{-1}\right), && \text{at } |\mathbf{r}| \to \infty
\end{aligned}
\qquad (2.16)
$$

where V is the gravitational potential;

$N_S(x'), S_S(x'), SST(x')$ are the known geoid height, sea surface height and sea surface topography

For both problems the classical definition of the telluroid cannot be used because the sea part of the boundary Γ is known and fixed, but on land the boundary surface is known up to a scalar (scalar free BVP). This will cause a broken type of Γ on the coast line.

2.2.1.1 Linearization of AGBVP I and AGBVP II

A general linearized form of both AGBVPs can be presented according to Lehmann (1999b) as:

$$
\begin{vmatrix}
\Delta T = 0 & \text{outside of } \Gamma \\
B_S(T) = g_S & \text{functional of the gravity potential at sea } \Gamma_S \\
B_L(T) = g_L & \text{functional of the gravity potential at sea } \Gamma_L \\
T = O(|\mathbf{r}|^{-2-n}), & |\mathbf{r}| \to \infty
\end{vmatrix} \tag{2.17}
$$

The regularity condition at infinity here means that the low-degree harmonics up to degree $n+1$ have been suppressed. After linearization the BVP becomes an oblique derivative BVP on land, but no other restrictions are necessary because the problem is not invariant under translation (as in the classical Molodensky problem). The reason for this situation is that on the sea part of the boundary surface the BVP is fixed (Sansò 1981).

2.2.1.2 Spherical approximation of AGBVP I and AGBVP II

The spherical approximation of AGBVP I and AGBVP II after Sansó (1993) will have the form

AGBVP I

$$
\begin{vmatrix}
\Delta T = 0 & \text{in } \Omega \text{ outside the sphere } \delta\Omega \\
T = \delta W_S + a, & \text{at sea part } \delta\Omega_S \text{ of the sphere} \\
N_S(\sigma) = S_S(\sigma) - SST(\sigma) & N_S(\sigma) \text{ is known} \\
-\frac{\partial T}{\partial r} - \frac{2}{R}T = \Delta g_L, & \text{on land part } \delta\Omega_L \text{ of the sphere} \\
\frac{1}{4\pi}\int T \, d\sigma = 0 & \text{over the sphere } \delta\Omega \\
T \sim O(r^{-1}), \;\; r \to \infty &
\end{vmatrix} \tag{2.18}
$$

AGBVP II

$$
\begin{vmatrix}
\Delta T = 0 & \text{in } \Omega \text{ outside the sphere } \delta\Omega \\
-\dfrac{\partial T}{\partial r} = \delta g_S + b, & \text{at sea part } \delta\Omega_S \text{ of the sphere} \\
N_S(\sigma) = S_{Ss}(\sigma) - SST(\sigma) & N(\sigma) \text{ is known} \\
-\dfrac{\partial T}{\partial r} - \dfrac{2}{R}T = \Delta g_L, & \text{on land part } \delta\Omega_L \text{ of the sphere} \\
\dfrac{1}{4\pi}\int T \, d\sigma = 0 & \text{over the sphere } \delta\Omega \\
T \sim O(r^{-1}), \;\; r \to \infty &
\end{vmatrix}
\tag{2.19}
$$

where σ represents a point on the sphere with spherical horizontal coordinates $(\varphi_\sigma, \lambda_\sigma)$. There are additional constants *a, b* for boundary conditions on land, which represent systematic differences between different types of data on land and at sea. These constants will be discussed later with respect to the higher level of regularity along the coastline.

2.2.2 Fixed AGBVP s

In Sansò (1993) a fixed AGBVP other than AGBVP I and AGBVP II was discussed and later it was called by Lehmann (1999b) as GBVP III. This type of BVP is possible because using GPS measurements the boundary surface on land becomes known and thus the AGBVP is a fixed BVP. Also, knowing geoid heights from GPS/leveling AGBVP II (which is scalar free on land) can be transformed to a scalar fixed AGBVP II. Table 2.2 shows the differences between the three AGBVPs from data coverage point of view as it is given in Lehmann (1999), where σ represents the horizontal coordinates in terms of spherical coordinates, $C = W_0 - W$ is the geopotential number and W_0 is the gravity potential on the geoid for a fundamental leveling reference point; *h* is the height above the sphere and *g* is the gravity. *AGBVPs I, II are scalar free-boundary problems on land and fixed BVPs at sea. AGBVP III is a fixed BVP both on land and sea.*

Table 2.2: Classification of AGBVPs with respect to the known and unknown parameters

AGBVPs	AGBVP I	AGBVP II	AGBVP III
Land			
Known	g,σ,C	g,σ,C	g,σ,h
Unknown	h	h	W
Sea			
Known	σ,h,C	$g\sigma,h$	σ,h,C
Unknown	g	W	g

2.3 Compatibility conditions along the coastline

The role of compatibility conditions for AGBVPs is quite complicated, guaranteeing the existence of the solution, smoothing the data (boundary conditions) at the boundary, and providing a higher level of regularization and smoothness of the solution. They are often used to guarantee the well-posedness of the problem (Sacerdote and Sansò, 1987; Svensson, 1988; Lehmann, 1999). The uniqueness and existence of the solution of AGBVPs depend upon the smoothness assumptions along the coastline.

Another use of compatibility conditions along the coastline is for the regularization of the solution in the neighbourhood of the coastline. According to Svensson (1988), unless the compatibility conditions are satisfied, the mixed problems cannot be solved with a higher degree of smoothness. Additional constraints on the data for the regularization of the solution along the coastline were derived in Sacerdote and Sansò (1987).

The addition of compatibility conditions may cause the problem to become well posed, but it is questionable whether these conditions upon the data are realistic for practical use. To answer this question, three preliminary numerical experiments have been conducted; see Chapter 6 or Grebenitcharsky and Sideris (2001a and 2002b), and Grebenitcharsky et al. (2001). The effect of data smoothing along the coastline on the final geoid solution (up

to 5 cm for a flat area and 30 cm for a mountainous coastline) is significant for cm-geoid determination. These preliminary numerical results were the starting point of a further theoretical investigation for finding solutions of AGBVPs, based on the combination of spherical harmonics, spherical pseudo-differential operators and spherical wavelets; see Chapter 5 or Grebenitcharsky and Sideris (2002a).

2.3.1 Effect of smoothness assumptions on the existence and uniqueness of the solution

The role of compatibility (smoothness) conditions for the existence and uniqueness of the solution of both AGBVP I and AGBVP II has been discussed in Svensson (1988). He showed that, in general, AGBVPs in their different forms do not have unique solutions and furthermore they do not have solutions unless a compatibility condition on the data is assumed at the coastline. For AGBVP I and AGBVP II (Sansò, 1993), it has been shown that with the introduction of additional compatibility conditions on the coastline, both problems become normal solvable (satisfying the Fredholm alternative). To achieve this, Svensson (1983b) introduced pseudo-differential operators. Using PDOs, it is possible not only to reformulate existing AGBVPs but to apply the compatibility conditions along the coastline. Together with new pseudo-differential operators *E, F, L* and *M*, the new form of AGBVP I and AGBVP II is possible. According to Eskin (1980; pp. 62) PDOs can be applied only on functions defined on the entire space $\delta\Omega$ on the sphere, but they can be applied on the parts $\delta\Omega_L$, $\delta\Omega_S$ only after extending the functions to the entire space $\delta\Omega$. In fact, *E, F, L* and *M* can be considered not only as extensions of function domains but also as extensions from one order of regularity, α*-2,* to another, α*,* for AGBVP II and from -*1/2* to *1/2* for AGBVP I, representing different types of boundary conditions. More details about those mappings will be given in Chapter 3 together with the background for PDOs theory.

Let $\mathbf{W}_k$ and $\overline{\mathbf{W}}_k$ are Sobolev spaces of k^{th} order and their closures. Sansò (1983) has proved that AGBVP II is normal solvable for $\delta g_S \in \mathbf{W}_{\alpha-1}$, $\Delta g_L \in \mathbf{W}_{\alpha-1}$, $1/2<\alpha<3/2$. In

addition, for $\alpha>3/2$, the Fredholm's alternative can be deduced if it is known in advance that on the coastline $-\frac{\partial T_S}{\partial r}-\frac{2}{R}T_S=\Delta g_L$, which will imply the condition

$$\Delta\left(\delta g_S-\frac{2}{R}T_S\right)=\Delta\left[\Delta g_L\right] \tag{2.20}$$

where Δ is Laplace-Beltrami operator. This condition, as it will be shown later, corresponds to the compatibility condition given by Svensson (1988). At the same time, uniqueness for the corresponding homogeneous problem is possible only for $T \in \mathbf{W}_\alpha$, $\alpha>3/2$, so no existence and uniqueness can be stated for the second problem (Sacerdote and Sansó, 1987). The non-uniqueness for AGBVP II has been proved by Svensson (1985) as well. To overcome this problem, it has to be modified by introducing an additional constant a to the boundary condition at sea (Sacerdote and Sansó, 1987); see Eq. (2.21) below as it will be discussed in the following section.

2.3.2 Compatibility conditions and the regularity of the data and the solution

As it has been mentioned in Svensson (1988), the mixed problems cannot be solved with a high degree of smoothness (comparing to the case when only datum problem is solved) unless the compatibility conditions are introduced. In addition, if a solution $T\in\mathbf{W}_\alpha$ is desired for large values of α, further compatibility (smoothness) conditions are needed. The regularization of the solution across the coastline has been studied by (Sacerdote and Sansò, 1987). According to their Theorem 5.1, higher level of regularity of the solution ($3/2<\alpha<5/2$) is possible, and the solution is unique if along the coastline the following condition is satisfied:

$$\delta g_S+b(\delta g_S,\Delta g_L)=\frac{2}{R}T(\delta g_S,\Delta g_L)+\Delta g_L \quad \text{along the coastline} \tag{2.21}$$

where $b(\delta g_S, \Delta g_L)$ is a constant which represents a systematic difference between data at sea and on land. It could be physically interpreted either, e.g., as orbital errors in the altimetry data or as datum inconsistence between the two sets of data. Assuming a sphere with radius R and $b(\delta g_S, \Delta g_L)=0$, which means that the systematic differences between land and sea data have been previously removed, the condition in Eq. (2.21) can be written as:

$$\delta g_S = \Delta g_L + 2\frac{T}{R} \tag{2.22}$$

where T depends on δg_S and Δg_L on land and at sea. *It will be shown later in Chapter 3 that the vertical datum condition Eq.(2.21) in the form of Eq.(2.22) is a part of the compatibility conditions corresponding to the requirement data on both sides of the coastline to be consistent.*

2.3.3 Compatibility conditions and the regularity of the weak (generalized) solution of AGBVPs

The variational method used for solving differential equations (Rektorys, 1977; Holota, 1997) provides so-called *weak* solutions. They can be considered as averaging in the neighborhood of the computational points. The weak solutions are based on base functions which are the eigenfunctions of the differential operator and correspond to the minimization of a certain functional. This method requires both the boundary surface and the boundary conditions (observations) to be smooth enough, i.e., to have continuous derivatives up to a certain order. This means they belong to the functional space $\mathbf{C}^{(2k)}$ (Rektorys, 1977), where k shows the order of generalized derivatives for the weak solution or the degree of regularity. In practice k (although $k\rightarrow\infty$) corresponds to the condition the boundary and boundary conditions being sufficiently smooth. Under such conditions, the weak (generalized) solution will be close enough to the classical (pointwise) solution for the given problem. The complete theory behind this statement can be found in Rektorys (1977, pp. 546-548). It has been shown that if the given data

(boundary conditions) are smooth enough, the weak solution is smooth enough, too, and as a result it can be considered as classical solution. In reality, however, irregularities exist on the coastline because different types of data with different observation procedures, accuracy and resolution are used. To overcome these problems, compatibility conditions along the coastline can be applied either in an explicit form or as a condition for coincidence of data and their higher order gradients along the coastline. The necessary background for the variational methods and the properties of the weak solution for the application of compatibility conditions will be given in Chapter 4.

2.3.4 Application of wavelet theory for imposing compatibility conditions along the coastline

The properties of wavelets which give not only the frequencies of a signal but also their spatial distribution in different scales can be used to detect discrepancies between different data along the coastline. A wavelet decomposition and reconstruction can be used to place compatibility (smoothness) conditions on the data and the boundary along the coastline. After the decomposition up to certain level, irregularities along the coastline in the high frequency part of the decomposition can be eliminated. This is equivalent to putting constraints on the n^{-th} derivatives (i.e., smoothness conditions used). Wavelet decomposition and reconstruction allow the restriction of the vertical, horizontal and diagonal coefficients up to certain level for every level of decomposition. The threshold value can be associated to a certain statistic of detail coefficients (for example the average or the RMS value). These constraints imply that additional smoothness conditions are implicitly used on the derivatives of the data. Restricting the detail coefficients on the coastline means that the horizontal gradients of the signal both on land and at sea are forced to be equal and to have as maximal values the threshold values for every level of decomposition. These restrictions are only for points which are very close to the coastline. The signal far from the coastal region remains unchanged. Using this procedure it can be expected that the irregularities along the coastline will be smoothed and this smoothing will affect only the coastal region. Detailed discussion for the application of wavelet theory in detecting irregularities and smoothing them is included in Chapter 5.

The main disadvantage of classical planar wavelets is the fact that they are not harmonic and they are not suitable to use as base functions to get solution for the harmonic disturbing potential. In order to be able to apply harmonic wavelet functions, new wavelet methods for approximating harmonic functions have been suggested in Freeden and Schreiner (1995). Applying spherical harmonic expansion (spherical Fourier transform) for the definition of pseudo-differential operators gives us the so-called spherical PDOs in the finite spherical domain. A complete description of the spherical PDOs and their application for imposing compatibility conditions together with spherical wavelets will be given in Chapter 5. The main advantages of PDOs will be discussed there including the following properties: after the transformation a BVP can become normal solvable or invertible because of the nature of the PDOs; both parts of a BVP - the differential equation and the boundary conditions can be written in one pseudo-differential equation; PDOs are uniformly regular and can be combined with local regular wavelets. In this case, the combination between spherical PDOs and spherical wavelets can help us overcome this problem. Spherical wavelets are a result of applying "rotation" and "dilation" operators. In the case of classical (planar) wavelets, the operators are "translation" and "dilation" of a mother wavelet. The combined solution consists of two parts: spherical harmonic expansion for low frequencies and wavelet transformation for the high frequency part of the disturbing potential and the observations. Having the spherical wavelet representation of every functional of the disturbing potential it is possible to apply the compatibility conditions in two different ways. The first method is to restrict the wavelet detail coefficients, which is equivalent to constraining the n^{th}-order horizontal gradients to coincide along the coastline. This approach will be presented later as a procedure for the numerical solution of AGBVP II. The second approach is to apply the compatibility conditions in an explicit form. The first method will be described in Chapter 5 and 6 as part of the numerical solutions with compatibility conditions. The explicit form of the compatibility conditions will also be given in Chapter 5.

2.4 Altimetry-gravimetry boundary value problems and compatibility (smoothness) conditions along the coastline

After presenting the theoretical background for altimetry-gravimetry boundary value problems and the role of the compatibility conditions in brief, the problems that need to be solved are stated as follows:

- *To find numerical solutions of altimetry-gravimetry boundary value problems using a combination of spherical PDOs, spherical harmonics, and spherical wavelets.*
- *To derive the compatibility conditions in an explicit form and to apply them as a conditions that data and their higher order derivatives coincide across the coastline.*
- *To investigate the effect of compatibility conditions at the coastline on the final geoid determination in terms of cm-geoid determination .*

Chapter 3

Compatibility conditions in terms of pseudo-differential operators – smoothness conditions for coincidence of data in coastal region

In this chapter the basic theory of PDOs will be briefly presented. PDOs are based on Sobolev spaces of generalized functions and their derivatives. A theoretical background about generalized functions will be provided as well. It is necessary because Sobolev spaces are considered as extensions of generalized functions with special spaces of periodic functions (Kirsch, 1996). The generalized derivatives allow us to define derivatives of a degree which is a real number. In this way, using different types of norms based on the degree of generalized functions (which is a real number) different types of data can be described. Also, different norms will have influence on the smoothness of the solution, especially when different types of data are used and discrepancies across the coastlines have to be smoothed. For example, the downward continuation can be represented as a lost of half degree of regularity and it will cause amplification of irregularities along the coastline. This background is necessary to clarify the uniform regularity (smoothness) of PDOs combined later with local regular wavelets. The role of factorization index representing the level of regularity will be discussed as well to show that the additional conditions along the coastline will increase the smoothness of the solution. Finally, the nature of compatibility conditions will be emphasized as conditions for coincidence of data and their gradients along the coastline.

3.1 Pseudo-differential operators – general aspects

The complete theory for the application of pseudo-differential operators to solutions of mixed boundary value problems for elliptic differential equations can be found in Eskin (1980). The definition of PDOs given in Eskin (1980) allows differential, integral and integro-differential operators to be presented as *slow growth* pseudo-differential

operators. The main advantage of PDOs is that they are invertible. After reformulation of a boundary value problem in terms of PDOs, it becomes normal solvable in the sense of generalized functions, because of the invertability of PDOs. According to Eskin (1980), for second order elliptic equations such as AGBVPs, it will be possible to select function spaces with a weight factor vanishing at the coastline, which will ensure the smoothness of solutions everywhere off the coastline, so that the AGBVP will be normal solvable. Also, not only normal solvability for an AGBVP can be achieved using PDOs; it could also be transformed into a generalized mixed boundary value problem with additional boundary conditions at the coastline.

The theoretical base of PDOs is the theory of generalized functions. This theory allows the solution of a problem to be found not only in the space of pointwise differentiable functions but also in a wider class of generalized functions based on infinitely differentiable test functions with compact support $\mathbf{C}_0^\infty(\mathbf{R}^n)$, whose members are distribution functions measurable in a Lebesgue sense (see the definition A.1 in the Appendix).

All integrals involved generalized functions are Lebesgue integrals which are defined uniquely up to sets of measure zero. In a Lebesgue sense, points or sets of points (lines in $\mathbf{R}^2$ or planes in $\mathbf{R}^3$) can be considered as having a zero measure, depending on the type of measure. The notation *almost everywhere* will be used instead of *with the exception of points with zero measure*. Generalized functions will produce a solution of a BVP almost everywhere, which means excluding the points on sets with a measure of zero. For AGBVPs with broken type boundary surface (sea and land parts of the boundary surface) and different types of data on land and at sea, generalized functions can be used for their solutions because discrepancies exist across the coastline. The coastline can be considered with *areal measure zero*, which will permit a *sufficiently smooth solution off* the coastline. A further extension of functional spaces of generalized functions are the Sobolev spaces, defined in terms of generalized functions whose Fourier transforms are locally integrable in a Lebesgue sense. Sobolev spaces contain not only generalized

functions but also generalized derivatives. Finally, PDOs are based on both generalized functions and Sobolev functional spaces and they will be discussed in more details in the following subsections.

Combining the foregoing theory with spherical harmonics and spherical wavelets, PDOs have been applied on the sphere by Freeden, Gervens and Schreiner (1998). Spherical PDOs will be discussed in more details in Chapter 5. Main operators such as Stokes' operator, integral operators of single layer potential and double layer potential used in gravity field modeling and some boundary conditions are presented in terms of PDOs in (Keller, 2003), and (Freeden, Gervens, and Schreiner, (1998), and (Freeden and Windheuser, 1997). Compatibility conditions along the coastline are implicitly expressed in terms of spherical PDOs (Svensson, 1988). It will be shown that they are equivalent to imposing conditions on data and their gradients to coincide with across the coastline; this clearly shows the relationships between compatibility conditions and smoothing data along the coastline. The compatibility conditions will be presented in an explicit way in Chapter 5.

3.1.1 Generalized functions in infinite domain

Following Eskin (1980), the background of generalized functions in $\mathbf{R}^3$ will be given; it is necessary for explaining PDOs and their role in solutions of mixed BVPs. Generalized functions will be defined after defining functions from the space $\mathbf{S} = \mathbf{S}(\mathbf{R}^3)$, which is the totality of all infinitely differentiable functions $v(x)$ in 3-dimensional space, $\mathbf{R}^3$, that together with all of their derivatives decrease more rapidly than any negative power of

$$\mathrm{r} = |x| = \sqrt{x_1^2 + x_2^2 + x_3^2} \to \infty . \tag{3.1}$$

Furthermore, the functional space **S** has the topology given by the norm

$$\left\|[v]\right\|_m = \max_x (1+|x|)^m \sum_{|k|\le m} \left| \frac{\partial^k \varphi(x)}{\partial x^k} \right|, \quad 0 \le m \le \infty \tag{3.2}$$

where the index k is a 3-tuple of non-negative integers, $|k| = k_1 + k_2 + k_3$ and

$$\frac{\partial^k \varphi(x)}{\partial x^k} = \frac{\partial^{k_1+k_2+k_3} \varphi(x)}{\partial x_1^{k_1} \partial x_2^{k_2} \partial x_3^{k_3}} \tag{3.3}$$

The convolution $v_1 * v_2$ of a pair of functions $v_1(x), v_2(x) \in \mathbf{S}$ is defined by

$$v_1 * v_2 = \int_{-\infty}^{+\infty} v_1(x-y) v_2(x) dy \tag{3.4}$$

Actually, the integral above in infinite domain represents a triple integral with respect to the 3D vectors x and y.

According to Eskin (1980) a lemma A.1 given in the Appendix justifies the application of functions of space **S** to obtain differentiable function even from a function with irregularities on sets of zero measure, such as the coastline in AGBVPs.

Using the lemma A.1 mentioned above, the solution of AGBVPs can be infinitely differentiable after convolving boundary data with base functions from the space **S** even if discrepancies exist across the coastline. This fact leads to generalized functions as a tool for solving AGBVPs and, together with the concept of generalized derivatives in Sobolev spaces, will constitute the base for the PDOs approach.

According to Rektorys (1977) a functional f is defined as a scalar product of two functions – *f(x)* and *v(x)* given in the form

$$(f, v) = \int_{-\infty}^{\infty} f(x) \bar{v}(x) dx \tag{3.5}$$

where $\bar{v}(x)$ is the complex conjugate function of $\bar{v}(x)$.

Definition 3.1: A functional *f* on *S* is said to be *semilinear* if

$$(f, \alpha_1 v_1 + \alpha_2 v_2) = \bar{\alpha}_1 (f, v_1) + \bar{\alpha}_2 (f, v_2) \tag{3.6}$$

for any $v_1, v_2 \in \mathbf{S}$ and complex numbers α_1, α_2 and *continuous* if

$$(f, v_n) \to (f, v) \tag{3.7}$$

for any convergent sequence $v_n(x) \to v(x)$ in **S**. Now, a continuous semilinear functional *f* on **S** will be called a *generalized function*.

The functions $v(x)$ belonging to **S** are called fundamental (base) functions. The space of generalized functions will be denoted by $\mathbf{S}' = \mathbf{S}'(\mathbf{R}^3)$. Suppose that $f(x)$ is a locally integrable function in the Lebesgue sense such that, for some *K>0*

$$\int_{-\infty}^{+\infty} |f(x)|(1+|x|)^{-K} dx < \infty \tag{3.8}$$

It can be shown that from $|(f, v) \le C[\![v]\!]_K$, the functional defined in Eq.(3.5) is continuous; in this discussion it will be called *regular functional*. The lemma A.2 provides the necessary condition for a semilinear functional to be a generalized function. The converse sufficient condition is also valid: if a semilinear functional satisfies (A.2), then it is continuous, or belongs to the space of generalized functions **S***'*.

A typical example of a generalized function is the delta function which in the traditional case, cannot be defined as a function

$$(\delta, v) = v(0), \quad \forall v \in \mathbf{S} \tag{3.9}$$

Definition 3.2 The derivative $\partial^k f / \partial x^k$ of a generalized function $f \in \mathbf{S}'$ is defined as a generalized function satisfying the relation

$$(\partial^k f / \partial x^k, v) = (-1)^{|k|}(f, \partial^k v / \partial x^k), \quad \forall v \in \mathbf{S} \tag{3.10}$$

Let $D^k = D_1^{k_1} D_2^{k_2} D_3^{k_3}$, where $D_r^{k_r} = \partial^{k_r} / \partial x^{k_r}$ and $1 \le r \le 3$,

Then Eq.(3.10) can be presented as

$$(D^k f, v) = (-1)^{|k|}(f, D^k v), \quad \forall v \in \mathbf{S}, \quad \forall k = (k_1, k_2, k_3) \tag{3.11}$$

It must be noted here that generalized functions have derivatives of all orders. This means that even functions with discontinuities can be approximated as a limit of infinitely smooth test functions. As an example let us consider a Heaviside (step) function $w(x)$ in 1D space with an argument x (Eskin, 1980).

Example 3.1 Suppose $w(x) = 1$ for $x>0$ and $w(x) = 0$ for $x<0$. Then $w(x)$ defines a regular functional on $\mathbf{S}(\mathbf{R}^1)$. The functional dw/dx will be given as

$$(dw/dx, v) = -(w, dv/dx) = -\int_0^\infty \frac{\overline{dv(x)}}{dx} dx = \overline{v(0)} \text{ or } dw/dx = \delta. \tag{3.12}$$

Furthermore, the k^{th} derivative of the delta function δ is defined as

$$(D^k \delta, \varphi) = \overline{D^k \varphi(0)}. \tag{3.13}$$

This example shows how a non-continuous (in the classical sense) function can be represented by a regular functional, which corresponds to a slowly increasing function. Furthermore, the classical step function has an infinite first derivative but the corresponding regular functional can have derivatives up to the k^{th} order.

This property of generalized functions makes them very useful in the formulation of PDOs, allowing the corresponding BVPs to become normal solvable and eliminating the singularities at certain points or lines of points (for example, along the coastline).

3.1.2. Generalized functions in a finite domain

The generalized functions considered in the previous subsection are defined in infinite domain covering the entire $\mathbf{R}^3$ space. Considering the application of PDOs for solutions of AGBVPs where different types of data are given on different parts of a boundary surface (or in other words on different domains) it is necessary to discuss generalized functions in finite domains. Also, the definition of *restriction* and *extension* operators in terms of generalized functions needs to be explained. This is necessary because, as will be seen later, PDOs must be applied on the entire $\mathbf{R}^3$ space, which means that the operators based on the generalized functions in a domain have to be preliminarily extended.

The theory for generalized functions in a domain will be presented, following Eskin (1980). The *support* of a continuous function $v(x)$ is the closure of the set of points at which $v(x) \neq 0$. Let $\mathbf{U}$ be an open domain in $\mathbf{R}^3$ that is generally unbounded and let $\mathbf{C}_0^\infty(\mathbf{U})$ be the space of all inifinitely differentiable functions with compact support in $\mathbf{U}$. The completion of $\mathbf{C}_0^\infty(\mathbf{U})$ in the topology of $\mathbf{S}(\mathbf{R}^3)$ will be denoted as $\mathbf{S}(\mathbf{U})$ and it is a closed subspace of $\mathbf{S}(\mathbf{R}^3)$.

Definition 3.3 A continuous semilinear functional on $\mathbf{S}(\mathbf{U})$ is a *generalized function in the domain* $\mathbf{U}$.

The space of generalized functions in a domain $\mathbf{U}$ will be denoted as $\mathbf{S}'(\mathbf{U})$. Let us assume a generalized function g as belonging to $\mathbf{S}'(\mathbf{R}^3)$.

Definition 3.4 A functional $g_0 \in \mathbf{S}'(\mathbf{U})$ is called *restriction* of g to $\mathbf{U}$ if $(g,v) = (g_0,v)$ for any $v \in \mathbf{S}(\mathbf{U})$. The restriction operator is denoted by $p : pg = g_0$

Downward continuation can be considered as an example of a restriction in physical geodesy. In this case the space $\mathbf{R}^3$ outside a certain boundary surface is restricted to this boundary surface, which can be considered as an $\mathbf{R}^2$ space.

Definition 3.5 Any continuous semilinear functional g_0 on $\mathbf{S}(\mathbf{U})$ can be extended although not uniquely to a continuous semilinear functional g (called *extension* of g_0) on $\mathbf{S}(\mathbf{R}^3)$. The extension operator is denoted as $l : g = lg_0$.

The upward harmonic continuation of disturbing potential ($\Delta T = 0$) from the boundary surface $\mathbf{R}^2$ to the space outside this boundary $\mathbf{R}^3$ can be considered as an example for extension in physical geodesy.

The support of a generalized function $g \in \mathbf{S}'(\mathbf{R}^3)$ is the complement of the largest open set $\mathbf{U}$ where the restriction of g to $\mathbf{U}$ vanishes (see Definition A.2).

The concept of restrictions and extensions of a generalized function can be applied in the formulation and the solution of AGBVPs. Assume that the extension of data on the land section of the boundary surface can be defined as zero values at the sea part and vice versa. The extension of data at the sea part will be defined as zeros on the land part of the boundary surface.

In Eskin (1980: 62, lemma 4.6) it has been shown that the type of extension does not have any influence on the solution of BVPs defined by PDOs; in general, the extension is not unique. The idea of extending land and sea data in AGBVPs will be discussed in Chapter 5 in terms of the explicit representation of compatibility conditions. The most suitable

type of function used by geophysicists (e.g. in ocean tide based on the extensions above is the so-called land-ocean function, described in Chapter 5 as well.

3.1.3. Sobolev spaces of generalized derivatives

Definition 3.6 By the Sobolev space $\mathbf{W}_\alpha(\mathbf{R}^3)$ is meant the space of those generalized functions *u* whose Fourier transform $\hat{u}(\xi)$ is locally integrable in the Lebesgue sense and such that

$$\|u\|_\alpha^2 = \int_{-\infty}^{\infty} |\hat{u}(\xi)|^2 \left(1+|\xi|\right)^{2\alpha} d\xi < \infty \tag{3.14}$$

where ξ is the frequency represented in $\mathbf{R}^n$

$\hat{u}(\xi)$ is the Fourier transform of *u*

α is the order of generalized derivatives, which can be not only integer but real number comparing to the integer order of generalized function k. As it can be seen later the degree of generalized functions is closely related to so-called Lipschitz regularity α, described in Chapter 4.

The Sobolev spaces $\mathbf{W}_\alpha(\mathbf{R}^3)$ are considered as an extension of generalized functions when the order of the derivatives *s* can be a real number, or when $\mathbf{W}_\alpha(\mathbf{R}^3)$ consists of all generalized derivatives. Introducing the generalized derivatives allows a more general interpretation of the regularity of a continuous semilinear functional. The order of regularity (the smoothness) can be expressed with a real number. For mixed BVPs like all AGBVPs with different types of data on both parts of the boundary surface, the level of regularity (smoothness) along the coastline can be described in a better way using generalized derivatives of Sobolev spaces.

For example, for AGBVP II the boundary conditions (observations) have to satisfy $\delta g_S \in \mathbf{W}_{\alpha-1}$, $\Delta g_L \in \mathbf{W}_{\alpha-1}$ where $1/2 < \alpha < 3/2$. Even more, to increase the regularity

additional conditions will increase α. Also, the downward continuation of data down to the boundary surface can be represented as decreasing the regularity with a half degree up to $\alpha - 1 - 1/2$. This is the reason why PDOs based on both spaces $\mathbf{S}'(\mathbf{R}^3)$ and $\mathbf{W}_\alpha(\mathbf{R}^3)$ can be applied to transform AGBVPs to normal solvable problems and to apply compatibility conditions along the coastline to increase the smoothness of the solution in a coastal area.

The space of Fourier transform of functions of $\mathbf{W}_\alpha = \mathbf{W}_\alpha(\mathbf{R}^3)$ is denoted by $\hat{\mathbf{W}}_\alpha = \hat{\mathbf{W}}_\alpha(\mathbf{R}^3)$. Eq.(3.14) defines the norm in $\mathbf{W}_\alpha$ and $\hat{\mathbf{W}}_\alpha$, together with a scalar product associated with it:

$$\langle u, v \rangle_\alpha = \int_{-\infty}^{\infty} \hat{u}(\xi)\overline{\hat{v}(\xi)}(1+|\xi|)^{2\alpha} d\xi \tag{3.15}$$

It can be shown that, for the functional $u \in \mathbf{W}_\alpha$, and $v \in \mathbf{S}$, the inner product can be expressed as

$$(u, v) = \frac{1}{(2\pi)^3} \int_{-\infty}^{\infty} \hat{u}(\xi)\overline{\hat{v}(\xi)} d\xi \tag{3.16}$$

A Sobolev space can be analyzed with respect to the value of α. Let us consider the following four cases:

Case 1: $\alpha = 0$.

Both $\mathbf{W}_0$ and $\hat{\mathbf{W}}_0$ are the spaces $\mathbf{L}^2(\mathbf{R}^3)$ of square integrable functions in the Lebesgue sense.

Case 2: $\alpha = m$, where m is a positive integer.

The norm Eq.(3.14) becomes, according to Eskin (1980),

$$\|u\|_m^{'2} = \sum_{|k|\le m} \int_{-\infty}^{\infty} \left|D^k u(x)\right|^2 dx = \sum_{|k|\le m} \frac{1}{(2\pi)^3} \int_{-\infty}^{\infty} \left|\xi^k \hat{u}(\xi)\right|^2 d\xi \tag{3.17}$$

where D^k is the partial derivative of order k, defined in Eq.(3.17), and the symbol prime denotes the type of the norm. *Thus* $\mathbf{W}_m(\mathbf{R}^3)$ *consists of those square integrable functions* $u(x)$ *whose generalized derivatives are also square integable functions for* $1 \le |k| \le m$.

Case 3: $\alpha = -m,$ where m is a positive integer.

It can be shown that

$$u = \sum_{|k|\le m} D^k v_k \tag{3.18}$$

where $v_k, \hat{v}_k \in \mathbf{L}^2(\mathbf{R}^3)$ and $\hat{v}(\xi) = (1+|\xi|)^{-m} \hat{u}(\xi)$

Thus the generalized functions in $\mathbf{W}_{-m}$ *are derivatives of order at most m of the functions which are in* $\mathbf{L}^2(\mathbf{R}^3)$.

Case 4: $\alpha = \lambda,\ \ 0 < \lambda < 1.$

This is the extension with respect to the space of generalized functions when the order of derivatives can be a non-integer value and the norm Eq.(3.15) becomes

$$\|u\|_\lambda^{'2} = \int_{-\infty}^{\infty}\int_{-\infty}^{\infty} \frac{\left|u(x+y)-u(x)\right|^2}{|y|^{3+2\lambda}} dxdy + \int_{-\infty}^{\infty} |u(x)|^2 dx \tag{3.19}$$

Case 5: $\alpha = m + \lambda,$ where m is a positive integer and $0 < \lambda < 1.$

This is a more general case and the norm Eq.(3.15) becomes

$$\|u\|_{m+\lambda}^2 = \|u\|_\lambda^{'2} = \sum_{|k|\le m} \int_{-\infty}^{\infty}\int_{-\infty}^{\infty} \frac{\left|D_x^k u(x+y) - D_x^k u(x)\right|^2}{|y|^{3+2\lambda}} dxdy + \int_{-\infty}^{\infty} |u(x)|^2 dx \tag{3.20}$$

Thus the space $\mathbf{W}_{m+\lambda}(\mathbf{R}^3)$ *can be defined as the completion of the space of infinitely differentiable functions with a compact support* $\mathbf{C}_0^{\infty}(\mathbf{R}^3)$.

The above five cases show that the functions from Sobolev spaces include generalized functions together with their generalized derivatives. It can be expected that a higher level of regularity (smoothness) can be achieved for the solution of AGBVPs using those functions even when irregularities along the coastline exist.

The following Sobolev's imbedding theorem justifies why Sobolev spaces are necessary in order to obtain differentiable solutions for AGBVPs of a certain order.

Theorem 3.1 (*Sobolev's imbedding theorem***).** Suppose $0 \le q < \alpha - 3/2$.
Then

$$\sum_{|k|=0}^{q} \max_{x \in \mathbf{R}^3} \left| D^k u(x) \right| \le C \left\| u \right\|_{\alpha}, \qquad \forall u(x) \in \mathbf{W}_{\alpha}(\mathbf{R}^3) \tag{3.21}$$

and hence $\mathbf{W}_{\alpha}(\mathbf{R}^3) \subset \mathbf{C}_0^{q}(\mathbf{R}^3)$.

This means that the sum of the maxima of the derivatives up to order *q* will always be restricted by the norm Eq.(3.14) in the topology of Sobolev spaces. *Or in other words it follows from this theorem that the functions in* $\mathbf{W}_{\alpha}(\mathbf{R}^3)$ *are sufficiently smooth if* α *is sufficiently large. In particular,* $u(x) \in \mathbf{C}^{\infty}(\mathbf{R}^3)$ *if* $u(x) \in \mathbf{W}_{\alpha}(\mathbf{R}^3)$ *for all* α. *To increase the smoothness along the coastline for AGBVPs, the order of generalized derivatives should be increased and additional compatibility conditions are necessary.*

By introducing Sobolev spaces, the restriction of a function to a plane can be described in terms of generalized functions. For this purpose let $x' = (x_1, x_2) \in \mathbf{R}^2$ and let $\left[v \right]_{\alpha}$ represent the norm in the space $\mathbf{W}_{\alpha}^{'} = \mathbf{W}_{\alpha}(\mathbf{R}^2)$ in the form

$$[v]_{\alpha}^{2} = \int_{-\infty}^{\infty} (1+|\xi'|)^{2\alpha} |\hat{v}(\xi')|^{2} \, d\xi' \tag{3.22}$$

In the following Theorem 3.2, the operator of the restriction is defined in terms of generalized derivatives belonging to Sobolev spaces.

Theorem 3.2 Suppose $\alpha > 1/2$. Then any function $u(x', x_3) \in \mathbf{W}_{\alpha}(\mathbf{R}^3)$ is a continuous function of $x_3 \in \mathbf{R}^1$ with values in $\mathbf{W}'_{\alpha-1/2} = \mathbf{W}_{\alpha-1/2}(\mathbf{R}^2)$, and the following relationship holds:

$$\max_{x_3 \in \mathbf{R}^1} [u(x', x_3)]_{s-1/2} \le C \|u\|_s, \quad \forall u \in W_s(\mathbf{R}^3), \tag{3.23}$$

so that the operator of the restriction to the plane $x_3 = const.$ is a bounded operator from $\mathbf{W}_{\alpha}(\mathbf{R}^3)$ into $\mathbf{W}_{\alpha-1/2}(\mathbf{R}^2)$.

In geodesy, taking into account this theorem the fact that a restriction operator such as downward continuation decreases the regularity in a half degree can be explained. *It can be expected that the smoothness will decrease going from a space outside a boundary surface to the surface itself. If the boundary surface is itself broken, the restriction of data to it will lead to less smoothness or amplification of the discrepancies. A possible situation for AGBVPs is with a mountainous coastline. After downward continuation of data on land to the boundary surface, the discrepancies along the coastline will be amplified in magnitude and the application of compatibility conditions across the coastline will have greater effect.*

3.1.4. Pseudo-differential operators in infinite domain

Pseudo-differential operators (PDOs) are defined as generalized functions acting on functions $u(x) \in \mathbf{S}(\mathbf{R}^3)$ and based on the space $\mathbf{S}_\alpha^0$ of measurable functions $A(\xi)$ satisfying

$$\left|A(\xi)\right| \le C(1+\left|\xi\right|)^\alpha . \tag{3.24}$$

The formula which defines a PDO A on $u \in \mathbf{S}(\mathbf{R}^3)$ is

$$Au = \frac{1}{(2\pi)^3} \int_{-\infty}^{\infty} A(\xi)\hat{u}(\xi)e^{-i(x,\xi)}d\xi , \tag{3.25}$$

The function $A(\xi)$ is called the *symbol* of A. Depending on the type of $A(\xi)$ two main types of PDOs can be considered which themselves can be split in different cases.

i) The PDOs symbol is an ordinary function

Case 1: (differential operator):

If the ordinary function $A(\xi)$ is a polynomial in ξ, i.e. $A(\xi) = \sum_{|k|\le m} a_k \xi^k$, then it can be shown that

$$Au = \frac{1}{(2\pi)^3} \int_{-\infty}^{\infty} \sum_{|k|\le m} a_k \xi^k \hat{u}(\xi)e^{-i(x,\xi)}d\xi = \sum_{|k|\le m} a_k D^k u(x) . \tag{3.26}$$

This means that A is a *differential* operator, and the class of PDOs contains the class of differential operators.

Case 2: (integral of convolution type)

When $\alpha < -3$ the symbol $A(\xi)$ is an absolutely integrable function and the inverse Fourier transform $a(x) = \mathbb{F}^{-1}A(\xi)$ is a bounded continuous function. The PDO *A* is an *integral operator of convolution type*

$$Au = \mathbb{F}^{-1}(A(\xi)\hat{u}(\xi)) = \int_{-\infty}^{\infty} a(x-y)u(y)dy \tag{3.27}$$

Case 3: (integro-differential operator)

When $\alpha > -3$, there exists a positive integer *m* such that $\alpha + 3 < 2m$. Then let A_1 be a new PDO with symbol

$$A_1(\xi) = \frac{A(\xi)}{(1+|\xi|\ )^{2m}} \tag{3.28}$$

Then $|A_1(\xi)| \le C(1+|\xi|)^{\alpha-2m}$ and A_1 is absolutely integrable such that $a_1 = \mathbb{F}^{-1}A_1(\xi)$. Finally, the PDO A is an integro-differential operator

$$Au = (-\Delta+1)^m \int_{-\infty}^{\infty} a_1(x-y)u(y)dy = \int_{-\infty}^{\infty} a_1(x-y)(-\Delta+1)^m u(y)dy \tag{3.29}$$

where $\Delta = \frac{\partial^2}{\partial x_1^2} + \frac{\partial^2}{\partial x_2^2} + \frac{\partial^2}{\partial x_3^2}$ is the Laplace operator. Now $A(\xi)u(\xi)$ satisfies

$$|A(\xi)u(\xi)| \le C_K(1+|\xi|)^K, \tag{3.30}$$

for any K, and the constant C_K depending on *K*, because $\hat{u}(\xi) \in \mathbf{S}(\mathbf{R}^3)$. In other words, the PDO $Au = \mathbb{F}^{-1}A(\xi)\hat{u}(\xi)$ is *a bounded infinitely differentiable operator* (Eskin, 1980).

For any value of α, the corresponding PDO can be considered as a pure differential, integral or integro-differential operator. In every case the product $A(\xi)\hat{u}(\xi)$ has bounded and continuous inverse Fourier transforms, which means that, for functions $\hat{u}(\xi) \in \mathbf{S}(\mathbf{R}^3)$ the corresponding PDO is normal solvable (invertible). This is one of the most important properties, and is one which makes them useful for the solution of mixed BVPs such as AGBVPs.

ii) The PDOs symbol is a generalized function

The existence of inverse Fourier transform in this case is guaranteed by the type of slow growth generalized functions (Hsu, 1984) used for applications. By choosing a generalized function $A(\xi) \in \mathbf{S}'(\mathbf{R}^3)$ it is possible to define a PDO A acting from $\mathbf{S}(\mathbf{R}^3)$ to $\mathbf{S}'(\mathbf{R}^3)$ and of the form

$$Au = \mathbb{F}^{-1}(A(\xi)\hat{u}) . \tag{3.31}$$

It can be shown that this PDO represents a convolution $Au = a * u$, where $a = \mathbb{F}^{-1}A(\xi) \in \mathbf{S}'(\mathbf{R}^3)$. As a consequence, the application of Au will lead to an differentiable function up to a certain order, making *PDOs ideally suited to solutions of AGBVPs, where discrepancies along the coastline exist. However, over and above this application , PDOs produce solutions that are smooth up to a certain order.* PDOs with *homogeneous* symbols $O^{\infty}_{\alpha+i\beta}$ play an important role in the application of PDO and are defined in the Definition A.3. The variables α and β are related to the degree of homogeneity.

The class of functions based on homogeneous symbols will be denoted as $O^{\infty}_{\alpha+i\beta}$. Two cases can be distinguished:

Case 1: when $-3 < \alpha < 0$, $A_0(\xi)$ defines a regular functional on $\mathbf{S}(\mathbf{R}^3)$;

Case 2: when $A_0(\xi) \in O^{\infty}_{\alpha+i\beta}$, $\alpha \leq$ -3, and $\alpha + i\beta + 3 \neq 0, -1, -2, \ldots\ldots$, $A_0(\xi)$ *does not define* a regular functional on $\mathbf{S}(\mathbf{R}^3)$.

Definition 3.7 By *homogeneous factorization* of an *elliptic* ($A(\xi) \neq 0, \forall \xi \neq 0$) homogeneous symbol with respect to the variable ξ_3 is meant a representation of

$$A(\xi', \xi_3) = A_-(\xi', \xi_3) A_+(\xi', \xi_3) \tag{3.32}$$

where $A_-(\xi', \xi_3)$ and $A_+(\xi', \xi_3)$ have the properties, given in the Appendix. The inverse of an elliptic homogenous symbol $A(\xi) \in O_{\alpha+i\beta}$ belongs to $A^{-1}(\xi) \in O_{-\alpha-i\beta}$. According to Theorem A.1 presented by Eskin (1980) every elliptic symbol admits a *unique* homogeneous factorization. Let us return to PDOs, to analyze how the parameter α affects the regularity of the functionals based on generalized functions used as symbols. The following cases deal with PDOs defined by symbols which are generalized functions induced by the homogeneous function $A_0(\xi)$:

Depending on α the following cases of PDOs with generalized functions as symbols are possible:

Case 1 (regular integral): In general if $\alpha > -3$, $A_0(\xi)$ defines a regular functional, which is analogous to the definition of a PDO, given by Eq.(3.25). This case can be split into two cases:

Case 1.1 (integral with weak singularity): $-3 < \alpha < 0$, $A_0(\xi)$ is an integral operator with a weak singularity

$$A_0 u = \int_{-\infty}^{\infty} a_0(x-y)u(y)dy \quad . \tag{3.33}$$

Case 1.2 (integro-differential operator): $\alpha > 0$, there exists a positive integer *m* such that $-1 \le \varepsilon = \alpha - m < 0$. In this case $A_0(\xi)$ can be presented as $A_0(\xi) = |\xi|^m B_0(\xi)$, where $B_0(\xi) \in O^{\infty}_{\gamma+i\beta}$. Now the function $A_0(\xi)$ can be presented as

$$A_0(\xi) = \sum_{k=1}^{3} P^k(\xi) B^k(\xi), \tag{3.34}$$

where $B^k(\xi) \in O^{\infty}_{\gamma+i\beta}$, $B^k(\xi)$ and $P^k(\xi)$ are homogeneous polynomials in ξ of degree $m = \alpha - \varepsilon$. As a consequence the PDO A_0 can be represented as an integro-differential operator

$$A_0 u = \sum_{k=1}^{3} \int_{-\infty}^{\infty} b_k(x-y) P_k(D_y) u(y) dy, \quad \forall u \in \mathbf{S}(\mathbf{R}^3), \tag{3.35}$$

where $b_k(x) = \mathbb{F}^{-1} B^k(\xi) \in O^{\infty}_{-\gamma-i\beta-3}$, $1 \le k < 3$. An analysis in Eskin (1980) shows that the functional $a_0 = \mathbb{F}^{-1} A_0(\xi) = \sum_{k=1}^{3} P^k(D) b_k$ is not regular for $\alpha \ge 0$ with singularity at the origin $\{0\}$. So, the restriction of the generalized function a_0 to the domain $\mathbf{R}^3 \setminus \{0\}$ will be a regular functional. In other words, *by using PDOs defined by generalized functions, it is possible to overcome existing singularities*.

Case 3 (singular integral): $\alpha = 0$, then $A_0(\xi)$ can be represented in the form of a *singular integral*, based on Theorem 3.3 proved in Eskin (1980).

Theorem 3.3 A PDO A_0 with symbol $A_0(\xi) \in O_0^\infty$ (see Definition A.3) can be represented in the form of a singular operator

$$A_0 = c_0 u(x) + p.v. \int_{-\infty}^{\infty} a_0(x-y)u(y)dy, \tag{3.36}$$

where c_0 is the average value of A_0 on the sphere $\partial\Omega$ and the *principal value (p.v.)* of the singular integral is presented as

$$p.v. \int_{-\infty}^{\infty} a_0(x-y)u(y)dy = \lim_{\varepsilon \to 0} \int_{|x-y|>\varepsilon} a_0(x-y)u(y)dy \tag{3.37}$$

or the singular integral Eq.(3.36) converges to its *Cauchy principal value*. Actually, the principal value exists if and only if the average of a_0 on the sphere $\partial\Omega$ is equal to zero or

$$\int_{\partial\Omega} a_0(\omega) d\sigma_\omega = 0, \tag{3.38}$$

where ω presents a point on the sphere, and $d\sigma_\omega$ the surface element on this sphere.

Case 4 (regular functional): When $\alpha \le -3$ an ordinary function $A_0(\xi) \in O_{\alpha+i\beta}^\infty$ itself does not define a regular functional on $\mathbf{S}(\mathbf{R}^3)$, but we can associate a generalized function $A_0 \in \mathbf{S}'$ as a symbol for the PDO A_0 and $\alpha + i\beta + 3 \neq 0, -1, \ldots$ Now, the corresponding PDO presents a regular functional given by $a_0(x) = \mathbb{F}^{-1} A_0$.

Finally, it is clear that different types of operators – differential, integral, integrodifferential, singular integral and even no regular functionals can be represented as PDOs; furthermore, such PDOs are invertible even when singularities exist on sets with measure zero. The application of PDOs for the formulation and solution of AGBVPs

will ensure uniqueness and a certain level of smoothness of the solution depending on the factorization index.

As shown above, α is part of the factorization index Eq.(3.35). The problem of regularity (smoothness) of a mixed BVP is very closely related to the value of the factorization index **k**. The next subsection will explain mixed BVPs of second order in a halfspace using PDOs defined in a finite domain.

3.2 Regularity of mixed boundary value problems of second order using PDOs in a halfspace

The primary task for this subsection is to explore how to apply PDOs on halfspaces to formulate mixed BVPs and to define the role of the factorization index for an elliptic equation of second order. Modifying an example for oblique derivative discontinuity given in Eskin (1980), it will be shown that the fixed AGBVP II (identical to AGBVP III) has a unique solution. The factorization index has influence on the smoothness of the solution of AGBVPs; to increase it across the coastline, additional conditions must be introduced.

3.2.1 Mixed boundary value problems of second order using PDOs in a halfspace

Let us consider an elliptic equation of second order with constant coefficients in the halfspace $\mathbf{R}^3_+$ defined by $x_3 \geq 0$ (the space above the plane $x_3 = 0,$ along with the plane itself)

$$L(D)u(x) = -\sum_{j,k=1}^{3} a_{jk} \frac{\partial^2 u(x)}{\partial x_j \partial x_k} = f(x), \text{ where } D = D^2 \tag{3.39}$$

where a_{jk} are real numbers such that $\sum_{j,k=1}^{3} a_{jk}\xi_j\xi_k > 0$ for $\xi = (\xi_1, \xi_2, \xi_3) \neq 0$ are real numbers. Let us give a graphical representation of the spaces $\mathbf{R}^3, \mathbf{R}^2, \mathbf{R}^2_+, \mathbf{R}^2_-$ and $\mathbf{R}^1$ and

associate them with the domain of the solution of an AGBVP, a boundary surface, different parts of boundary surface and the coastline.

Let $\mathbf{R}^2 \equiv \Gamma$ denote the 2-dimensional boundary plane defined by $x_3 = 0$, where $x = (x', x_3) \in \mathbf{R}^3$ and $x' = (x_1, x_2)$. Let $\mathbf{R}^2_+ \equiv \Gamma_1 \subset \mathbf{R}^2$ represent the 2-dimensional halfspace $x_2 > 0, x_3 = 0$ which is part of the boundary surface and $\mathbf{R}^2_- \equiv \Gamma_2 \subset \mathbf{R}^2$ represent the halfspace $x_2 < 0, x_3 = 0$ which is the second part of the boundary surface. Finally, the boundary between both spaces $\mathbf{R}^1 = \mathbf{R}^2_+ \cap \mathbf{R}^2_-$ $(\gamma_c = \Gamma_1 \cap \Gamma_2)$ and $\gamma_c \equiv x_1$ is the line representing the coastline in AGBVPs. To solve Eq.(3.39), mixed boundary conditions need to be imposed on the plane $x_3 = 0$, or one boundary condition must be assigned on $\mathbf{R}^2_+$ and another on $\mathbf{R}^2_-$ in a similar treatment as that applied to (2.14). Now the following general mixed BVP in a general case will be defined:

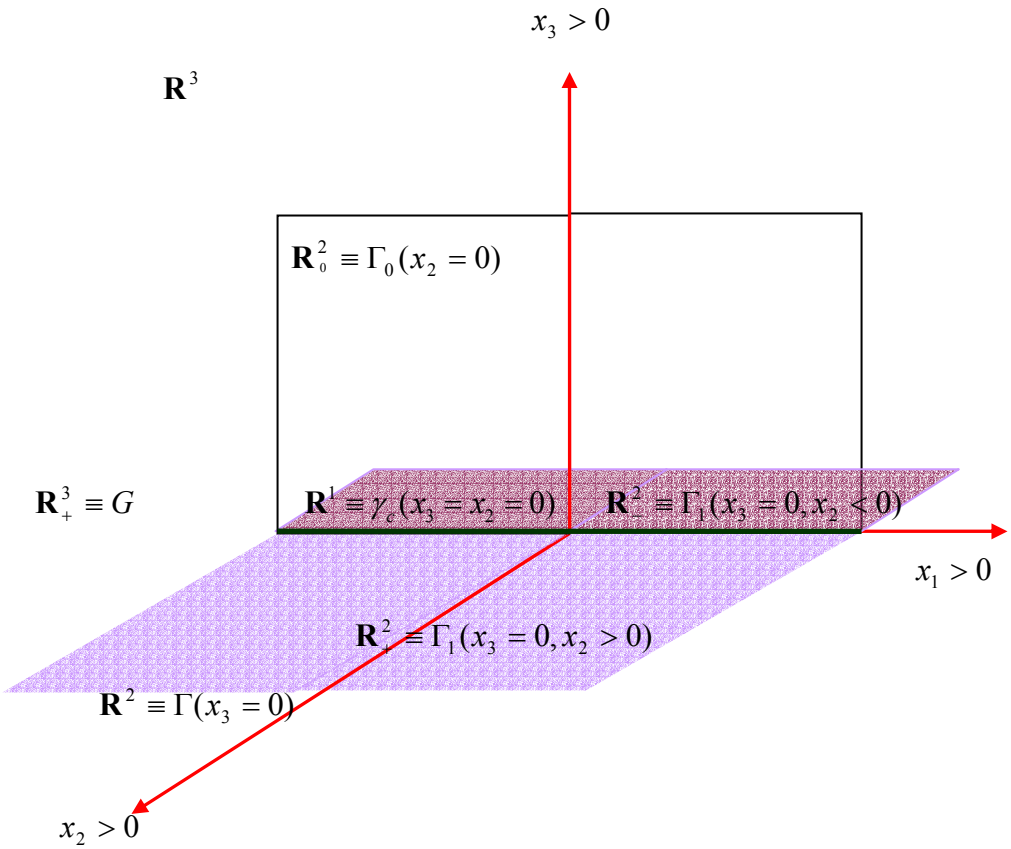

Figure 3.1: Representation of a mixed problem in 3D infinite space

$$\begin{cases} L(D)u(x) = f(x) \\ B_1(D)u(x)\big|_{\mathbf{R}^2_+ \equiv \Gamma_1} = g_1(x') \\ B_2(D)u(x)\big|_{\mathbf{R}^2_- \equiv \Gamma_2} = g_2(x') \end{cases}, \tag{3.40}$$

where $B_1(D)$ and $B_2(D)$ are homogeneous differential operators of orders m_1 and m_2 with constant coefficients. *For L(D) denoting the Laplacian, $f(x) = 0$, and $B_1(D)$ and $B_2(D)$ being the differential operators corresponding to gravity anomalies and gravity disturbances ($m_1 = m_2 = 1$), Eq.(3.40) will present AGBVP II.*

Let us assume $L(\xi_1, \xi_2, \xi_3)$, $B_i(\xi_1, \xi_2, \xi_3)$, $i = 1,2$ are the symbols of the differential operators $L(D)$, $B_i(D)$ and denote by $\widetilde{L}, \widetilde{B}_i$ PDOs with following symbols:

$$\begin{aligned} \widetilde{L}(\xi_1, \xi_2, \xi_3) &= L\left(\frac{\xi_1}{|\xi|} + 1, \xi_2, \xi_3\right) \\ \widetilde{B}_i(\xi_1, \xi_2, \xi_3) &= B_i\left(\frac{\xi_1}{|\xi|} + 1, \xi_2, \xi_3\right) \end{aligned} \tag{3.41}$$

They are differential operators only with respect to x_3, x_2 but not with respect to x_1. Now the problem Eq.(3.40) can be reformulated as

$$\begin{cases} \widetilde{L}(D)u(x) = f(x) \\ \widetilde{B}_1(D)u(x)\big|_{\mathbf{R}^2_+ \equiv \Gamma_1} = g_1(x') \\ \widetilde{B}_2(D)u(x)\big|_{\mathbf{R}^2_- \equiv \Gamma_2} = g_2(x') \end{cases} \tag{3.42}$$

It is mentioned in Eskin (1980) that even though $f(x), g_1(x')$ and $g_2(x')$ are infinitely differentiable, the solution of Eq.(3.42) generally has a *singularity* at $\gamma_c(x_3 = x_2 = 0)$ while being infinitely differentiable elsewhere. There are two ways to overcome this problem:

The first approach is to study the solution $u(x) \in \mathbf{W}_\alpha(\mathbf{R}^3_+)$ after multiplication by a weight factor that vanishes at $\gamma_c(x_3 = x_2 = 0)$. If α is sufficiently large, such functions are sufficiently smooth off the plane line $\gamma_c(x_3 = x_2 = 0)$. In general, boundary conditions defined by PDOs in terms of generalized functions have a global support covering the entire boundary plane. Even PDOs can be applied after the extension from $\mathbf{R}^2_+$ or $\mathbf{R}^2_-$ to $\mathbf{R}^2$. To localize the PDOs only on $\gamma_c(x_3 = x_2 = 0)$, *wavelets* can be applied because of their very good localizing properties not only in the frequency but also in the spatial domain. *The wavelet coefficients can be considered as vanishing at* $\gamma_c(x_3 = x_2 = 0)$.

The second way is to formulate a BVP with a *"jump"* condition (Eskin, 1980), on $\gamma_c(x_3 = x_2 = 0)$ of the type

$$B_{j1}(x, D)u_+ - B_{j2}(x, D)u_- = g_j(x') \tag{3.43}$$

The elliptic differential equation is given on the space $G \setminus \Gamma_0$ (see Figure 3.1) and the jump condition on Γ_0 where the plane Γ_0 has as a boundary the line γ_c. Also, $u_+(x)$ or $u_-(x)$ are the limits of the solution for $x \to \Gamma_0$ from one or the other side of Γ_0. In general, it is necessary to assign additional boundary conditions on γ_c. This approach has been applied in Svensson (1988) to reformulate AGBVPs and to apply compatibility conditions at the coastline. Again, wavelets can be useful to localize PDOs and to apply the conditions on γ_c. Wavelet theory will be discussed in the treatment of *frame theory* in Chapter 4, from an application point of view (depicting and smoothing of discrepancies in data along the coastline). The efficacy of this application stems from the fact that wavelets can be considered as multiscale differential operators.

In both cases, the regularity (smoothness) and the uniqueness of the solution depend on the factorization index; its effect on α will be discussed in the next subsection.

3.2.2 Regularity of mixed boundary value problems of second order using PDOs in a halfspace

The uniqueness and the regularity (smoothness) of the solution of a mixed BVP depends on the factorization index; it will be demonstrated through an example dealing with *oblique derivative discontinuity* given in Eskin (1980). This example will be adjusted to the case of AGBVP II with a known boundary surface on land. The elliptic differential equation given by Eq. (13.31) in Eskin (1980) presented here by Eq.(3.44) can be transformed to the Laplace's equation by assuming $z = 0$. Our starting point will be the Theorem A.2, valid for the case when $z = 0$. Notations necessary for this theorem can be found in the Appendix. *The Theorem A.2 shows the conditions for α related to the factorization index under which the mixed BVP Eq.(3.42) has a unique solution and can have a higher level of regularity (smoothness).*

Let us apply this theorem on the fixed AGBVP II to see the impact of the factorization index on the uniqueness of the solution and how it can be used to increase the regularity of the solution.

Let us consider the following second order elliptic equation to be solved in $\mathbf{R}^3_+$

$$-\frac{\partial^2 u}{\partial x_3^2}-\frac{\partial^2 u}{\partial x_2^2}+(L_1(D_1)+z)^2 u=0, \quad \text{for } x_3>0 \tag{3.44}$$

where $L_1(D_1)$ is a PDO with symbol $|\xi_1|$ and $z>0$. If $r=0$ then $\left(L_1(D_1)\right)^2=-\frac{\partial^2}{\partial x_1^2}$ and Laplace's equation is obtained in the space $\mathbf{R}^3_+$:

$$-\frac{\partial^2 u}{\partial x_3^2}-\frac{\partial^2 u}{\partial x_2^2}-\frac{\partial^2 u}{\partial x_1^2}=-\Delta u=0,\ \text{ for } x_3>0\,. \tag{3.45}$$

The general solution of Eq.(3.45) is a double-layer potential and to get a partial solution additional boundary conditions will be used on both parts of the boundary surface. As a result the BVP can be defined in the same way as in Eq.(3.40) assuming $f=0\in \mathbf{W}_{\alpha-2}(\mathbf{R}^3_+)$. Now, *the first operator* $B_1(D)$ represents the derivative along the vertical normal to the boundary surface. If the boundary surface is equipotential (geoid), $B_1(D)$ represents negative gravity disturbances on Γ_1, which is a first order differential equation ($m_1=1$); *the second first order operator* $B_2(D)$ represents gravity anomalies on the second part Γ_2 of the boundary surface, which again is a first order differential equation ($m_2=1$).

A new theorem is proved taking into account the Example13.3 given in Eskin (1980) for a mixed BVP with oblique derivative discontinuity having boundary conditions similar to gravity anomalies on the land and gravity disturbances at sea.

Theorem 3.4 *The mixed BVP with oblique derivative discontinuity corresponding to the AGBVP II with known boundary on land has a unique solution belonging to* $\mathbf{W}_{\alpha}(\mathbf{R}^3_+)$ *for any* $g_{1\equiv Sea}(x')\in \mathbf{W}_{\alpha-3/2}(\mathbf{R}^2_+)$ *and* $g_{2\equiv land}(x')\in \mathbf{W}_{\alpha-3/2}(\mathbf{R}^2_+)$.

The fact that the land and sea parts of the boundary surface are known means that the normal derivatives to the boundary can be computed almost everywhere excluding the singularity points with discontinuity along the coastline. Following the expressions for the symbols of geodetic PDOs given in Keller (2003) the PDOs presenting the boundary conditions in terms of their symbols will be given as:

$$\hat{B}_1(\xi)=a_1^{(1)}\xi_1+a_2^{(1)}\xi_2+a_3^{(1)}\xi_3=\left|\xi\right|/4\pi \tag{3.46}$$

where $\hat{B}_1(\xi)$ is the *the symbol of normal potential derivative*;

$$\hat{B}_2(\xi) = a_1^{(2)}\xi_1 + a_2^{(2)}\xi_2 + a_3^{(2)}\xi_3 = -|\xi|/4\pi \tag{3.47}$$

where $\hat{B}_2(\xi)$ is the *symbol of gravity anomalies.* Then the coefficients of both symbols will be equal to

$$a_k^{(1)} = \frac{\xi_k}{4\pi|\xi|},\ a_k^{(2)} = -\frac{\xi_k}{4\pi|\xi|}. \tag{3.48}$$

Following the example in Eskin (1980) it can be assumed that $a_3^{(1)} = a_3^{(2)} = 1$ to insure that $b_k(\xi') \neq 0,\ k = 1,2$. Then $\xi_3 = 4\pi|\xi|$ for gravity disturbances and $\xi_3 = -4\pi|\xi|$ for gravity anomalies. Now, for both cases

$$\xi_1^2 + \xi_2^2 = 0 \text{ or } \xi_1 = \xi_2 = 0 \Rightarrow a_1^{(1)} = a_1^{(2)} = a_2^{(1)} = a_2^{(2)} = 0 \tag{3.49}$$

Also, for the factorization index of $\tilde{b}_1\tilde{b}_2^{-1}$ it is valid

$$\mathbf{k} = \frac{1}{\pi}\arctan(a_2^{(2)}) - \frac{1}{\pi}\arctan(a_2^{(1)}) = 0 \tag{3.50}$$

Consequently, $\mathbf{k}_0 = \mathbf{k} + m_2 = 1$. Taking the inequalities from Theorem A.2

$$|\alpha - 1/2 - \mathrm{Re}\,\mathbf{k}_0| < 1/2 \text{ and } \quad \alpha > \max(m_1 + 1/2, m_2 + 1/2) \tag{3.51}$$

and assuming $k_0 = \mathrm{Re}\,\mathbf{k}_0$ Eq.(3.51) will have the form

$$k_0 < \alpha < k_0 + 1 \text{ and } \alpha > 3/2. \tag{3.52}$$

It is apparent that, for the fixed AGBVPs α always exists and satisfies Eq.(3.52). Following Theorem A.2, it can be concluded that AGBVP II with a known boundary on land will have a unique solution $u(x) \in \mathbf{W}_\alpha(\mathbf{R}^3_+)$ for any $g_{1\equiv Sea}(x') \in \mathbf{W}_{\alpha-3/2}(\mathbf{R}^2_+)$ and $g_{2\equiv land}(x') \in \mathbf{W}_{\alpha-3/2}(\mathbf{R}^2_+)$. *For AGBVP II, it means that when the boundary on land is known a unique solution exists satisfying the gravity anomalies on the land and gravity disturbances at sea. Furthermore, a higher level of regularity (smoothness) is possible by increasing* α *if additional compatibility (smoothness) conditions are introduced and* k_0 *is increased.* The existence and uniqueness of the solution of the fixed AGBVP II has been proven by Keller (1996) and Lehmann (1999b); but the current proof extends this work by taking advantage of PDO theory.

The *behavior* of the solution of a mixed BVP near the line $\gamma_c(x_3 = x_2 = 0)$ has been investigated in Eskin (1980) and the smoothness of the solution across γ has been expressed as d^{k_0} or $d^{k_0} \ln d$, where $d = \sqrt{x_3^2 + x_2^2}$ is the distance to the plane Γ_0, which has the boundary line $\gamma_c(x_3 = x_2 = 0)$. It is interesting to see that the smoothness will increase with the distance to the coastline and with the parameter $\mathbf{k}_0$. Finally, as a result of Theorem 3.4, *if the boundary conditions on land are transformed from gravity anomalies to gravity disturbances or vice versa at sea and, after that inverse, Hotine's or inverse Stokes' are applied, it will be certain that both methods represent the same unique solution. After such a transformation, the transformed boundary conditions will still belong to* $\mathbf{W}_\alpha(\mathbf{R}^2_+)$ *and* $\mathbf{W}_\alpha(\mathbf{R}^2_-)$.

Now, all known AGBVPs can be expressed by PDOs (Svensson, 1988) in terms of the compatibility conditions given in an implicit form. To increase the regularity (smoothness) of the solution (the order of generalized derivatives α) across the coastline, it will be enough to apply additional smoothness conditions. It will be shown in the next subsection that imposing compatibility conditions is equivalent to forcing data and their first and second degree gradients to coincide with each other across the coastline.

3.3 Compatibility conditions for AGBVPs in terms of PDOs as smoothness conditions for coincidence of data and their gradients across the coastline

Svensson (1983b) introduced for the first time the pseudo-differential operators to physical geodesy. He pointed out the main advantages of using PDOs, including the fact that all differential and integral formulae in physical geodesy can be expressed by PDOs. Following Keller (2003), representations of most-often used geodetic operators are given for the infinite case in Table 3.1 by their symbols.

$$\alpha_1 \hat{A}_1(\xi) + \alpha_2 \hat{A}_2(\xi) \quad \text{if} \quad \alpha_1 A_1 + \alpha_2 A_2 \tag{3.53a}$$

$$\hat{A}_1(\xi)\,\hat{A}_2(\xi) \quad \text{if} \quad A_1 A_2 \tag{3.53b}$$

$$1/\hat{A}_1(\xi) \quad \text{if} \quad A_1^{-1}\,, \tag{3.53c}$$

Table 3.1: Geodetic pseudo-differential operators

Geodetic operator	symbol
Upward continuation	$he^{-(\xi)}$
Normal derivative (negative gravity isturbance)	$\lvert\xi\rvert/4\pi$
Gravity anomaly	$-\lvert\xi\rvert/4\pi$
Stokes'	$1/2\pi\gamma\lvert\xi\rvert$

where *h* is the height above the boundary surface and γ is the normal gravity. Using the properties of symbols

the remaining geodetic operators can be easily expressed in terms of PDOs. The simplicity of PDO algebra is the other advantage pointed out by Svensson. Another very important characteristic of PDOs is that an ordinary BVP consisting of two parts – differential equation to be solved and boundary conditions given on the boundary surface – can be represented by only one equation. For example, Stokes' problem can be represented with only one pseudo-differential equation $Au = \Delta g$, where the symbol of A in the planar case is $\hat{A}(\xi) = -|\xi|/4\pi$ and it is based on the PDO corresponding to the Laplacian, which has the symbol $|\xi|^2$. For BVPs with irregularities across the coastline the combination with wavelets can produce operators with local smoothness assumptions. In physical geodesy most operators are applied on a sphere and this is the reason why Svensson (1983, 1988) has defined geodetic PDOs on a sphere with radius R. The combined application of spherical wavelets and spherical PDOs will be presented further in chapter 5.

3.3.1 AGBPVs and compatibility conditions along the coastline in terms of PDOs

After the reformulation of AGBVPs in terms of PDOs, it is possible to impose compatibility conditions expressed in PDOs as well. Compatibility conditions will increase the regularity of the solution and will help AGBVPs to become normal solvable. The main role in the formulation of PDOs on the sphere is related to the Laplace-Beltrami operator which, on a sphere with radius R has the form

$$\Delta_\sigma = R^{-2}(\partial^2/\partial\varphi_\sigma^{\,2} + \tan\varphi_\sigma \partial/\partial\varphi_\sigma + \cos^{-2}\varphi_\sigma \partial^2/\partial\lambda_\sigma^{\,2}), \tag{3.54}$$

where $\sigma=(\varphi_\sigma, \lambda_\sigma)$ are latitude and longitude of the point σ on the sphere. The Laplace-Beltrami operator itself is a PDO of order two. Let us define the following PDOs based on the Laplace-Beltrami operator on the sphere:

$$\begin{aligned} A &= [-\Delta_\sigma + 1/(4R^2)]^{1/2} - 3/(2R), \\ C &= [-\Delta_\sigma + 1/(4R^2)]^{1/2} + 3/(2R), \end{aligned} \tag{3.55}$$

$$AC = CA = -\Delta_\sigma - 2/R^2, \quad C = A + 3/R. \tag{3.56}$$

The following explanations of the fact that PDOs A and C are invertible can be found in (Freeden at al., 1998). PDOs contain Δ_σ which is not invertible for degree $n = 0$ because its symbol is 0. But, for unit sphere the symbol of $(-\Delta_\sigma + 1/4)$ is $(n + 1/2)^2$, which is different from zero for any integer degree including zero. In this case the inverse of both operators A and C.

It can be shown that the inverse spherical PDOs A^{-1}, C^{-1}, $(AC)^{-1}$, and different combinations of them, do exist and that they have certain physical meanings. For example, $S=A^{-1}$ is Stokes' operator and $(I-C)^{-1}$ is Hotine's operator. The operator C itself is the gradient operator. Taking into account that inverse PDOs exist, AGBVPs can be redefined, compatibility conditions can be established, and the solution can be found numerically. Let $u = T$ represent the disturbing potential, then (2.18) and (2.19) - assuming that systematic effects a, b have been previously removed together with the sea surface topography - can be expressed as

AGBVP I (problem (2.18) in terms of PDOs)

$$\begin{vmatrix} T = T_S, & \text{at the sea part } \delta\Omega_S \text{ of the sphere} \\ AT = \Delta g_L, & \text{on the land part } \delta\Omega_L \text{ of the sphere}, \\ SE\Delta g_L + SFCAT_S - T_S + T_1 = 0 & \text{at coastline } \delta\Omega_C \end{vmatrix} \tag{3.57}$$

where T_1 is the first degree harmonic and E, F are extensions from land and sea parts to the entire sphere $\delta\Omega$; and $\bar{\mathbf{W}}_{1/2}(\delta\Omega_S) \xrightarrow{F} \mathbf{W}_{1/2}(\delta\Omega)$, $\bar{\mathbf{W}}_{-1/2}(\delta\Omega_L) \xrightarrow{E} \mathbf{W}_{1/2}(\delta\Omega)$ are discussed before in terms of generalized functions. The third equation represents the compatibility condition. The problem becomes normal solvable and if $T \in \mathbf{W}_\alpha(\delta\Omega), T_S \in \bar{\mathbf{W}}_\alpha, \Delta g_L$ for $1 < \alpha < 2$ further compatibility conditions are necessary.

AGBVP II (problem (2.19) in terms of PDOs)

$$\begin{vmatrix} (A+2/R)(A+3/R)AT=(-\Delta_\sigma-2/R^2)\delta g_S, & \text{at the sea part } \partial\Omega_S \\ AT=\Delta g_L, & \text{on the land part } \partial\Omega_L \\ (A+2/R)SL\Delta g_L+(A+2/R)SM(-\Delta_\sigma-2/R^2)\delta g_S & \\ +(A+2/R)T_1=0, & \text{at coastline } \partial\Omega_C \end{vmatrix} \tag{3.58}$$

where L,M are extensions from land and sea part to the entire sphere and $\bar{\mathbf{W}}_\alpha(\partial\Omega_L)\xrightarrow{L}\mathbf{W}_\alpha(\partial\Omega)$, $\bar{\mathbf{W}}_{\alpha-2}(\partial\Omega_S)\xrightarrow{M}\mathbf{W}_\alpha(\partial\Omega)$. In both problems $\mathbf{W}_k$ and $\bar{\mathbf{W}}_k$ are Sobolev spaces of k^{th} order and their closures. The third equation represents the compatibility condition along the coastline. The problem becomes normal solvable and, if *s* increases, additional compatibility conditions are necessary to be applied.

Both mixed problems cannot be solved with a higher degree of smoothness unless the compatibility conditions are recognized at the coastline (Svensson, 1988). To understand the nature of compatibility conditions subsection 3.3.2 will show that compatibility conditions are equivalent to imposing conditions for coincidence of data and their gradients up to a certain order. Because AGBVP II is applicable for local and regional geoid determination some attention will be focused on it, assuming that for AGBVP I, the compatibility conditions will have the same role.

3.3.2 Compatibility conditions used as smoothness conditions for coincidence of data and their gradients along the coastline – spherical case

It will be proven that on the sphere the compatibility conditions (in spherical approximation) correspond to the following conditions:

$$\begin{vmatrix} \delta g_S=\Delta g_L+2T/R & \text{at coastline} \\ C\delta g_S=C\Delta g_L-4A^{-1}T/R^3 & \text{at coastline} \\ \Delta_\sigma\delta g_S=\Delta_\sigma\Delta g_L & \text{at coastline} \end{vmatrix} \tag{3.59}$$

It is interesting to mention that the first condition corresponds to

$$\delta g_S = \Delta g_L + 2\frac{T}{R}, \tag{3.60}$$

where T depends on δg_S and Δg_L, which is discussed in Chapter 2. The third condition can be derived from

$$\Delta_\sigma\left(\delta g_S - \frac{2}{R}T\right) = \Delta_\sigma \Delta g_L, \tag{3.61}$$

applied to data on land (right hand side) and at sea (left hand side). The second conditions can be derived from the first one by applying the PDO $AC = -\Delta_\sigma^2 - 2/R^2$.
Let us start with the second condition in the form

$$AC\delta g_S = AC\Delta g_L - 4T/R^3 \tag{3.62}$$

and assume that L and M are two complementary operators such that $L+M=P$, where the operator P could be simply interpreted as merging data on land and at sea. Then Eq.(3.62) can be modified in the following way by applying on both sides by $L=(P-M)$:

$$LAC\Delta g_L - 4LT/R^3 = (P-M)AC\delta g_S \tag{3.63}$$

After applying the operator $(A+2/R)S$ on both sides and some additional manipulations, and applying the identity operator I, it is obtained

$$(A+2/R)SLAC\Delta g_L - (A+2/R)S(P-M)AC\delta g_S = 4(A+2/R)SLT/R^3$$

$$(A+2/R)SL(AC-I+I)\Delta g_L - (A+2/R)S(P-M)AC\delta g_S = 4(A+2/R)SLT/R^3$$

$$(A+2/R)S\left[L(AC-I)\Delta g_L - PAC\delta g_S\right]+(A+2/R)SL\Delta g_L+(A+2/R)SMAC\delta g_S$$
$$=4(A+2/R)SLT/R^3$$

$$(A+2/R)S\left[-L\Delta g_L + LAC\Delta g_L - PAC\delta g_S\right]+(A+2/R)S\left[L\Delta g_L + MAC\delta g_S\right]$$
$$=4(A+2/R)SLT/R^3$$

From (3.66), it can be written that $LAC\Delta g_L = LAC\delta g_S + 4LT/R^3$. After substituting above,

$$(A+2/R)S\left[4LT/R^3 - L\Delta g_L + \left(LAC\delta g_S - PAC\delta g_S\right)\right]+$$
$$(A+2/R)S\left[L\Delta g_L + MAC\delta g_S\right]=4(A+2/R)SLT/R^3$$

But $\left(LAC\delta g_S - PAC\delta g_S\right)=(L-P)AC\delta g_S=-MAC\delta g_S$ and as a result

$$4(A+2/R)SLT/R^3+(A+2/R)S\left[-L\Delta g_L + MAC\delta g_S\right]+$$
$$(A+2/R)S\left[L\Delta g_L + MAC\delta g_S\right]=4(A+2/R)SLT/R^3$$

$$(I-I)[(A+2/R)SL\Delta g_L+(A+2/R)SMAC\delta g_S]=0$$

The expression in brackets can have an arbitrary value.

$$(A+2/R)SL\Delta g_L+(A+2/R)SMAC\delta g_S=-(A+2/R)T_1 \qquad (3.64)$$

where T_1 is the first degree spherical harmonic. As a final result, the compatibility condition along the coastline given by (3.58) is exactly obtained. It is *proven that the compatibility condition for AGBVP II Eq.(3.58) is equivalent to the conditions that the data and their first and second order gradients (Eq.(3.59)) should be consistent along the coastline.*

3.3.3 Compatibility conditions used as smoothness conditions for coincidence of data and their gradients along the coastline – planar case

The proof is similar in the planar case taking into account that the radius of the sphere $R \to \infty$. The following conditions related to the data and their gradients along the coastline are assumed:

$$\begin{vmatrix} \Delta g_L = \delta g_S & \text{at the coastline} \\ C\Delta g_L = C\delta g_S & \text{at the coastline} \\ \nabla^2(\Delta g_L) = \nabla^2(\delta g_S) & \text{at the coastline} \end{vmatrix} \tag{3.65}$$

where ∇ is the gradient operator. It is easy to see that ∇^2 is the Laplacian in 2D Euclidean space. Gravity disturbances at the coastline are considered equal to the gravity anomalies, which is possible of course if the sea surface topography is known with sufficient accuracy.

Now, it will be shown that conditions Eq.(3.65) are closely related to the condition at the coastline in Eq.(3.58) and that, in fact, the coastline condition Eq.(3.58) is satisfied under the assumption of Eq.(3.65) and $T_1=0$ for planar case. As usual, it is assumed that the first degree term T_1 is zero; i.e., the coordinate system is placed at the centre of the Earth. After extracting a certain type of geopotential model for the disturbing potential, the data residuals can be applied on a plane and then the first degree term can be assumed zero. Let the operator P is defined such as $P=L+M$, where the operators L,M and P have the same meaning as in the spherical case. All PDOs used in AGBVPs and defined on the sphere (Svensson, 1988) have their equivalent PDOs defined on the plane (Keller, 2003). To go from sphere to plane it can be assumed that $R \to \infty$ for the radius of the sphere. From equations (3.65) and (3.56) the following can be immediately obtained

$$AC\Delta g_L = AC\delta g_S \qquad \text{on the coastline}. \tag{3.66}$$

Under the assumption above the operator $A+2/R$ will become A. Applying the *L* (or *P-M*) and then the *AS=I* operator to both sides of Eq.(3.66),

$$LAC\Delta g_L = (P-M)AC\delta g_S \qquad \text{at the coastline}, \tag{3.67}$$

$$ASL(AC-I+I)\Delta g_L = AS(P-M)AC\delta g_S \quad \text{at the coastline} \tag{3.68}$$

or, equivalently,

$$AS\{L(AC-I)\Delta g_L - PAC\delta g_S\} + \{ASL\Delta g_L + ASMAC\delta g_S\} = 0. \tag{3.69}$$

Taking into account that at the coastline $LAC\Delta g_L = LAC\delta g_S$ the following condition is derived:

$$(I-I)\{ASL\Delta g_L + ASMAC\delta g_S\} = 0. \tag{3.70}$$

It is clear that the equation in brackets could have any value. Now, it can be assumed that

$$ASL\Delta g_L + ASMAC\delta g_S = 0. \tag{3.71}$$

Using Eq.(3.56) adapted to planar case it can be seen that the condition Eq.(3.71) is equal to the compatibility condition Eq.(3.58) given in a planar approximations. But, this is exactly the compatibility conditions in planar approximation along the coastline in Svensson's representation of the AGBVP II. Thus it makes sense to use conditions Eq.(3.65) for smoothing the data along the coastline.

3.4 Concluding remarks and summary

In this chapter, the background of PDO theory (after Eskin ,1980) has been presented for a better understanding of the application of PDOs for the formulation and solution of AGBVPs. Special attention has been paid to the application of generalized functions and

Sobolev spaces in the theory of PDOs and their contribution to the solution of mixed AGBVPs with irregularities at the coastline. It has been shown that, by using PDOs, the problems become normal solvable and the regularity (smoothness) of the solution increases. Also, the role of the factorization index and its relationship to the order of generalized derivatives has been discussed.

For the fixed AGBVP II (considered as identical to AGBVP III), it has been proven that there exists a unique solution and the proof is based on PDO theory. This proof can be considered as complementary to the proofs given in Keller (1996) and Lehmann (1999) and it shows how the factorization index can be used to increase the regularity of the solution. As a result, a higher order of smoothness can be achieved by increasing the order of the PDOs employed (generalized derivatives) and imposing additional conditions along the coastline.

It has been shown that compatibility conditions applied by Svensson (1988) for AGBVPs correspond to the conditions that the data and their first and second order gradients should coincide along the coastline. An even higher order of smoothness is possible if these conditions involve a higher order of gradients.

For the numerical application of the compatibility conditions, two options exist. The first one is to give them in an explicit form (see Chapter 5), and the second one is to improve the regularity of the data (and consequently the regularity of the solution as well) by imposing these conditions on the data, and their first and second order gradients (and even on higher order gradients). This can be done with the application of wavelets as multiscale differential operators (Mallat, 1998). Their application for detecting and smoothing irregularities along the coastline will be discussed in Chapter 4 .

Chapter 4

Wavelet frames as a generalization of base functions for detecting and smoothing discrepancies along the coastline in solutions of AGBVPs

The methods most often used for solving AGBVPs are the *variational* methods for solving differential equations. They are based on the minimization of a functional of base (test or fundamental) functions. In the geodetic context the base functions correspond to the eigenfunctions of the Laplacian differential operator. These base functions are linearly independent and orthogonal which, together with the minimization problem, lead to the uniqueness of the solution. *Frames* are generalizations of base functions and they accept dependent and non-orthogonal functions. As a result, the solution is not unique and can provide more flexibility, especially along the coastline. One of the main questions discussed in this chapter is the following: *what are the advantages of wavelet frames compared to the variational methods with base functions?* From the previous chapter, the application of PDOs is associated with infinitely smooth solutions based on data in the entire region of support. To obtain higher level of smoothness along the coastline (by using vanishing weight functions) and to localize the solution, PDOs can be combined with wavelets in terms of frames. The second question discussed in this chapter is this: *How can wavelets be used as multiscale differential operators to detect and smooth discrepancies along the coastline?* Once the role of wavelets as multiscale differential operators is analyzed, it is possible to apply them for imposing smoothness conditions. It is possible because of the conclusion in Chapter 3 that compatibility conditions are equivalent to the coincidence of data and their higher order gradients across the coastline. The application of smoothness conditions on boundary conditions (data) can be considered as a preprocessing step which leads to an improvement of the solution (becoming closer to the classical solution) and guaranteeing the necessary smoothness of the geoid along the coastline. Although the preprocessing character of smoothness

conditions they are a part of the computational procedure providing the numerical solution.

4.1 Variational methods and weak solution of a boundary value problem - general description

The transition from the unique weak solution given by variational methods to the solution in terms of spherical wavelets used as frames requires more details about the variational methods. Only a brief overview of the application of variational methods for solutions of AGBVPs will be presented here. The theory of variational methods will be presented as it is given in Rektorys (1977) for the one-dimensional case, assuming that it can be extended to 2D or 3D spaces.

4.1.1 Classical solution of a boundary value problem

The general formulation of a boundary value problem in 1D is

$$\begin{cases} Au = f \quad \text{in } G \equiv \mathbf{R}^1 \\ B(u) = g \text{ on } \Gamma \end{cases}, \tag{4.1}$$

where A is a differential operator of n^{th} -order; f is a continuous function with continuous n^{th} derivatives in the domain G; G is a bounded domain; and $B(u)$ is a functional representing the boundary conditions (measurements) on the boundary of Γ of G. The classical solution of a boundary value problem is a sufficiently smooth function satisfying the partial differential equation and the respective boundary conditions *pointwise* (Rektorys, 1977). This definition assumes that the classical solution u_0 belongs to the space D_A of all functions over which the differential operator A can be applied. *This means that all functions with irregularities are excluded*. All functions in D_A should be very smooth because, in the classical sense in terms of ordinary functions, the definition of derivatives is pointwise.

4.1.2 Generalized (weak) solution of a boundary value problem

Generalized derivatives belong to the Sobolev spaces defined in Definition 3.6. A similar interpretation of generalized derivatives can be found in Rektorys (1977). It is known that if $v(x)$ has continuous derivatives in G up to the m^{th} order, its classical derivative agrees with the generalized derivative. Also, generalized derivatives are uniquely determined up to a set of measure zero. Now it is possible to obtain a solution of a boundary value problem in terms of generalized derivatives which is called the *generalized* or *weak* solution. The weak solution does not need to have even derivatives of the order of the differential operator. For example for the Laplacian, it will be enough to have generalized derivatives of first order. The conditions related to the smoothness in the generalized sense are not so strict (the *weaker*) as the smoothness conditions in the classical sense. This is the reason why the generalized solution is called "*weak*", as well. The weak solution may be considered as an approximation of the classical solution. Very often, as in the case of altimetry-gravimetry boundary value problems, the classical solution is not possible in the usual integral form. The idea then is to find a weak solution which will be as close as possible to the classical solution.

4.1.3 Variational methods and the weak solution of a boundary value problem

Let a new scalar product for the boundary value problem Eq.(4.1) be defined in the form:

$$(u,v)_A = (Au,v), \quad \text{where } u \in \mathbf{D}_A \tag{4.2}$$

It is interesting to see how the new scalar product for a certain differential operator will look like.

Example 4.1. Let us consider the one dimensional space $\mathbf{L}^2(a,b)$ over the interval $[a,b]$ with inner product

$$(u,v)=\int_a^b u(x)v(x)dx \tag{4.3}$$

Let us apply Eq.(4.3) for a homogeneous BVP

$$\begin{vmatrix} Au=-u_{xx}=0 \\ u(a)=0,\ \ u(b)=0 \end{vmatrix} \tag{4.4}$$

For the new scalar product

$$(u,v)_A=(u_x,v_x) \tag{4.5}$$

where u_x and u_{xx} are the first and second derivatives respectively. It is clear that the new scalar product will contain not only the functions themselves but their derivatives as well. Now, introducing the new scalar product in the space $\mathbf{D}_A$ a new space $\mathbf{S}_A$ can be defined After the extension of $\mathbf{S}_A$ by additional elements, a new complete Hilbert space $\mathbf{H}_A$ will be defined by the inner product $(u,v)_A$, which is actually a completion of the space $\mathbf{D}_\mathrm{A}$.

Let us assume that instead of searching directly for the solution of the partial differential equation, there exist a function u_0 which minimizes the functional

$$Fu=(Au,u)-2(f,u), \qquad u\in \mathbf{D}_A \tag{4.6}$$

Under the assumption that the operator A is positive on the linear space $\mathbf{D}_A$ and if the equation $Au=f$ has a solution u_0, the functional Fu assumes in $\mathbf{D}_A$ its minimal value for u_0. The converse assertion is true as well. It is shown (Rektorys, 1977) that, if the functional is extended to the space $\mathbf{H}_A$, the minimum of the functional is uniquely determined. The idea of the weak solution in terms of variational methods can be formulated as: *to find the solution u_0 (minimizing the functional) of the boundary value problem not in the space*

$\mathbf{D}_A$ *(classical solution) but in the wider (with additional elements) space* $\mathbf{H}_A$. The question is h*ow to construct the additional elements of the space* $\mathbf{D}_A$?

Introducing a scalar product which is the sum of the scalar products of functions u and v together with the scalar product of all their derivatives up to k^{th} order, a new function space $\mathbf{W}_k$ will be constructed.

$$(u,v)_{W_k} = \sum_{i=0}^{k} \int_G u^{(i)}(x) v^{(i)}(x) dx \tag{4.7}$$

All functions from this space should have generalized derivatives up to the k^{th} order. It can be shown that $\mathbf{H} \subset \mathbf{H}_A \subset \mathbf{W}_k$. This means that the additional elements necessary to extend the space $\mathbf{D}_A$ will form a subspace of the space $\mathbf{W}_k$. The space $\mathbf{W}_k$ is the Sobolev space defined in Chapter 3 and it is an extension of Hilbert space $\mathbf{H}$. Actually $\mathbf{H}_A$ includes all functions with generalized derivatives up to the k^{th} order, and this space is generated by an inner product of type Eq.(4.7).

The main characteristic of *variational methods* is the minimization of the norm corresponding to Eq.(4.7) after representing the solution in series with respect to base functions. The base functions are usually assumed to be linearly independent and orthogonal. *The solution found by variational methods is unique because it is an linear optimization problem*. In general, according to Rektorys (1977), a weak (generalized) solution of the AGBVP exists and it consists of a functional u satisfying the stable boundary conditions (related to geoid heights N_S or disturbance potential T_S as measurements at sea) plus a "refinement" of u based on the unstable conditions (gravity disturbances δg_S at sea or gravity anomalies Δg_L on land as measurements). It is expected that the weak solution for Laplace's operator has generalized derivatives of all orders Rektorys (1977). The higher the degree of derivatives included in the compatibility conditions, the closer the weak solution is to the classical solution of the problem. According to Sacerdote and Sansò (1987), infinitely differentiable solutions can be

expected only for points that are far from the coastline (inner regularity). Additional constraints must be imposed on the data along the coastline. In this way, the irregularities between the data along the coastline need to be regularized by introducing compatibility conditions. Actually, smoothness conditions can be assumed for derivatives up to an infinite degree along the coastline.

Finally, the conclusion given in Rektorys (1977) that "if all data of the considered problem (including the boundary surface) are sufficiently smooth, then the weak solution is the classical solution of the considered problem" is the underlying reason for investigating the smoothing procedure along the coastline for AGBVPs. From this point of view, the transition from variational methods with base functions to wavelet frames needs to be discussed.

4.2 The transition from base functions and variational methods to wavelet frames for solutions of AGBVPs

Once, having a weak solution produced by variational methods (using wavelets as base functions, which will correspond to exact decomposition and reconstruction), the wavelet coefficients could be restricted along the coastline using the frame theory. In this way, smoothing of data or applying compatibility conditions in a coastal region become possible. To describe the application of variational methods to AGBVPs, the general formulation (2.17) given by Lehmann (1999) can be used. The fixed AGBVP II will be discussed, which means that the boundary surface on land and at sea will be treated as known. Assuming that there is no systematic effect or that it has been previously removed together with the known SST, Eq.(2.19) becomes Eq.(4.8).

$$\begin{cases} \Delta T = 0 & \text{in } \Omega \text{ outside the sphere } \delta\Omega \\ -\dfrac{\partial T}{\partial r} = \delta g_S, & \text{at the sea part } \delta\Omega_S \text{ of the sphere} \\ -\dfrac{\partial T}{\partial\, r} - \dfrac{2}{R}T = \Delta g_L, & \text{on the land part } \delta\Omega_L \text{ of the sphere} \\ \text{with geoid heights } N_S \text{ and } N_L \text{ known on land and sea.} \end{cases} \tag{4.8}$$

If a bilinear form Eq.(4.9) similar to the one in Holota (1983), Keller (1996) and Holota (2000) is introduced, the following is valid

$$((T,v))_B = B(T,v) = (\Delta T, v) + g(T,v)\,, \tag{4.9}$$

which contains not only the inner product $(\Delta T, v)$ related to the differential operator, but the inner product $g(T,v)$ of boundary conditions as well. The problem above could be presented as a *variational equation* in the form

$$B(T,v) = \int_{\delta\Omega} g v d\sigma = \int_{\delta\Omega_S} g(\delta g_S, \Delta g_L) v d\sigma + \int_{\delta\Omega_L} g(\delta g_S, \Delta g_L) v d\sigma\,, \tag{4.10}$$

where the function g is tied to the boundary conditions (data). For example, for AGBVPII, $g=g(\delta g_S, \Delta g_L)$; v are base (test) functions which belong to the Sobolev weighted space $\mathbf{W}_1$ defined in Chapter 3; $d\sigma$ is the surface element on the sphere, and $\sigma = \eta(\eta_1, \eta_2, \eta_3)$ represents a point on the sphere. The variational equation is the result of minimizing the functional

$$F(T) = \big((T,T)\big)_B - 2(f,T) = B(T,v), \text{ where } T \in \mathbf{W}_1\,, \tag{4.11}$$

and assuming $f = 0$, because Laplace equation is homogeneous.

The space $\mathbf{W}_1$ is a space of functions that are square integrable on the sphere $\delta\Omega$ under the weight $|\eta|^{-2}$ and which have first derivatives in a generalized sense. It is equipped with the inner product

$$(T,v)_{\mathbf{W}_1} = \int_{\delta\Omega} \frac{Tv}{|\eta|^2} d\sigma + \sum_{i=1}^{3} \int_{\delta\Omega} \frac{\partial T}{\partial \eta_i} \frac{\partial v}{\partial \eta_i} d\sigma . \tag{4.12}$$

Now, instead of looking for a solution of problem Eq.(4.8) satisfying the differential equation and boundary conditions pointwise in the classical sense, a weak (generalized) solution in space $\mathbf{W}_1$ based on a certain type of base function can be found. If T is represented as a series with respect to a certain type of base functions, the solution for T can be given as

$$T(\eta) = \sum_{j=0}^{n} c_j^{(n)} v_j(\eta), \tag{4.13}$$

where $\eta \in \Omega \cup \delta\Omega$, and $c_j^{(n)}$ are numerical coefficients. The coefficients can be found as a solution of the Galerkin system

$$\sum_{j=0}^{n} c_j^{(n)} B(v_j, v_k) = \int_{\delta\Omega} v_k g d\sigma, \quad k = 0...., n . \tag{4.14}$$

The weak solution will minimize the functional Eq.(4.11) and will be a solution to the variational equation Eq.(4.10). *The set of coefficients is unique because of the linear optimization problem in terms of eigenfunctions which are orthogonal.*

To apply wavelets, frame theory needs to be introduced in brief as a generalization of base functions (Christensen, 2001; Mallat, 1998). Instead of base functions v_n, wavelets ψ_n are used as frames.

Definition 4.1: A family of elements $\{v_n\} \subseteq \mathbf{H}$ (where $\mathbf{H}$ is a separable Hilbert space) is called a frame for $\mathbf{H}$ if there exist constants $P,Q>0$ such that

$$P\|g\|^2 \le \sum |(g, v_n)|^2 \le Q\|g\|^2, \quad g \in \mathbf{H}, \tag{4.15}$$

where P,Q are called frame bounds, $\{v_n\}$ is a family of wavelets; and g is tied to the boundary conditions (data).

The frame bounds *are not unique* and the wavelet coefficients in this case are not unique either. The optimal frame bounds are the biggest possible value for P and the smallest possible value for Q. If $P=Q$, the frame is called *tight* and when $P=Q=1$ the basis become orthonormal. Since the orthonormal basis condition is very strong, it would be difficult to find a basis that satisfies additional conditions such as the compatibility conditions at the coastline. From a mathematical point of view, the lack of uniqueness is not desirable but the wavelet frames could provide more flexibility in the application of compatibility conditions at the coastline. The frame definition allows changes in wavelet coefficients along the coastline, which is equivalent to imposing smoothness conditions. More details about wavelet frames are presented in subsection 4.3 after Mallat (1998). The application of spherical pseudo-differential operators and spherical wavelets for compatibility (smoothness) conditions is discussed in Chapter 5.

4.3 Pointwise regularity of wavelet frames - detecting and smoothing singularities and edges

4.3.1 Non-uniqueness of frame coefficients and non-uniqueness of frame reconstruction

The advantage of frames relative to bases is that the set of coefficients can be changed which is useful for irregular sampling such as wavelet decomposition on the sphere or

reconstruction of a signal after suppressing some coefficients up to a certain value, which can result in a smoothness effect. If the frame condition Eq.(4.15) is satisfied, the operator

$$Ug = \left(g, v_n\right) \tag{4.16}$$

is called a frame operator. The condition Eq.(4.15) guarantees that the frame operator is invertible and has a bounded inverse. A frame defines a complete and stable signal representation but it may be *redundant*. This redundancy can be measured by the frame bounds. If $\{v_n\}$ are linearly independent, then $P \le 1 \le Q$; but if $P > 1$, then the frame is redundant. For a non-orthogonal wavelet frame or spherical wavelets with irregular sampling on the sphere redundancy appears (that is the set of coefficients is not unique), which means that the inverse frame operator is not unique. To define the inverse frame operator the *left pseudo-inverse* operator has to be defined as

$$\tilde{U}^{-1} = \left(U^* U\right)^{-1} U^*, \tag{4.17}$$

where U^* denotes the adjoint operator of U such that $\left(Ug, y\right) = \left(g, U^* y\right)$. The pseudo-inverse of a frame operator is related to the so-called *dual frame family* (with oversymbol '~') and it is used for reconstructing the signal from its frame coefficients. Theorem 4.1 given in Mallat (1998) justifies the application of dual frames.

Theorem 4.1 Suppose that $\{v_n\}$ is a frame with frame bounds *P* and *Q*. Let $\tilde{v}_n = \left(U^* U\right)^{-1} v_n$. For any $g \in \mathbf{H}$,

$$\frac{1}{Q}\|g\|^2 \le \sum_n \left|\left(g, \tilde{v}_n\right)\right|^2 \le \frac{1}{P}\|g\|^2 \tag{4.18}$$

and

$$g = \tilde{U}^{-1}Ug = \sum_n (g, v_n)\tilde{v}_n = \sum_n (g, \tilde{v}_n)v_n \tag{4.19}$$

If the frame is tight (i.e., $P = Q$), then $\tilde{v}_n = \frac{1}{P}v_n$.

If frame vectors are linearly independent, the frame is called the *Ritz basis* and its dual frame consists of linearly independent vectors as well. These types of frames are called *bi-orthogonal* frames. Ritz bases represent such kinds of frames and, if they are normalized, then $P \le 1 \le Q$. It can be seen that the assumption $P = Q = 1$ transforms a frame into an orthonormal basis which leads to uniqueness of decomposition and reconstruction of the signal; or, in other words, the frames can be considered as a generalization of the orthonormal base function approach. *The ability to vary the scalar product of signal and frames (frame coefficients) in certain boundaries allows us to change the frame coefficients, which is the key point in using wavelet frames to impose smoothness conditions at points where singularities or edges exist.* This aspect of wavelet frames will help us to overcome the restriction of orthonormal base functions in variational methods coming from the uniqueness of coefficients along the coastline for AGBVPs. Now the application of wavelet frames as compatibility (smoothness) conditions can be admitted and justified from a theoretical prospective point of view.

4.3.2 Wavelet frames – general aspects

Wavelet frames are constructed by sampling the time and scale of a continuous wavelet transform defined by

$$\mathrm{Wg}(x,s) = \left(g, \psi_{x,s}\right), \tag{4.20}$$

where

$$\psi_{x,s}(y) = \frac{1}{\sqrt{s}}\psi\left(\frac{y-x}{s}\right) \tag{4.21}$$

is shifted in time and dilated in scale version of the mother wavelet ψ. To construct a wavelet frame the time-frequency plane needs to be covered with "boxes". The scale s is sampled with an exponential sequence $\{a^j\}$ with dilation step a. The time is sampled uniformly at intervals that are proportional to the scale $s = a^j$. The discrete version of a frame is given as

$$\psi_{j,n}(y) = \frac{1}{\sqrt{a^j}}\psi\left(\frac{y-nxa^j}{a^j}\right) \tag{4.22}$$

Graphically, the boxes can be presented in Figure 4.1, see Mallat (1998).

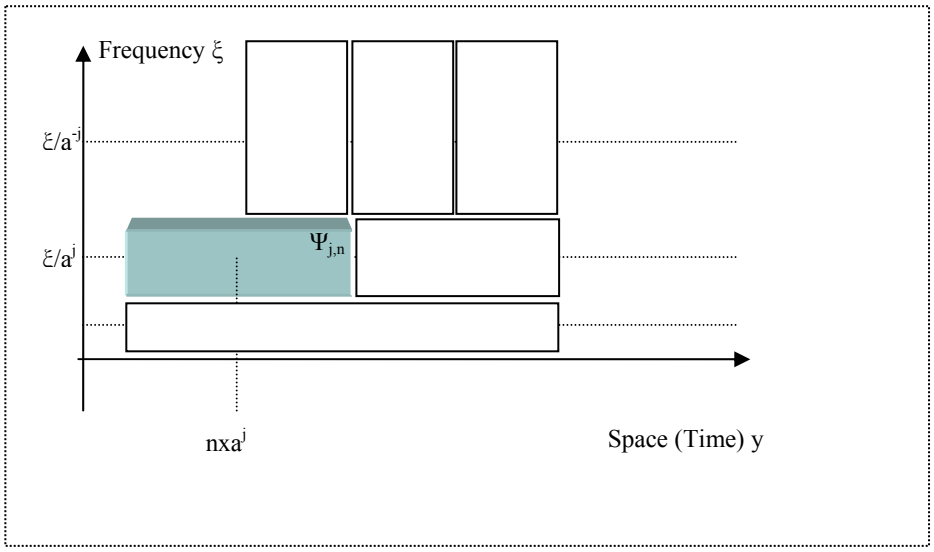

Figure 4.1: Time and frequency localization of wavelets

The size of the box along the frequency axis depends on the scale a^{-j} while the width stays uniform along the time axis but it is changed by a^j as the box is translated along the vertical frequency axis. The following theorem provides the necessary and sufficient condition for a discrete wavelet to be a frame.

Theorem 4.2 The necessary and sufficient condition for a wavelet to be a frame of the space $\mathbf{L}^2$ of all square integrable functions is that its bounds must satisfy

$$P \le \frac{C_\psi}{x \ln a} \le Q, \tag{4.23}$$

where

$$C_\psi = \int_0^\infty \frac{\left|\tilde{\psi}(\xi)\right|^2}{\xi} d\xi < \infty. \tag{4.24}$$

The frequency equivalent of Eq.(4.23) will have the form for every frequency ξ

$$P \le \frac{1}{x_0} \sum_{j=-\infty}^{\infty} \left|\hat{\psi}\left(a^j \xi\right)\right|^2 \le Q, \qquad \forall \xi \in \mathbf{R} \setminus \{0\} \tag{4.25}$$

The inequality Eq.(4.23) relates the sampling density $x \ln a$ to the bounds of the frame. According to Theorem 4.1, the dual wavelet frame can be computed by substituting $\tilde{v}_n$ by $\tilde{\psi}_{j,n}$, and the following expression will hold:

$$\tilde{\psi}_{j,n} = \left(U^* U\right)^{-1} \psi_{j,n} \tag{4.26}$$

According to Mallat (1998), a wavelet frame can be determined by computing the basic wavelet $\tilde{\psi}_{j,o}$ by Eq.(4.26) and after that translating it along the time axis *y* by

$$\tilde{\psi}_{j,n}(y) = \tilde{\psi}_{j,0}(y - na^j x) \tag{4.27}$$

4.3.3 Dyadic wavelet transform

Continuous wavelet transforms such as windowed Fourier transforms provide translation-invariant representation, but sampling the translation parameter (having discretization along the time axis) will destroy this translation invariance. The translation invariance means that after translation, a signal pattern will be only translated but not modified. The loss of translation invariance appears if the translation factor is not equal to the grid interval. It is necessary t*o preserve the property of translation invariance for detecting singularities or edges in wavelet applications for AGBVPs.* There are two reasons to use so-called *dyadic wavelets* (when $a = 2$): (i) they maintain translation invariance, and (ii) fast computations are possible through the use of filter banks based on dyadic wavelets. The dyadic wavelet transform is defined in the following form:

Definition 4.2 Assuming the scale to be $s = a^j = 2^j$, where j denotes the level of wavelet decomposition, the dyadic wavelet transform of $g \in \mathbf{L}^2(\mathbf{R})$ is defined as

$$\mathrm{W}g(x, 2^j) = \int_{-\infty}^{+\infty} g(x) \frac{1}{\sqrt{2^j}} \psi\left(\frac{y-x}{2^j}\right) dy = g * \overline{\psi}_{2^j}(x), \tag{4.28}$$

where

$$\overline{\psi}_{2^j}(x) = \psi_{2^j}(-x) = \frac{1}{\sqrt{2^j}} \psi\left(\frac{-x}{2^j}\right) \tag{4.29}$$

The following theorem gives the presentation of a dyadic transform in terms of wavelet frames. It allows changes in wavelet coefficients in frame boundaries in view of smoothing the data or imposing smoothness conditions.

Theorem 4.3 If there exist two constants $P > 0$ and $Q > 0$ such that

$$P \le \sum_{j=-\infty}^{+\infty} \left| \hat{\psi}\left(2^j \xi\right) \right|^2 \le Q, \quad \forall \xi \in \mathbf{R} \tag{4.30}$$

then

$$P\|g\|^2 \le \sum_{j=-\infty}^{+\infty} \left\| \mathrm{W}g\left(x, 2^j\right) \right\|^2 \le Q\|g\|^2 . \tag{4.31}$$

Furthermore, if a dual wavelet $\tilde{\psi}$ satisfies

$$\sum_{j=-\infty}^{\infty} \hat{\psi}^*\left(2^j \xi\right)\hat{\tilde{\psi}}\left(2^j \xi\right) = 1 \quad \forall \xi \in \mathbf{R} \setminus \{0\},$$

(4.32)

which means that the wavelet frames become orthonormal bases, then perfect reconstruction of $g(y)$ is possible in the form

$$g(y) = \sum_{j=-\infty}^{+\infty} \mathrm{W}g(\bullet, 2^j) * \tilde{\psi}_{2^j}(y) . \tag{4.33}$$

It is interesting to see that *once the frame boundaries are determined for certain types of wavelets by Eq.(4.30,) the wavelet coefficients can be changed within these frame boundaries, meeting the requirements of being wavelet frames and smoothing singularities or edges in* $g(y)$. The energy equivalence Eq.(4.31) proves that the *normalized dyadic wavelet transform operator*

$$Ug(j, x) = \frac{1}{\sqrt{2^j}} Wg(x, 2^j) = \left(g, \frac{1}{\sqrt{2^j}} \psi_{2^j}(y - x) \right) \tag{4.34}$$

has the same properties as a frame operator given by Mallat (1998). The equation Eq.(4.35) is valid for the Fourier transform of the dual wavelets

$$\hat{\tilde{\psi}}(\xi) = \frac{\hat{\psi}(\xi)}{\sum_{j=-\infty}^{\infty} \left|\hat{\psi}\left(2^j \xi\right)\right|^2}. \tag{4.35}$$

Application of spherical pseudo-differential operators and spherical wavelets for compatibility (smoothness) conditions will be discussed in Chapter 5.

4.3.4 Multiresolution analysis

Multiresolution analysis (MRA) gives the tool to apply the wavelet theory numerically to decompose and reconstruct a signal g. The concept of MRA is the key to the construction of orthogonal wavelet bases and fast decomposition and reconstruction of a signal into *different frequency* bands (Keller, 2000). MRA is the base of constructing *filter banks* to design dyadic wavelets described in Mallat (1998). The procedure for an MRA as an application of *low*- and *high*-pass filters together with downsampling and upsampling will be discussed following Keller (2000) to explain the mathematical background of MRA in terms of orthogonal projections between functional spaces.

Let us assume g to be a signal from a certain space $\mathbf{A}_j \subset \mathbf{L}^2(\mathbf{R})$, where j denotes the level of decomposition. This signal needs to be decomposed into low-frequency and high-frequency components. The low-frequency part can be considered as an orthogonal projection $l_{j+1}g$ onto a smaller space $\mathbf{A}_{j+1} \subset \mathbf{A}_j$ containing smooth functions. The orthogonal complement of $\mathbf{A}_{j+1}$ is the space $\mathbf{D}_{j+1}$ and the projection of the signal into this space will be denoted as $h_{j+1}g$. Later, $\mathbf{A}_j$ will be associated with the *approximated* coefficients at level j, and $\mathbf{D}_j$ will be associated with *detail* coefficients at level j. The signal g can be decomposed into two frequency bands

$$g = l_{j+1}g + h_{j+1}g \tag{4.36}$$

where the corresponding spaces are presented as an operator of *space addition* $\mathbf{A}_j = \mathbf{A}_{j+1} \oplus \mathbf{D}_{j+1}$. The procedure can continue to the next $j+2$ level of decomposition. If both low-pass and high-pass projections are generated by dyadic orthogonal wavelets, the exact reconstruction of the signal is possible. Later the scheme will be presented in terms of low- and high-pass filters. At this point, it is necessary to define the MRA.

Definition 4.3 A nested sequence (Mallat, 1998; Keller, 2000)**,**

$$\{0\} \subset \cdots \mathbf{A}_{-2} \subset \mathbf{A}_{-1} \subset \mathbf{A}_0 \subset \mathbf{A}_1 \subset \cdots \subset \mathbf{L}^2(\mathbf{R}) \tag{4.37}$$

of closed subspaces $\mathbf{A}_m \subset \mathbf{L}^2(\mathbf{R})$ is called a MRA of $\mathbf{L}^2(\mathbf{R})$ if the following four statements hold:

1. $\overline{\underset{m\in\mathbf{Z}}{\cup} \mathbf{A}_m} = \mathbf{L}^2(\mathbf{R})$, there are no elements of a MRA outside $\mathbf{L}^2(\mathbf{R})$ (4.38)
2. $\underset{m\in\mathbf{Z}}{\cap} \mathbf{A}_m = \{0\}$,there is no redundancy in the number of elements of MRA (4.39)
3. $g(n) \in \mathbf{A}_m \Leftrightarrow g(2^m n)$ in $\mathbf{A}_0$, which means that all spaces of MRA are scaled versions of the space $\mathbf{A}_0$ (4.40)
4. There is a function $\varphi \in \mathbf{L}^2(\mathbf{R})$ with $\mathbf{A}_0 = \overline{\text{span}\{\varphi(n-k) | k \in \mathbf{Z}\}}$ and

$$P\sum_{k\in\mathbf{Z}} c_k^2 \le \left\| \sum_{k\in\mathbf{Z}} c_k \varphi(n-k) \right\|_{L^2}^2 \le Q\sum_{k\in Z} \mathrm{c}_\mathrm{k}^2, \quad 0 < P, Q \tag{4.41}$$

and this last equation corresponds to the frame bounds definitions with $\{c_k\}_{k\in\mathbf{Z}} \in l^2(\mathbf{Z})$.

The space $\mathbf{A}_0$ itself is spanned by shifted versions of the so-called *scaling function* φ. If $m \to \infty$ the elements of $\mathbf{A}_m$ become more extended and dilated and, if $m \to -\infty$, the

spaces $\mathbf{A}_m$ contain an increasingly finer structure. The spaces $\mathbf{A}_m$ are spanned by shifted versions of $\varphi_{m,k} = 2^{-m/2}\varphi\left(2^{-m} - k\right)$ or $\mathbf{A}_m = \text{span}\left\{\varphi_{m,k} \,|k \in \mathbf{Z}\right\}$. A MRA can be represented as a filter bank with low-pass and high-pass filters corresponding to certain types of wavelets.

4.3.5 Multiresolution analysis using dyadic wavelets

Let us assume that a MRA with discrete dyadic wavelets is numerically applied using two filters, namely l for the low-pass and h for the high-pass filter (Mallat, 1998). A scaling function can be constructed whose Fourier transform has the form

$$\hat{\varphi}(\xi) = \frac{1}{\sqrt{2}}\hat{l}\left(\frac{\xi}{2}\right)\hat{\varphi}\left(\frac{\xi}{2}\right) \tag{4.42}$$

The corresponding wavelet has a Fourier transform defined by

$$\hat{\psi}(\xi) = \frac{1}{\sqrt{2}}\hat{h}\left(\frac{\xi}{2}\right)\hat{\varphi}\left(\frac{\xi}{2}\right) \tag{4.43}$$

The number of vanishing moments for ψ will be equal to the number of zeros of $\hat{\psi}(\xi)$ at $\xi = 0$. Both Eq.(4.42) and Eq.(4.43) represent the decomposition step. The dual scale functions and wavelets for the reconstruction step are given through their Fourier transforms

$$\hat{\tilde{\varphi}}(\xi) = \frac{1}{\sqrt{2}}\hat{\tilde{l}}\left(\frac{\xi}{2}\right)\hat{\tilde{\varphi}}\left(\frac{\xi}{2}\right) \tag{4.44}$$

$$\hat{\tilde{\psi}}(\xi) = \frac{1}{\sqrt{2}}\hat{\tilde{h}}\left(\frac{\xi}{2}\right)\hat{\tilde{\varphi}}\left(\frac{\xi}{2}\right), \tag{4.45}$$

where $\tilde{l}, \tilde{h}$ are the dual filters for the reconstruction step. The following proposition found in Mallat (1998) gives the sufficient condition that Eq.(4.45) represents the dual wavelet for the reconstruction step.

Proposition 4.1 If the filters satisfy

$$\hat{\tilde{l}}(\xi)\hat{l}(\xi) + \hat{\tilde{h}}\hat{h} = 2, \quad \forall \xi \in [-\pi, \pi] \tag{4.46}$$

then

$$\sum_{j=-\infty}^{\infty} \hat{\psi}^*(2^j \xi)\hat{\tilde{\psi}}(2^j \xi) = 1, \quad \forall \xi \in \mathbf{R} - \{0\}. \tag{4.47}$$

This proposition gives the condition that the filters should satisfy to have exact reconstruction.

To apply fast dyadic transforms let us assume that the *samples of discrete input signal* $a_0[n]$ *(data)* are considered as averages of a function g weighted by the scale kernel $\varphi(y-n)$

$$a_0[n] = (g(y), \varphi(y-n)) = \int_{-\infty}^{\infty} g(y)\varphi(y-n)dy \tag{4.48}$$

Now, for every level of decomposition $j > 0$, the scale function (approximated) coefficients are

$$a_j[n] = \left(g(y), \varphi_{2^j}(y-n)\right) \tag{4.49}$$

and the dyadic wavelet (detail) coefficients over the integer grid are

$$d_j[n] = \mathrm{W}g(n, 2^j) = \left(g(y), \psi_{2^j}(y-n)\right). \tag{4.50}$$

The index j for the filters h_j, g_j shows that there are $2^j - 1$ zeros inserted between each sample of $h[n]$ or $l[n]$. These zeros create holes called '*trous*' in French and the name of this algorithm is known as '*Algorithme à Trous*' (Mallat, 1998). Assuming the notation $\bar{l}_j[n] = l_j[-n]$, $\bar{h}_j[n] = h_j[-n]$, the following proposition gives the formulas for this algorithm.

Proposition 4.2 For any $j \geq 0$ for the decomposition step

$$a_{j+1}[n] = a_j * \bar{l}_j[n], \quad d_{j+1}[n] = a_j * \bar{h}_j[n], \tag{4.51}$$

and for the reconstruction step

$$a_j[n] = \frac{1}{2}\left(a_{j+1} * \bar{l}_j[n] + d_{j+1} * \bar{h}_j[n]\right). \tag{4.52}$$

Figure 4.2. shows the procedure of applying discrete dyadic wavelets as filter banks for the decomposition and reconstruction steps between levels $j, j+1, j+2$.

This procedure will be applied for the solutions of AGBVPs to impose compatibility (smoothness) conditions along the coastline, and will be discussed in greater detail in Chapters 5 and 6.

4.4 Application of wavelet frames in imposing smoothness conditions in AGBVPs

It was mentioned in Chapter 3 that PDO theory is related to generalized linear operators acting upon infinitely smooth test functions. The regularity of the solution of AGBVPs is a uniform, global regularity, based on data distributed all over the region of support. This

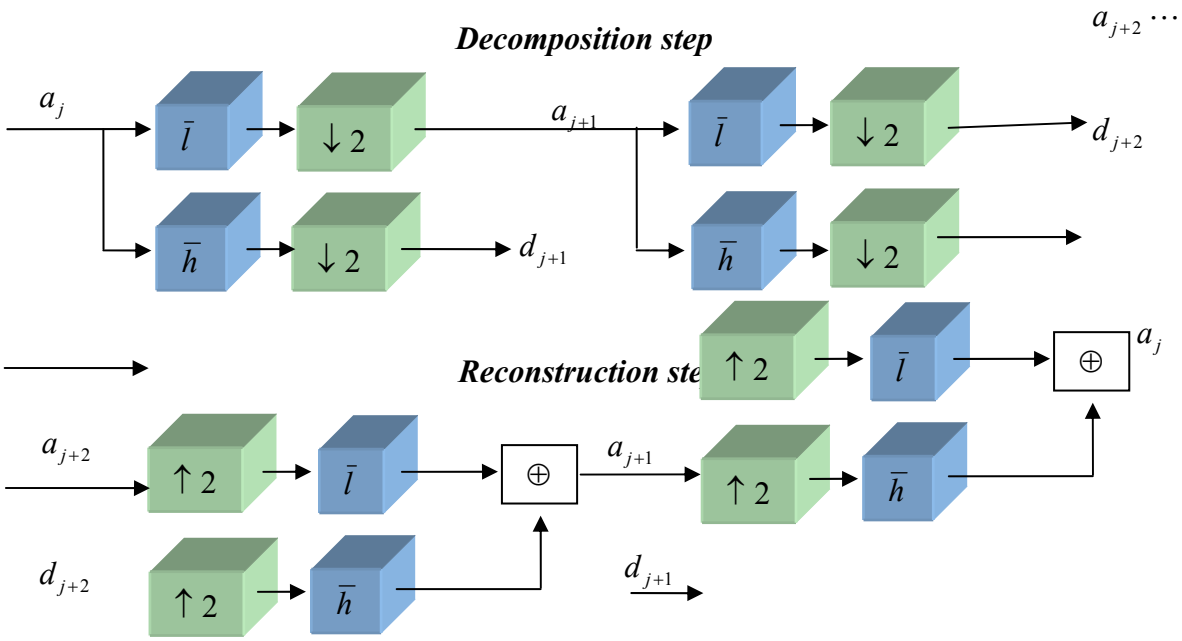

Figure 4.2 : Decomposition and reconstruction steps

regularity is not enough if the local behavior of the solution along the coastline needs to be investigated. To detect singularities and edges across the coastline, local estimation of regularity is necessary. Because wavelets have a very good space localization property, they are considered very useful for this purpose. The combination of PDOs and wavelets can help to overcome and to change the smoothness of the solution along the coastline. It has been shown in Chapter 3 that the solution of an AGBVP can be infinitely differentiable in points away from the coastline; and that at the coastline the smoothness can be changed by introducing vanishing weight functions. Because of good localizing

properties of wavelets, they can play the role of weight functions assuming the detail coefficients to become zero at the coastline for every level of decomposition. This main role in detecting and smoothing singularities and edges is described by the so called *Lipschitz regularity* α. The parameter α characterizing the regularity corresponds to the degree of generalized derivatives of Sobolev spaces, described in Chapter 3. Lipschitz exponents, which will be explained in subsection 4.4.1 below, provide a uniform estimation of regularity over a space interval but also, if a function g has singularity at point x, then the Lipschitz exponent will characterize this singular behavior. *The following analysis of uniform and local Lipschitz regularity, used for detecting and smoothing singularities and edges, will help to explain wavelet application for imposing smoothness conditions in AGBVPs.*

4.4.1 Lipschitz regularity

The uniform regularity of g is related to the asymptotic decay of the amplitude of its Fourier transform over the entire space $\mathbf{R}$ (Mallat, 1998). It can be considered a *global* measure of the regularity. However, for analyzing a signal at certain points it will be not enough. Nevertheless, it will be briefly discussed herein to illustrate the meaning of regularity.

The *Taylor formula* relates the differentiability of a signal to its polynomial approximation. Let us assume that g is a m times differentiable function in the interval $[x_0 - \Delta x, x_0 + \Delta x]$. Let p_x be the Taylor polynomial representing the function in the neighborhood of x,

$$p_x(x) = \sum_{k=0}^{m-1} \frac{g^{(k)}(x_0)}{k!}\left(x - x_0\right)^k . \tag{4.53}$$

The approximation error is

$$\left|e_x(x)\right| = \left|g(x) - p_x(x)\right| \le \frac{\left|x_0 - x\right|^m}{m!} \sup_{t\in[x_0-\Delta x, x_0+\Delta x]} \left|g^m(t)\right|, \quad \forall x \in \left[x_0 - \Delta x, x_0 + \Delta x\right] \tag{4.54}$$

When m is an integer, the m^{th} order differentiability of g in the neighborhood of x represents the upper bound on the error $e_x(x)$ when $x \to x_0$. *The meaning of Lipschitz regularity is that it refines this upper bound with respect to non-integer exponents*. Lipschitz exponents are also called *Hölder* exponents. The following theorem represents both types of regularity – *uniform* and *local*.

Theorem 4.4 (Lipschitz)

- A function g is *pointwise Lipschitz* $\alpha \ge 0$ at x, if there exists $C > 0$ and a polynomial p_x of degree $m = \lfloor \alpha \rfloor$ such that

$$\left|g(x) - p_x(x)\right| \le C\left|x_0 - x\right|^\alpha, \forall x_0 \in \mathbf{R} \tag{4.55}$$

- A function g is *uniformly Lipschitz* α over $[a,b]$, if it satisfies Eq.(4.55) for all $x \in [a,b]$, with a constant C that is independent of x.
- The Lipschitz regularity of g at x or over $[a,b]$ is the sup of the α such that g is Lipschitz α.

Pointwise Lipschitz exponents vary from point to point and, in contrast to the uniform Lipschitz exponents which provide a more global estimation of regularity are applied to the entire interval. If g is uniformly Lipschitz α $(\alpha > m)$ in the neighborhood of x, then g is at least m times continuously differentiable in this neighborhood. If $0 \le \alpha < 1$,then the function is equal to the polynomial itself and

$$\left|g(x_0) - g(x)\right| \le C\left|x_0 - x\right|^\alpha, \forall x_0 \in \mathbf{R}. \tag{4.56}$$

If a function is bounded but discontinuous at x it is Lipschitz 0 at this point. When $\alpha < 1$, g is not differentiable at x and α characterizes the singularity type.

The following theorem provides the necessary condition for a function to be bounded and uniformly Lipschitz α.

Theorem 4.5 A function g is bounded and uniformly Lipschitz α over $\mathbf{R}$ if

$$\int_{-\infty}^{\infty} |\hat{g}(\xi)|\left(1+|\xi|^{\alpha}\right)d\xi < +\infty \tag{4.57}$$

The uniform Lipschitz regularity means that there exists a constant $C > 0$ such that, for all pairs $(x_0, x) \in \mathbf{R}^2$

$$\frac{|g(x_0) - g(x)|}{|x_0 - x|^{\alpha}} \leq C \tag{4.58}$$

In subsection 4.4.2 this theorem will be used to prove that all PDOs based on the generalized derivatives from Sobolev spaces $\mathbf{W}_{\alpha}$ are Lipschitz α. The uniform regularity measures the *minimum global regularity* of functions. However the regularity at a particular point cannot be measured from the decay of $|\hat{g}(\xi)|$. To the contrary, because of well-localized wavelets, the wavelet transform provides local Lipschitz regularity over intervals and at points (Mallat, 1998).

4.4.2 Pseudo-differential operators with Lipschitz α regularity

The theory of PDOs discussed in Chapter 3 is called $\mathbf{C}^{\infty}$-theory, because PDOs themselves can be considered as infinitely differentiable generalized function. The regularity discussed is a global uniform regularity as will be shown in the next proposition 4.3.

Proposition 4.3 *Pseudo-differential operators based on generalized derivatives of Sobolev spaces* $\mathbf{W}_\alpha$ *are uniformly Lipschitz* α .

Proof:

Let $g \in \mathbf{W}_\alpha$. Then, according to Eq.(3.14) in Chapter 3,

$$\int_{-\infty}^{\infty} \left|\hat{g}(\xi)\right|^2 (1+|\xi|)^{2\alpha}\, d\xi < \infty \tag{4.59}$$

Let us assume that

$$u(\xi) = \hat{g}(\xi)(1+|\xi|)^{\alpha} \tag{4.60}$$

On the other hand, the Schwarz (Hölder, Cauchy-Buniakovski) inequality states that

$$\int_{-\infty}^{\infty} u(\xi)v(\xi)d\xi \le \sqrt{\int_{-\infty}^{\infty} u^2(\xi)d\xi}\sqrt{\int_{-\infty}^{\infty} v^2(\xi)d\xi} \ . \tag{4.61}$$

If it is assumed that $v(\xi) = 1$; the second term goes to ∞ Then (4.61) will have the form

$$\left|\int_{-\infty}^{\infty} u(\xi)d\xi\right| \le \int_{-\infty}^{\infty} |u(\xi)|\, d\xi < \infty.\sqrt{\int_{-\infty}^{\infty} u^2(\xi)d\xi} \ . \tag{4.62}$$

Taking into account Eq.(4.59) for g we will have

$$\int_{-\infty}^{\infty} |\hat{g}(\xi)|(1+|\xi|)^{\alpha}\, d\xi < \infty.\sqrt{\int_{-\infty}^{\infty} \left|\hat{g}(\xi)\right|^2 (1+|\xi|)^{2\alpha}\, d\xi} < \infty \ . \tag{4.63}$$

Also, it is possible to show that

$$\int_{-\infty}^{\infty} |\hat{g}(\xi)|(1+|\xi|^{\alpha})d\xi \leq \int_{-\infty}^{\infty} |\hat{g}(\xi)|(1+|\xi|)^{\alpha}\, d\xi\,, \tag{4.64}$$

because $(1+|\xi|^{\alpha}) \leq (1+|\xi|)^{\alpha}$ for every $\xi \in \mathbf{R}$.

As a result, it is obtained

$$\int_{-\infty}^{\infty} |\hat{g}(\xi)|(1+|\xi|^{\alpha})d\xi < \infty\,, \tag{4.65}$$

which is exactly Theorem 4.5 and, because g represents PDOs from Sobolev spaces, it can be concluded that *PDOs are uniformly Lipschitz* α.

The importance of the proposition just proved is that uniformly regular PDOs can be combined with local regular wavelets in solutions of AGBVPs to increase the regularity along the coastline.

4.4.3 Wavelets as multiscale differential operators and regularity measurements with wavelets

The theory of wavelets as multiscale differential operators and the estimation of regularity at a certain point will be presented following Mallat (1998). To measure the local regularity of a signal, vanishing moments of wavelets will give the order of a multiscale differential operator. In subsection 4.4.1, the regularity exponent α was associated with the error of the polynomial approximating function g. Applying the wavelet transform, the exponent α can be estimated without the need of this polynomial but wavelets with $n > \alpha$ vanishing moments have to be used.

$$\int_{-\infty}^{\infty} x^{k}\psi(x)dx = 0, \quad 0 \leq k < n \tag{4.66}$$

A wavelet with *n* vanishing moments is orthogonal to polynomials of degree *n-1*, since the polynomial has degree at most $n-1$ because $\alpha < n$.

Theorem 4.6 (Mallat, 1998) proves that a wavelet with n vanishing moments can be considered as the n^{th} derivative of a function τ. As a result, the wavelet transform represents a *multiscale differential operator*. Let us assume that the wavelet has a fast decay, which fact means that for every *decay exponent* $m \in \mathbf{N}$ there exists a constant C_m such that

$$|\psi(x)| \le \frac{C_m}{1+|x|^m}, \quad \forall x \in \mathbf{R}. \tag{4.67}$$

Theorem 4.6 A wavelet with a fast decay has n vanishing moments if and only if there exists τ with a fast decay such that

$$\psi(x) = (-1)^n \frac{d^n \tau(x)}{dx^n}. \tag{4.68}$$

As a result, the wavelet transform can be represented as a differential operator

$$\mathrm{W}g(x,s) = s^n \frac{d^n}{dx^n}\left(g * \bar{\tau}_s\right)(x), \tag{4.69}$$

with $\bar{\tau}_s(x) = \frac{1}{\sqrt{s}}\tau\left(-\frac{x}{s}\right)$. Moreover, ψ has no more than n vanishing moments if and only if $\int_{-\infty}^{+\infty} \tau(x)dx \neq 0$.

It is clear that Theorem 4.6 gives the necessary and sufficient condition for a wavelet to represent a multiscale differential operator of degree n, which has n vanishing moments. It has been shown in Mallat (1998) that since τ has a fast decay then

$$\lim_{s\to 0}\frac{1}{\sqrt{s}}\overline{\tau}_s = C\delta(x)\,. \tag{4.70}$$

For a function g which is n times continuously differentiable in the neighborhood of x, the limit when the scale is approaching zero is equal to

$$\lim_{s\to 0}\frac{\mathrm{W}g(x,s)}{\mathrm{s}^{\mathrm{n}+1/2}} = \lim_{s\to 0} g^{(n)} * \frac{1}{\sqrt{s}}\overline{\tau}_s(x) = Cg^{(n)}(x)\,. \tag{4.71}$$

It is interesting to note that for zero scale the wavelet transform is similar to the n^{th} derivative of the function. To measure the regularity uniformly over an interval, the following theorem gives the relationship between the amplitude of the wavelet transform and the regularity exponent at a certain continuous scale.

Theorem 4.7 If $g \in \mathbf{L}^2(\mathbf{R})$ is uniformly Lipschitz α (i.e., $\alpha \le n$ over $[a,b]$) then there exists a constant $C > 0$ such that

$$\left|\mathrm{W}g(x,s)\right| \le Cs^{\alpha+1/2}, \quad \forall(x,s) \in [a,b]\times \mathbf{R}^+\,. \tag{4.72}$$

Conversely, if $\mathrm{W}g(x,s)$ satisfies Eq.(4.72) and if $\alpha < n$ is not an integer then g is uniformly Lipschitz α on $[a+\Delta x, b-\Delta x]$, for any $\Delta x > 0$.

According to Mallat (1998), if the scale s decreases, the wavelet transform measures scale variations in the neighborhood of x and its amplitude decays such as $s^{\alpha+1/2}$ over intervals where the function g is uniformly Lipschitz α. Theorem 4.8 describes how to measure the pointwise Lipschitz regularity.

Theorem 4.8 (Jaffard) If $g \in \mathbf{L}^2(\mathbf{R})$ is uniformly Lipschitz $\alpha \le n$ at point x_0, then there exists a constant $C > 0$ such that

$$\left|\mathrm{W}g(x,s)\right| \le Cs^{\alpha+1/2}\left(1+\left|\frac{x-x_0}{s}\right|^{\alpha}\right), \quad \forall(x,s)\in \mathbf{R}\times\mathbf{R}^{+}. \tag{4.73}$$

Conversely, if $\mathrm{W}g(x,s)$ satisfies Eq.(4.73) and if $\alpha < n$ is not an integer and there exists C and $\alpha' < \alpha$ such that

$$\left|\mathrm{W}g(x,s)\right| \le Cs^{\alpha+1/2}\left(1+\left|\frac{x-x_0}{s}\right|^{\alpha'}\right), \quad \forall(x,s)\in \mathbf{R}\times\mathbf{R}^{+}, \tag{4.74}$$

then g is Lipschitz α at point x_0.

This theorem allows the local Lipschitz regularity to be measured at every point using the amplitude of the wavelet transform. Using wavelet transforms, it is possible to detect singularities and edges at certain points in space at different scales and, furthermore, to smooth them.

4.4.4 Detecting and smoothing singularities by wavelets

The decay of $\left|\mathrm{W}g(x,s)\right|$ can be controlled by its local maximum values instead of computing it directly in the space-scale domain. The theory and more details about isolated, smoothed singularities and the propagation of the singularities through the scales can be found in Mallat (1998).

4.4.4.1 Wavelet modulus maxima

The term *modulus maximum (maxima)* plays a basic role in detecting and smoothing singularities. It is related to the point x_0 at scale s_0 where $\left|\mathrm{W}g(x_0,s_0)\right|$ is a local maximum or where

$$\frac{\partial Wg(x_0,s_0)}{\partial x} = 0. \tag{4.75}$$

A maxima line is any connected curve in the space-scale domain consisting of points which are modulus maxima. The singularities can be detected by the abscissas to which wavelet modulus maxima converge at fine scales (Mallat, 1998). If a wavelet has one vanishing moment, wavelet modulus maxima are points where the first *derivative* is maximum. For wavelets with two vanishing moments, the curve in space-scale plane will have more maxima and minima which means more modulus maxima. When $|\mathrm{W}g(x,s)|$ does not have modulus maxima at fine scales, the function is *locally regular*. The measure of regularity can be computed for every modulus maximum point by Eq.(4.67).

In image processing, after detecting singularities they can be used to reconstruct the image, because the modulus maxima contain information about sharp signal transitions, edges and singularities. *By contrast, in the case of AGBVPs, data and the solution can be considered smooth enough everywhere except the coastline. All modulus maxima can be expected in the coastal area and, after changing their magnitude, the singularities can be decreased or apply certain level of smoothing*. For AGBVPs, expected singularities are situated along the coastline and it can be considered as a maxima line. *The key point in applying wavelets as smoothness condition is the statement in Mallat (1998): "The strength of singularities can be modified by changing the amplitude of the maxima and some singularities can be removed by suppressing the corresponding maxima"*.

4.4.4.2 Reconstruction from dyadic modulus maxima

For numerical applications, the dyadic wavelet transform is considered because it is complete, stable and has the same properties as a continuous wavelet transform. A *reconstruction algorithm of the signal from dyadic maxima* is presented in Mallat (1998). At each scale 2^j the positions $\{x_{j,p}\}$ of dyadic maxima are known as are the values of the local maxima, in the form

$$\mathrm{W}g(x_{j,p},2^j) = \left(g,\psi_{j,p}\right) \tag{4.76}$$

where

$$\psi_{j,p}(x) = \frac{1}{\sqrt{2^j}}\psi\left(\frac{x - x_{j,p}}{2^j}\right). \tag{4.77}$$

The reconstruction algorithm will recover a function $\widetilde{g}$ such that

$$W\widetilde{g}\left(x_{j,p}, 2^j\right) = \left(\widetilde{g}, \psi_{j,p}\right) = \left(g, \psi_{j,p}\right) \tag{4.78}$$

whose wavelet modulus maxima are located at points $\left\{x_{j,p}\right\}$. The *reconstructed function* $\widetilde{g}$ should satisfy the frame boundary condition in the form

$$P\left\|\widetilde{g}\right\|^2 \le \sum_{j=-\infty}^{\infty} 2^{-j}\left\|\mathrm{W}\widetilde{g}(x, 2^j)\right\|^2 \le Q\left\|\widetilde{g}\right\|^2. \tag{4.79}$$

4.4.4.3 Extension of reconstruction algorithm for smoothing singularities

The reconstruction algorithm can be modified to smooth the singularities in addition to the reconstruction of the signal. In the frame bounds, the wavelet norm can be reduced by decreasing the absolute value of wavelet coefficients $\left|\mathrm{W}\widetilde{g}(x, 2^j)\right|$ for the reconstructed signal at the modulus maxima points. To reach the highest level of smoothing, the wavelet coefficients can be restricted to zero or up to a value representative of the certain level j of decomposition. *As in Chapter 3 for the application of PDOs to AGBVPs, modulus maxima coefficients (along the coastline) can be assumed to be weights that vanish at the coastline. The solution can be improved or certain degree of smoothness can be achieved by smoothing data along the coastline. As a result, the determined geoid will be closer to the real equipotential surface along the coastline overcoming existing sharp transition across the coastline.* In the case of a 2D spatial signal and dyadic wavelets, the maxima line at a certain scale 2^j will represent lines with maximum n^{th} derivatives for wavelets with $n-1$ vanishing moments.

4.5 Concluding remarks and summary

In this chapter the transition from variational methods for solutions of AGBVPs with orthonormal base functions to wavelet frame theory has been discussed. It has been shown that wavelet frames can provide more flexibility in imposing compatibility (smoothness) conditions along the coastline compared to the unique solution by variational methods. For this purpose, both the theory of variational methods and frame theory have been presented briefly, pointing out their specific applications to AGBVPs.

Dyadic wavelet frames have been discussed together with dyadic multiresolution analysis in the form of filter banks. This procedure will be applied later in Chapter 5 and 6 for finding solutions of AGBVPs by a combination of spherical wavelets and spherical PDOs.

The uniform and local Lipschitz regularities have been discussed for wavelets. The local regularity of wavelets can be used to detect singularities and edges because of the very good space localization properties of wavelets. In AGBVPs, the singularities are expected along the coastline and the estimation of local regularity can help to detect them. The combination of uniformly regular PDOs with local regular wavelets can increase the regularity of the AGBVP solutions across the coastline.

In addition, in subsection 4.4.2, it has been proven that PDOs are uniformly Lipschitz α. The impact of Proposition 4.3 is that it helps to combine PDOs and wavelets for AGBVPs considering that they are complimentary in terms of Liptschitz regularity. *This means that PDOs will provide the necessary smoothness off the coastline and wavelets will detect and smooth the singularities and edges along the coastline.*

Finally, the detection and smoothing of singularities by wavelets have been presented following Mallat (1998), and a modified procedure for reconstruction of the signal was presented to smooth the singularities. The representation of the wavelet transform as a multiscale differential operator together with the concept of modulus maxima allows the

reconstruction of a signal by its modulus maxima points. In the case of AGBVPs, the wavelet coefficients can be changed along the coastline and this is possible because of the properties of wavelet frames. In this way, additional smoothing can be achieved in the modified reconstruction of the signal.

Chapter 5

Combination of spherical harmonics, pseudo-differential operators and wavelets for solutions of AGBVPs and explicit compatibility conditions in a coastal region

In this chapter spherical harmonics, spherical PDOs and spherical wavelets will be discussed both separately and in combination for solutions of AGBVPs following Freeden and Windheuser (1997). Two approaches for solutions of AGBVPs with compatibility (smoothness) conditions will be discussed: *the first one* is based on the application of wavelets for the solution of Neumann's BVP (Freeden and Schneider, 1998) and restricting the wavelet coefficients as it has been described in Chapter 4; *the second solution* is related to the combination of spherical PDOs and wavelets to apply compatibility conditions for *the first time in an explicit form*. Actually a third solution is possible and it will be discussed in subsection 5.3; it can be considered as combination of both solutions mentioned above.

5.1 Spherical harmonics and Abel-Poisson singular integral

5.1.1 Spherical harmonics

The theory of spherical harmonics will be briefly presented according to Freeden and Windheuser (1997) as it will be used later to describe spherical PDOs and spherical wavelets. Let us assume a point $x \in \mathbf{R}^3$ with coordinates (x_1, x_2, x_3). If the directional unit vector from the origin of the coordinate system to the point is denoted by $\mathbf{i} = \left(\frac{x_1}{|x|}, \frac{x_2}{|x|}, \frac{x_3}{|x|} \right)$ and $r = |x| = \sqrt{x_1^2 + x_2^2 + x_3^2}$, then $x = r\mathbf{i}$. For spherical coordinates of point $\sigma=(\varphi_\sigma, \lambda_\sigma)$

on a unit sphere $\delta\Omega$ and orthonormal basis $e=(e_1,e_2,e_3)$, (representing unit vectors along the coordinate axes) the following equation holds:

$$\begin{aligned}\mathbf{i} &= \sin(\varphi_\sigma)e_3+\cos(\varphi_\sigma)\cos(\lambda_\sigma)e_1+\cos(\varphi_\sigma)\sin(\lambda_\sigma)e_2= \\ &= pe_3+\sqrt{1-p^2}\left(\cos(\lambda_\sigma)e_1+\sin(\lambda_\sigma)e_2\right),\end{aligned} \tag{5.1}$$

where $p=\sin(\varphi_\sigma)=\cos(90^\circ-\varphi_\sigma)$

Let ∇_σ us denote the *surface gradient* on the unit sphere $\delta\Omega$. The *Beltrami (surface Laplace)* operator Δ_σ on the sphere with radius *R* is expressed as in Eq.(3.54) in the form

$$\Delta_\sigma=\nabla_\sigma^2=R^{-2}(\partial^2/\partial\varphi_\sigma{}^2+\tan\varphi_\sigma\partial/\partial\varphi_\sigma+\cos^{-2}\varphi_\sigma\partial^2/\partial\lambda_\sigma{}^2). \tag{5.2}$$

Definition 5.1 The *infinitely differentiable eigenfunctions* of the Laplace (Beltrami) operator on the unit sphere $\delta\Omega$ are called *spherical harmonics* Y_n *of order n*. They correspond to the eigenvalues of the Laplace (Beltrami) operator $\hat{\Delta}_\sigma(n)=-n(n+1)$, which will be later called *spherical symbols* in terms of the representation of the spherical Laplace (Beltrami) operator as a spherical PDO.

The functions $H_n:\mathbf{R}^3\to\mathbf{R}^1$ defined as $H_n(x)=r^nY_n(x/r)$; represent polynomials of $x\in\mathbf{R}^3$ satisfying Laplace's equation $\Delta H_n=0$ in rectangular coordinates. Such kinds of polynomials are *Legendre polynomials* $P_n(\cos\theta)$, where θ is the spherical distance between two points on the sphere or the angle between two unit vectors. They are considered as infinitely differentiable eigenfunctions of the *Legendre operator,*

$$L_p=(1-p^2)\frac{d^2}{dp^2}-2p\left(\frac{d}{dp}\right). \tag{5.3}$$

Legendre functions of order *n* and degree *m* are denoted as $P_{nm}(\cos\theta)$ (Moritz, 1980). Let the space of all spherical harmonics of order *n* be denoted as $Harm_n$. This space is linear with a dimension of $\dim(Harm_n) = 2n+1$. This means that there exist $2n+1$ linearly independent spherical harmonics, which form an orthogonal basis and can even be normalized. In physical geodesy spherical harmonics are used to describe the gravity potential and they have the form Eq.(5.6) in terms of latitude and longitude of a point $\sigma(\varphi_\sigma, \lambda_\sigma) \in \delta\Omega$ on the unit sphere:

$$Y_{nm} = \begin{cases} P_{n,m}(\sin(\varphi_\sigma))\cos(m\lambda_\sigma) & , \quad m \geq 0 \\ P_{n,|m|}(\sin(\varphi_\sigma))\sin(|m|\lambda_\sigma), & \quad m < 0 \end{cases}, m = -n,\ldots -1,0,1,\ldots n \tag{5.6}$$

Let us assume the following notation for points ω, η, ς on the unit sphere:

$$\begin{aligned} \omega &= (\omega_1, \omega_2, \omega_3) = \left[\cos(\varphi_\omega)\cos(\lambda_\omega),\ \cos(\varphi_\omega)\sin(\lambda_\omega),\ \sin(\varphi_\omega)\right] \\ \eta &= (\eta_1, \eta_2, \eta_3) \quad = \left[\cos(\varphi_\eta)\cos(\lambda_\eta),\ \cos(\varphi_\eta)\sin(\lambda_\eta),\ \sin(\varphi_\eta)\right] \\ \varsigma &= (\varsigma_1, \varsigma_2, \varsigma_3) \quad = \left[\cos(\varphi_\varsigma)\cos(\lambda_\varsigma),\ \cos(\varphi_\varsigma)\sin(\lambda_\varsigma),\ \sin(\varphi_\varsigma)\right] \end{aligned} \tag{5.7}$$

If the spherical harmonics are normalized (Moritz, 1980), then

$$\left(Y_{n,m}, Y_{j,k}\right) = \int_{\delta\Omega} Y_{n,m}(\eta) Y_{j,k}(\eta) d\sigma(\eta) = \delta_{n,j}\delta_{m,k} \tag{5.8}$$

where $\delta_{n,j}$ and $\delta_{m,k}$ are Kronecker symbols and $d\sigma(\eta)$ is the surface element on the unit sphere at point η. The so-called *Addition Theorem* and *Funk-Hecke Formula* play an important role in the theory of spherical harmonics and wavelets. Both will be presented as they are given in Freeden and Windheuser (1997).

Theorem 5.1 (Addition theorem) For any two points $(\omega,\eta)\in\partial\Omega\times\partial\Omega$ on the unit sphere

$$\sum_{m=-n}^{n} Y_{n,m}(\omega)Y_{n,m}(\eta)=\frac{2n+1}{4\pi}P_n(\omega\cdot\eta), \tag{5.9}$$

where $\omega\cdot\eta=\cos\theta$ is the scalar product of the two unit vectors ω,η, and θ is the spherical distance between the two points on the sphere.

This theorem is important for the understanding of spherical wavelets because it represents the spherical harmonics on the unit sphere $\partial\Omega$ by a univariate Legendre polynomial.

Theorem 5.2 (Funk-Hecke Formula) For a function $y(\omega\cdot\eta)$ defined on the interval $[-1,1]$, it holds that

$$\int_{\partial\Omega} y(\omega\cdot\eta)P_n(\varsigma\cdot\eta)\,d\sigma(\eta)=\hat{y}(n)P_n(\omega.\varsigma), \tag{5.10}$$

where the *Legendre transform* $\hat{y}(n)$ (for a spherical cap it can be considered as spherical harmonic expansion) is defined as

$$\hat{y}(n)=2\pi\int_0^{p_1} y(p)P_n(p)d(p). \tag{5.11}$$

The Funk-Hecke formula will be applied later to derive the discrete form of the integral representing a PDO of gravity potential; the Legendre transform can be used to get the spherical symbol of the ocean-land function when it has the shape of a spherical cap. The functions of the type $y_\omega(\eta)=y(\omega\cdot\eta)$ are called *zonal functions* which are constant on every η such that $\omega\cdot\eta=v, v\in[-1,1]$. In this case all points η can be considered as boundaries of a spherical cap.

5.1.2 Spherical harmonic expansion

Let the space $\boldsymbol{\chi}[-1,1]$ include the continuous functions $\mathbf{C}[-1,1]$, together with spaces defined by q-norm $\mathbf{L}^q[-1,1]$, given in the form

$$\|y\|_{\mathbf{L}^q[-1,1]} = \left(2\pi \int_{-1}^{1} |y(p)|^q \, dp \right)^{1/q}. \tag{5.12}$$

The same functional spaces can be defined on the sphere taking into account that for the spherical distance it is valid, and $-1 \le p = \cos\theta \le 1$.

Definition 5.3 Let the function $y \in \boldsymbol{\chi}(\delta\Omega)$ belong to the functional space of square integrable functions on the unit sphere. The *spherical harmonic transform* is defined as

$$y(n,m) = \left(y, Y_{n,m} \right)_{\mathbf{L}^2(\delta\Omega)}, \tag{5.13}$$

where spherical harmonics play the role of orthonormal base functions.

The Fourier transform can be considered as mapping from the space $\mathbf{L}^2(\delta\Omega)$ into the space $l^2(\mathbf{N})$ of all sequences $\mathbf{N} = \{(n,m) | n = 0,1,2,..., m = -n,...-1,0,1...n\}$. The sequence is called the *spherical symbol* for the case of spherical PDOs, which are defined later using spherical harmonics as base functions. The *inverse spherical harmonic transform* is defined as

$$y(\omega \cdot \eta) = \sum_{n=0}^{\infty} \sum_{m=-n}^{n} \hat{y}(n,m) \overline{Y}_{n,m} \tag{5.14}$$

where $\overline{Y}_{n,m}$ are conjugate spherical harmonics. If, in addition the function y is *Lipschitz continuous (regular; see Chapter 4)* on the sphere, then it can be recovered by its Fourier transform in a uniform sense. The continuous *spherical convolution* of two functions $y_1(\partial\Omega)$ and $y_2(\partial\Omega)$ is defined by

$$(y_1 * y_2)(\omega) = \int_{\partial\Omega} y_1(\omega\cdot\eta)\, y_2(\eta)\, d\sigma(\eta), \qquad (\omega,\eta) \in \partial\Omega. \tag{5.15}$$

The discrete form of the convolution on the sphere using traditional spherical grid is not commutative. To be applied for the entire sphere, a set of equidistant points is required (see Freeden and Windheuser, 1997). The problems related to the gridding and the discrete spherical convolution will be discussed in more details in section 6.1.

5.1.3 Abel-Poisson kernel and Abel-Poisson singular integral

The Abel-Poisson kernel can be used to construct spherical wavelets for solving the Laplace equation in physical geodesy. The main advantage of wavelets constructed in this way is that they are harmonic and that the solution of AGBVPs representing the disturbing gravity potential will be harmonic as well. As it is discussed later, the Abel-Poisson kernel is used as a scaling function for generating spherical wavelets. Also, the theory of PDOs has been developed for solving singular integrals as discussed in subsection 3.1.4. Because of the role of the Abel-Poisson kernel and the Abel-Poisson singular integral in the application of spherical PDOs and spherical wavelets for AGBVPs, both will be discussed in more detail in the sequel. A detailed discussion about singular integrals was provided in Chapter 3; now, only the spherical equivalent will be given, paying special attention to the Abel-Poisson integral.

Definition 5.4 Let us consider a subfamily $\{\Phi_s\} \in \mathbf{L}^1[-1,1]$ similar to function $y(\omega\cdot\eta)$ and satisfying the condition $\hat{\Phi}_s(0) = 1$ for all $s \in (0,\infty)$. Then, for a function $g \in \boldsymbol{\chi}(\Omega)$, the sequence $\{I_s\}$ defined by $I_s = \Phi_s * g$ is called *spherical singular integral*.

The sequence $\{\Phi_s\}$ is called the *kernel* of the singular integral $\{I_s\}$. *As will be seen later* s *plays the role of the scale as in the planar case and is connected to the different levels of spherical MRA.*

A singular integral is assumed to be an *approximate identity* in $\chi(\delta\Omega)$ if

$$\lim_{\substack{s\to 0\\ s>0}} \left\| g - I_s(g) \right\|_{\chi(\delta\Omega)} = 0, \quad \text{for all } g \in \chi(\delta\Omega) \ . \tag{5.16}$$

The definition of approximate identity shows that at zero scale, the spherical singular integral approximates the function g *itself.* If the kernel $\{\Phi_s\}$ is uniformly bounded or

$$2\pi \int_{-1}^{1} \left| \Phi_s(p) \right| dp \le C \,, \tag{5.17}$$

then the corresponding singular integral $\{I_s\}$ is an approximate identity if and only if

$$\lim_{\substack{s\to 0\\ s>0}} \left(\hat{\Phi}_s(n) \right) = 1 \tag{5.18}$$

for all nonnegative n. If the kernel is nonnegative $(i.e.\,, \Phi_s(p) \ge 0)$ for all $s \in (0,\infty)$ then (Freeden and Windheuser ,1997) the following properties are equivalent:

- $\{I_s\}$ is an approximate identity in $\chi(\delta\Omega)$ (5.19.1)
- $\lim\limits_{\substack{s\to 0\\ s>0}} \hat{\Phi}_s(n) = 1, \quad \text{for all } n \in \mathbf{N}$ (5.19.2)
- $\lim\limits_{\substack{s\to 0\\ s>0}} \hat{\Phi}_s(1) = 1$ (5.19.3)
- $\lim\limits_{\substack{s\to 0\\ s>0}} \int_{-1}^{\vartheta} \Phi_s(p)dp = 0, \quad \text{for } \vartheta \in (-1,+1)$ (5.19.4)

All these properties of the Abel-Poisson singular integral can be applied in constructing spherical wavelets using an Abel-Poisson integral as a scale function.

Definition 5.5 For $g \in \chi(\delta\Omega)$, $\rho = e^{-s}$, $s \in (0,\infty)$ then the operator $A_\rho(g) : \omega \to A_\rho g(\omega)$ defined by the integral

$$A_\rho g(\omega) = \int_{\delta\Omega} Q_\rho(\omega \cdot \eta) g(\eta) d\sigma(\eta), \quad \omega, \eta \in \delta\Omega \tag{5.20}$$

is called an *Abel-Poisson mean* with an *Abel-Poisson kernel* $Q_\rho(\omega.\eta)$*;* the integral has the name *Abel-Poisson singular integral*, which has all the properties outlined in Eq.(5.19).

The kernel has the well-known closed form

$$Q_\rho(\omega.\eta) = \frac{1}{4\pi} \frac{1-\rho^2}{\left(1+\rho^2-2\rho(\omega\cdot\eta)\right)^{3/2}} = \sum_{n=0}^{\infty} \frac{2n+1}{4\pi} \rho^n P_n(\omega \cdot \eta). \tag{5.21}$$

Then the infinitely differentiable function $A_\rho g$ can be represented on the unit sphere as

$$A_\rho g(\omega) = \sum_{n=0}^{\infty} \sum_{m=-n}^{n} \rho^n \hat{g}(n,j) Y_{n,m}(\omega). \tag{5.22}$$

The form Eq.(5.21) of the Abel-Poisson integral with $\rho \in (0,1)$ *represents a upward continuation from the space inside to the unit sphere. This continuation is not related to the physics of the problem, it represents mathematically only the fact that the density of data decreases with increasing the scale and it corresponds to smoothing. The form Eq.(5.22) will be used later to define the scaling function necessary to construct spherical wavelets. It is interesting to mention that the scale function based on the Abel-Poisson*

integral for a spherical MRA in every j-level of decomposition is defined on a sphere extended as the scale increases. For example, for j level of decomposition the radius is $\rho = e^{-2^{-j}}$.

5.2 Spherical pseudo-differential operators and spherical wavelets

5.2.1 Spherical pseudo-differential operators

Applying a spherical harmonic transform (SHT) equivalent to spherical harmonic expansion for the definition of pseudo-differential operators will give us the so-called spherical PDOs in the *finite spherical domain*. The theory of spherical PDOs is given in Freeden and Windheuser (1997) and in Freeden et al. (1998) and will be used to briefly present the subject of PDOs on a sphere.

Before defining spherical PDOs, it is necessary to see how the Sobolev spaces discussed in Chapter 3 will look on a unit sphere. Consider a linear space $\mathbf{E}$ of all sequences $\{E_{n,m}\}$ of real numbers such that $E = \{E_{n,m} \,|\, E_{n,m} \in \mathbf{R}, n = 0,1,..., \;\; m = -n,...-1,0,1,...,n\}$. Also, let $\{E_n\} \in E$ be a sequence, assuming that $E_{n,m} = E_n$, for $m = -n,...,-1,0,1,...,n$. Consider the set $\mathbf{E}^\infty(\{E_n\})$ of all infinitely differentiable functions g on $\partial\Omega$ as satisfying the condition,

$$\sum_{n=0}^{\infty} \sum_{m=-n}^{n} |E_n|^2 \left(g, Y_{n,m}\right)^2 < \infty \tag{5.23}$$

Now, if $g_1, g_2 \in \mathbf{E}^\infty$, then the following inner product can be defined in $\mathbf{E}^\infty$:

$$(g_1, g_2)_{\mathbf{W}} = \sum_{n=0}^{\infty} \sum_{m=-n}^{n} |E_n|^2 (g_1, Y_{n,m})(g_2, Y_{n,m}) \tag{5.24}$$

and the associated norm will have the form

$$\|g\|_{\mathbf{W}} = (g, g)_{\mathbf{W}} = \sum_{n=0}^{\infty} \sum_{m=-n}^{n} |E_n|^2 (g, Y_{n,m})^2 . \tag{5.25}$$

At this point it is appropriate to define Sobolev spaces on a sphere as following:

Definition 5.6 The Sobolev space $\mathbf{W}^{\partial\Omega} = \mathbf{W}(\{E_n\}; \partial\Omega)$ on the sphere $\partial\Omega$ is the completion of $\mathbf{E}^{\infty}$ under norm Eq.(5.25). The Sobolev spaces on the unit sphere are considered generalized Hilbert spaces with an inner product Eq.(5.24).

As in the case of infinite Euclidean space in Chapter 3, it can be expected that Sobolev spaces on the sphere contain generalized derivatives. The spaces $\mathbf{W}^{\partial\Omega}$ have elements which can be considered as generalized functions (Freeden and Windheuser, 1997). Also, Sobolev spaces can be identified with a subspace of $\mathbf{E}$ by associating to every $g \in \mathbf{W}^{\partial\Omega}$ its sequence $\{\hat{g}(n, j)\}$ such that $\hat{g}(n, m) = (g, Y_{n,m})$. The Laplace (Beltrami) operator applied on spherical harmonics is presented as

$$\Delta_{\sigma} Y_{n,m} = -n(n+1) Y_{n,m} . \tag{5.26}$$

Consider the following operator containing the Laplace (Beltrami) operator applied on the function g on the unit sphere:

$$Bg = (-\Delta_{\sigma} + 1/4)^{\alpha/2} g, \text{ with} \tag{5.27}$$

$$\left[\left(-\Delta_\sigma + 1/4\right)^{\alpha/2} g\right]^{\wedge}(n,m) = \left(n+1/2\right)^{\alpha} \hat{g}(n,m) \tag{5.28}$$

Actually, the operator B is included in the definition of PDOs Eq.(3.55) given by Svensson (1988) assuming a unit sphere with radius $R = 1$. This operator is used to define the Sobolev space $W_\alpha^{\delta\Omega}$ of generalized derivatives of degree α on a unit sphere $\delta\Omega$.

$$\mathbf{W}_\alpha^{\delta\Omega} = \mathbf{W}_\alpha\left(\delta\Omega\right) = \mathbf{W}\left(\left\{\left(n+1/2\right)^{\alpha}\right\}; \delta\Omega\right) \text{ with norm} \tag{5.29}$$

$$\left\|g\right\|_{W_\alpha(\delta\Omega)} = \left\|\left(-\Delta_\sigma + 1/4\right)^{\alpha/2}\right\|_{L^2(\delta\Omega)} . \tag{5.30}$$

It is clear that for $\alpha = 0$, $\mathbf{W}_0(\delta\Omega) \equiv \mathbf{L}^2(\delta\Omega)$ and the norm Eq.(5.30) is simply an $\mathbf{L}^2$-norm. Let $t < \alpha$; then the operator $\left(-\Delta_\sigma + 1/4\right)^{t/2}$ is a bounded operator from $\mathbf{W}_{\alpha+t}(\delta\Omega)$ to $\mathbf{W}_\alpha(\delta\Omega)$, which means it has an inverse operator $\left(-\Delta_\sigma + 1/4\right)^{-t/2}$. The definition of spherical PDOs is slightly different from the PDOs in an infinite domain, due to the use of spherical harmonic expansions.

Definition 5.7 For some $t \in \mathbf{R}^1$ let $\left\{\hat{\Lambda}(n)\right\}_{n=0.1....}$ be a sequence of real numbers $\lim_{n\to\infty}\left|\hat{\Lambda}(n)\right|/(n+1/2)^t = const \neq 0$, $t \in \mathbf{R}^1$. Then the operator $\Lambda : \mathbf{W}_\alpha(\delta\Omega) \to \mathbf{W}_{\alpha-t}(\delta\Omega)$, defined by

$$\Lambda(g) = \sum_{n=0}^{\infty}\sum_{m=-n}^{n} \hat{\Lambda}(n)\hat{g}(n,m)Y_{n,m}, \quad g \in \mathbf{W}_\alpha(\delta\Omega) \tag{5.31}$$

is called a *spherical pseudo-differential operator* of order t and $\left\{\hat{\Lambda}(n)\right\}$ is called a *spherical symbol*. Here, g is a function given on $\delta\Omega$, $\hat{\Lambda}, \hat{g}$ are spherical harmonic expansions of the PDO and the function, and $Y_{n,m}$ are surface spherical harmonics.

If $\lim_{n\to\infty}\left|\hat{\Lambda}(n)\right|/(n+1/2)^t = 0$ for all $t \in \mathbf{R}^1$, then the operator $\Lambda : \mathbf{W}_\alpha(\delta\Omega) \to \mathbf{C}^\infty(\Omega)$ is called a *pseudo-differential operator of order* ∞. Spherical symbols have the following important properties:

$$\left(\Lambda_1 + \Lambda_2\right)^{\wedge} = \hat{\Lambda}_1 + \hat{\Lambda}_2 \tag{5.31.1}$$

$$\left(\Lambda_1\Lambda_2\right)^{\wedge} = \hat{\Lambda}_1\hat{\Lambda}_2 \tag{5.31.2}$$

$$\left(\Lambda^{-1}\right)^{\wedge} = 1/\hat{\Lambda} \tag{5.31.3}$$

$$\Lambda(Y_{n,m}) = \hat{\Lambda}(n)Y_{n,m}\,. \tag{5.31.4}$$

The following lemma 5.1, taken from Freeden and Windheuser (1997), gives the error of substituting a function $g \in \mathbf{W}_\alpha(\delta\Omega)$ by its N^{th} truncated spherical harmonic expansion.

Lemma 5.1 For $g \in \mathbf{W}_\alpha(\delta\Omega)$, $\alpha > 1$ the approximation error is

$$\sup_{\omega\in\delta\Omega}\left|g(\omega) - \sum_{n=0}^{N}\sum_{m=-n}^{n}\hat{g}\left(n,m\right)Y_{n,m}\right| \le \frac{C}{N^{\alpha-1}}\left\|g\right\|_{\mathbf{W}_\alpha(\delta\Omega)}, \tag{5.32}$$

where the constant C depends only on α.

Using these properties of spherical symbols and after some derivations, the analogies between PDOs used by Svensson (1988) and Rummel, (1997), and known geodetic operators are derived and shown in Table 5.1. They can be also found in Chapter 3 but for the planar case (Keller, 2003).

Table 5.1: Spherical PDOs, spherical symbols and geodetic operators

Name	Symbol	PDO - Spherical symbol	Name	Symbol	Inverse PDO - Spherical symbol
Gravity anomalies	A	(n-1)/R	Stokes' formula	A^{-1}	R/(n-1)
Gravity disturbances	(I-C) =A+2/R	(n+1)/R	Hotine's formula	$(I-C)^{-1}$ $=(A+2/R)^{-1}$	R/(n+1)
Gradient operator	-C	-(n+2)/R		$-C^{-1}$	-R/(n+2)
	AC=CA	$(n+2)(n-1)/R^2$		$(AC)^{-1}$	$R^2/(n+2)/(n-1)$
Second radial derivative	C(I-C)	$(n+2)(n+1)/R^2$		$(C(I-C))^{-1}$	$R^2/(n+2)/(n+1)$

All PDOs are generalized functions, which in fact creates difficulties in the application of compatibility conditions along the coastline. At the same time, compatibility conditions have to be locally applied. In this case, the combination between spherical PDOs and spherical wavelets can help us to overcome this problem.

5.2.2 Spherical wavelets

The application of multiresolution analysis (MRA) and wavelets with well known types of wavelet transforms is not suitable for the solution of AGBVPs because known wavelets for an infinite (planar) domain are not harmonic functions. To solve the problem, new wavelet methods for approximating harmonic functions have been suggested in Freeden and Schreiner (1995). Spherical wavelets are useful for the solution of AGBVPs; they are harmonic and have good space and spectral localization properties, which are necessary for the application of compatibility (smoothness) conditions. Spherical wavelets are a result of applying "rotation" and "dilation" operators. In the case

of classical wavelets, the operators are "translation" and "dilation" of a mother wavelet. Another characteristic of spherical wavelets is the way of deriving the mother wavelet. The kernels of spherical singular integrals are used as spherical scaling functions. As a spherical scaling function for the solution of AGBVPs, the most suitable kernel is the Abel-Poisson kernel because it is harmonic (Freeden and Windheuser, 1996) and correspond to the nature of the Earth's gravity potential.

5.2.2.1 Continuous spherical wavelet transform

The following definition provided in Freeden and Windheuser (1997) gives the spherical wavelet transform which is continuous in both spatial and scale domains.

Definition 5.8 A subfamily $\{\psi_s\}$ of the space $\mathbf{L}^2[-1,1]$ is called a *spherical wavelet of order l* if the corresponding sequence $\{\hat{\psi}_s(n)\}$ satisfies the following *admissibility* conditions:

(i) for $n = l+1, l+2, \ldots$

$$\int_0^\infty \left(\hat{\psi}_s(n)\right)^2 \frac{ds}{s} = 1 \tag{5.33}$$

(ii) for $s \in (0,\infty)$ and $n = 0,\ldots l$

$$\hat{\psi}_s(n) = 0 \tag{5.34}$$

(iii) for $R \in (0,\infty)$

$$\sum_{n=m+1}^{\infty} \frac{2n+1}{4\pi} \int_R^\infty \left(\hat{\psi}_s(n)\right)^2 \frac{ds}{s} < \infty \tag{5.35}$$

(iv) for all $R \in (0,\infty)$

$$2\pi \int_{-1}^{1} \left| \int_{R}^{\infty} \left(\psi_s(p)\right)^2 \frac{ds}{s} \right| dp \le C, \tag{5.36}$$

where C is a positive constant independent of R.

The function $\psi = \psi_1$, when $s = 1$, is called the *spherical mother wavelet*. The condition Eq.(5.34) represents the fact that the wavelet has m vanishing moments and it is of order m. The wavelet corresponding to scale s and point η on the sphere is defined as:

$$\psi_{s,\eta} : \omega \to \psi_{s,\eta}(\omega) = \psi_s(\omega,\eta) = \mathbf{R}_\eta \mathbf{D}_s \psi(\bullet.\omega),\ \omega \in \delta\Omega \tag{5.37}$$

or *it can be considered a rotated and dilated version of the mother wavelet, where the 'η – rotation* operator $\mathbf{R}_\eta$*' and the 's – dilation* operator $\mathbf{D}_s$*' are given by*:

$$\mathbf{R}_\eta : \psi(\bullet.\omega) \to \mathbf{R}_\eta \psi(\bullet.\omega) = \psi(\eta.\omega), \text{ and} \tag{5.38}$$

$$\mathbf{D}_s : \psi(\bullet.\omega) \to \mathbf{D}_s \psi(\bullet.\omega) = \psi_s(\bullet.\omega). \tag{5.39}$$

Continuous spherical wavelets use the scale $s \in (0,\infty)$ which is defined as continuous.

Definition 5.9 Let $\{\psi_s\}, s \in (0,\infty)$, be a spherical wavelet of order l. Then the spherical wavelet transform $WT_\psi g(s;\eta) : \mathbf{L}^2(\delta\Omega) \to \mathbf{L}^2\left((0,\infty)\times\delta\Omega\right)$ is defined by

$$WT_\psi g(s;\eta) = \left(\psi_{s,\eta} g\right)_{\mathbf{L}^2(\delta\Omega)} = \int_{\delta\Omega} \psi_{s,\eta}(\omega) g(\omega) d\sigma(\omega). \tag{5.40}$$

The continuous spherical wavelet transform WT_ψ is invertible on function space $g \in \mathbf{L}^2(\delta\Omega)$ under the conditions $\hat{g}(n,m) = 0$ for $n = 0,1...l$ and $m = -n...0...n$. This means that the inverse transform exists and it is given by the reconstruction formula.

Theorem 5.2 (Reconstruction formula) Let $\{\psi_s\}, s \in (0,\infty)$ be a spherical wavelet of order l. If $g \in \mathbf{L}^2(\Omega)$ satisfies $\hat{g}(n,m) = 0$ *for* $n = 0,1...l$ and $m = -n...0...n$, then

$$g = \int_{\delta\Omega} \int_0^\infty WT_\psi g(s,\eta) \psi_{s;\eta}(\bullet) \frac{ds.d\sigma(\eta)}{s}, \tag{5.41}$$

For an arbitrary function $y_R : p \to y_R(p), p \in [-1,1]$ it is possible to have

$$y_R(p) = \sum_{n=0}^{l} \frac{2n+1}{4\pi} P_n(p) + \sum_{n=l+1}^{\infty} \left(\int_R \left(\hat{\psi}_s(n)\right)^2 \frac{ds}{s} \right) P_n(p). \tag{5.42}$$

The form Eq.(5.42) gives the link between singular integral theory (background of PDOs) and spherical wavelets. Furthermore, this form is used to construct scaling functions by using certain types of wavelets or vice versa.

5.2.2.2 Continuous spherical scaling function

There are two main ways of constructing spherical MRA, the first one is by using given wavelets to construct the corresponding *scaling function*. The second one is using a given scaling function to define the corresponding wavelet function. The first way is given by the following definition.

Definition 5.10 Let $\{\psi_s\}, s \in (0,\infty)$ be a spherical wavelet of order l. Then the *corresponding continuous spherical* function $\{\varphi_R\}, R \in (0,\infty)$ is defined by

$$\varphi_R = \sum_{n=0}^{\infty} \frac{2n+1}{4\pi} \hat{\varphi}_R(n) P_n \tag{5.43}$$

and

$$\hat{\varphi}_R(n) = \begin{cases} 1, & n = 0,1,...,l \\ \left(\int_R^{\infty} \left(\hat{\psi}_s(n) \right)^2 \frac{ds}{s} \right)^{1/2}, & n = l+1, l+2,... \end{cases} \tag{5.44}$$

If the wavelet is known the spherical symbol of the scaling function can be determined by Eq.(5.44). *The following corollary gives the procedure for determining the spherical wavelet if the scaling function is known. It can be useful to construct spherical wavelets based on the use of the Abel-Poisson kernel as a scaling function*.

Corollary 5.1 Suppose that $\{\varphi_R\}, R \in (0,\infty)$, is the uniformly bounded kernel of an approximate identity. Furthermore,let the coefficients $\hat{\varphi}_R(n), R \in (0,\infty), n = l+1, l+2,...$ as function of R be differentiable and decreasing. Moreover, assume that

$$\begin{aligned} &\hat{\varphi}_R(n) = 1, n = 0,...l \\ &\lim_{R \to \infty} \hat{\varphi}_R(n) = 0, n = l+1, l+2,... \end{aligned} \tag{5.45}$$

Then the associated spherical wavelet $\{\psi_s\}, s \in (0,\infty)$ of order l is given by

$$\hat{\psi}_s(n) = \left(-s \frac{d}{ds} \left(\hat{\varphi}_s(n) \right)^2 \right)^{1/2} \tag{5.46}$$

for $s \in (0,\infty)$ and $n = 0,1,...$

If the Abel-Poisson kernel is used as spherical scaling function (Freeden and Windheuser, 1997) as presented by

$$\varphi_R(p)=\sum_{n=0}^{l}\frac{2n+1}{4\pi}P_n(p)+\sum_{n=l+1}^{\infty}\frac{2n+1}{4\pi}e^{-nR}P_n(p), \tag{5.47}$$

the *continuous spherical Abel-Poisson wavelet* $\{\psi_s\}, s\in(0,\infty)$ will have the form

$$\psi_s(p)=\sum_{n=l+1}^{\infty}\frac{2n+1}{4\pi}\hat{\psi}_s(n)P_n(p), \qquad \cos\theta=p\in[-1,+1] \tag{5.48}$$

where

$$\hat{\psi}_s(n)=\begin{cases}\left(-s\dfrac{d}{ds}\left(e^{-2ns}\right)\right)^{1/2}=\sqrt{2s}\sqrt{n}e^{-ns}, & n>l\\ 0, & \text{else}\end{cases}. \tag{5.49}$$

As a consequence, the continuous version of an Abel-Poisson spherical wavelet is

$$\psi_s(p)=\sqrt{2s}\sum_{n=l+1}^{\infty}\frac{2n+1}{4\pi}\sqrt{n}e^{-ns}P_n(p), \quad p\in[-1,+1]. \tag{5.50}$$

5.2.2.3 Scale discretized spherical wavelet transform

The continuous wavelet transform is defined over the entire scale domain. To discretize the wavelets along the scale axis, the so-called *spherical wavelet packet (P-wavelet)* is introduced by

$$\hat{\psi}_j^P(n)=\left(\int_{s_{j+1}}^{s_j}\left(\hat{\psi}_s(n)\right)^2\frac{ds}{s}\right)^{1/2}, n=0,1... \tag{5.51}$$

It is clear that it for $n=l+1,l+2,...$, the following equation holds:

$$\sum_{j=-\infty}^{\infty}\left(\hat{\psi}_j^P(n)\right)^2=\int_0^{\infty}\left(\hat{\psi}_s(n)\right)^2\frac{ds}{s}=1 \tag{5.52}$$

The corresponding *P-scale Abel-Poisson* scaling function and wavelet are defined by

$$\varphi_j(p)=\sum_{n=0}^{l}\frac{2n+1}{4\pi}P_n(p)+\sum_{n=l+1}^{\infty}\frac{2n+1}{4\pi}e^{-ns_j}P_n(p) \tag{5.53}$$

with

$$\psi_j(p)=\sum_{n=l+1}^{\infty}\frac{2n+1}{4\pi}\hat{\psi}_j(n)P_n(p),\qquad \cos\theta=p\in[-1,+1] \tag{5.54}$$

where

$$\hat{\psi}_j(n)=\begin{cases}\left(e^{-2ns_{j+1}}-e^{-2ns_j}\right)^{1/2}, & n>l\\ 0, & \text{else}\end{cases}. \tag{5.55}$$

Further discretization is also possible with so-called modified *M-scale wavelets* given by

$$\begin{aligned}\psi_j^M&=\varphi_{j+1}^P-\varphi_j^P\\ \tilde{\psi}_j^M&=\varphi_{j+1}^P+\varphi_j^P\end{aligned} \tag{5.56}$$

which satisfy the property

$$\sum_{j=-\infty}^{\infty}\hat{\psi}_j^M(n)\hat{\tilde{\psi}}_j^M(n)=1,\ \text{for}\ n=l+1,l+2,... \tag{5.57}$$

where $\tilde{\psi}_j^M$ is the dual wavelet necessary for the reconstruction step.

The discretization of the scale integral is based on its division in subsequent subintegrals. This representation leads to wavelet packets (P-wavelets). The next step of discretization is to use the sum of discrete scale sequences $\{s_j\}$, as implemented in Daubechies' idea (Mallat, 1998) for discretization of a continuous integral. In this case a *stability condition* needs to be satisfied to ensure the reconstruction step. *The stability conditions are the same as the frame limits discussed in Chapter 4 and they have all the properties of frame conditions discussed there*. Discretized in this way, wavelets are called a *D-wavelets* (that is named after D(aubechies)-scale discretized wavelet).

Definition 5.11 Suppose that $\{s_j\}, j \in \mathbf{Z}$ is a scale sequence satisfying $\lim_{j=-\infty} s_j = \infty$ and $\lim_{j=\infty} s_j = 0$. Let $\{\psi_s\}$ be a spherical wavelet of order m with corresponding scale discretized sacle function $\{\varphi_j^P\}, \varphi_j^P = \varphi_{s_j}, j = \mathbf{Z}$. Then the family $\{\psi_j^D\}, \psi_j^D = \psi_{s_j}, j \in \mathbf{Z}$ is called a *spherical D-wavelet* of order l if, for $n = l+1, l+2, \ldots$ if the *D-stability condition Eq.(5.58) is satisfied.*

$$P \le \sum_{j=-\infty}^{\infty} \left(\psi_j^D(n)\right)^2 \le Q, \tag{5.58}$$

This is equivalent to the condition

$$P\|g\|^2_{\mathbf{L}^2(\delta\Omega)} \le \left\|WT_\psi^D g\right\|^2_{\mathbf{L}^2(\mathbf{Z}\times\delta\Omega)} \le Q\|g\|^2_{\mathbf{L}^2(\delta\Omega)} \tag{5.59}$$

and can be used to apply smoothness conditions as explained in Chapter 4. For the dual D-wavelets required for the reconstruction step, it holds that

$$\hat{\tilde{\psi}}_j^D(n) = \frac{\hat{\psi}_j^D(n)}{\sum_{k=-\infty}^{\infty} \left(\hat{\psi}_k^D(n)\right)^2}, j \in \mathbf{Z} \tag{5.60}$$

stated in terms of stability conditions,

$$\frac{1}{Q} \le \sum_{j=-\infty}^{\infty} \left(\hat{\tilde{\psi}}_j^D(n)\right)^2 \le \frac{1}{P}.$$

Eq.(5.61)

In the case of orthogonal spherical wavelets, or $P = Q$, the spherical symbol of the dual wavelet is simply

$$\hat{\tilde{\psi}}_j^D(n) = \frac{1}{P}\hat{\psi}_j^D(n). \tag{5.62}$$

Finally, as a D-scaling function at the $J - level$ of decomposition, the function will be considered

$$\hat{\varphi}_J^D(n) = \left(\sum_{j=-\infty}^{J-1} \hat{\psi}_j^D(n)\hat{\tilde{\psi}}_j^D(n) \right)^{1/2}. \tag{5.63}$$

It provides an approximation of a function corresponding to the $J - level$ of the MRA.

5.2.2.4 Spherical Abel-Poisson multiresolution analysis

According to Freeden and Windheuser (1997) the usual dyadic MRA on the plane is not applicable on a sphere. The reason is because the translations on the plane are substituted by rotations on the sphere and, instead of the infinite plane, a finite sphere is used as a boundary on which data are given. To explain the meaning of the spherical Abel-Poisson MRA, let us assume the scale $s = 2^{-J}$ to be discretized in a dyadic way, but now the MRA means "*blowing up*" the spheres $\delta\Omega_J$ to the unit sphere $\delta\Omega$; see Figure 5.1. The spherical MRA produced by the Abel-Poisson kernel is considered as a *harmonic upward*

continuation from the inner space to $g \in \mathbf{L}^2(\partial\Omega)$, which means going from a sphere with radius $\rho_J = e^{-2^{-J}}$ to the unit sphere $\partial\Omega$.

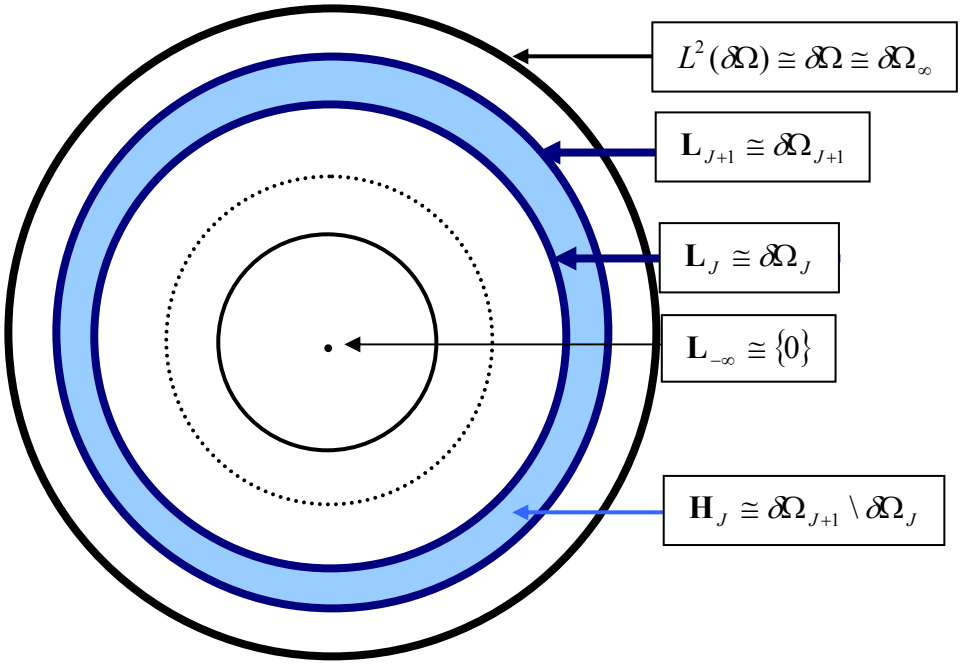

Figure 5.1: Abel-Poisson multiresolution analysis

5.3 Spherical pseudo-differential operators and spherical wavelets for solutions of AGBVPs and explicit form of compatibility conditions along the coastline

In general, spherical PDOs, spherical harmonics and spherical wavelets can be combined to solve the AGBVPs. The disturbing potential T and the observations (boundary conditions) can be related through PDOs; (see diagram in Figure 5.2).

5.3.1. Solution of the Neumann BVP in terms of spherical wavelets for the fixed AGBVP

The boundary condition can be formulated on land for the fixed AGBVP using geoid heights N_{GPS} from GPS/leveling. It will take the form

$$\left| -\frac{\partial T}{\partial r} = \delta g_L = \Delta g_L + \frac{2\gamma}{R} N_{GPS} \quad on \quad \delta\Omega_L \right. , \tag{5.64}$$

where γ is the normal gravity and N_{GPS} is the geoid height. After merging gravity disturbances at sea and on land, the wavelet solution of Neumann's problem discussed in Freeden and Schneider (1998) can be applied. The form of this solution is

$$\begin{aligned} T_J(\omega) = & \sum_{n=1}^{M_0} \boxed{b_n^0} \sum_{k=0}^{m} \sum_{l=1}^{2k+1} \sum_{i=1}^{M} \boxed{a_i^{k,l}} \hat{\Phi}_0(k) \delta g(\eta_i^M) Y_{-k-1,l}(R; \varsigma_n^{M_0}) \Phi_{0;y_n^{M_0}}(\omega) \\ & + \sum_{j=0}^{J} \sum_{n=1}^{M_J} \boxed{b_n^j} \sum_{k=0}^{m} \sum_{l=1}^{2k+1} \sum_{i=1}^{M} \boxed{a_i^{k,l}} \hat{\Psi}_j(k) \delta g(\eta_i^M) Y_{-k-1,l}(R; \varsigma_n^{M_0}) \tilde{\Psi}_{0;y_n^{M_0}}(\omega) \end{aligned} \tag{5.65}$$

where T is the disturbing potential; $\omega, \eta, \varsigma \in \delta\Omega$, $Y_{-k-1,l}$ are the outer harmonics; $\Phi, \tilde{\Psi}$ are the scale function and the dual wavelet; $\hat{\Phi}, \hat{\Psi}$ are the spherical symbols for scale function and wavelet function; δg are the boundary conditions (gravity disturbances); and J is the level of wavelet decomposition. For detailed information about the notation used, see Eqs. (67) in Freeden and Schneider (1998).

All coefficients b_n^0, b_n^j, a_i^k in front of the scale functions (approximate coefficients) and those in front of the wavelet functions (detail coefficients) are spatially distributed in every J-level of decomposition. These coefficients can be determined separately and independently for a certain configuration and J-level of wavelet approximation. Now, the coefficients could be limited up to a certain magnitude using the stability conditions for different types of wavelets. The stability conditions correspond to the definition of the frames (see 5.66) and they will have the form

$$\begin{aligned} & P \le \sum_{j=-\infty}^{\infty} ((\hat{\Psi}_j)\ (n))^2 \le Q \quad or \\ & P \left\| \delta g \right\|^2_{\mathbf{L}^2(\delta\Omega)} \le \sum_{j=-\infty}^{\infty} \left\| (WT)_\Psi (\delta g)(j;.) \right\|^2_{\mathbf{L}^2(\delta\Omega)} \le Q \left\| \delta g \right\|^2_{\mathbf{L}^2(\delta\Omega)} \end{aligned} . \tag{5.66}$$

Restricting the detail (wavelet) coefficients is equivalent to putting smoothing conditions on the derivatives. Typical for this numerical solution is that the smoothing conditions are imposed on the boundary data.

5.3.2. Combination of spherical harmonics, wavelets and PDOs for solution of AGBVPs

The following Figure 5.2 shows how to combine spherical harmonics, spherical wavelets and spherical PDOs to represent every functional of the disturbing potential and the potential itself. This scheme is based on the idea in Freeden and Windheuser (1997) for combining spherical harmonics (for low frequencies) and spherical wavelets (for high frequencies), with spherical PDOs representing different functionals of disturbing potential. The following notations are used: ξ and η are points on the sphere; $\widetilde{\psi}_{j;\eta}$ is the dual wavelet; $(\hat{\psi}_j)(n)$ is the spherical wavelet symbol; $\widetilde{\psi}_{j;\eta} * K_\Lambda$ is the convolution of the dual wavelet and the kernel of the corresponding PDO; and j is the level of wavelet decomposition.

Now, it will be proceeded with the answer of the two main questions : *How to apply spherical PDOs and spherical wavelets to obtain numerical solutions of the fixed AGBVP II; and how to have an explicit form of the compatibility conditions along the coastline.*

5.3.3. Numerical solution of AGBVPs by combination of spherical harmonics, wavelets and PDOs

This numerical solution is based on the representation of functionals of the disturbing potential as PDOs through their spherical symbols, which can be considered as eigenvalues of respective PDOs. The extension and restriction operators used in Eskin (1980) can be applied to define the mappings *L* and *M*. In the end, the compatibility

COMBINED SOLUTION

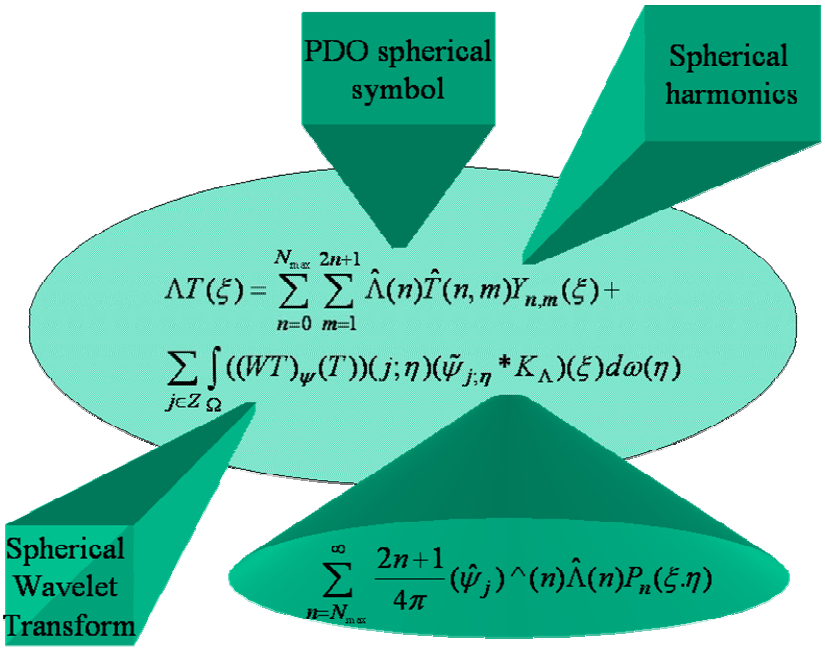

Figure 5.2: Combined solution in a general form

conditions can be applied in an explicit way to have a numerical solution of the fixed AGBVP. To combine a spherical harmonic expansion with spherical PDOs and wavelets according to the diagram in Figure 5.2, the spherical harmonic solution (in the form of a geopotential model) must be subtracted from the data. For the residual part of every functional of the disturbing potential it is valid

$$\begin{aligned} \Lambda T(\xi) &= \sum_{j \in z} \int_{\delta\Omega} (WT)_{\psi}^{Z}(T)(j;\eta)(\tilde{\Psi}_{j;\eta}^{A} * K_{\Lambda}) d\sigma(\eta) \\ &= \sum_{j \in z} \int_{\delta\Omega} (WT)_{\psi}^{Z}(T)(j;\eta) \sum_{n=N_{\max}}^{\infty} \frac{2n+1}{4\pi} (\hat{\tilde{\psi}}_j^{Z})(n)\hat{\Lambda}(n)P_n(\xi \cdot \eta) d\sigma(\eta) \end{aligned} \tag{5.67}$$

where Z is the type of the *wavelet packet* used. For example, Z can be used as equal to *P, M or D-wavelet packets* described in detail in Freeden and Windheuser (1997). Changing the order of integration and summation yields

$$\Lambda T(\xi)=\sum_{j\in\mathbf{Z}}\sum_{n=N_{\max}}^{\infty}\frac{2n+1}{4\pi}\left(\hat{\tilde{\psi}}_j^{A}\right)(n)\hat{\Lambda}(n)\int_{\delta\Omega}\left(WT\right)_{\psi}^{A}(T)(j;\eta)P_n(\xi.\eta)d\sigma(\eta)\,. \tag{5.68}$$

The integral could be transformed in a discrete form using discrete wavelet representation (Freeden and Windheuser ,1997, pp. 32-33) in the following way:

$$\begin{aligned}(WT)_{\Psi}^{Z}(T)(j;\eta)&=\int_{\delta\Omega}T(\xi)\Psi_{j;\eta}^{Z}(\xi)d\sigma(\xi)\\&=\sum_{l=1}^{M}c_l^{j;\eta}T(\xi_l)\\&=\sum_{l=1}^{M}\psi_{j;l}^{Z}(\eta)T(\xi_l)\end{aligned} \tag{5.69}$$

$$\Downarrow$$

$$\begin{aligned}\int_{\delta\Omega}(WT)_{\Psi}^{Z}(T)(j;\eta)P_n(\xi\cdot\eta)d\sigma(\eta)&=\int_{\delta\Omega}\sum_{l=1}^{M}(\tilde{\Psi}_{j;l}^{Z})T(\xi_l)P_n(\xi\cdot\eta)d\sigma(\eta)\\&=\sum_{l=1}^{M}T(\xi_l)\int_{\delta\Omega}\tilde{\Psi}_j(\xi_l\cdot\eta)P_n(\xi\cdot\eta)d\sigma(\eta)\end{aligned} \tag{5.70}$$

After applying the Funk-Hecke formula, we will have for the discrete representation of the integral,

$$\begin{aligned}\int_{\delta\Omega}(WT)_{\Psi}^{Z}(T)(j;\eta)P_n(\xi\cdot\eta)d\sigma(\eta)&=\sum_{l=1}^{M}T(\xi_l)(\hat{\tilde{\Psi}}_j^{Z})(n)P_n(\xi_l\cdot\xi)\\&=(\hat{\tilde{\Psi}}_j^{Z})(n)\sum_{l=1}^{M}T(\xi_l)P_n(\xi_l\cdot\xi)\end{aligned} \tag{5.71}$$

Now the functional can be represented as

$$\Lambda T(\xi)=\sum_{n=0}^{\infty}\frac{2n+1}{4\pi}\hat{\Lambda}\ (n)\sum_{l=1}^{M}T(\xi_l)P_n(\xi_l\cdot\xi)\sum_{j=-\infty}^{\infty}((\hat{\tilde{\Psi}}_j^{A})(n))^2\,. \tag{5.72}$$

Example 5.1 Representation of the upward continuation in discrete form (5.72) using the combined application of spherical PDOs and wavelets.

$$\hat{\Lambda}(n) = \left(\frac{R}{r}\right)^{n+1} \text{-upward continuation,} \tag{5.73}$$

$$\sum_{j=-\infty}^{\infty} ((\hat{\tilde{\Psi}}_j^A)(n))^2 = 1 \text{- wavelets are orthonormal,} \tag{5.74}$$

$$\sum_{l=1}^{M} T(\xi_l) P_n(\xi_l.\xi) = \sum_{\lambda'} \sum_{\varphi'} T(\varphi', \lambda', R) P_n(\cos(\theta)) \cos\varphi', \text{ where } \xi = (\varphi, \lambda, r), \quad \xi_l = (\varphi', \lambda', R)$$

and $P_n(\xi_l.\xi) = P_n(\cos(\theta))$, where θ represents the spherical distance between the two points on the sphere and the functional becomes

$$T(\varphi, \lambda, R) = \sum_{n=0}^{N_{\max}} \frac{2n+1}{4\pi} \left(\frac{R}{r}\right)^{n+1} \sum_{\lambda'} \sum_{\varphi'} T(\varphi', \lambda', R) P_n(\cos(\theta)) \cos\varphi'. \tag{5.75}$$

However, this is exactly the discrete form of Poisson's integral. The equations Eq.(5.72) can be successfully used for representing any kind of functional of the disturbing potential as a PDO.

Finally, gravity anomalies on land and gravity disturbances at sea can be represented in the form

$$\Lambda T(\xi) = \sum_{j=0}^{J} \sum_{n=N_{\max}+M_{j-1}+1}^{N_{\max}+M_j} \frac{2n+1}{4\pi} \hat{\Lambda}(n) \left[\left(\hat{\tilde{\psi}}_j^Z\right)(n)\right]^2 \sum_{l=1}^{M} T(\xi_l) P_n(\xi_l.\xi) \tag{5.76}$$

Only the proper spherical symbol must be chosen from Table 5.1. For example, $\hat{A} = (n-1)/R$ for gravity anomalies and $(I-C)\hat{} = (A+2/R)\hat{} = (n+1)/R$ for gravity disturbances.

5.3.4. Explicit form of compatibility conditions

The spherical symbols for PDOs on the unit sphere used in the formulation of compatibility conditions can be written as

$$\begin{aligned}
&\hat{A} = (n+1/2) - 3/2 = (n-1), \\
&\hat{C} = (A+3)^{\wedge} = n+2 \\
&(A+2)^{\wedge} = n+1, \quad \hat{S} = 1/(n-1) \\
&(AC)^{\wedge} = (-\nabla^2 - 2)^{\wedge} = \hat{A}\ \hat{C} = (n-1)(n+2)
\end{aligned} \tag{5.77}$$

According to Eskin (1980), the mappings L and M could be simply considered as extensions assuming zeros for the sea and land. Let us introduce two complementary extensions:

$$\chi = \begin{cases} 1 & on \quad land \\ 0 & at \quad sea \end{cases}, \quad \vartheta = \begin{cases} 0 & on \quad land \\ 1 & at \quad sea \end{cases} \tag{5.78}$$

Then the mappings L and M can be represented as the inverse Fourier transforms of Eq.(5.79):

$$\begin{aligned}
&\hat{L}(\Delta g_L) = \hat{\chi} * \Delta\hat{g} \\
&\hat{M}(\Delta g_L) = \hat{\vartheta} * \Delta\hat{g}
\end{aligned} \tag{5.79}$$

For the specific case of a spherical cap, the Legendre transform will give us the spherical symbol for both extensions as

$$\begin{aligned}
&\hat{L}(n) = 2\pi \int_0^{t_1} \chi(t) P_n(t) dt \\
&\hat{M}(n) = 2\pi \int_0^{t_2} \chi(t) P_n(t) dt
\end{aligned} \tag{5.80}$$

.

For a more complicated coastline, a window in the form of a continent-ocean function can be applied and expanded into spherical harmonics (Simons et al., 1997) over the entire unit sphere, and the spherical symbols can be calculated. In this case, the χ and θ functions will not have only zonal non-null harmonic coefficients. Possible complications may arise from a numerical point of view, when these non-zero harmonic coefficients have to be determined.

Assuming the first term T_1 of the disturbing potential to be zero, the compatibility conditions along the coastline for AGBVP II discussed in Chapter 3 can be given in an explicit form in terms of PDOs and wavelets as

$$\Lambda_L(T) + \Lambda_S(T) = 0 \tag{5.81}$$

with spherical symbols on a unit sphere

$$\begin{aligned} \hat{\Lambda}_L(n) &= (A+2)^{\wedge}\hat{S}\hat{A}\hat{L} = (n+1)\hat{L}(n) \\ \hat{\Lambda}_S(n) &= (A+2)^{\wedge}\hat{S}\,\hat{M}(AC)^{\wedge}\hat{A} \\ &= (n+1)(n+2)(n-1)\hat{M}(n) \end{aligned} \quad . \tag{5.82}$$

Now, the compatibility conditions can be explicitly applied on the detail coefficients in the coastal area at every J-level of decomposition using the representation of Λ_L, Λ_S in terms of spherical PDOs and spherical wavelets.

The possible difficulty will be the determination of spherical symbols for mappings L and M for general shape of the coastline (different from a spherical cap). The reason is that the ocean-land function behaves as a step function, which implies that its spherical harmonic transform contains all frequencies. It is necessary to find a proper way to determine numerically the spherical symbols for both mappings.

5.4 Concluding remarks and summary

In this chapter the theoretical background for the combined application of spherical harmonics, spherical PDOs and spherical wavelets for solutions of AGBVPs was presented. The entire theory has been developed in Freeden and Windheuser (1997) and it is presented to support the final goal of this chapter – numerical solutions of AGBVPs based on spherical harmonics, PDOs and wavelets and an explicit form of compatibility conditions.

The theory of spherical harmonics and spherical harmonic expansions has been briefly presented, along with the theory of singular integrals focused on the Abel-Poisson singular integral. The theory of spherical PDOs, based on singular integrals, has been briefly discussed in terms of its application for AGBVPs providing infinitely smooth solutions. To change the smoothness of the solution along the coastline, spherical PDOs can be combined with spherical wavelets which have a very good localizing property in the spatial domain. The theory of spherical wavelets has been presented again discussing mainly the continuous wavelet transform on the sphere; its scale discretization in the form of different wavelet packets, and the application of the Abel-Poisson kernel as a scaling function to generate the harmonic wavelets necessary to model the harmonic disturbing potential and its functionals.

In subsection 5.3.1, a solution of Neumann's BVP given in Freeden and Schneider (1998) has been used to develop a solution of the fixed AGBVP II. The compatibility conditions can be applied as restrictions of wavelet coefficients and, although the smoothnees conditions are incorporated into the solution, they are applied to the boundary conditions (data). Difficulties in processing are expected due to the huge number of coefficients but, for a certain type of wavelets and data configuration, they could be computed once and separately.

Subsections 5.3.2 and 5.3.3 include a discussion of the combination of spherical harmonics, spherical PDOs and wavelets to generate solutions of AGBVPs including both

the low and high frequency components of disturbing potential. *The discrete form Eq.(5.76) of functionals of disturbing potential has been derived; this is necessary to model both types of observations for a AGBVP in terms of PDOs and wavelets on the sphere. It has been applied in the case of upward continuation showing that, under certain conditions, the equation Eq.(5.75) for upward continuation is exactly the Poisson integral for the space outside the sphere.*

In subsection 5.3.4 the compatibility conditions given by Svensson (1988) in an implicit form were derived in *an explicit form* Eq.(5.81) as two PDOs Eq.(5.82) on land and at the sea. The compatibility conditions are applied directly to the solution (disturbing potential) along the coastline. The main difficulties in this approach are the non-orthogonality of the Abel-Poisson wavelets, which will slow down the processing, and the application of an equidistant grid. Also, the computation of the spherical symbol for the ocean-land function can be considered a serious problem, because this function acts as a step function across the coastline and its spherical spectrum will contain all possible frequencies.

Chapter 6

Numerical solutions of AGBVPs with compatibility conditions along the coastline

In this chapter numerical solutions of the fixed AGBVP II will be presented taking into account the combined use of gravity and GPS/leveling data on land and altimetry plus shipborne gravity data at sea.

A global solution with compatibility conditions along the coastlines is first discussed in a general way in Section 6.1. It will provide the necessary link between the globally defined compatibility conditions and their local applications in terms of spherical wavelets. Also, the local planar applications can be considered as a part of a global procedure for improving global geoid models taking advantage of the availability of very high degree spherical harmonic expansions.

Two *preliminary* solutions are presented first with homogenous data (gravity anomalies) on both sides of the boundary surface only to investigate the effect of smoothing data on the final geoid solution. It is obvious that these two cases do not even present a real AGBVP, but they are necessary as a starting point for further theoretical and practical investigations for finding solutions with compatibility (smoothness) conditions along the coastlines. Two experiments are conducted over the flat coastline of Eastern Canada and over the mountainous and very complicated coastline of Western Canadian and the U.S. coast.

A third solution was obtained, which can be considered as a solution of the fixed AGBVP after the transformation of gravity anomalies on land to gravity disturbances. The smoothness conditions are applied on the boundary conditions (measurements) and on the boundary surface to investigate both effects on the final geoid. The used planar wavelets are not harmonic. But because they have been used on the derivatives of disturbing

potential which are not harmonic either but this is still acceptable. The final solution is applied using FFTs with Hotine's kernel, because on both parts gravity disturbances are available after the transformation of gravity anomalies on land.

The fourth numerical solution is considered as an application of compatibility in the form of coincidence of data and their derivatives across the coastline. The smoothness conditions are incorporated in the solution using combined application of spherical harmonics, spherical PDOs and spherical wavelets. Because spherical wavelets are based on the harmonic Abel-Poisson kernel they are harmonic as well and are more suitable for modeling the disturbing potential than classical planar wavelets.

6.1 Global application of compatibility conditions – complexity and numerical difficulties

The entire theory for the application of PDOs and wavelets was presented on the sphere. The main reason for this is that spherical wavelets based on the spherical harmonics are *harmonic* and the resulting solution for the disturbing potential will be harmonic as well. Also, compatibility conditions were originally defined on the sphere and the complete theory for combination of PDOs and wavelets was developed on the sphere. The global application of the spherical wavelet approach can face many problems like non-orthogonality of wavelets, non-equiangular grids on the sphere, problems with spherical convolution, etc. However, the application of compatibility conditions is local in coastal areas, and the global application will be discussed to provide the necessary link between the globally defined problem and its local application. The global multiresolution applications based on the spherical harmonic analysis and synthesis have been discussed in detail in (Blais and Provins, 2002). The scheme of finding solutions to AGBVPs for global applications is different from the local planar solutions mainly because of different gridding procedures, different properties of spherical convolution, polar complications, non-orthogonality of spherical wavelets, etc. The main steps of global solution are similar to those of local solutions and they will be considered in detail together with the

principal complications and difficulties that can arise. The following general steps can be used to have a global solution with compatibility conditions along the coastlines:

Step 1: *Use of reference gravity field based on spherical harmonic expansion* to extract the contribution of low frequency part of the signal. This can be done by using different geopotential models such as EGM 96 or geopotential models derived by new gravity satellite missions such as CHAMP, GRACE and GOCE, providing high accuracy for low and middle parts of the spectrum.

The usual geodetic spherical harmonic formulation can be used in the form:

$$g(\vartheta,\lambda)=\sum_{n=0}^{\infty}\sum_{m=0}^{n}\left[\bar{C}_{nm}\cos m\lambda+\bar{S}_{nm}\sin m\lambda\right]\bar{P}_{nm}(\cos\vartheta) \tag{6.1}$$

where ϑ is the co-latitude, $\bar{C}_{nm},\bar{S}_{nm}$ are the (geodetically) normalized spherical harmonic coefficients, $\bar{P}_{nm}(\cos\vartheta)$ are the (geodetically) normalized Legendre functions.

Step 2: *Global gridding for improving spherical harmonic coefficients*. Improvements of the spherical harmonic models by adding additional measurements and increasing the degrees and orders both for land and sea part are now computationally feasible. Increasing degrees to 3600 will provide an approximate resolution of 5 km, as demonstrated in resent spherical harmonic computations to very high degrees and orders (Blais and Soofi, 2004). Also, it is possible to carry out the computations separately on land and at sea by simply assuming zeros on the complementary parts. As a result, these improved spherical harmonic coefficients on land ($\bar{C}^{L}_{nm},\bar{S}^{L}_{nm}$) and at sea ($\bar{C}^{S}_{nm},\bar{S}^{S}_{nm}$) can be combined for global gridding resulting in new spherical harmonic coefficients ($\bar{C}^{G}_{nm},\bar{S}^{G}_{nm}$). Different gridding procedures can be applied such as for equiangular or Gaussian grids using the zeros of Legendre polynomials (Sneeuw, 1994; Blais et al., 2000) or Chebyshev quadrature (Blais et al.,

2004). The main disadvantage of Gaussian grids is the fact that in latitude, the zeros of the Legendre polynomials are not equispaced and hence the grid is not equiangular. Other types of gridding such as equilateral or "igloo-like" can be applied as well, with the poles included in or excluded from the grid.

Step 3: *Decomposition and reconstruction step of MRA with spherical wavelets for smoothing data along the coastlines.* Depending on the applications the smoothing can be done globally, regionally and locally. It is possible to separate wavelets from the PDOs because of their linearity. The procedure for smoothing developed for local applications of spherical wavelets can be applied successfully on a regional and local scale. Using the smoothed near- the coastline data the spherical harmonic coefficients can be modified and recomputed providing corrected ($\bar{C}^{C}_{nm}, \bar{S}^{C}_{nm}$).

Step 4: *Application of spherical PDOs to* ($\bar{C}^{C}_{nm}, \bar{S}^{C}_{nm}$) in spectral domain. Different spherical PDOs can be applied corresponding to different data types represented as functionals of the disturbing potential. Furthermore, the compatibility conditions can be globally applied in the explicit form given by (5.81) as a sum of two functionals represented in the form of spherical PDOs (5.82).

Step 5: *Performing inverse SHT and getting the spatial global solution.* Because the compatibility conditions applied globally, regionally and locally, the resulting PDO solution in the form of a global geopotential model of very high resolution will reflect the compatibility (smoothness) conditions along the coastlines.

The third steps can be locally applied on a plane after using appropriate type of map projections. All numerical experiments in the following sections are locally applied on spherical grids. The transition from global to local applications has is discussed in the next Section 6.2.

6.2 From global theoretical formulation to local application of the solution of AGBVP II with compatibility conditions

The problem needed to be solved in this dissertation was defined globally on the sphere but the numerical solutions are given on a spherical grid corresponding to so-called “plate carre map projection” (Svensson, 2003). Actually, spherical scale functions and wavelets were computed on the sphere, but applied as corresponding filters on the planar grid based on spherical coordinates. There are several compromises which allow this procedure to be applied in local areas:

(i) The proof by Svensson (2003) that the solution of the Laplacian locally on the sphere will be different from this on a plane only by a scale constant;
(ii) Keller (2003) has shown that spherical PDOs can be locally applied on a part of the sphere or using suitable projection on a plane tangent to the sphere;
(iii) after subtracting the spherical harmonic part from measurements in the form of a geopotential model the residual part of the gravity signal (different functionals of disturbing potential) can be applied on a local spherical grid;
(iv) spherical wavelets have a very narrow local support and the non-equiangular spherical grid can be acceptable.

The main problem of spherical wavelets – non-orthogonality – still can cause computational difficulties. To overcome them an orthogonalization procedure using Slepian functions (Albertella, A. et al., 1999) can be applied. Another approach is to use certain types of spherical wavelets – for example, H-Shannon spherical wavelets (Freeden and Michel, 2002) – which are orthogonal. In general, Shannon wavelets are band-limited. The Shannon scaling function can be considered as a simple box function in the spectral domain and as a result oscillations in special domain can be expeted (Blais and Provins, 2002). It is considered as an analog of the Haar scaling functions in spatial domain which creates oscillations in spectral domain. Proposed H-Shannon wavelets are bandlimited on the sphere as well. Based on the addition theorem discussed in Chapter 5 these wavelets admit a simple representation and realization. They can be considered as

radial base functions on the sphere. The form of H-Shannon scale and wavelet functions based on the Abel-Poisson kernel is given by:

$$\Phi_j(\psi) = \sum_{n=n_{GPM}}^{N_j} h^n \frac{2n+1}{4\pi} P_n(\cos(\psi))$$
$$\psi_j(\psi) = h^{N_j+1} \frac{2N_j+3}{4\pi} P_{N_j+1}(\cos(\psi)) \qquad (6.2)$$

where if $h=r/R=1$ all data are on the sphere, N_j is the degree of Legendre polynomials corresponding to *j-level*, n_{GPM} is the degree of the used reference geopotential model; ψ is the spherical distance. Finally, H-Shannon scale and wavelet functions can be used to construct corresponding low-pass and high-pass filters necessary for the reconstruction step of a dyadic MRA. In this way, numerical solutions are applied on the spherical grid considered as a projection from the sphere to a plane.

As a reference the global geopotential model EGM96 has been used for all numerical experiments with a resolution of $1^\circ \times 1^\circ$. The resolution of altimetry data corresponds to the resolution of 3-4 km of geodetic altimetry missions. The resolution of land gravity data is not homogenous in mountainous and flat areas, their average resolution is comparable to those of altimetry data. Shipborne gravity data have very high density in coastal areas, but in the ocean they have lower resolution. Again, an average resolution of 3-4 km can be considered acceptable. The lowest resolution is for GPS/levelling data on land (around 40 GPS points all over the area) but they can be considered as most accurate with an vertical error of 1-2 cm. A priori noise level for different types of data is quite different. For altimetry sea surface height it can be considered as 3-4 cm, but the accuracy of altimetry derived geoid depends on the accuracy of the used sea surface topography model. Land gravity data are collected in different time periods and it is difficult to have relevant a priory estimation of the accuracy but an average accuracy of 1 mGal can be considered as representative enough. It is known that the a priori precision of gravity shipborne data is around 3 mGal.

Taking into account the high level of non-homogeneity of the resolution and the noise level of data different irregularities and discrepancies exist and the application of smoothness conditions along the coastline will improve the solution of AGBVPs in terms of a geoid with a less sharp transition across the coastline.

6.3 Preliminary numerical investigations of smoothness effects on geoid determination

6.3.1 Smoothness effects along the coastline on the geoid – flat terrain and simple coastline

6.3.1.1 Area of investigation and data used

Gravity data on land and gravity data derived from altimetry (provided by KMS – solution KMS99) at sea have been used in the region of Newfoundland, Eastern coast of Canada, for the numerical solution of AGBVP II, applying smoothness conditions along the coastline using wavelets. The size of the area is 14x14 degrees and the resolution of the grid is 2x2 arc minutes. To show more details along the coastline, some results are presented in a smaller window (see Figure 6.1).

In the numerical experiment, “Daubechies 4” wavelet decomposition up to third level has been used as it was described in subsection 2.3.4. to detect existing irregularities between both data types and to place additional compatibility conditions on the data along the coastline.

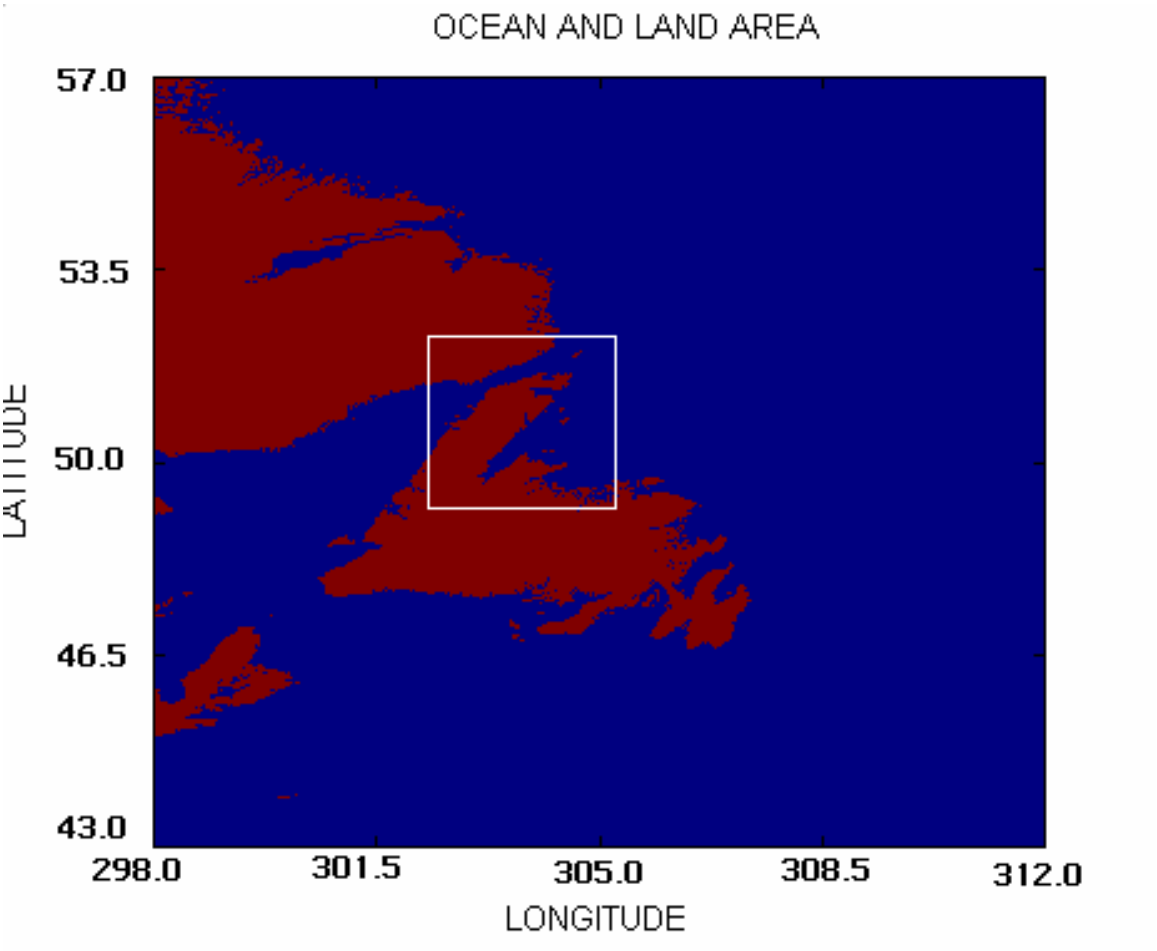

Figure 6.1: Area under study

6.3.1.2 Description of the procedure

The experiment was conducted in the following steps:

- Separate gridding of residual gravity anomalies (referenced to EGM96) on land and at sea, and merging both types of data. This experiment investigates only the effect of smoothing between same types of data and it is not completely equivalent to the formulation of AGBVP II.
- Geoid computation using Stokes formula with the original spherical kernel (by 1D-FFT) applied to the merged data.

- Smoothing gravity anomalies at the coastline using Daubechies fourth wavelet decomposition and reconstruction up to the third level. For every level of decomposition, detail coefficients were restricted up to the RMS values of the coefficients that are not on the coastline. These constraints are equivalent to using additional smoothness conditions on the derivatives of the solution as it was previously discussed in subsections 2.3.4 and 4.4.4.3. The threshold value could be restricted to zero if maximum smoothness is desired, but to take into account the accuracy of the detail coefficients the suggested threshold value is more realistic.
- Geoid computation using Stokes formula with the original spherical kernel (by 1D-FFT) applied to gravity anomalies smoothed only along the coastline.
- Comparison between original and smoothed gravity anomalies and between final geoid solutions from original and smoothed anomalies.

6.3.1.3 Analysis and summary of results for flat and simple coastline

Figure 6.2 shows the ability of "Daubechies 4" wavelets to detect irregularities between different types of data along the coastline.

It is obvious that the greatest values of wavelet coefficients are along the coastline. After this, an investigation of the influence of these conditions on the final geoid solution in the coastal region was conducted. The statistics of the original and smoothed data and of their differences are presented in Table 6.1, Table 6.2 and Table 6.3.

Smoothed gravity anomaly residuals are a result of placing compatibility conditions along the coastline using "Daubechies 4" wavelet decomposition and reconstruction

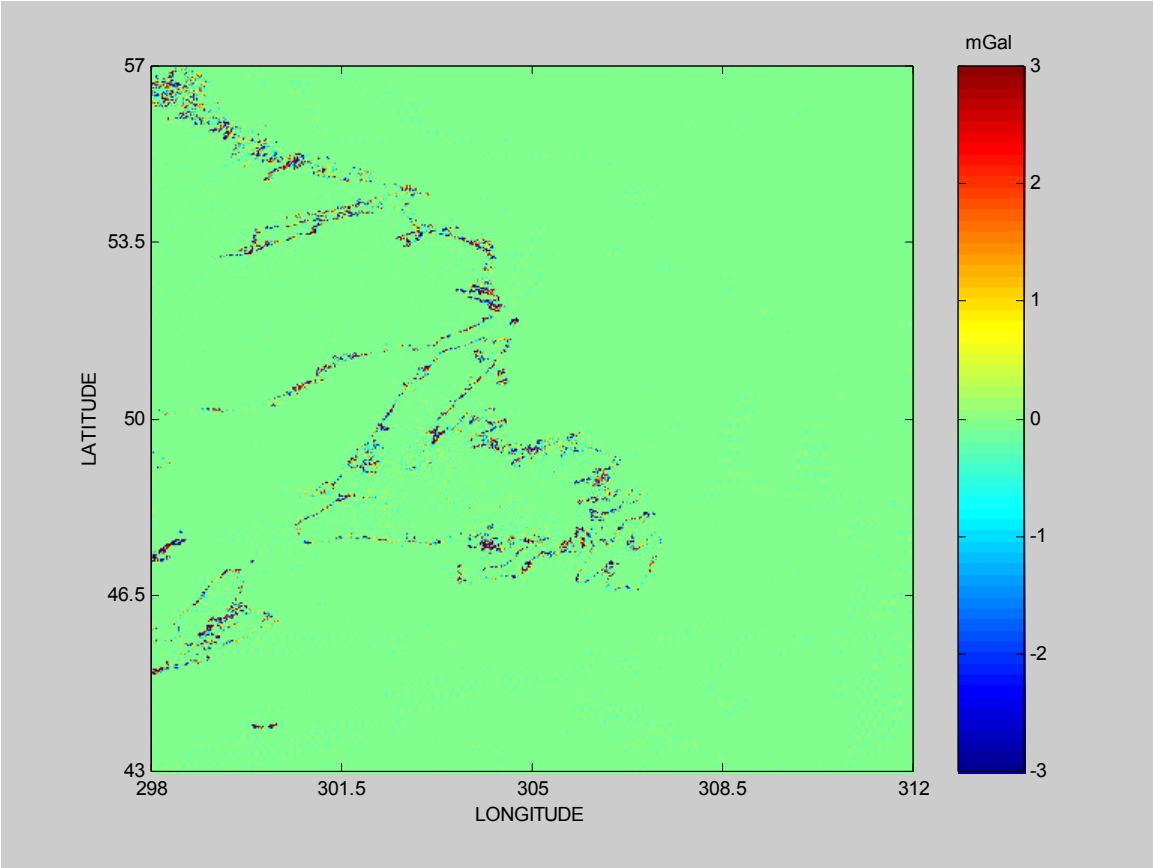

Figure 6.2: Magnitude of diagonal detail coefficients after the first level of "Daubechies 4" wavelet decomposition. Unit: [mGal]

Table 6.1. Original gravity anomaly residuals referenced to EGM96. Unit: [mGal].

max	min	mean	RMS	STD
97.26	-67.81	-0.93	9.65	9.65

Table 6.2. Smoothed gravity anomaly residuals referenced to EGM96 Unit: [mGal].

max	min	mean	RMS	STD
83.89	-65.54	-0.92	9.64	9.60

Table 6.3. Residual gravity anomaly differences (smoothed-original). Unit: [mGal].

max	Min	mean	RMS	STD
42.49	-38.54	0.00	1.76	1.76

(see subsections 2.3.4, 4.4.4.3. and Eq. (4.78)). It is known that "Daubechies 4" has three vanishing moments or it can be considered as a multiscale differential operator of order 3. It is evident that the mean, rms and standard deviation are not changed significantly. In general, the signal is not changed except along the coastline. The discrepancies between the land and KMS gravity data are clearly visible along the coastline (see Figure 6.3). Wavelets have been applied to smooth these discrepancies. It is evident that the irregularities have been smoothed along the coastline, but for the areas away from the coastline there are no significan changes. Applying such a smoothing procedure influences only the coastal area. The differences between smoothed and original data are given in Figure 6.5.

The differences in the entire area range between –39 mGal and 43 mGal. The colour graphs are only for the zoomed area and have been chosen to show more details along the coastline. It is clear that the corrections to the original data from smoothing along the coastline are concentrated along the coastline.

Both original and smoothed data were used to determine the geoid heights in the area under study. The remove-restore technique was applied by removing the effect of geopotential model EGM96 and terrain corrections provided together with the gravity anomalies. The geoid was determined by using 1D FFT spherical Stokes kernel described in Sideris (1999). The differences between these two solutions give us information about the influence of the compatibility conditions on the final geoid solution for the region of investigation. The statistics for the final geoid solutions using original and smoothed gravity anomalies are given in Table 6.4, Table 6.5 and Table 6.6. The differences between the residual geoid heights derived from original residual gravity anomalies and residual geoid heights derived from smoothed residual gravity anomalies show that the smoothing along the coastline does not change the statistics of the entire area. The effect of smoothness is only along the coastline. The magnitude of the effect of the smoothness conditions is between –5 and +5 cm. There are greater values than these

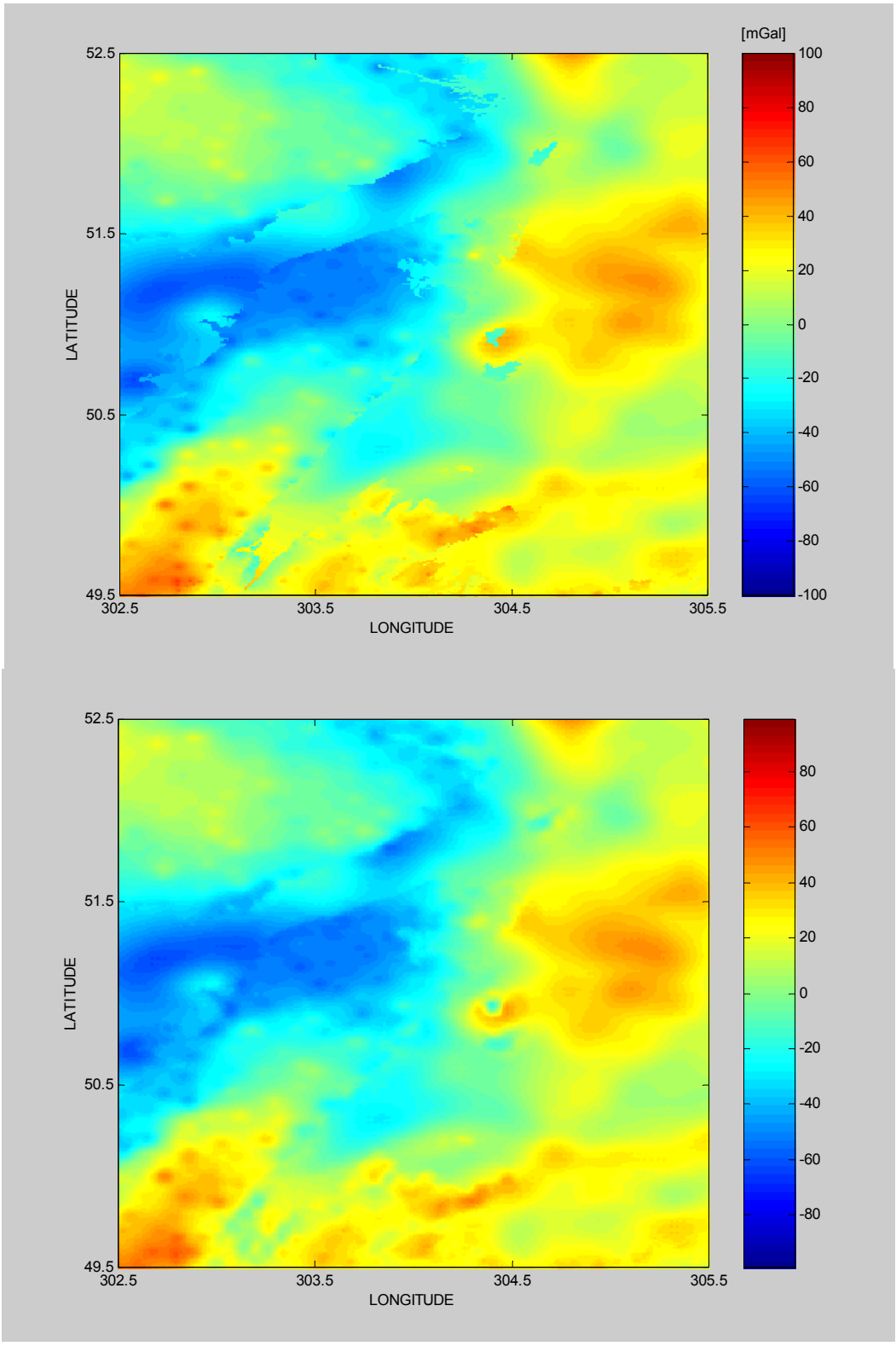

Figure 6.3-6.4: Original and smoothed land gravity and gravity data from altimetry in the area under study. Unit: [mGal]

Table 6.4. Original residual geoid heights. Unit: [m].

max	Min	mean	RMS	STD
0.711	-0.845	-0.045	0.189	0.183

Table 6.5. Smoothed residual geoid heights. Unit: [m].

max	min	mean	RMS	STD
0.719	-0.844	-0.045	0.188	0.183

Table 6.6. Residual geoid heights differences (smoothed-original). Unit: [m].

max	min	mean	RMS	STD
0.045	-0.050	0.000	0.001	0.001

but they are due to edge effects. Smoothing again does not change the mean and rms of the geoid results in the area under study but only the values along the coastline (see Figures 6.6 and 6.7).

Summarizing the results from the numerical experiment the following conclusions are possible:

It was shown that wavelet transforms using wavelets with (n-1) vanishing moments (multiscale differential operators of n^{th} order) can be used successfully for detecting irregularities along the coastline and for smoothing data (compatibility conditions along the coastline). In the numerical experiment, "Daubechies 4" wavelets are considered as 4^{th} order multiscale differential operator.

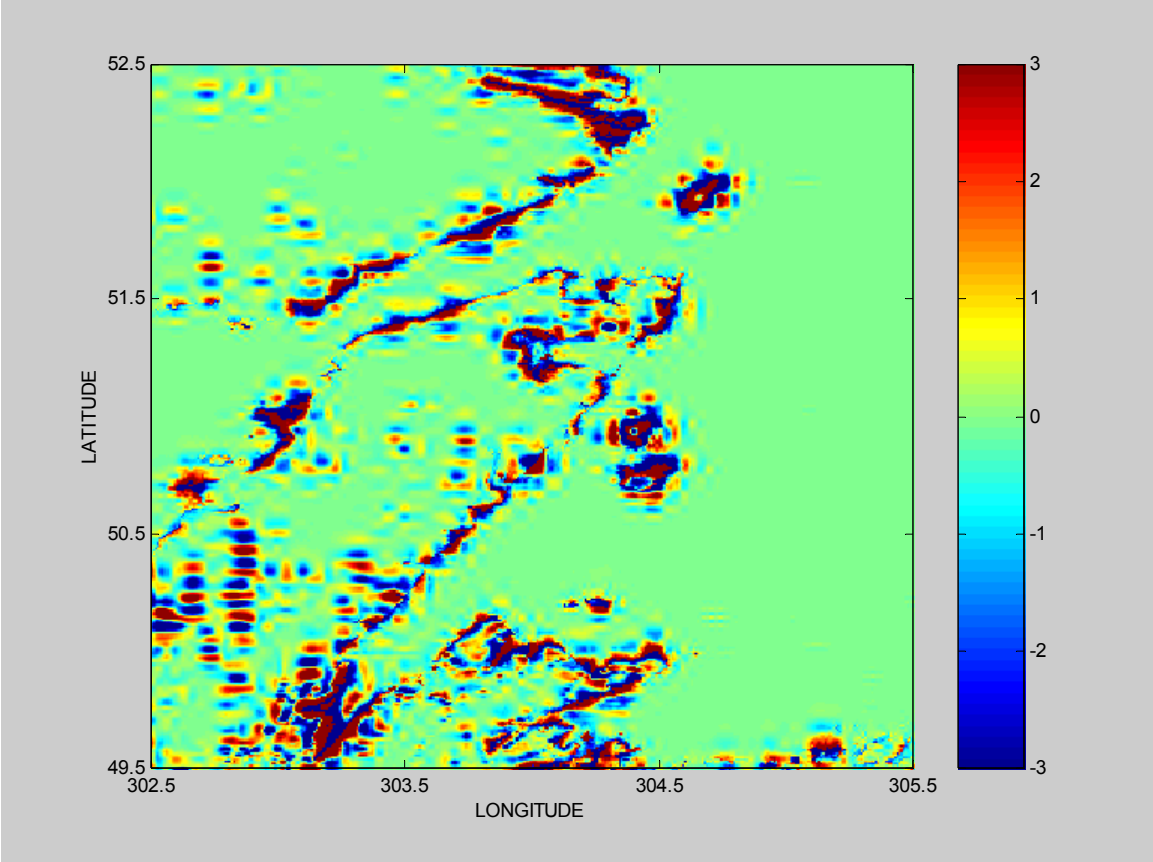

Figure 6.5. Differences between original and smoothed land gravity and gravity data from altimetry in the area under study. Unit: [mGal]

To smooth the data along the coastline, the detail coefficients need to be restricted in every level of decomposition to a certain value. The threshold value could be the average of all detail coefficients, excluding the values along the coastline. The maximum smoothness is possible if detail coefficients are restricted to zero, but to take into account possible errors in the computation of detail coefficients the suggested threshold value seems more realistic.

The differences between smoothed and original gravity anomalies were -39 mGal and 43 mGal for entire area. After the smoothing procedure, the greatest differences were located mostly along the coastline. For areas away from the coastline the differences are negligible, i.e., the used smoothing procedure has influence only along the coastline.

The effect of smoothness on the final geoid solution along the coastline is between ±5 cm in our test area. There is no effect on the regions away from the coastline, except for edge effects.

Although the smoothness effect is not large in this area, the final geoid solution using smoothness conditions along the coastline is theoretically closer to the classical solution (see the discussion in subsection 4.1.3). A numerical solution of an AGBVP should take into account the compatibility conditions along the coastline, especially for cm-level geoid determination.

The area under study is characterized by a flat topography relief. It is expected that in regions with mountains along the coastline or in areas of rougher gravity field in general the smoothness effect will be larger and should be investigated.

6.3.2 Smoothness effects along the coastline on the geoid – mountainous and complicated coastline

6.3.2.1 Area of investigation and data used

Gravity data on land and gravity data derived from satellite altimetry (Sandwell and Smith 1997) at sea have been used in a region of the western Canadian coast, applying smoothness conditions along the coastline using wavelets. The size of the area is 20x20 degrees with a data resolution of 2x2 arc minutes. Figure 6.8 shows the complicated coastline with a lot of small islands. To show more details along the coastline, some results are presented in a smaller window.

The area under study is located between $40° \le \varphi \le 60°$ and $220° \le \lambda \le 240°$ (i.e., the Western US and Canadian Pacific coast). It is characterized by high mountains, which are very close to the coastline. The maximum altitude and depth are 3729 m and –5149 m., respectively. The topography and bathymetry are presented in Figures 6.8 and 6.9.

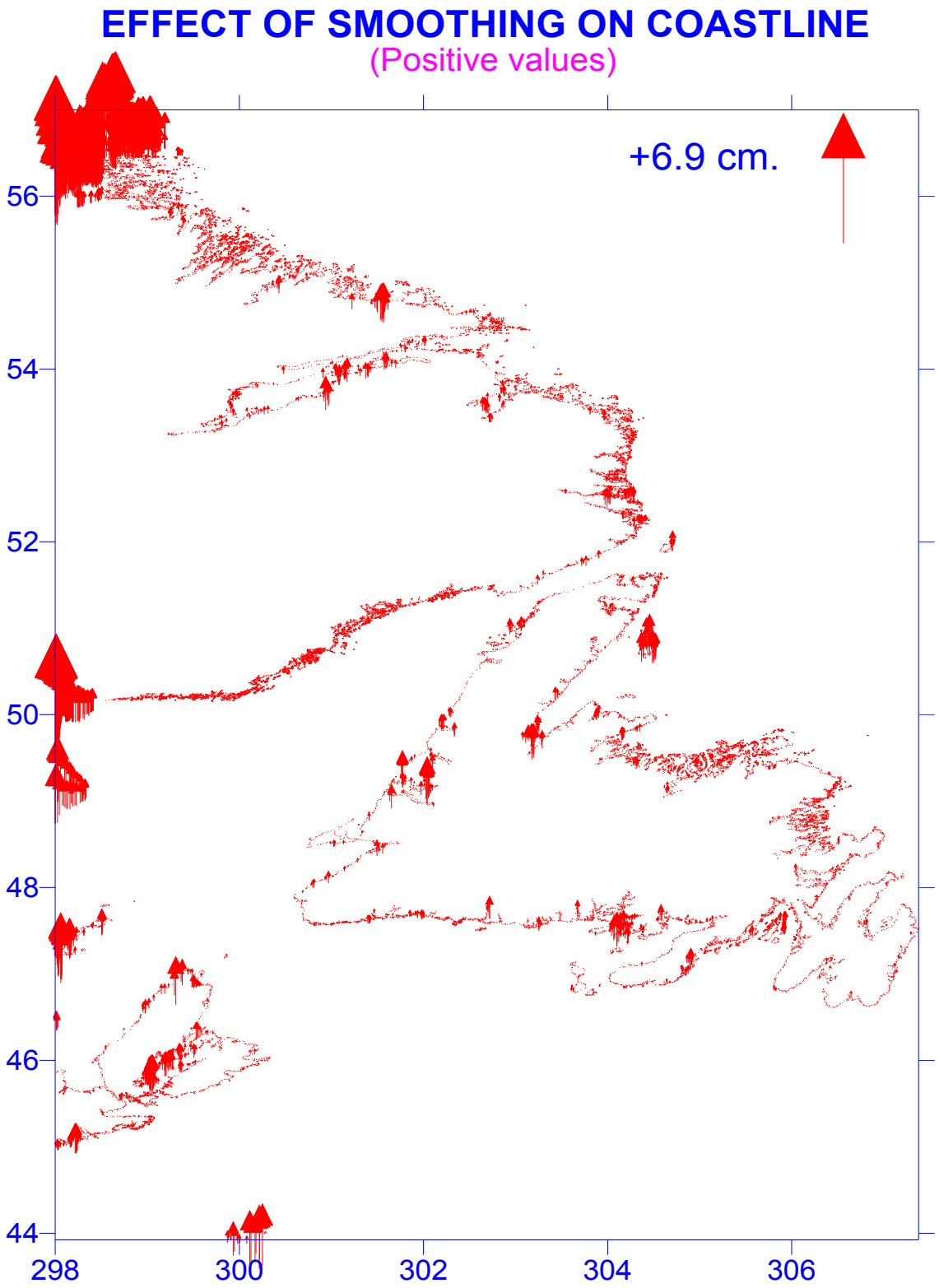

Figure 6.6. Positive effect of smoothness conditions on the points along the coastline.

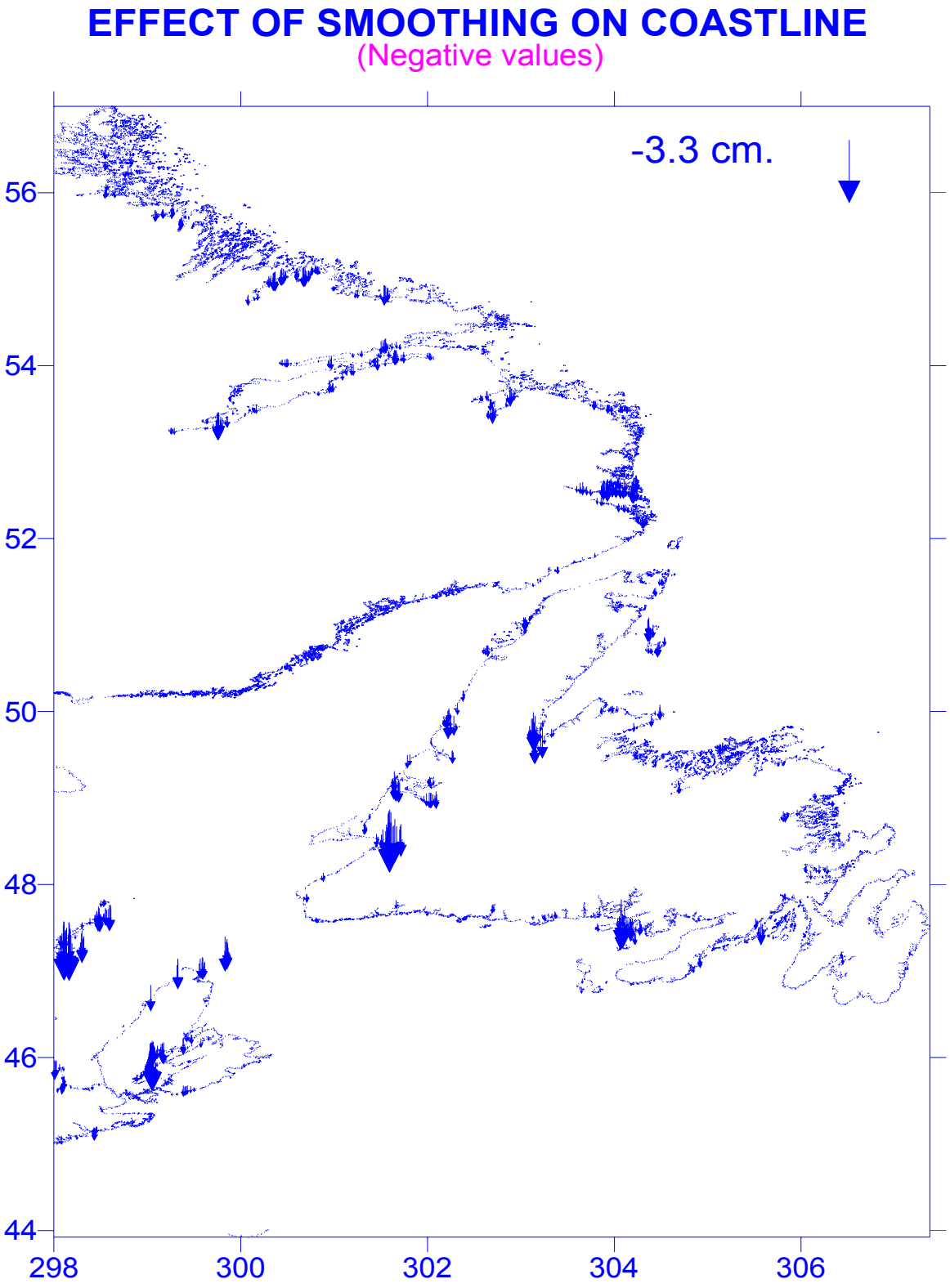

Figure 6.7. Negative effect of smoothness conditions on the points along the coastline.

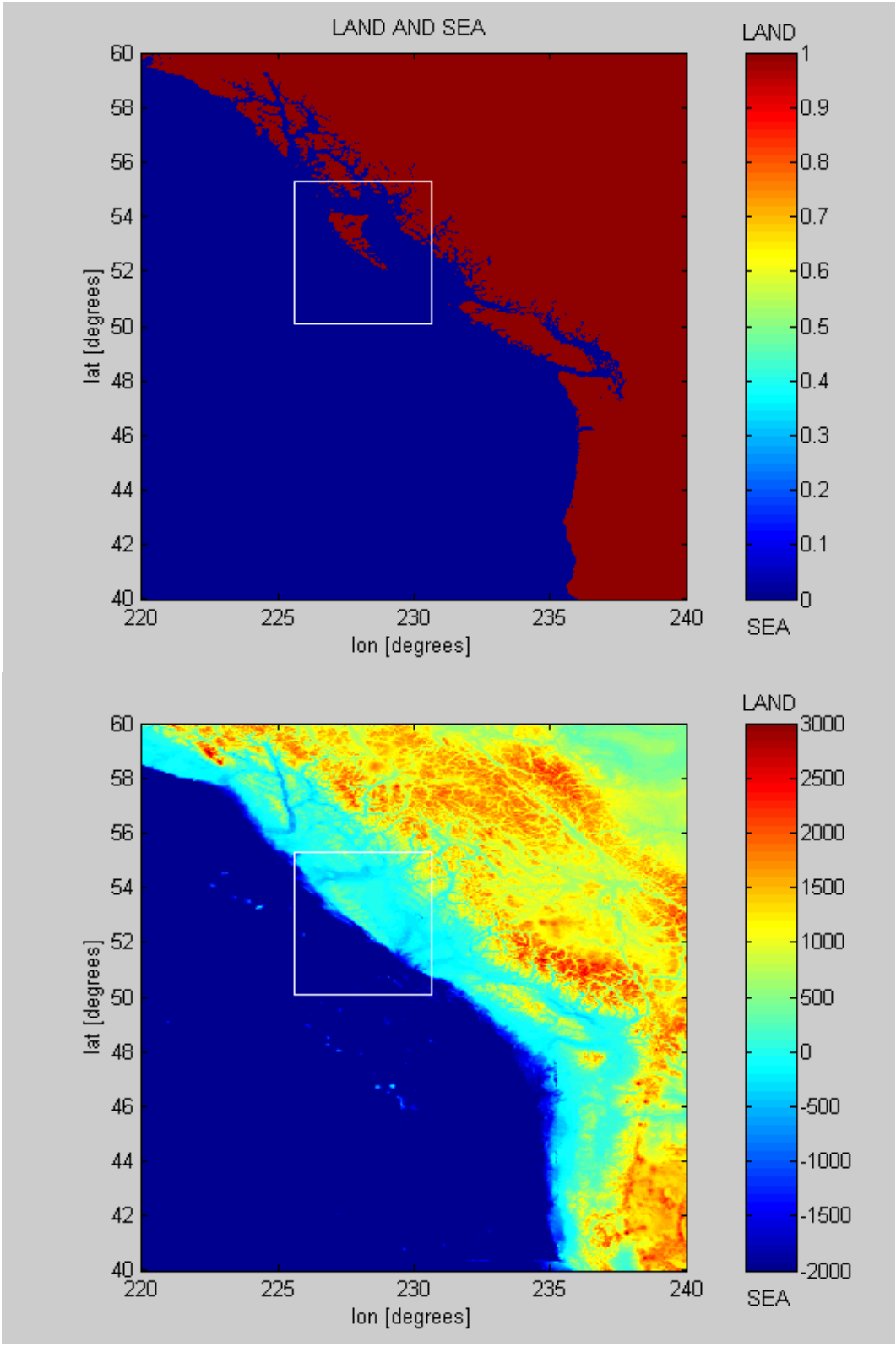

Figure 6.8-6.9: Area under study, topography and bathymetry

6.3.2.2 Description of the procedure

The experiment was conducted following the procedure already described in section 6.2.1.2 for the flat area. For completeness, it will be briefly presented again.

- Separate gridding of residual gravity anomalies (referenced to EGM96) on land and at sea, and merging both types of data.
- Geoid computation using Stokes' formula with the original spherical kernel (by 1D-FFT) applied to the merged data.
- Smoothing gravity anomalies at the coastline using Daubechies fourth wavelet decomposition and reconstruction up to the third level. For every level of decomposition, detail coefficients are restricted up to the RMS values of the coefficients that are not on the coastline.
- Geoid computation using Stokes' formula with the original spherical kernel (by 1D-FFT) applied to gravity anomalies smoothed only at the coastline.
- Comparison between original and smoothed gravity anomalies and between final geoid solutions from original and smoothed anomalies.

6.3.2.3 Analysis and summary of results for mountainous coastline

The following figures (Figure 6.10) show the effect of smoothing on the data along the coastline (smaller window). From Tables 6.7 and 6.8, the mean, RMS and standard deviation of the residual gravity anomalies are not significantly changed after the smoothing procedure. However, the effect of smoothing can be clearly seen in the restricted area; data away from the coastline remain unchanged. The differences between the original merged and the smoothed data are shown in Fig 6.11; their statistics are given in Table 6.9.

All the differences are concentrated along the coastline. Their magnitude is between –91.30 mGal and 97.45 mGal. The differences are zero away from the coastline, and the smoothing is in the coastline area only.

Table 6.7. Original gravity anomaly residuals referenced to EGM96. Unit: [mGal].

max	min	mean	RMS	STD
240.60	-138.60	0.60	16.80	16.80

Table 6.8. Smoothed gravity anomaly residuals referenced to EGM96 Unit: [mGal].

max	min	mean	RMS	STD
212.40	-124.10	0.60	16.10	16.10

Table 6.9. Residual gravity anomaly differences (smoothed minus original) Unit: [mGal].

max	min	mean	RMS	STD
97.50	-91.30	0.00	3.40	3.40

Geoid residuals (referenced to EGM96) have been computed with the original merged and smoothed data. The effect of smoothing on the final geoid solution can be seen in Fig 6.13 (circular window area). The statistics for both solutions are very close each other, which means that there are no significant differences for entire area and the effect of smoothing is in the coastline area only. The geoid after applying the compatibility (smoothing) conditions is smoother than the one from merged only data.

The differences between both geoid solutions for the entire area are shown in Fig 6.12. These differences are located along the coastline only and the effect of smoothing has a magnitude between –33.1 cm and 24.7 cm

The summary of the results allows us to draw the following conclusions:

As in the flat area wavelet transforms using wavelets with *n*-vanishing moments can be used successfully for detecting irregularities along a mountainous and complicated coastline and for smoothing data applying compatibility conditions along the coastline.

The differences between smoothed and original gravity anomalies are between –91.30 mGal and 97.45 mGal for the entire area, with an RMS value of 3.4 mGal. After the

Table 6.10. Original residual geoid heights. Unit: [m].

max	min	mean	RMS	STD
3.245	-1.733	0.568	0.734	0.466

Table 6.11. Smoothed residual geoid heights. Unit: [m].

max	min	mean	RMS	STD
3.501	-1.980	0.567	0.743	0.466

Table 6.12. Residual geoid heights differences (smoothed minus original) Unit: [m].

max	min	mean	RMS	STD
0.247	-0.331	0.000	0.017	0.017

smoothing procedure, the greatest differences were located mostly along the coastline and, for areas away from the coastline the differences are negligible, i.e., the used smoothing procedure has influence only along the coastline.

The effect of smoothness on the final geoid solution along the coastline is between –33.1 cm and 24.7 cm in the test area, with an RMS value of 1.7cm. There is no effect on the other regions, which are located away from the coastline, except for edge effects in the FFT geoid computations.

The magnitude of the smoothing effect in rough terrain and complicated coastline is much greater than in the flat area (between –5 cm and 5 cm), as determined in the previous subsection and in Grebenitcharsky and Sideris (2001). This is significant when aiming for a cm-geoid and thus the numerical solution of an AGBVP should take into account the compatibility conditions along the coastline.

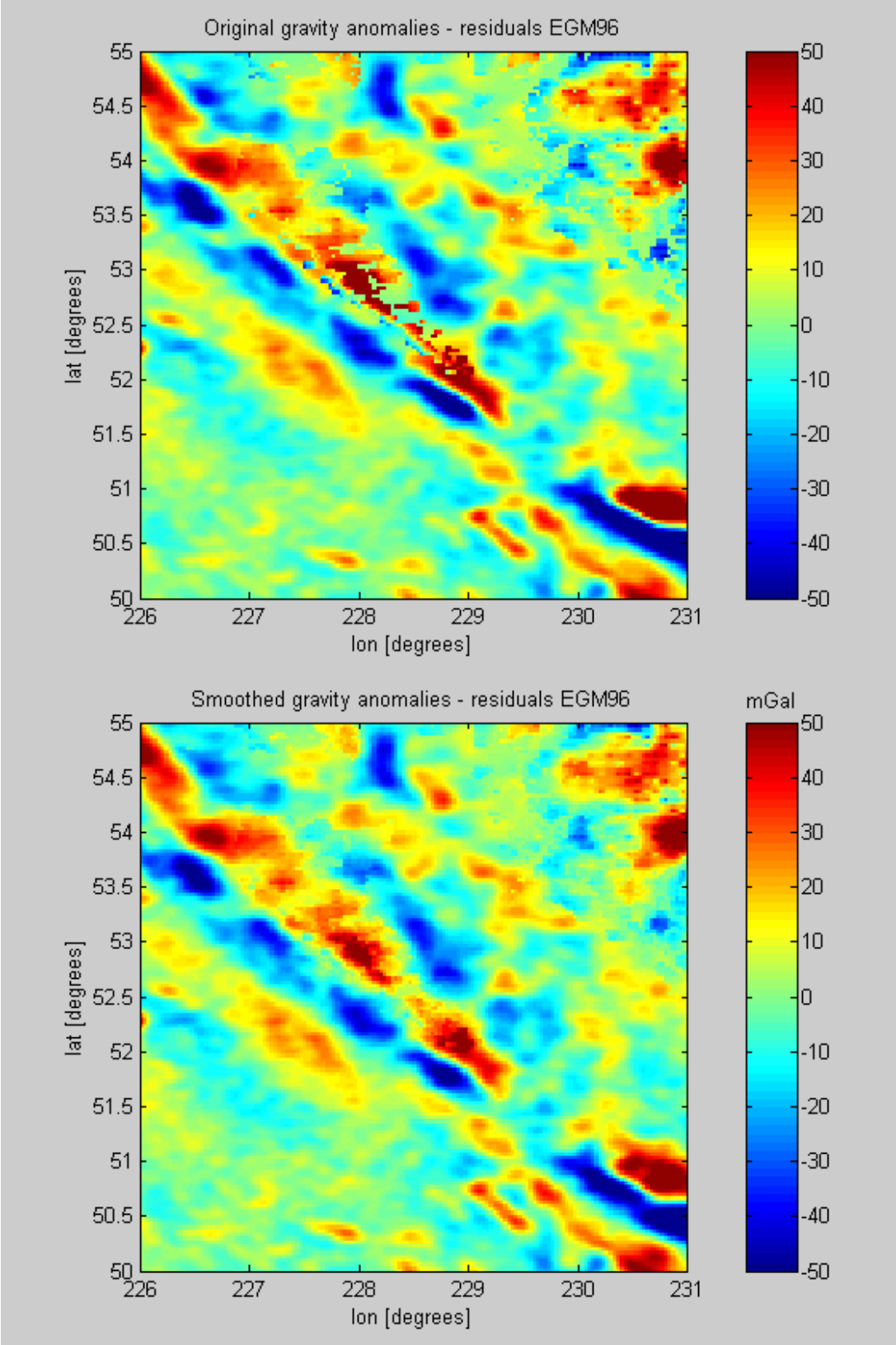

Figure 6.10: Merged gravity anomalies (top) and smoothed gravity anomalies (bottom).

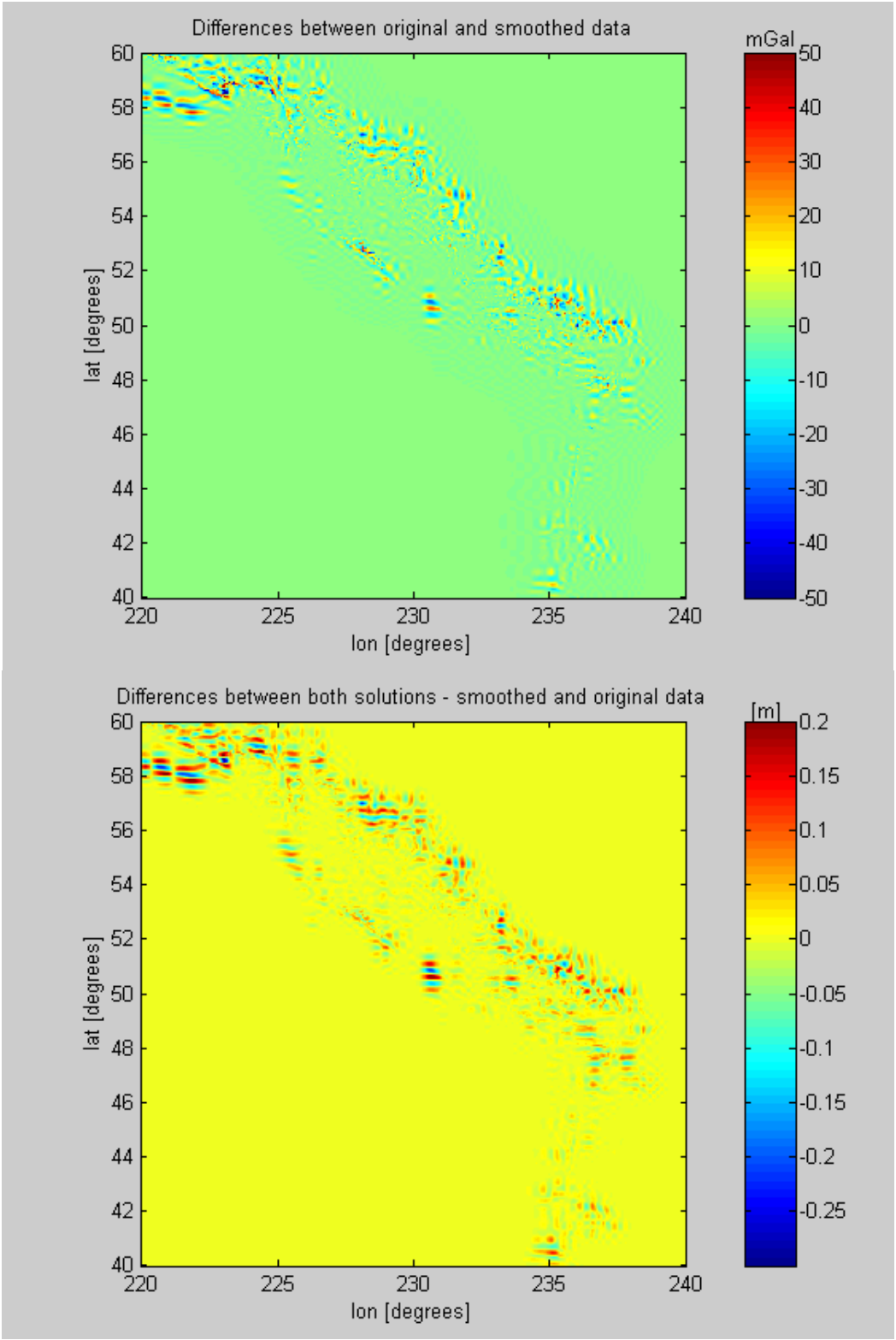

Fig. 6.11-6.12: Differences between original and smoothed gravity data. Unit:[mGal]
Differences between geoid solutions from original and smoothed data. Unit:[m]

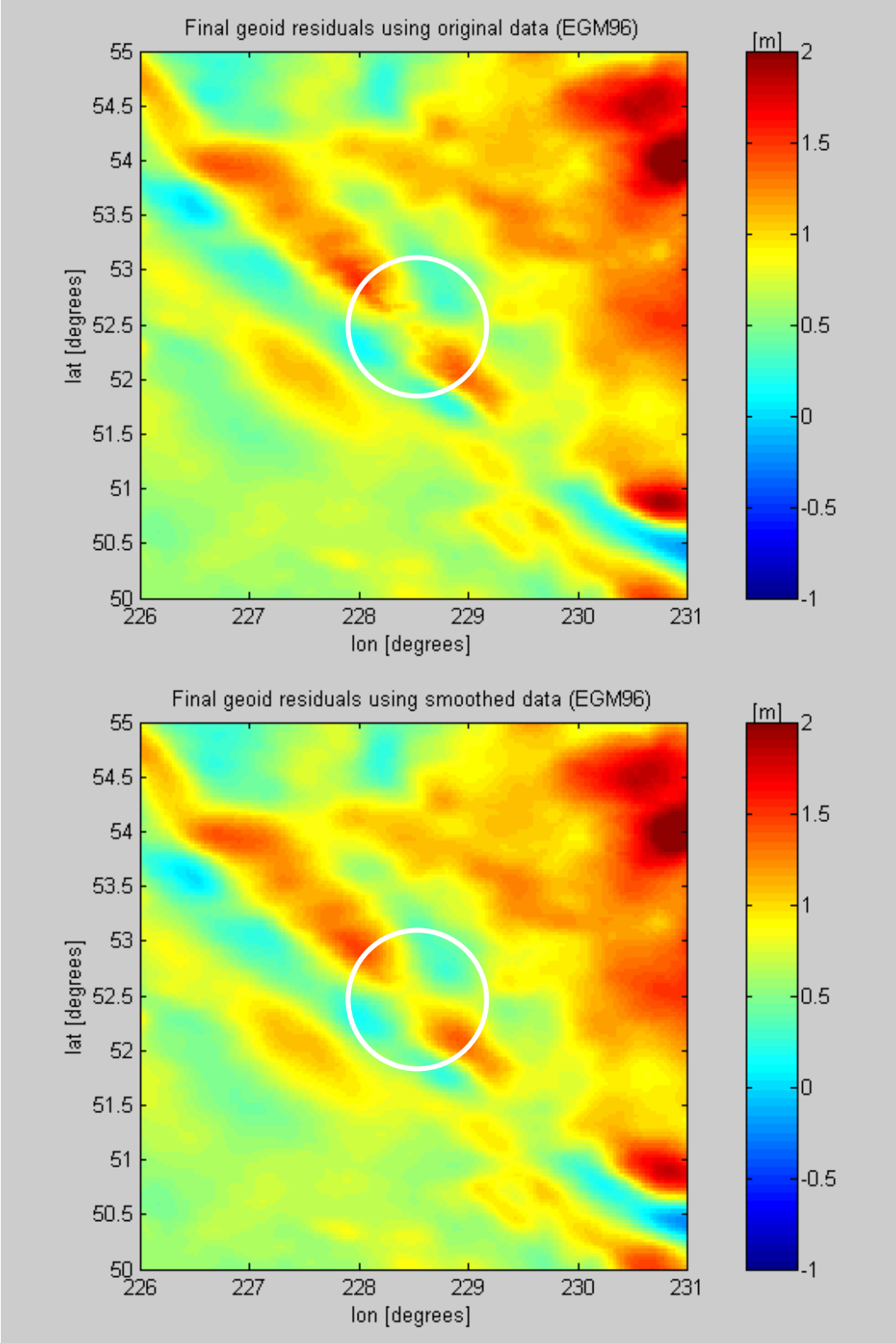

Figure 6.13: Final geoid solutions from original and smoothed data (restricted window)

6.4 Effect of smoothness of boundary surface and boundary conditions on the numerical solution of fixed AGBVP II using classical planar wavelets

6.4.1 Area of investigation and data used

The area under study is $43° \leq \varphi \leq 57°$ and $298° \leq \lambda \leq 312°$ (Newfoundland, Eastern Canada); see Figure 6.1. The size of the area is 14x14 degrees with data resolution 2x2 arc seconds. The following data were used: free air gravity anomalies on land from the Geological Survey of Canada, GPS/Levelling data on benchmarks from the Geodetic Survey Division, shipborne free-air gravity anomalies from the Geological Survey of Canada, and GEOSAT geodetic mission (GM) satellite altimetry data at sea from NOAA (NOAA, 1997).

The EGM96 geopotential model was used as a reference field. The global quasi-stationary sea surface topography (QSST) model derived from the simultaneous EGM96 adjustment complete to degree and order 20 was used for the reduction of the data from the sea surface to the geoid.

To assess the accuracy of the numerical solution, a comparison with the Canadian geoid CGG2000 was performed. Also, a comparison with a Multiple Input Multiple Output System Theory (MIMOST, Sideris, 1996) solution was done to assess the accuracy of the numerical solution with respect to a standard heterogeneous data combination method.

6.4.2 Description of the solution and its validation

The mixed AGBVP II in spherical approximation given by (2.19) was simplified assuming that the bias in sea data and the effect of SST have been previously removed. Also, assuming that GPS/leveling can provide a known boundary surface on land, the

fixed AGBVP II, which can be considered as identical to AGBVP III, can be defined as follows:

$$
\begin{cases}
\Delta T = 0 & \\
-\dfrac{\partial T}{\partial r} - \dfrac{2}{R} T - 2\dfrac{\Delta W_0}{R} = \Delta g_L & \text{on land part } \delta\Omega_L \text{ of the sphere} \\
T_L = \dfrac{N_{GPS}}{\gamma_0} & \text{on land part } \delta\Omega_L \text{ of the sphere} \\
-\dfrac{\partial T}{\partial r} = \delta g_S & \text{at sea part } \delta\Omega_S \text{ of the sphere} \\
T \sim O(r^{-1}), & r \to \infty
\end{cases}
\tag{6.2}
$$

where the constant $2W_0 / R$ is due to the fact that potential differences are observed and can be related to the constant in Eq. (2.19). It is necessary to assume that this constant is removed from the boundary conditions or assumed to be zero. The boundary condition on land can be reformulated using geoid heights from GPS/leveling and Bruns's equation as follows:

$$
-\frac{\partial T}{\partial r} = \delta g_L = \Delta g_L + \frac{2\gamma}{R} N_{GPS} \tag{6.3}
$$

After reformulation of the land boundary condition and applying smoothness conditions along the coastline (to have regular boundary surface and regular boundary conditions, i.e., data) the fixed AGBVP II is transformed to a Neumann boundary value problem (Rektorys, 1977). Evaluating by 1D FFT or 2D FFT the spherical Hotine convolution integral with 50 kilometers integration radius, a numerical solution for the fixed AGBVP II is obtained.

Two solutions were derived by the following steps:

Numerical solution with smoothed boundary conditions:

- Gridding GPS/levelling derived geoid heights at land gravity points and merging them with the gridded geoid heights from altimetry data (corrected by SST).
- Transformation of the boundary conditions (using unsmoothed geoid heights on land) to get gravity disturbances on land.
- Merging the residual gravity disturbances on land and gravity disturbances at sea (both referenced to EGM96).
- Smoothing the boundary conditions (gravity disturbances at the coastline) using Daubechies fourth wavelet decomposition and reconstruction up to the third level. For every level of decomposition, detail coefficients were restricted up to the RMS values of the coefficients that are not on the coastline. These constraints mean that additional smoothness conditions have been used *to smooth the boundary conditions*.
- Geoid computation using Hotine's formula with the Hotine's spherical kernel (by 1D-FFT) applied to the smoothed gravity disturbances.

Numerical solution with smoothed boundary surface (geoid from GPS/levelling and altimetry):

- Gridding GPS/levelling derived geoid heights at land gravity points and merging them with the gridded geoid heights from altimetry data (corrected by SST).
- Smoothing the boundary surface (the geoid) along the coastline using Daubechies fourth wavelet decomposition and reconstruction up to the third level. Restricting the detail wavelet coefficients for the geoid means that the *smoothness conditions were applied on the boundary surface*.
- Transformation of the boundary conditions (using smoothed geoid heights along the coastline) to get gravity disturbances on land.
- Merging the residual disturbances on land and gravity disturbances at sea (both referenced to EGM96).
- Geoid computation using Hotine's formula with the Hotine's spherical kernel (by 1D-FFT) applied to the transformed (with smoothed boundary surface – geoid heights) disturbances.

The second solution will be later referred as numerical solution *with smoothed boundary surface.*

To assess the results of both numerical Hotine solutions, they were compared to the following three solutions:

Solution 1: Evaluation by 2D FFT of the spherical Stokes integral kernel (Sideris, 1999) after simple merging of gravity anomalies on land and at sea.

Solution 2: Application of multiple input, multiple output system theory (MIMOST) method (Andritsanos et al., 2000) for combination of gravity anomalies (on land and at sea) and geoid heights (GPS/leveling on land and GEOSAT-GM altimetry data at sea).. Due to the lack of specific information about the errors in both altimetric and gravimetric solutions, simulated noises were used as input error. Randomly distributed fields (white noise) were generated in Matlab® using 10 cm standard deviation for the altimetry derived geoid heights and 3 mGal standard deviation for the gravimetrically-derived gravity anomalies. The final solutions from the combination method were calculated according to the following equation (Andritsanos et al., 2000):

$$\hat{N} = \left[H_{N,\Delta g}, H_{N,N_a} \right] \left\{ \begin{pmatrix} P_{\Delta g,\Delta g} & P_{\Delta g,N_a} \\ P_{N_a,\Delta g} & P_{N_a,N_a} \end{pmatrix} - \begin{pmatrix} P_{m_{\Delta g},m_{\Delta g}} & 0 \\ 0 & P_{m_{N_a},m_{N_a}} \end{pmatrix} \right\} \times \begin{pmatrix} P_{\Delta g,\Delta g} & P_{\Delta g,N_a} \\ P_{N_a,\Delta g} & P_{N_a,N_a} \end{pmatrix}^{-1} \begin{bmatrix} \Delta\hat{g} \\ \hat{N}_a \end{bmatrix} \tag{6.4}$$

where $\hat{N}$ is the estimated output spectrum of geoid heights, H_{xy} is the theoretical frequency impulse response of the system with $x = N, y = \Delta g, N_a$; $\begin{bmatrix} \Delta\hat{g} \\ \hat{N}_a \end{bmatrix}$ is the input observation spectrum for gravity anomalies (on land and sea) and geoid heights (from

GPS/levelling and altimetry); $P_{y,z}$ is the input observation PSD with $z = \Delta g, N_a, y = \Delta g, N_a$, $P_{m_x m_y}$ is the input noise PSD.

Solution 3: The most recent gravimetric geoid of Canada, CGG2000. The CGG2000 residuals to EGM96 show a mean value of –0.680 m with a standard deviation of 0.268 m.

6.4.3 Analysis of results

6.4.3.1 Comparisons and validation of the numerical solution of AGBVP II

To validate the numerical solution of AGBVP II with smoothed boundary conditions, it was compared to the 2D FFT spherical Stokes' solution with gravity anomalies, the CGG 2000 geoid and the MIMOST solution.

Table 6.13. Statistics of the numerical solution with smoothed boundary conditions. Unit: [m].

Solution (data)	max	min	mean	STD
Num. solution	0.418	-0.821	-0.241	0.151

Table 6.14 Statistics of differences of the numerical solution from other solutions. Unit: [m].

Differences with	max	min	mean	STD
Solution 1	0.349	-0.371	-0.058	0.042
CGG2000	1.476	-0.539	0.459	0.310
MIMOST	0.398	-1.236	-0.419	0.205

The numerical solution is closest to Solution 1. The differences with Stokes' solution are quite small. These differences are due to GPS/leveling and GEOSAT data. In the

numerical solution, GPS/leveling and GEOSAT (corrected for the QSST) data can be considered as part of the known boundary. The solution depends mostly on the gravity data. Differences with CGG2000 are mainly due to the QSST, which was not removed in the CGG2000 solution (the numerical solution does not contain the effect of QSST). After restoring the effect of QSST on the numerical solution, the mean value of the differences with CGG2000 is close to zero.

The main contribution to the numerical solution comes from the gravity data. In terms of mean value, the numerical solution is closer to CGG2000 (see Table 6.14), which shows again the gravimetric character of the numerical solution. A comparison with the MIMOST solution shows a better geoid agreement on land (see Figure 6.14 and Figure 6.15), which can be seen in the differences between the numerical and MIMOST solutions (Figure 6.17), as well.

Table 6.15. Statistics of differences to the altimetry and shipborne solution at sea only.Unit: [m].

Differences	**max**	**Min**	**mean**	**STD**
Num. Solution	0.645	-0.892	0.005	0.240
MIMOST	1.257	-0.628	0.424	0.232

Table 6.16. Statistics of MIMOST solution. Unit: [m].

Solution (data)	**max**	**min**	**mean**	**STD**
MIMOST	0.759	-0.592	0.191	0.154

Table 6.17. Statistics of differences of MIMOST solution from other solutions. Unit: [m].

Differences with	**max**	**min**	**mean**	**STD**
GPS&GEOSAT	0.970	-1.071	-0.003	0.209
Solution 1	1.264	-0.473	0.366	0.209
CGG2000	1.740	-0.194	0.926	0.267

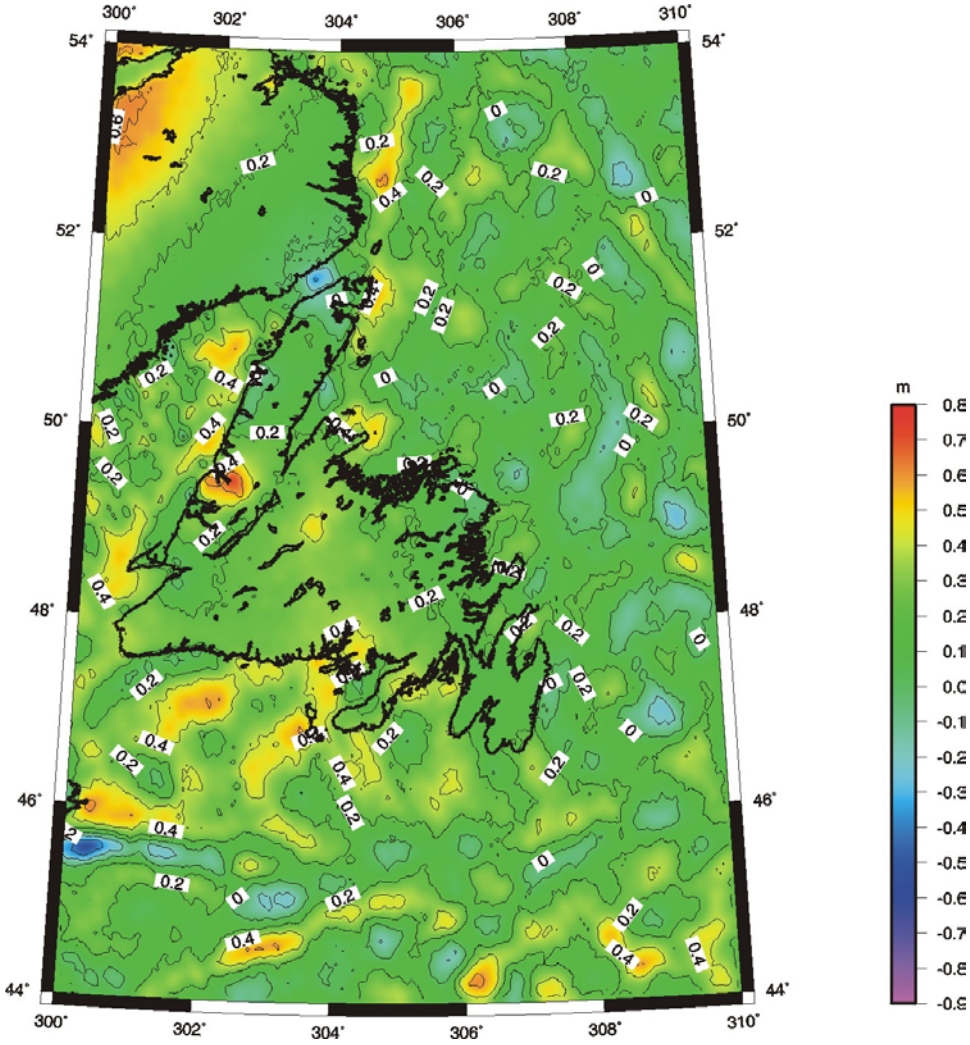

Figure 6.14: MIMOST solution (residuals to EGM96). Unit:[m]

Both the numerical solution and the MIMOST solution have been compared to a previous altimetry and shipborne gravity solution at sea only (Vergos et al., 2001). The changes in the coastline region due to the gravity data and GPS/leveling on land exist in both solutions. At the same time, a comparison to the solution with altimetry and shipborne data only at sea showed that the numerical solution is closer in terms of mean value (see Table 6.15) and the standard deviations are very close (see also Figure 6.18) as well.

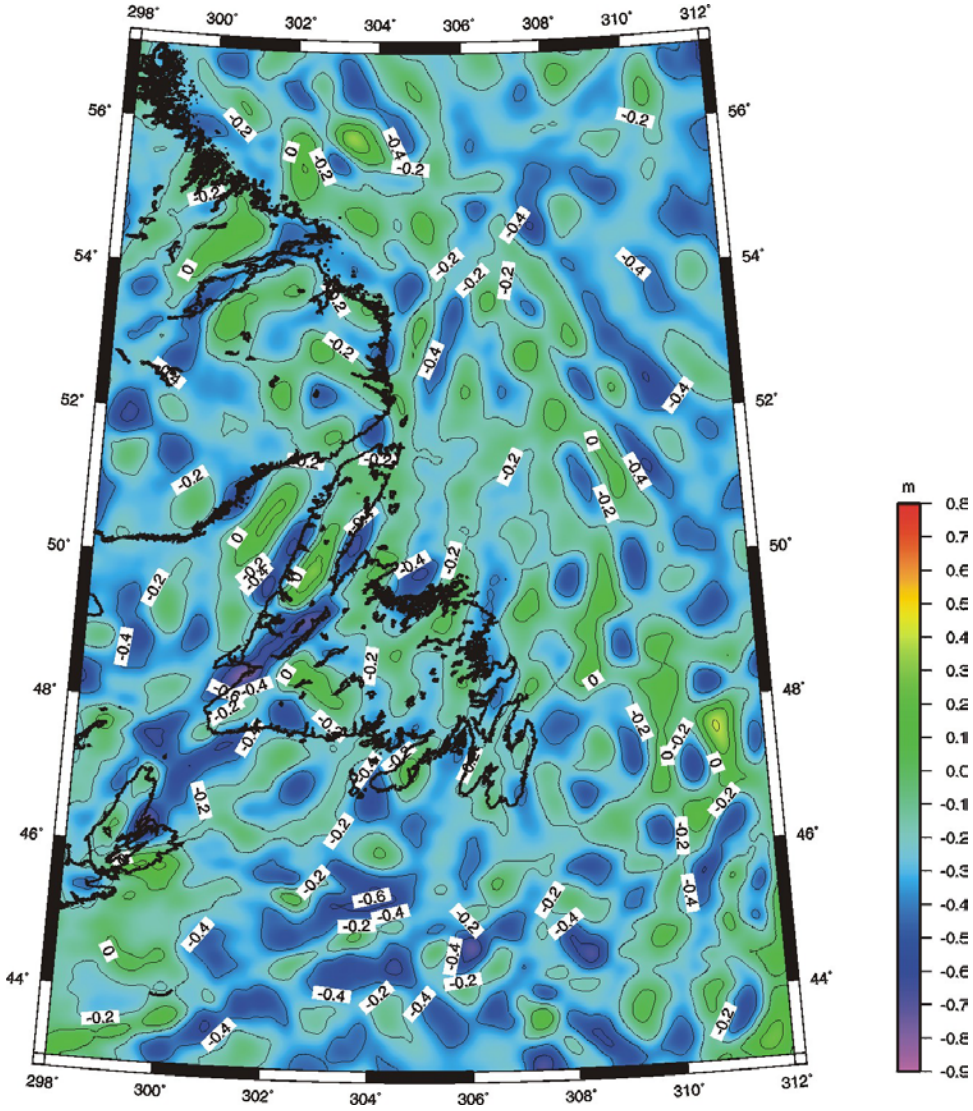

Figure. 6.15: Numerical solution (residuals to EGM96). Unit:[m]

6.4.3.2 Validation of MIMOST solution

Before the comparison of our numerical solution to the MIMOST solution, it was necessary to validate the MIMOST solution itself. The solution using the MIMOST method was compared with GPS/leveling and GEOSAT GM data, the 2D FFT spherical Stokes solution with gravity anomalies, and the CGG2000 geoid. GPS and GEOSAT data were referenced to EGM 96.

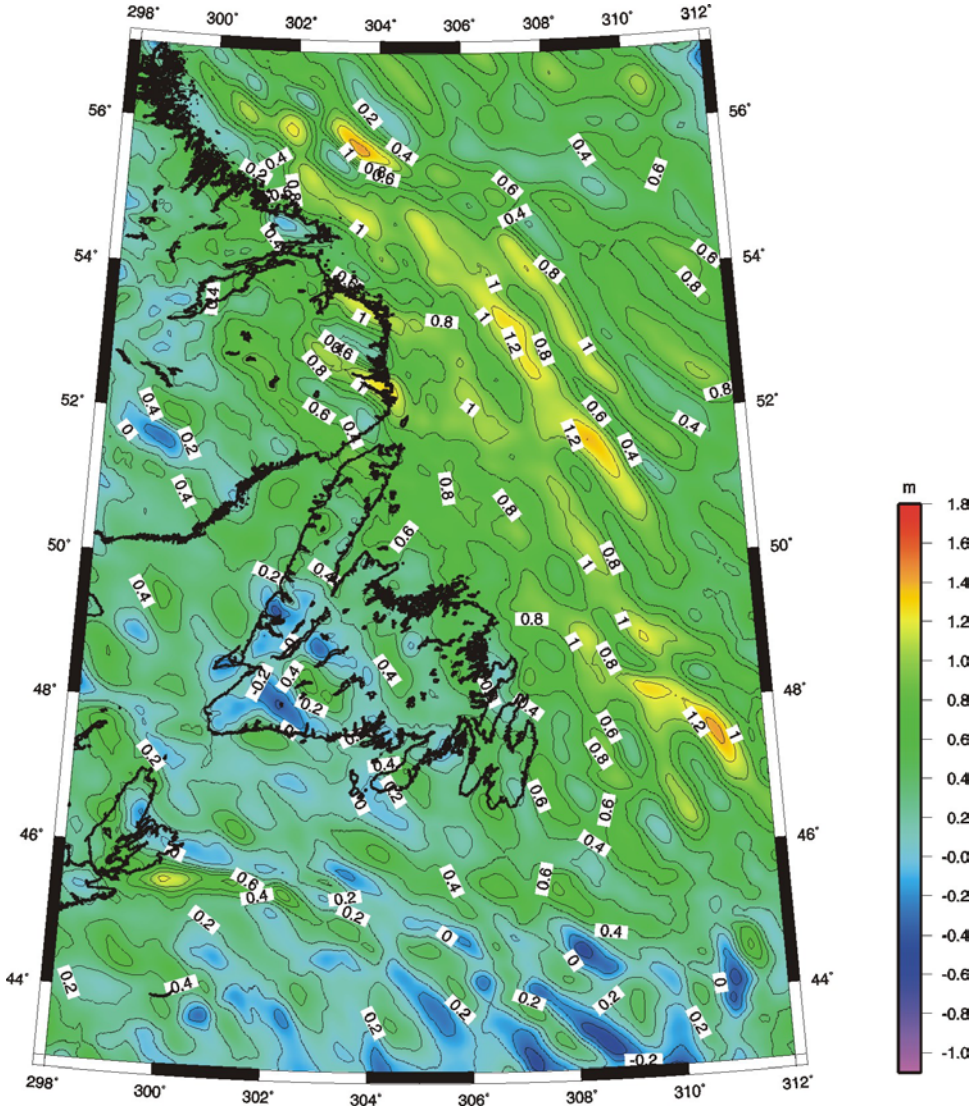

Figure 6.16: Differences between numerical solution and CGG2000. Unit:[m]

Table 6.18. Statistics of smoothing effects. Unit: [m].

Differences	**max**	**min**	**mean**	**STD**
Num. Solution	0.645	-0.892	0.005	0.240
Num. Solution-boundary	0.001	-0.001	0.000	0.001
MIMOST	1.257	-0.628	0.424	0.232

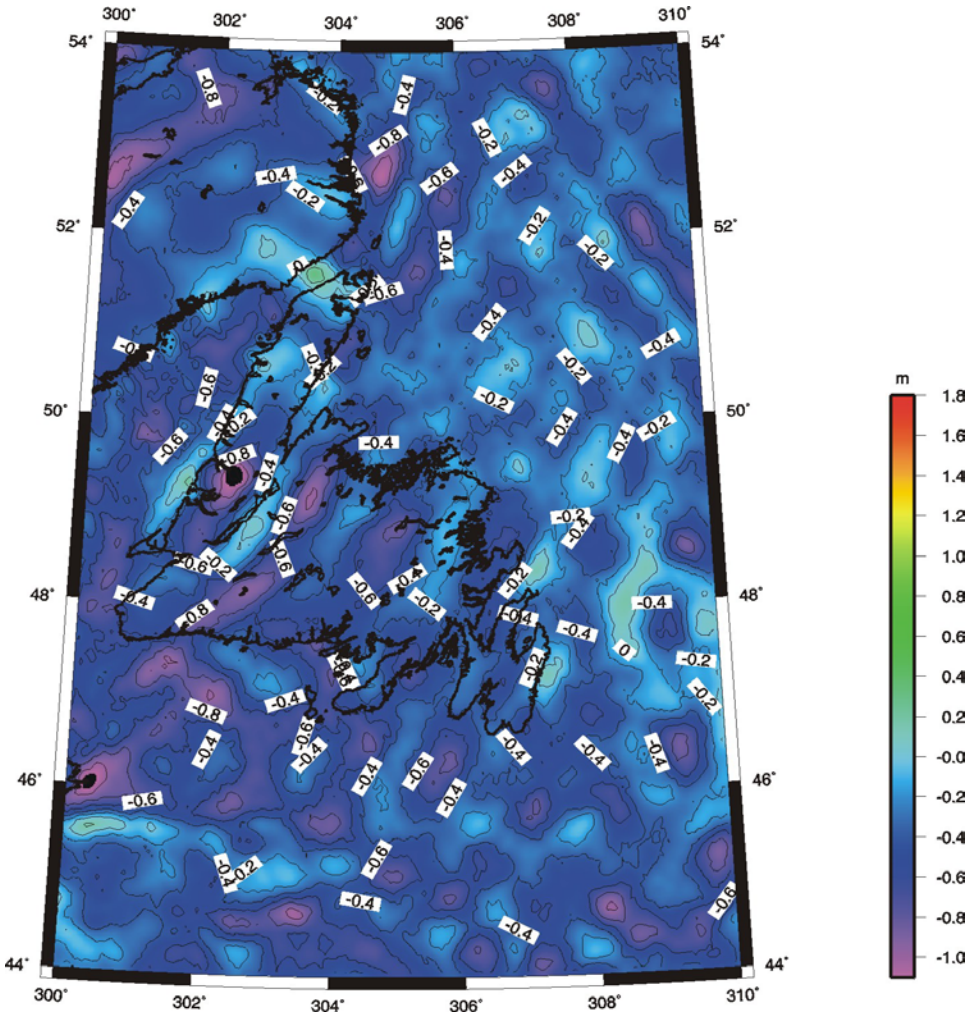

Figure 6.17: Differences between numerical solution and MIMOST. Unit:[m]

The MIMOST solution is presented graphically in Figure 6.14. The smoother surface on land is due to the influence of the resolution of GPS/leveling data. The MIMOST solution is closest to the data from GPS/levelling and GEOSAT (see Table 6.17) because of the higher a priory accuracy used for GPS and GEOSAT data. Differences with Solution 1 (see Table 6.17) are due to the small weight of the gravity anomalies in MIMOST. The differences between the mean values in Table 6.17 are due to the different referencing. CGG2000 refers to the mean sea level at several tide gauges; altimetry data are related to

the sea surface and solution 1 is referenced to the geoid (sea surface corrected for the QSST).

6.4.3.3 Effect of smoothness conditions along the coastline on the numerical and MIMOST Solutions

In numerical and MIMOST solutions gravity data are considered as boundary conditions (data) and at the same time, GPS/leveling and GEOSAT can be considered as part of the known boundary surface. Smoothing conditions along the coastline are applied on boundary surface and boundary conditions (data) before the computation of the geoid. The effects of smoothing along the coastline induce the differences between the geoid determined from the original data and the geoid determined from smoothed data along the coastline. For the numerical solution, the effects of smoothing conditions on the boundary surface and on the data have been investigated separately. The color scale in Figure 6.19 is different from the values in Table 6.18, because the figure represents a smaller area.

The smoothing effects in Table 6.18 represents the statistics of the differences between the solutions with smoothed boundary conditions (Numerical solution and MIMOST) and the one merged only data; and between the solution with smoothed boundary surface (geoid) and the geoid with merged data. The effects in case of numerical solution range between -0.137m and 0.103 m. For MIMOST, they have greater magnitude, between -0.234 m and 0.165 m. For the MIMOST method, the smoothing effects on the boundary (GPS and altimetry data) are larger, because of larger weight of these data in the combined solution and existing discrepancies between GPS and altimetry data. The smoothing of the boundary surface does not have an effect on the geoid (see Table 6.18), in the numerical solution. The MIMOST solution is more sensitive to the smoothing on the boundary surface than the numerical solution. In both cases, the smoothing effects are concentrated in the coastal region.

6.4.4 Summary of the effect of smoothness of boundary surface and boundary conditions on the numerical solution of fixed AGBVP II

After the analysis of the obtained results, the following conclusions are drawn:
The suggested numerical solution with gravity disturbances as boundary data both on land and at sea can be successfully applied for the solution of the fixed AGBVP II.

The numerical solution is closer to the pure gravity solution taking into account GPS and GEOSAT data. These data describe the boundary surface and take part in the solution implicitly through the transformation of the boundary condition.

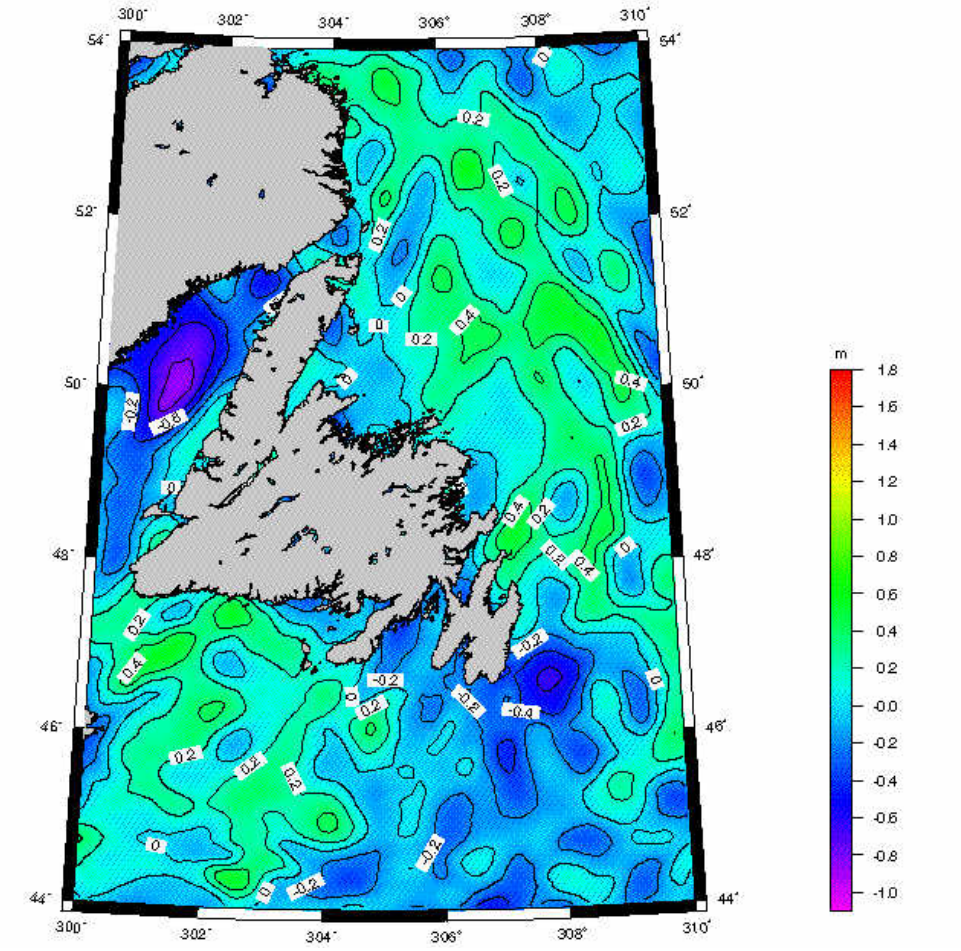

Figure 6.18: Differences between numerical solution and altimetry and shipborne solution at sea only. Unit:[m]

The significant differences with CGG2000 are because the numerical solution does not contain the effect of QSST while CGG2000 does. After restoring the effect of the SST in numerical solution, the mean value of the differences became zero.

The smoothing of the boundary surface does not have an effect on geoid determination as evidenced by the magnitude of this effect which is only 1mm! The smoothing on the

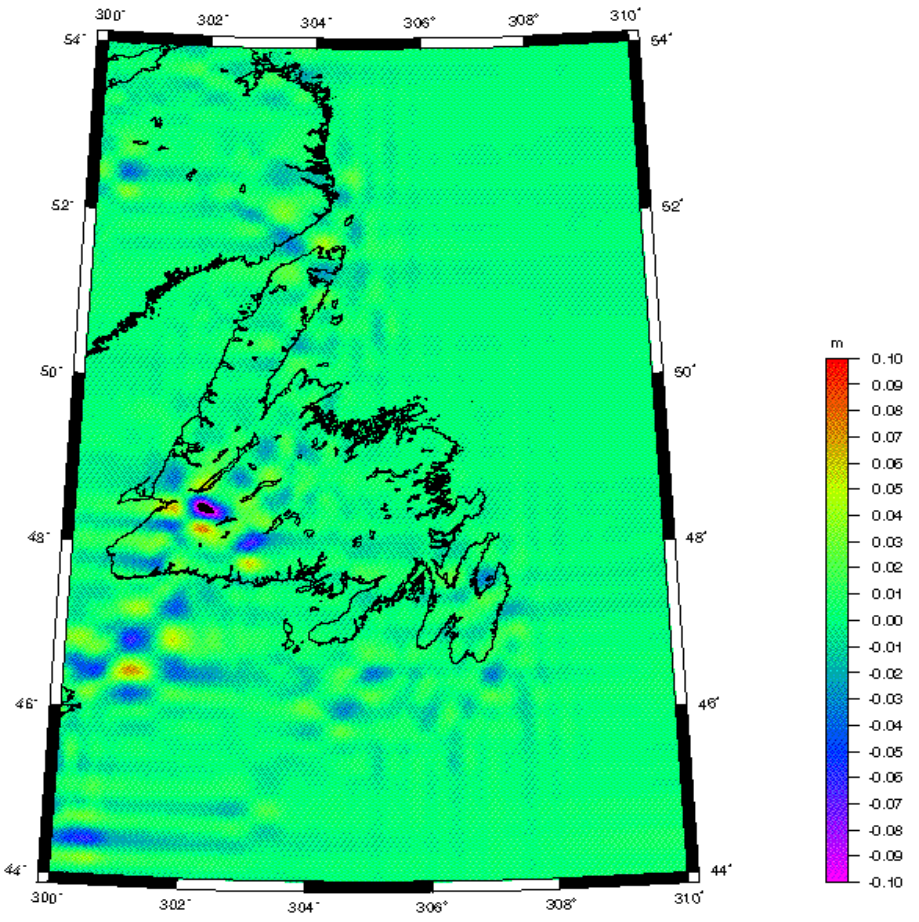

Figure 6.19: Effect of smoothing along the coastline on the numerical solution

boundary conditions (data) gives a maximum effect on the final geoid solution between -0.137 m and 0.103 m.

The numerical solution is less sensitive to discrepancies between GPS/leveling and altimetry data. Even greater discrepancies between GPS/levelling and altimetry data do not have smoothing effects along the coastline.

6.5 Numerical solution of AGBVP II with compatibility conditions for coincidence of data along the coastline – combination of spherical harmonics, PDOs and wavelets

6.5.1 Area of investigation and data used

A numerical experiment has been conducted to investigate the proposed procedure for the solution of AGBVPII. The area under study is $43° \leq \varphi \leq 57°$ and $298° \leq \lambda \leq 312°$ (Newfoundland, Eastern Canada, Figure 6.1). The size of the area is 14x14 degrees with data resolution 2x2 arc minutes. The following data were used: free air gravity anomalies on land from the Geological Survey of Canada, shipborne free air gravity anomalies at sea from the Geological Survey of Canada and the GEOSAT geodetic mission (GM) satellite altimetry data at sea from NOAA. The EGM96 geopotential model was used as the reference field. To show more details along the coastline, some results are presented in a smaller window (see Figure 6.1).

6.5.2 Description of the solution and its procedure for the solution

The mixed AGBVP II in spherical approximation given by (2.19) was simplified assuming that the bias in sea data and the effect of SST were previously removed. Also, assuming that altimetry data will provide known boundary surface at sea and together with gravity disturbances from shipborne data the AGBVP II can be defined in a similar way like in the previous subchapter as:

$$
\begin{cases}
\Delta T = 0 & \\
-\dfrac{\partial T}{\partial r} - \dfrac{2}{R} T = \Delta g_L & \text{on land part } \delta\Omega_L \text{ of the sphere} \\
T_S = \gamma N_{altim} & \text{at sea part } \delta\Omega_S \text{ of the sphere} \\
-\dfrac{\partial T}{\partial r} = \delta g_S & \text{at sea part } \delta\Omega_S \text{ of the sphere} \\
T \sim O(r^{-1}) & r \to \infty
\end{cases}
\tag{6.3}
$$

where T is the disturbing potential, Δ is the Laplace's operator, r is the radial distance from the center of the sphere, R is the radius of the sphere, Δg_L are the land gravity anomalies and δg_S are the sea gravity disturbances, γ is mean normal gravity and N_{altim} is the geoid height from altimetry at sea. The boundary condition at sea can be reformulated using geoid heights from altimetry and Bruns's equation as follows:

$$
-\frac{\partial T}{\partial r} - \frac{2}{R} T = \Delta g_S = \delta g_S - \frac{2\gamma}{R} N_{altim} \tag{6.4}
$$

In the numerical experiment gravity anomalies at sea are provided directly, but in general case it is necessary gravity disturbances to be transformed to gravity anomalies. Having gravity anomalies both at sea and on land the Stokes' kernel can be applied in terms of spherical PDOs together with spherical wavelets (Freeden and Windheuser, 1997). After the wavelet decomposition step, the detail coefficients are restricted to a certain value (zero for the numerical experiment) for every level of decomposition, which is equivalent to the restriction of gradients of first or higher order. As a result, the data along the coastline will be smoothed and the reconstruction step with the convolution between the dual wavelet and the Stokes' kernel will give the solution for the smoothed data along the coastline. The computational procedure to get the numerical solution is the following:

Step 1: Transform gravity disturbances at sea to gravity anomalies using geoid heights from the altimetry data. Remove the contribution of the geopotential model (EGM96) up to degree n_{GPM}=360. As a result, residual gravity anomalies Δg_{GPM} are obtained.

Step 2: Grid the residual gravity anomalies for land and sea separately. Merge both sets of data using a topographic model to identify grid points at sea and on land.

Step 3: Determine the low-pass filter L_D and high- pass filter H_D (see subsection 4.3.5) for the decomposition step.

3.1 Determine the scale function and corresponding wavelet function using the formulas for *H*-Shannon spherical wavelets given by Freeden and Michel (2002):

The scale function Φ_j for *j-level* of decomposition is

$$\Phi_j(\psi) = \sum_{n=n_{GPM}}^{N_j} h^n \frac{2n+1}{4\pi} P_n(\cos(\psi))$$

The wavelet function Ψ_j for *j-level* of decomposition is

$$\psi_j(\psi) = h^{N_j+1} \frac{2N_j+3}{4\pi} P_{N_j+1}(\cos(\psi))$$

if $h=r/R=1$ all data are on the sphere without upward continuation, N_j is the degree of Legendre polynomials corresponding to *j-level*, N_j depends on the resolution of data, n_{GPM} is the degree of the used reference geopotential model.

3.2 Determine both decomposition filters based on the scale and the wavelet functions.

Step 4: Determine the low pass filter L_R and high pass filter H_R for the reconstruction step (see subsection 4.3.5).

4.1 Determine the Stokes kernel as a Legendre polynomial series according to Freeden and Windheuser (1997) as

$$K_\Lambda(\psi) = \sum_{n=0}^{N_j} \frac{2n+1}{4\pi} \hat{\Lambda}(n) P_n(\cos(\psi))$$

where the spherical symbol for the Stokes operator is $\hat{\Lambda}(n) = 1/(n-1)$. For other types of data the only change is the spherical symbol. For example, for gravity disturbances it would be $\hat{\Lambda}(n) = 1/(n+1)$.

4.2 Determine the corresponding low-pass and high- pass filters for the reconstruction step by convolving the ones from the decomposition step with the Stokes kernel. In terms of formulas

$L_R(\psi) = L_D(\psi) * K_\Lambda(\psi)$, $H_R(\psi) = H_D(\psi) * K_\Lambda(\psi)$

Step 5: Perform one level of wavelet decomposition and reconstruction using the corresponding low-pass and high-pass filters after smoothing the data along the coastline by limiting detail coefficients to zero.

5.1 Perform decomposition step using L_D and H_D filters resulting in the approximation plus detail coefficients. The coastline is expected to be detected in the detail coefficients because of existing discrepancies between data along the coastline.

5.2 Apply the compatibility (smoothing) conditions by setting the detail coefficients to zero value.

5.3 Perform reconstruction step using L_R and H_R filters resulting in the approximated (within a scale constant) geoid height residuals $\Delta\check{N}_{GPM}$ smoothed along the coastline.

Step 6: Compute the final smoothed geoid heights on the grid points for the area under study.

6.1 Scale the approximated geoid height residuals to have the correct geoid height residuals ΔN_{GPM} on the grid

$$\Delta N_{GPM} = \frac{R\Delta\varphi\Delta\lambda\cos(\varphi)}{\gamma}\Delta\breve{N}_{GPM},$$

where $\Delta\varphi, \Delta\lambda$ is the resolution of the spherical grid.

6.2 Obtain final smoothed geoid heights by restoring the contribution of the geopotential model.

$N = N_{GPM} + \Delta N_{GPM}$.

6.5.3 Analysis of results

The effect of smoothing on the measurements can be seen in Fig. 6.20. The original gravity anomalies, the smoothed gravity anomalies and the differences between both show the ability of spherical wavelets to detect irregularities in data along the coastline. The greatest differences were along the coastline. The effect of smoothing on the measurements was between -45.5 and +61.4 mGal (Table 6.19). The smoothing effect is mostly along the coastline; data further from the coastline change only slightly.

A comparison with one level of decomposition and reconstruction with classical planar Daubechies 8 wavelets (see Figure 6.21) showed much better smoothing properties for spherical wavelets. It is known that "Daubechies 8" has 7 vanishing moments or it can be considered as a multiscale differential operator of order 7 (see Eq.(4.69) in subsection 4.4.3). *Daubechies 8 will provide a very high level of regularity related to the 7^{th} order derivatives to be compared with the smoothness effects of spherical wavelets.* In this case, the data along the coastline have been changed a little bit but still the discrepancies exist.

Table 6.19. Residual gravity anomaly differences (smoothed minus original) Unit: [mGal].

max	**min**	**mean**	**RMS**	**STD**
61.40	-45.50	0.00	1.60	1.60

The main advantage of the proposed numerical procedure is that the geoid heights are available immediately after the reconstruction procedure. Also, for other types of data, it is necessary to only change the spherical symbol in the kernel represented by a Legendre polynomial series.

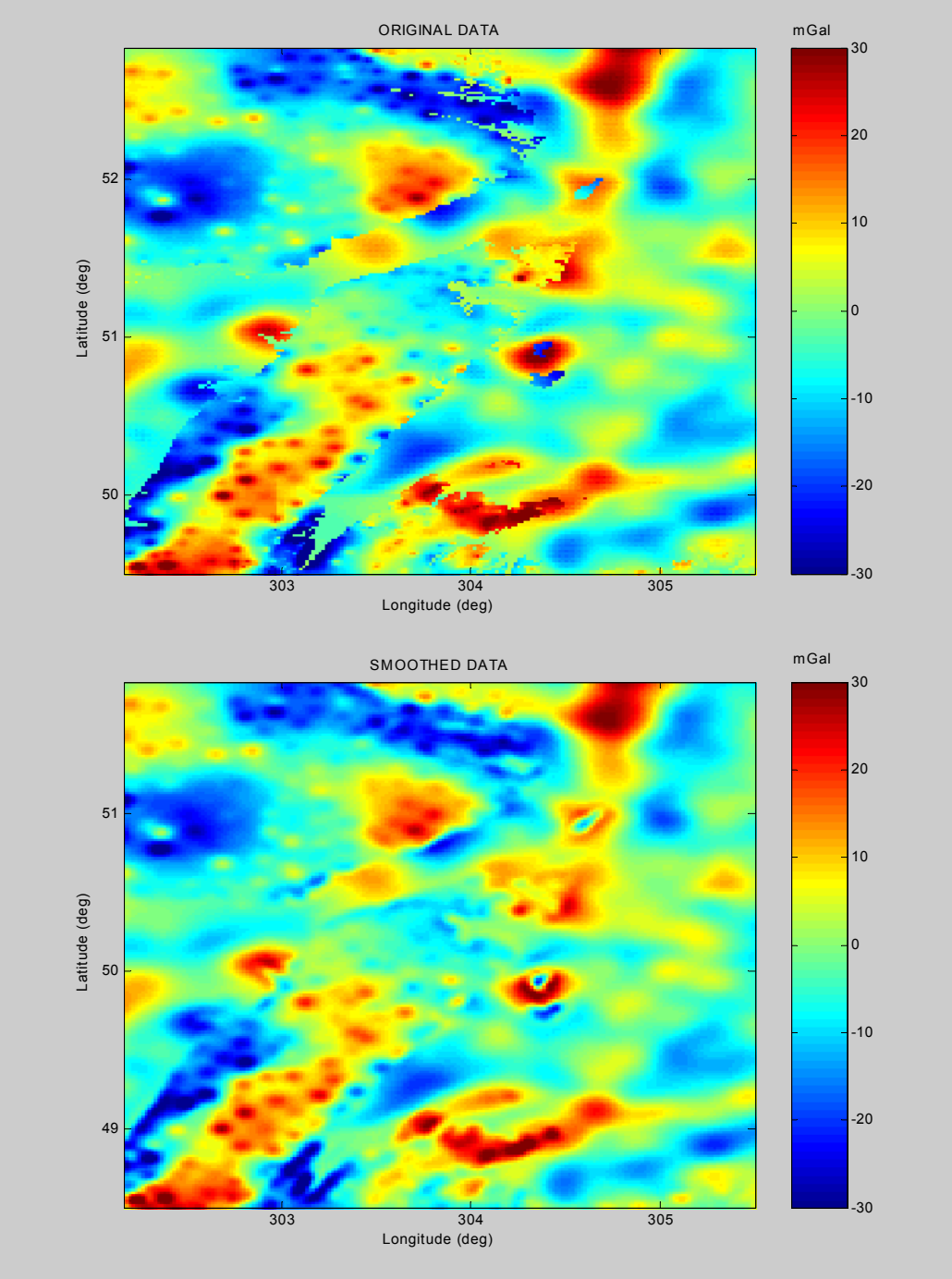

Figure 6.20: Effect of smoothing with spherical wavelets. Unit:[mGal]

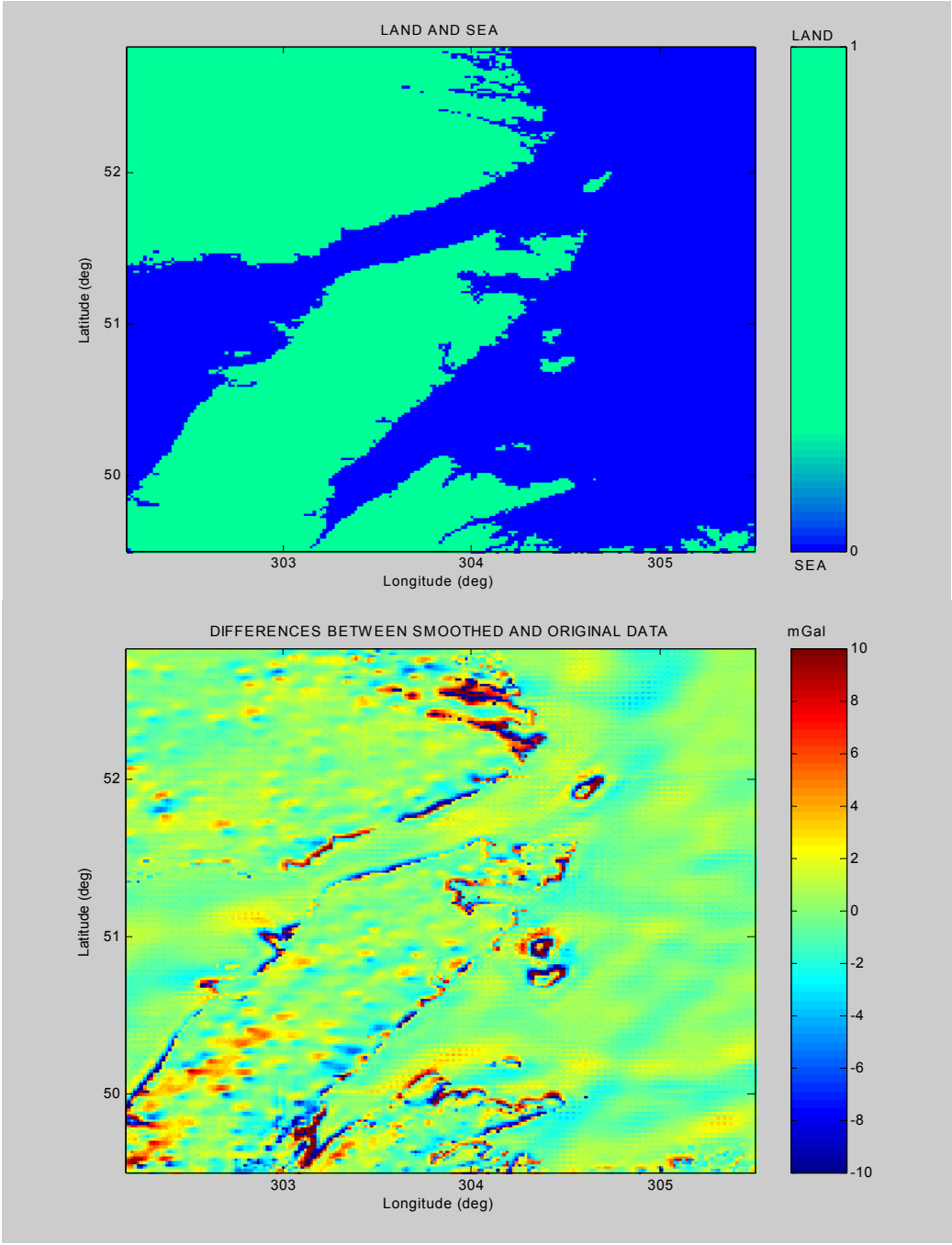

Figure 6.21: Differences between original and smoothed data for spherical wavelets. Unit:[mGal]

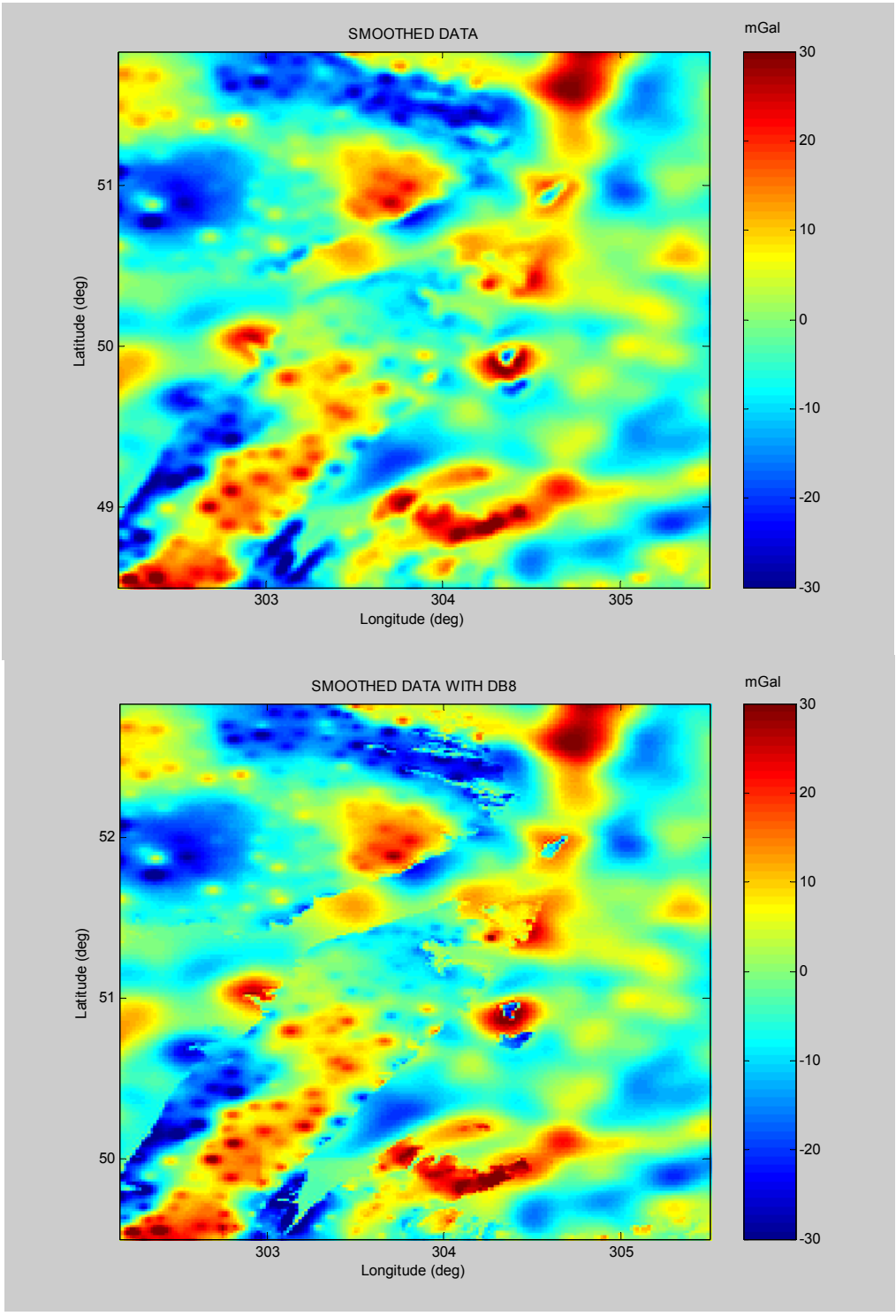

Figure 6.22: Comparison between spherical wavelets and Daubechies8 wavelets . Unit:[mGal]

To validate the numerical solution, the statistics of the differences in geoid heights between the proposed numerical solution and the 1D FFT spherical Stokes convolution with 50 km integration radius (Sideris, 1999) were computed and are shown in Table 6.20.

Table 6.20. Geoid height differences with respect to 1D FFT Unit: [m].

max	min	mean	RMS	STD
0.510	-0.301	0.001	0.101	0.100

The statistics show that the proposed numerical solution is close to the one by 1D FFT (with a RMS difference of 10 cm) and that further investigation of the effect of smoothing on the final geoid heights is necessary.

Figure 6.23 shows the smoothing effect of compatibility conditions on the final geoid heights. Again, all changes were along the coastline and between -3.4 and +3.6 cm; see Table 6.21.

Table 6.21. Differences between the geoids from smoothed and original data. Unit: [m].

max	min	mean	RMS	STD
0.036	-0.034	0.000	0.001	0.001

A smoothing effect of 4 cm is significant for cm-geoid determination. It agrees with what was seen in the preliminary study of the smoothing effect. Taking into account the fact that the area under study is flat, the effect of smoothing for a mountainous and very complicated coastline is expected to be much greater.

6.5.4 Summary for the numerical solution with compatibility conditions by combination of spherical harmonics, spherical PDOs and spherical wavelets

Spherical Shannon wavelets with Abel-Poisson kernel can be very successfully applied in the numerical solution of the AGBVP II. From a theoretical point of view, the solution for the disturbing potential will be harmonic because the used wavelets are harmonic. From a practical point of view, the orthogonality of wavelets helps us overcome a lot of technical complications. The very narrow local support of scale and wavelet function allows the computation to be done in a local area using a grid on the sphere.

The geoid heights can be immediately computed in the reconstruction step. The application for other types of data requires only changes in the spherical symbols used for different functionals of the disturbing potential.

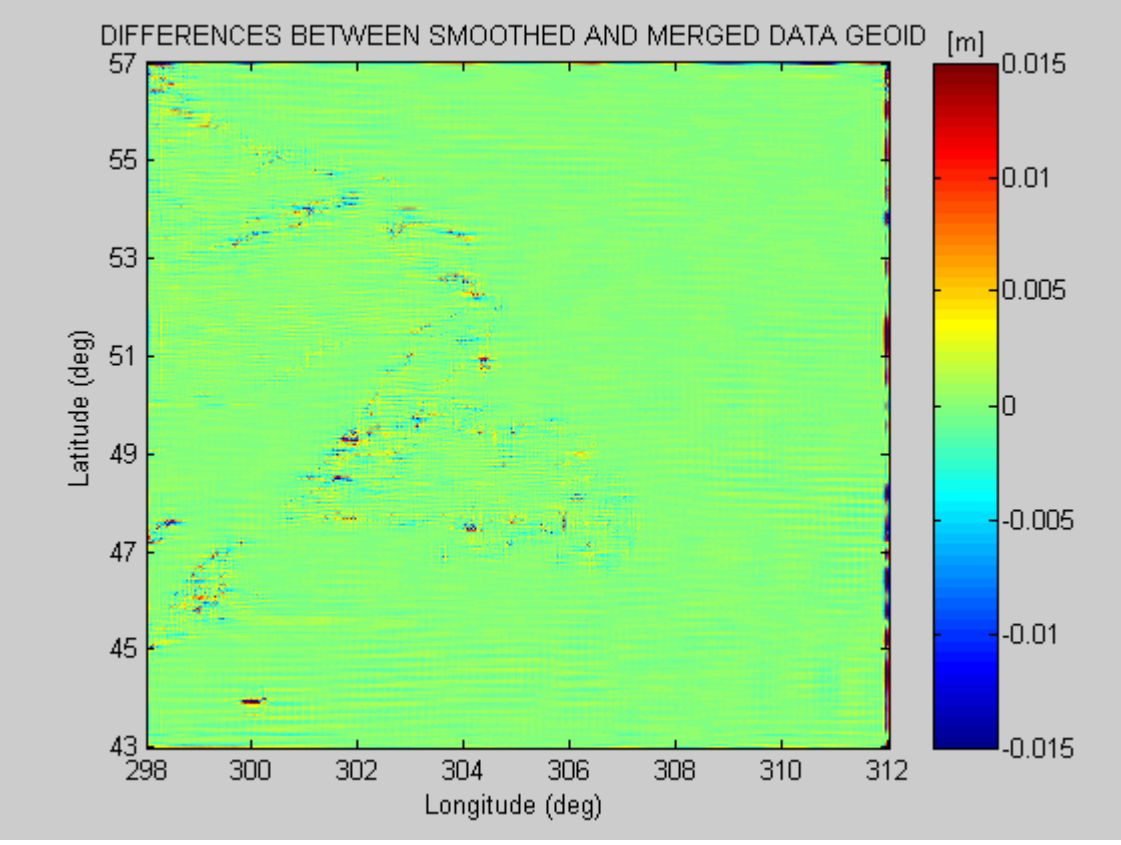

Figure 6.23: Effect of smoothing on the final geoid heights. Unit:[m]

The smoothing effect of spherical wavelets is much more effective, compared to classical planar type of wavelets (see Fig. 6.22), and it is concentrated along the coastline. No additional information about the coastline is necessary for the procedure to detect and smooth automatically the data irregularities along the coastline.

The smoothing effect on the coastline has a magnitude of -4 to 4 cm, which corresponds to our previous investigations and is significant for cm-geoid determination.

The proposed solution has to be applied in a mountainous and complicated coastline like the western coast of Canada and the US. The expected smoothing effect under these conditions should be much larger than those exhibited in the flat area we studied here.

Chapter 7

Summary, conclusions and recommendations

7.1 Summary of the contributions

In this subsection the main contributions of this dissertation are summarized. The following achievements can be considered as theoretical and practical contributions to the determination of the local and regional geoid in coastal areas, based on the solutions of AGBVPs with compatibility conditions along the coastline:

1. The theory of spherical PDOs, spherical wavelets and spherical harmonics is combined for local and regional geoid determination in coastal areas. This is done under the assumption that systematic differences between land and sea data have been removed previously.

2. It has been proven in Theorem 3.6 of subsection 3.2.2 that the fixed AGBVP II (identical to AGBVP III) has a unique solution. This was done through the use of the theory of PDOs. This theorem guarantees that different methods applied to solve this problem will lead to a unique solution.

3. It has been shown in subsections 3.3.2 and 3.3.3 that the compatibility conditions given by Svensson (1988) are equivalent to the condition that data and their first and second order gradients coincide with each other along the coastline.

4. It has been proven in proposition 4.3 of subsection 4.4.2 that PDOs are uniformly Lipschitz α. In this case, they can be combined with wavelets that are locally Lipschitz α to increase the regularity (smoothness) of the solution along the coastline.

5. A modified algorithm for reconstruction of a signal using wavelet modulus maxima points is suggested in subsection 4.4.4.3. It can be used to detect and to smooth existing discrepancies and irregularities along the coastline.

6. For combined use of spherical harmonics, PDOs and wavelets, the functional (5.67) of disturbing potential given in subsection 5.3.3 is presented in a discrete form, which allows different numerical methods to be applied. Every functional can be represented in this discrete form by taking into account only the spherical symbol that corresponds to it.

7. Compatibility conditions are derived in an explicit form in subsection 5.3.4. They can be represented as a sum of two functionals of disturbing potential on land and at sea.

8. Two solutions of the fixed AGBVP II have been proposed only from a theoretical point of view: one is based on the Neumann BVP; the second one is based on the explicit form of compatibility conditions.

9. Three preliminary solutions are tested to investigate the effect of smoothness conditions on the final geoid solution. For our flat test area, this effect is estimated to have a magnitude of -4 cm to 4 cm and, for our mountainous test area with complicated coastline, the magnitude is between -30 cm and 30 cm.

10. A final solution of AGBVP II with compatibility (smoothness) conditions is proposed and tested numerically. It has the following characteristics: it uses orthogonal spherical Shannon wavelets based on the Abel-Poisson kernel; it is harmonic; because Shannon wavelets have very narrow support, the procedure is applied in a local area using a spherical grid; for different types of measurements, only changes in the spherical symbols are necessary; it produces a much greater smoothness effect, as compared to classical planar wavelets and it is concentrated along the coastline; no additional information about the coastline is necessary for the procedure to detect and smooth the data irregularities along the coastline

automatically; the smoothness effect is consistent with previous investigations and is significant for cm-geoid determination.

7.2 Conclusions

In this subsection, conclusions and recommendations corresponding to the main objectives of the thesis originally formulated in Chapter 2 are provided.

1. The theory of PDOs and wavelets can be successfully applied for finding solutions of AGBVPs with compatibility (smoothness) conditions along the coastline. PDOs based on generalized functions and generalized derivatives from Sobolev spaces will provide infinite smoothness of the solution off the coastline. At the same time the very good localizing properties of wavelets will help to increase the smoothness of the solution along the coastline.

2. For the fixed AGBVP II, it has been proven that there exists *a unique solution* and the proof is based on the theory of PDOs. This proof can be considered as complementary to the proofs provided in Keller (1996) and Lehmann (1999), and it shows how the factorization index can be used to increase the regularity of the solution. As a result, a higher order of smoothness can be achieved by increasing the order of the used PDOs (generalized derivatives) and imposing additional conditions along the coastline.

3. It has been shown that the compatibility conditions applied by Svensson (1988) for AGBVPs correspond to the conditions that data and their first and second order gradients should coincide along the coastline. An even higher order of smoothness is possible if these conditions involve higher order gradients.

4. The transition from variational methods for solutions of AGBVPs with orthonormal base functions to the frame theory by wavelets is possible. It has been shown that wavelet frames can provide more flexibility in imposing compatibility

(smoothness) conditions along the coastline compared to the unique solution by variational methods.

5. The local regularity of wavelets can be used to detect singularities and edges, because of the space localizing properties of wavelets. For AGBVPs, the singularities are expected along the coastline and the local regularity estimation can help to detect them. The combination of uniformly regular PDOs with local regular wavelets can increase the regularity of the AGBVPs solutions across the coastline.

6. In subsection 4.4.2 it has been proven that PDOs are *uniformly Lipschitz* α. The impact of the proved *preposition 4.3* is that it will help to combine both PDOs and wavelets for AGBVPs considering they are complementary in terms of Lipschitz regularity. This means that PDOs will provide the necessary smoothness off the coastline and wavelets will detect and smooth the singularities and edges along the coastline.

7. From a theoretical point of view, the detection and the smoothing of singularities presented by Mallat (1998) and a *modified procedure* based on wavelets local modulus maxima points, for reconstruction of the signal can be applied in AGBVPs to smooth the irregularities across the coastline. The representation of the wavelet transform as a multiscale differential operator together with the concept of modulus maxima allows for the reconstruction of a signal by its modulus maxima points. In the case of AGBVPs the wavelet coefficients can be changed along the coastline and this is possible because of the properties of wavelet frames. As a result, additional smoothing can be achieved in the modified reconstruction of the signal.

8. It has been shown that for the numerical application of the compatibility conditions, two options exist. The first one is to give them in an explicit form (see

Chapter 6), and the second one is to improve the regularity of the data (and the regularity of the solution, as well) by imposing these conditions on the data, and their first and second order gradients (and even on higher order gradients). This can be successfully done with the application of wavelets as multiscale differential operators, and their abilities for detecting and smoothing irregularities along the coastline. The second procedure has been used in the numerical applications.

9. The threshold value plays an important role for the level of smoothing along the coastline. Maximum smoothing can be achieved by suppressing the detail coefficients to zero. Another option to take into account the accuracy of the coefficients is to us as threshold value some statistics of the detail coefficients – average, RMS or standard deviation of the coefficients.

10. Spherical harmonics, spherical PDOs and spherical wavelets for solutions of AGBVPs presented in Freeden and Windheuser (1997) can be successfully applied to find numerical solutions of AGBVPs with compatibility (smoothness) conditions along the coastline.

11. In subsection 5.3.1 a solution of Neumann's BVP given in Freeden and Schneider (1998) has been used to propose a numerical solution of the fixed AGBVP II (identical to AGBVP III). The compatibility conditions can be applied as restrictions of wavelet coefficients and although the smoothness conditions are incorporated in the solution, they are applied to the boundary conditions (data).

12. The discrete form (5.76) of functionals of the disturbing potential has been derived, which is necessary to model the type of observations for a AGBVP in terms of both PDOs and wavelets on the sphere. It has been applied in the case of downward continuation, showing that under certain conditions equation (3.76) for downward continuation is exactly the spherical Abel-Poisson integral for the space outside of the sphere.

13. In subsection 5.3.4 the compatibility conditions given by Svensson (1988) in an implicit form are derived in *explicit form* (5.81) as two PDOs (5.82) on land and at sea. The compatibility conditions are applied directly to the solution (disturbing potential) along the coastline. The main difficulties in this approach are the non-orthogonality of the Abel-Poisson wavelets, which will slow down the processing, and the application of an equidistant grid. Also, the computation of spherical symbol for the ocean-land function can be considered as a serious problem, because this function acts like a step function across the coastline and its spherical spectrum will contain all possible frequencies.

14. A general scheme for finding a global solution using compatibility conditions is presented. It is based on very high degrees of spherical harmonic expansions, which are possible because of the current level of numerical computations and recent developments in the theory of exact spherical harmonic transforms and their inverse. This presents the link between globally defined theory and local applications of compatibility conditions in coastal areas. The local smoothing along the coastlines can be considered as a part of a procedure for global potential modeling with very high resolution.

15. The two preliminary numerical solutions for investigating the effect of smoothing along the coastline show that for a flat and uncomplicated coastline the effect of smoothing is between -4 and 4 cm. and for a complicated mountainous coastline this effect increases to between -30 and 30 cm. In view of cm-geoid determination this effect can be considered as significant and the compatibility (smoothness) conditions need to be applied for solutions of AGBVP in coastal regions. These two experiments motivate further theoretical investigations for the application of compatibility conditions.

16. The third experiment, dedicated to the solution of the fixed AGBVP II, shows the same magnitude of the smoothness effect for flat area and it shows that the smoothing of the boundary surface (the geoid from GPS/leveling and altimetry data) does not have significant influence on the final geoid solution. The main contribution is due to the smoothing of boundary conditions, gravity anomalies on land and gravity disturbances at sea.

17. The final numerical solution of AGBVP II using spherical PDOs and spherical wavelets has the following properties from an application point of view:

- Spherical Shannon wavelets with Abel-Poisson kernel can be very successfully applied in the numerical solution of the AGBVP II. From a theoretical point of view, the solution for the disturbing potential will be harmonic because the used wavelets are harmonic. From a practical point of view, the orthogonality of wavelets helps us to overcome a lot of technical complications. The very narrow local support of scale and wavelet function allows the computation to be done in a local area using a grid on the sphere.
- The geoid heights can be immediately computed in the reconstruction step. The application for other types of data requires only changes in the spherical symbols used for different functionals of the disturbing potential.
- The smoothing effect of spherical wavelets is much more effective, compared to classical planar wavelets, and it is concentrated along the coastline. No additional information about the coastline is necessary for the procedure to detect and smooth automatically the data irregularities along the coastline.
- The smoothing effect at the coastline (the case of flat area) corresponds to our previous investigations and is significant for cm-geoid determination.

18. Different types of wavelets can be used for imposing compatibility conditions, but for modeling the disturbing potential it is important for them to be harmonic. In such way different spherical wavelets based on Abel-Poisson kernel are very suitable. Other types of harmonic wavelets can be useful as well if they are

orthogonal. Another main issue in the choice of wavelets is their orthogonality because this property of wavelets can overcome numerical difficulties on the sphere.

7.3 Recommendations for future work

The methods for solving AGBVPs with compatibility conditions can be used in other applications. For example, to combine geoids or gravity data in different areas (different countries) the methodology described in this dissertation could help to produce one common geoid with a smooth transition along the boundaries between seemingly disjoint parts. Some possible and potentially beneficial developments of this work in the future could be done in the following directions:

1. To find a proper equidistant grid on the sphere; the solution can be applied on much larger areas or even on the entire sphere.
2. To find a procedure for orthogonalization of spherical wavelets; this will facilitate the application of other types of spherical wavelets. A possible solution can be to use the so-called Slepian functions on the sphere.
3. A more realistic threshold value for the limit of detail wavelet coefficients can be found based on the spherical modulus maxima; it can be more effective than assuming a zero value (corresponding to the maximum smoothing), or by simply using the RMS of detail coefficient at every level of decomposition.
4. To find the spherical symbol for the ocean-land function. For a general distribution of land and sea, all frequencies are presented in the spherical spectrum because this function is a step function across the coastline. A proper procedure for finding the spherical Fourier transform is necessary. Having the spherical symbol for the land-ocean function will make possible the application of explicit compatibility conditions.
5. The proposed numerical solution with Shannon spherical wavelets needs to be applied in a mountainous coastal area. The smoothness effect of compatibility conditions is expected to be much greater because larger discrepancies exist between the data along the coastline.

6. The existence of random noise in the data needs to be taken into account. The smoothing of the noise can be done by wavelets but additional research is necessary in terms of minimization of the noise along the coastline.

REFERENCES

Albertella, A., Sansò, F., Sneeuw, N. (1999): Band-limited functions on a bounded spherical domain: the Slepian problem on the sphere, J of Geodesy, vol. 73, pp. 436-447.

Andritsanos, V., Sideris, M.G., Tziavos, I.N. (2000): A survey of gravity field modelling applications of the Input-Output System Theory (IOST). IGeS Bulletin, vol. 10, pp.1-17.

Arnold, K. (1983): The mixed boundary value problem of geodesy, Gerlands Beitr. Geophys., vol. 92, pp. 391-406.

Arnold, K. (1984): The compatibility conditions, the uniqueness and the solution of the mixed boundary value problem of geodesy. Gerlands Beitr Geophys., vol 93, pp. 339-355.

Blais, J.A.R. and Provins, D. and Tan C.J. (2000): Optimization of computations in spherical geopotential field applications, in Sideris M.G. (ed.) Gravity, Geoid and Geodynamics 2000, Banff, Canada, July31-August 4, 2000, pp. 55-59.

Blais, J.A.R. and Provins, D. (2002): Spherical harmonic analysis and synthesis for global multiresolution applications, J of Geodesy, vol. 76, 1, pp. 29-35.

Blais, J.A.R. and Soofi, M. (2004): Spherical harmonic transforms and global communications, presentation at 8th Canadain Geoid Workshop, Montreal, May 16, 2004

Christensen, O. (2001): Frames, Riesz bases and discrete Gabor/Wavelet expansions. Bulletin of the American Mathematical Society, vol. 38, num. 3, pp. 273-291.

Eskin, G. (1980): Boundary value problems for elliptic pseudodifferential equations. Tran. of Mathematical Monographs, vol. 52, American Mathematical Society.

Farlow, S. (1993): Partial Differential Equations for Scientists and Engineers , Dover Publications, Inc., New York.

Freeden, W. and Schneider, F. (1998): Wavelet approximation on closed surface and their application to boundary-value problems of potential theory. Math. Meth in Appl. Sciences, vol. 21, pp. 129-163.

Freeden, W. and Windheuser, U. (1996): Spherical wavelet transform and its discretization. Adv. Comp. Math., vol. 5, pp. 51-94.

Freeden, W. and Windheuser, U. (1997): Combined spherical harmonic and wavelet expansion – A future concept in Earth's gravitational determination. Appl. Comp. Harm. Anal., vol. 4, pp. 1-37.

Freeden, W. and Michel, V. (2002): Orthogonal non-bandlimited wavelets on the sphere, University of Kaiserslautern, Laboratory of Technomathematics, pp. 21-22.

Freeden, W. and Schreiner, M. (1995): New wavelet methods for approximating harmonic functions. In: Geodetic theory today (F. Sansò, ed.), International Association of Geodesy Symposia, vol. 114, Springer, pp. 112-121.

Freeden, W. Gervens, T. and Schreiner, M. (1998): Constructive approximation on the sphere, with applications to geomathematics. Oxford Science Publications.

Gelfand, I. and Shilov, G. (1968): Generalized functions, in "Spaces of fundamental and generalized functions", vol 2, Academic press, London

Grebenitcharsky, R. and Sideris, M.G. (2001a): Altimetry-gravimetry boundary value problems with smoothness conditions in coastal regions, in Tziavos I. N. and Barzaghi R. (eds.) EGS 2001-G7 Session "Regional and local gravity field approximation", Nice, France, 25-30 March, 2001, Bulletin of IGeS, vol. 13, special issue, pp. 121-132.

Grebenitcharsky, R., Vergos, G.S., and Sideris, M.G. (2001b): Combination of gravity, altimetry and GPS/Leveling data for the numerical solution of the altimetry-gravimetry boundary value problems, In: Adam J., Schwarz K.,P. (eds) Vistas for geodesy in the new millennium, IAG Scientific Assembly, Budapest, Hungary, September 2-7, pp. 150-155.

Grebenitcharsky, R. and Sideris, M.G. (2002a): Application of spherical pseudo-differential operators and spherical wavelets for numerical solutions of the fixed altimetry-gravimetry boundary value problem. V Hotine-Marussi Symposium on Mathematical Geodesy, Matera, 17-22 June.

Grebenitcharsky, R. and Sideris, M.G. (2002b): Data smoothing along a mountainous coastline for use in altimetry-gravimetry boundary value problem solutions, in "3rd Meeting of International Gravity and Geoid Commission", Tziavos (ed.), Gravity and Geoid 2002 - GG2002, 2003, pp. 223-228.

Grebenitcharsky, R. and Sideris M.G. (2003): A numerical study of solving the altimetry-gravimetry boundary value problem in coastal regions, IUGG XXIII General Assembly – IAG G3 Symposium, June 30-July 11, 2003, Sapporo, Japan.

Heck, B. (1997): Formulation and linearization of boundary value problems: from observables to a mathematical model. In: Sansò, F., Rummel, R. (eds) Geodetic boundary value problems in view of the one centimeter geoid. Lecture Notes in Earth Sciences, vol. 65, Springer, Berlin Heidelberg New York, pp 121-160.

Holota, P. (1980): The Altimetry-gravimetry boundary value problem. presented at the International Scientific Conference of Sec. 6 Intercosmos, Albena, Bulgaria.

Holota, P. (1983a): The altimetry gravimetry boundary value problem I: linearization, Friedrich's inequality. Boll. Geod. Sci. Afini., vol. 42, pp. 14-32.

Holota, P. (1983b) The altimetry gravimetry boundary value problem II: weak solution, V-ellipticity. Boll Geod. Sci. Afini., vol. 42, pp. 70-84.

Holota, P. (1997): Variational methods for geodetic boundary value problems. In: Sansò F., Rummel R. (eds.) Geodetic boundary value problems in view of the one centimeter geoid. Lecture notes in Earth sciences, vol. 65, Springer, Berlin Heidelberg New York, pp. 469-481.

Holota, P. (2000): Variational methods in the recovery of the gravity field – Galerkin's matrix for an ellipsoidal domain, in Sideris (ed.), Gravity, Geoid, and Geodynamics, 2000, IAG Symposia, vol. 123, pp. 277-283.

Hsu, H. (1984): Applied Fourier series, HBJ College outline series, New York, pp. 97

Jaffard, S. and Meyer, Y. (1996): Wavelet methods for pointwise regularity and local oscillations of functions, Memoirs of the American Mathematical Society, vol. 123, No. 587

Jinghai, Y. and Xiaoping, W. (1997): The solution of mixed boundary value problems with the reference ellipsoid as boundary. J of Geodesy, vol. 71, pp. 454-460.

Keller, W. (1996): On a scalar fixed altimetry-gravimetry boundary value problem. J of Geodesy, vol. 70, pp. 459-469.

Keller, W. (2000): Applications of wavelets, Lecture notes, The University of Calgary, Calgary, Canada.

Keller, W. (2003): Geodetic pseudo-differential operators and the Meissl scheme, in Geodesy - the challenge of the 3rd millennium, E., Grafarend, F., Krumm, V.S. Schwarze (eds.) , Springer-Verlag Berlin Heidelberg, pp. 207-212.

Kirsch, A. (1996): An introduction to the mathematical theory of inverse problems, Applied Math. Sciences., vol. 120, Springer-Verlag, New York.

Kotsakis, C. (2000): Multiresolution aspects of linear approximation methods in Hilbert spaces using gridded data, UCGE Reports, no. 20138, Calgary, Canada

Lehmann, R. (1999a): Studies on the altimetry-gravimetry problems for geoid determination. Phys. Chem. Earth., PA: Solid Earth Geod., vol. 24, pp. 47-52.

Lehmann, R. (1999b): Boundary value problems in the complex world of geodetic measurements, J of Geodesy, vol. 73, 491-500.

Lehmann, R. and Klees, R. (1999): Numerical solution of geodetic boundary value problems using a global reference field, J of Geodesy, vol. 73, pp. 543-554

Mainville, A. (1986): The altimetry-gravimetry problem using orthonormal base functions. Rep 373, Department of Geodetic Science and Surveying, The Ohio State University, Columbus, USA.

Mallat, S. (1998): A wavelet tour of signal processing. Academic Press, New York, USA.

Martinec, Z. (1995): Numerical stability of the least squares solution to the discrete altimetry-gravimetry boundary-value problem for determination of the global gravity model. Geophys. J. Int. vol. 123, pp. 715-726.

Mayer, J.P. (1997): Zur Lösung von geodätischen Randwertproblemen durch einen hypersingulären Potentialansatz. Dissertation, Mathematisch-Naturwissenschaftliche Fakultät der Christian Albrechts-Universität zu Kiel.

Moritz, H. (1980): Advanced physical geodesy, Herbert Wichmann Verlag, Karlsruhe.

National oceanographic and atmospheric administration – NOAA (1997): The GEOSAT-GM Altimeter JGM-3 GDRs.

Provins, D. (2004): Earth synthesis: Determining Earth's structure from geopotential fields, UCGE Report, no. 20189, Calgary, Canada.

Rektorys, K. (1977): Variational methods in mathematics, science and engineering. D. Reidel Publishing Company, Dordecht/ Boston, USA.

Rummel, R. (1997): Spherical spectral properties of the Earth's gravitational potential and its first and second derivatives. In: Sansò, F. and Rummel, R. (eds) Geodetic boundary value problems in view of the one centimeter geoid. Lecture Notes in Earth Sciences, No. 65, Springer, Berlin Heidelberg, New York, pp.359-404.

Rummel, R. and Teunissen, P. (1988): Height datum definition, height datum connection and the role of the geodetic boundary value problem. Bull. Geod., vol. 62, pp. 477-498.

Sacerdote, F. and Sansò, F. (1983): A contribution to the analysis of altimetry gravimetry problems. Bull. Geod., vol. 57, pp. 183-201.

Sacerdote, F. and Sansò, F. (1987): Further remarks on the altimetry-gravimetry problems. Bull. Geod., vol. 61, pp. 183-201.

Sandwell, D.T. and Smith, W.H.F. (1997): Marine gravity anomaly from Geosat and ERS 1 satellite altimetry, J. Geophys. Res., vol. 102(B5), pp. 10039-10054.

Sansò, F. (1981): Recent advances in the theory of the geodetic boundary value problem. Review of Geoph. and Space phys., vol. 19, no.3.

Sansò, F. (1983): A discussion on the altimetry-gravimetry problems. In Geodesy in transition,U of Calgary, pp. 71-107.

Sansò, F. (1993): Theory of geodetic boundary value problems applied to the analysis of altimeter data. in: Rummel, R. and Sansò, F. (eds.) Satellite altimetry in geodesy and oceanography, Lecture Notes in Earth Sciences, vol. 50, pp. 318-371.

Sansò, F. (1995): The long road from measurements to boundary value problems in physical geodesy. Manuscr. Geod., vol. 20, pp. 326-344.

Sansò, F. and Stock, B. (1985): A numerical experiment in the altimetry-gravimetry problem II. Manuscr. Geod. vol. 10, pp. 23-31.

Sansò, F. and Usai, S. (1995): Height datum and local geodetic datums in the theory of geodetic boundary value problems. Allg. Verm. Nachr., vol. 95, no.8-9, pp. 343-355.

Sideris, M.G. (1996): On the use of heterogeneous noisy data in spectral gravity field modeling methods, J of Geodesy, vol. 70, pp. 470-479.

Sideris, M.G. (1999): Geoid Determination by FFT techniques – International school for the determination and use of the geoid, International Geoid Service, DIIAR-Politecnico di Milano, pp. 165-229.

Simons, M., Solomon, S.C. and Hager, B.H. (1997): Localization of gravity and topography: constraints on the tectonics and mantle dynamics of Venus. Geophys. J. Int., vol. 131, pp. 24-44.

Sneeuw, N., (1994): Global spherical harmonic analysis by least-squares and quadrature methods in historical prospective. Geophys J Int, 118, pp. 707-716.

Svensson, L. (1983a). Solution of the altimetry-gravimetry problem. Bull. Geod., 57, 332-353.

Svensson, L. (1983b): Pseudodifferential operators – New Approach to the boundary problems of physical geodesy. Manuscr. Geod., vol. 8, pp. 1-40.

Svensson, L. (1985): Some remarks on the altimetry-gravimetry problem. Proceedings of the I Hotine-Marussi Symposium on Mathematical Geodesy, Rome, pp. 559-582.

Svensson, L. (1988): Some remarks on the altimetry-gravimetry problem. Manuscr. Geod., vol. 13, pp. 63-74.

Svensson, L. (2003): Map projections and boundary value problems, in Geodesy - the challenge of the 3rd millennium, E., Grafarend, F., Krumm, V.S. Schwarze (eds.) , Springer-Verlag Berlin Heidelberg, pp. 257-260.

Vergos, G., Grebenitcharsky, R. and Sideris M.G. (2001): Combination of multi-satellite altimetry and shipborne gravity data for geoid determination in a coastal region of eastern Canada, XXVI General Assembly of EGS, Nice, France, 25-30 March, 2001.

Xu, G. (1992): Spectral analysis and geopotential determination. Reihe C, Heft No 397, Deutsche Geodätische Kommission, bei der Bayerischen Akademie der Wissenschaften, München.

APPENDIX

Important mathematical formulations and theorems related to the general theory of PDOs

Definition A.1: A set *M* is called *measurable in a Lebesque sense* (*Lebesque measurable* or simply *measurable*) if the greatest lower bound of the measures of all bounded open sets of *M* is equal to the least upper bound of all bounded closed sets contained in *M.*

Lemma A.1 Suppose $f(x)$ is a measurable function such that $|f(x)| \le C(1+|x|)^t$, and $v(x) \in \mathbf{S}$. Then the convolution $f * v = \mathbf{C}^\infty$ satisfies the estimate

$$\left|\frac{\partial^k}{\partial x^k}(f * v)\right| \le C[\![v]\!]_m (1+|x|)^t, \quad 0 \le |k| < \infty \tag{A.1}$$

where $m = \max(|k|, |t|+4)$ and constant *C* does not depend on v.

Lemma A.2 Suppose $f \in \mathbf{S}'$. Then there exists an integer $m(f) \ge 0$ such that

$$|(f, v)| \le C_m [\![v]\!]_m \text{ for any } v \in \mathbf{S} \tag{A.2}$$

Definition A.2 The complement of the largest open set **U** on which $(g, v) = 0$ for all $v \in \mathbf{S}(\mathbf{U})$ is called a *support* of the functional *g*. It is noted as *supp g*.

Definition A.3 Assume $A_0(\xi) \in \mathbf{C}^\infty$ for $\xi = (\xi_1, \xi_2, \xi_3) \neq 0$ and is homogeneous $O^\infty_{\alpha+i.\beta}$ of degree $\alpha + i.\beta$, which means that

$$A_0(\mu\xi) = \mu^{\alpha+i.\beta} A_0(\xi), \quad \forall \mu > 0 . \tag{A.3}$$

Properties of $A_-(\xi', \xi_3)$ and $A_+(\xi', \xi_3)$**:**

a) $A_+(\xi', \xi^3)$ admits an analytical continuation with respect to ξ_3 into the upper halfplane $z > 0$ for $\xi' \neq 0$; is continuous and different from zero for $z > 0$, $|\xi'| + |\xi_3| + z > 0$; and is homogeneous of degree $\mathbf{k} = \mathbf{k}_1 + i.\mathbf{k}_2$.

b) $A_-(\xi', \xi^3)$ admits an analytical continuation with respect to to ξ_3 into the halfplane $z < 0$ for $\xi' \neq 0$, is continuous and different from zero for $z \leq 0$, $|\xi'| + |\xi_3| + |z| > 0$ and is homogeneous of degree $\alpha + i.\beta - \mathbf{k}$.

Theorem A.1 (Eskin, 1980) Suppose $A(\xi) \in O^\infty_{\alpha+i.\beta}$ is an elliptic symbol and $A(\xi) = |\xi|^{\alpha+i.\beta} A_0(\xi)$. Then $A(\xi)$ admits a unique homogeneous factorization and the degree of homogeneity $\mathbf{k} = \mathbf{k}_1 + i.\mathbf{k}_2$ of the function $A_+(\xi', \xi_3)$ is called the factorizarion index of an elliptic symbol $A(\xi', \xi^3) \in O^\infty_{\alpha+i.\beta}$ and

$$\mathbf{k} = (\alpha + i.\beta)/2 + m + \varepsilon \tag{A.4}$$

where $\varepsilon = (1/2\pi i)\ln(\alpha_2/\alpha_1) = \varepsilon_1 + i.\varepsilon_2$ is generally a complex number

$$\alpha_1 = \lim_{\xi_3 \to +\infty} A_0(\xi', \xi_3) = \lim_{\xi_3 \to +\infty} A_0\left(\frac{\xi'}{\xi_3}, +1\right) = A_0(0, +1) \tag{A.5a}$$

$$\alpha_2 = \lim_{\xi_3 \to -\infty} A_0(\xi', \xi_3) = \lim_{\xi_3 \to -\infty} A_0\left(\frac{\xi'}{|\xi_3|}, \frac{\xi_3}{|\xi_3|}\right) = A_0(0,-1) \qquad \text{(A.5b)}$$

Theorem A.2 (Eskin, 1980) Suppose that $b_k(\xi') \neq 0,\ k = 1,2$, where $\mathbf{k}$ is the factorization index of $\widetilde{b}_1\widetilde{b}_2^{-1}$, $\boldsymbol{\kappa}_0 = \boldsymbol{\kappa} + m_2$ and the number α satisfies both inequalities $|\alpha - 1/2 - \mathrm{Re}\,\mathbf{k}_0| < 1/2$ and $\alpha > \max(m_1 + 1/2, m_2 + 1/2)$. Then the mixed BVP Eq.(3.42) has a unique solution $u(x) \in \mathbf{W}_\alpha(\mathbf{R}^3_+)$ for any $f \in \mathbf{W}_{\alpha-2}(\mathbf{R}^3_+)$, $g_1 \in \mathbf{W}_{\alpha-m_1-1/2}(\mathbf{R}^2_+)$, and $g_2 \in \mathbf{W}_{\alpha-m_2-1/2}(\mathbf{R}^2_-)$.

Major notations: Let the operator $L(\xi', \xi_3)$ have the factorization $L(\xi', \xi_3) = a_{33}(\xi_3 - \lambda_1(\xi'))(\xi_3 - \lambda_2(\xi'))$, where $\xi' = (\xi_1, \xi_2)$. Also, let $\widetilde{\lambda}_2(\xi') = \lambda_2\left(\xi_1/|\xi_1| + \xi_1, \xi_2\right)$, then the PDO $\widetilde{b}_k(\xi') \in \mathbf{R}^2$ has the symbol $\tilde{b}_k(\xi') = iB^k\left(\xi_1/|\xi_1| + \xi_1, \xi_2\right)$. Finally, the factorization of $\widetilde{b}_1\widetilde{b}_2^{-1}$ with respect to ξ_3 will be denoted as $\widetilde{b}_1\widetilde{b}_2^{-1} = \widetilde{b}_-\widetilde{b}_+$ and the factorization index is equal to $\mathbf{k} = \deg_{\xi'} b_+(\xi_1, \xi_2)$, which means the degree of $b_+(\xi_1, \xi_2)$.